

Live-Cell Analysis Handbook

A Guide to Real-Time Live-Cell Imaging and Analysis
Fourth Edition

Simplifying Progress

SARTORIUS



Table of Contents



Chapter 1

Introducing Real-Time Live-Cell Analysis

The biomedical world has come a long way since Anton van Leeuwenhoek first observed living cells with a basic microscope in 1674. Using fluorescent probes and modern high resolution imaging techniques it is now possible to view labeled sub-cellular structures at the 10-50 nanometer scale. For researchers working with fixed (dead) cells, organelles can be studied at even higher resolution using electron microscopy. These methods provide tremendous insight into the structure and function of cells down to the molecular and atomic level.


The further development of cell imaging techniques has largely focused on resolving greater spatial detail within cells. Examples include higher magnification, three dimensional viewing and enhanced penetration into deep structures. Significant attention has also been paid to temporal resolution – time-lapse imaging has evolved for high-frame rate image capture from living cells to address “fast”

biology such as synaptic transmission and muscle contractility. Any consideration for technology advances at lower spatial or temporal detail may initially seem mundane, or even unnecessary. However, this would fail to recognize some key unmet user needs.

First, there is an increasing realization that many important biological changes occur over far longer time periods than current imaging solutions enable. For example, maturation and differentiation of stem cells can take hours, days and sometime weeks, which is hard to track using existing methods. Second, imaging techniques are not readily accessible to all researchers nor on an everyday basis. This lack of accessibility is either due to virtue of instrumentation that is expensive and use-saturated or by complex software that renders image acquisition and analysis the sole domain of the expert user. Third, and particularly with regard to time-lapse measurement,

the throughput of current solutions is typically too low for frontline use in industrial applications. Finally and most importantly, researchers are increasingly aware that any perturbation of the cells in the process of imaging (e.g. fixing, loss of environmental control) can introduce unwanted and misleading experimental artefacts. Together, these factors frame up the requirement for solutions that enable longer-term, non-perturbing analyses of cells at a throughput and ease of use commensurate with non-specialist users, and at industrial scale.

A new generation of specialized compact microscopes and live-cell imaging devices, are now emerging to meet this need. Designed to reside within the controlled, stable environment of a cell incubator, these systems gather cell images (phase contrast, bright-field and/or fluorescence) from assay micro-plates automatically, repeatedly and around the clock. Image acquisition is completely non-invasive



and non-perturbing to cells, opening up the opportunity to capture the full, and as needed, long-term time course of the biology. Acquisition scheduling, analysis and data viewing can be conducted easily and remotely, without in-depth knowledge of image processing. Data is analyzed on the fly, image by image, to provide real-time insight into cell behavior. We refer to this paradigm, which is differentiated from straight live-cell imaging by the provision of analysed data at scale as opposed to simply images, as 'real-time live-cell analysis'.

In an ideal world, the images acquired from a live-cell imaging device would be collected only from photons produced by the sample of interest, and in perfect focus. However, this is not the usual case. There are multiple sources of confounding signal present in an image, each needing correction, removal, or cleaning in order to reveal information which has been generated by the sample elements of interest. Corrections are needed due to systematic aberrations in an imaging system stemming from multiple sources. For example, detector anomalies (e.g. detector bias, dark current variability, field flatness and thermal or gamma-ray noise), optical


issues (non-flat optical components and illumination imperfections) or undesired signal introduced by the sample are common issues. Autofluorescence from cellular components or media, or non-biological signal sources such as shading, or patterns arising from sample matrices or non-uniform illumination due to meniscus effects in microwells must be removed before usable, replicable information can be extracted.

In order to perform these corrections, one must be aware of the effects of each process, and manipulations on the raw images must be repeatable, to ensure faithful capture of the measured biological signal across images, experiments, and devices. There are many tutorials and software toolkits available to process images, however systems that perform these corrections as a matter of course provide consistency and ease of use, particularly when coupled with standardized assays, reagents and consumables which normalize the experimental process (e.g. the Incucyte® Live-Cell Analysis System, and the assays and reagents available from

Sartorius). The consistency with which images are acquired and processed strongly influences the ability to analyze the collected data. This can be a time-consuming task, and purpose-built software that presents only the tools necessary for a specific scientific question can remove what can be a significant hurdle in the image analysis workflow.

While traditional compact microscopes typically only image from a single micro-plate or flask at a time, new live-cell analysis devices such as Incucyte® can automatically capture and analyze images from multiple micro-plates in parallel, thereby significantly increasing throughput (e.g. Incucyte = 6 x 384 well plates). With the Incucyte® Live-Cell Analysis System, a unique moving optical path design means that the cells and cell plates remain stationary throughout the entire experiment. This further minimizes cell perturbation and enables imaging and analyses of both adherent and non-adherent cell types.

This combination of functionality, throughput and ease of use revolutionizes



the way researchers can think about imaging assays in living cells. Real-time live-cell analysis has now been applied to a wide range of phenotypic cellular assays including cell proliferation, cell death and apoptosis, immune-cell killing, migration, chemotaxis, angiogenesis, neurite outgrowth and phagocytosis. In each case, the full time-course data and 'mini-movies' of the assay provide greater biological insight than end point assays. Novel analyses such as area under curve, time to signal onset or threshold, and rate parameters (dx/dt) are at times highly value adding. Simply calculating the assay signal at its peak time-point and/or at the optimal signal/background all helps in assembling robust and reproducible assays. Of course, transient effects of treatments can be detected by kinetic imaging that may otherwise be missed with end-point reads.


Due to its non-invasive nature, measurements from cells can be made not only during the assay itself but also during the cell preparation and 'pre-assay' stage. For example, the morphology and proliferation rates of cells can be

monitored throughout the cell culture period and immediately post-seeding on the micro-titer assay plate. The parameter/phenotype of interest can be measured prior to the addition of treatments to provide a within well baseline measure. Quality control of cells and assay plates in this way helps improve assay performance and consistency by ensuring that experiments are only conducted on healthy, evenly plated cultures with the expected cell morphology.

The real-time live-cell analysis approach also provides the opportunity to make data driven decisions while the experiment is in progress. A researcher studying the biology of vascular or neuronal networks, for example, may wish to first establish a stable network before assessing the effects of compound treatments or genetic manipulations (e.g. siRNAs). With continuous live-cell analysis, it is straightforward to temporally track network parameters and use the real time data to judge when best to initiate the treatment regimes. The timing of adjunct studies such as analysis of metabolites or secreted proteins in supernatants can

also be guided. Drug washout studies may be performed using the real time data to identify when an equilibrium response occurs and to trigger the timing of the washout regime. If for any reason it transpires that the experiment is not performing as expected, then treatments could be withheld to save expensive reagents and follow-on experiments can be initiated more quickly to make up time.

Real-time live-cell analysis is extremely helpful when developing, validating and troubleshooting phenotypic assays. Within a small number of assay plates it's usually possible to obtain a clear understanding of the relationship over time between assay signal and treatments, cell plating densities, plate coatings and other protocol parameters. Scrutiny of the kinetic data and 'mini-movies' from each well help to rapidly pinpoint sources of within- and across-plate variance and to validate the biology of interest. This is particularly true for more advanced cell systems such as co-cultures where far more permutations and combinations of protocol parameters exist (e.g. cell plating ratios) and the biology is more complex.



In summary, real-time live-cell analysis is re-defining the possibilities and workflows of cell biology. The combination of ease of use, throughput, long term stability and non-invasive measurement enables researchers to monitor and measure cell behaviors at a scale and in ways that were previously not possible, or at the least, highly impractical. In the following chapters of this handbook, we illustrate this with a range of different application examples.

Chapter 2

From Images to Answers

Introduction

The nature of cell biology research typically requires that image-based methods are used to capture moments in time to enable comparisons between treatment groups and across imaging modalities. Sample information is typically acquired using a microscope and a digital camera, and those moments in time are processed and analyzed. Images captured with a typical microscope camera are digital representations of the analog information contained in the sample, providing a means to automatically analyze the information in the sample. Once these digital snapshots are acquired, image processing is used to clean up the data, and image analysis is used to extract usable information for analysis.

At the core of all of these manipulations are numbers – images are comprised of pixels (picture elements), and each pixel in an image has a digital value representing the brightness or intensity of that portion of the sample, at a specific moment in time. By operating on these values, either in isolation, or while considering nearby values, the information in the images can be cleaned of aberrant information, and data relevant to the imaged sample can be extracted and measured.

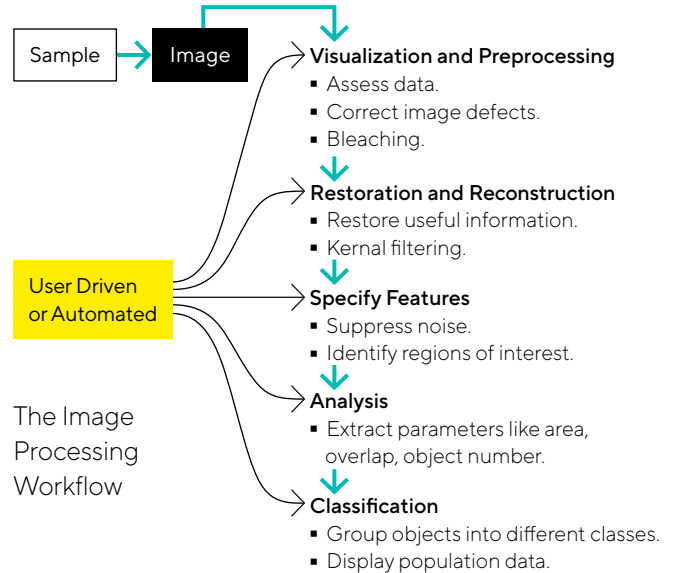


Figure 1. Image processing and analysis is accomplished using a number of techniques, guided by expert knowledge and software guidance. To ensure processing consistency across static and kinetic data, it is important to establish a set of image processing parameters which enable operation on all images in an identical manner. This contextually derived data processing workflow will seamlessly and automatically perform all of the necessary pre- and post- image processing steps, up to and including object analysis and graphical representation of the experimental result. Properly designed image analysis workflows are intended to require no human intervention and processes image archives, generating consistent and actionable results either in real-time, or post-acquisition.

Performing these steps on individual images to generate sufficient statistical power to support a hypothesis can be a tedious process. However, when operating on large numbers of images which have been collected in a substantially similar manner, the series of operations performed to clean up the data, extract desired information, and compare images may be recorded and automatically applied to many images in a single experiment. Once this data has been extracted, treatment groups may be compared to assess differences, and hypotheses evaluated. Scaling this to the analysis of live-cell experiments allows for the evaluation of temporal data, and extending this to microplate microscopy means that population data may be studied with ease. This basic workflow is the subject of countless tutorials and books, and the domain of numerous software packages that offer a cornucopia of tools intended to answer a broad range of scientific questions.

Image Processing to Remove Systematic or Sample-Induced Artifacts

The image data we have described above is typically captured by detectors that convert analog information, specifically photons, into digital signals. This analog information is collected in a matrix fashion, spatially rendered according to location in the sample. Ideally, the signal undergoing analog to digital conversion would come only from photons produced by the sample of interest, and in perfect focus. However, this is not the usual case. There are multiple sources of confounding signal present in an image, each needing correction, removal, or cleaning in order to reveal information which has been generated by the sample elements of interest. Corrections are needed due to systematic aberrations in an imaging system stemming from multiple sources. For example, detector anomalies (e.g. detector bias, dark current variability, field flatness and thermal or gamma-ray noise), optical issues (non-flat optical components and illumination imperfections) or undesired signal

introduced by the sample are common issues. Autofluorescence from cellular components or media, or non-biological signal sources (i.e. shading or patterns arising from sample matrices, micro-fluidic channels, or non-uniform illumination effects in microwells) must be removed before usable, replicable information can be extracted.

In order to perform these corrections, one must be aware of the effects of each process, and manipulations on the raw images must be repeatable to ensure faithful capture of the true biological signal across images. There are many tutorials and software toolkits available to process images, however systems that perform these corrections as a matter of course provide consistency and ease of use, particularly when coupled with standardized assays, reagents and consumables which normalize the experimental process (e.g. the Incucyte® Live-Cell Analysis System, and the assays and reagents available from Sartorius). The consistency with which images are acquired and processed will influence the ability to analyze the collected data.

Identifying Biology of Interest via Image Masking or “Segmentation”

Once an image has been appropriately processed to remove aberrant signal, the next step is to identify the biology of interest. Image segmentation is a binary process, meaning pixels are classified as either “in” and are included in any enumeration process, or “out” and not considered as part of the sample. The simplest method for determining which pixels are in or out is by thresholding, or setting a boundary above which all pixels are “in”, and below which, all pixels are “out”. More complex tools do exist, and more complex interactions can be performed with multiple masks, and Boolean operations (e.g., AND, OR, NOT) in order to hone in on the exact pixels of scientific interest. Again, this can be a time-consuming task, and purpose-built software that presents only the tools necessary for a specific scientific question can remove what can be a significant hurdle in the image analysis workflow.

Generating Actionable Data

After the pixels which satisfy all of the measurement criteria are identified in an image, it is possible to operate on this binary mask of pixels. The mask may be analyzed whole (for total area, or confluence measurements) or broken into multiple subparts, for example when defining or counting objects in the image. Depending upon the labeling of the sample, e.g. label-free or tagged with a specific marker such as a fluorescent reagent labeling a specific organelle or structure, a wide variety of statistics may be generated. In the case of fluorescent reagent-labeled images, these statistics may include the mean intensity value of all the pixels in the mask, the total additive intensity, the minimum, maximum, or standard deviation of the collective intensity, or the fluorescence mask may be used to count numbers of objects. Statistics may be global for the image as just described (e.g. total size of the mask, or mean intensity of the mask) or per object (e.g., area occupied by individual cells). Once again, the appropriate choice

of labels, image processing, and object identification can require deep technical expertise, as the number of options available to differentiate objects is very broad. For example, if you are looking for all red-labeled nuclei that are also labeled with a green reagent (for example, apoptotic cells labeled with Incucyte® Caspase 3/7 Green Dye, it is possible to identify individual cells first using a transmitted light image [mask 1], breaking that mask into objects representing cells using image processing tools like watershed split, and then classifying those objects/cells based on the included red and green mean intensity of the included nuclei. This task is more easily performed when the scientific question is well-defined, the appropriate tools are utilized, and the images processed automatically, and without bias.

Analyzing Image Data at Throughput

Now that a specific set of operations has been constructed to process and analyze a representative image, this same set of operations may be applied to all images in an experiment in exactly the same manner. If this set of operations inadequately processes the population of images included in an experiment, it may be necessary to make adjustments to the set of processing operations based upon the population of images collected for the task. In a live-cell imaging experiment performed in a 96-well plate, a data set containing thousands of images is perfectly reasonable. Many data sets will be considerably larger when capturing multiple channels, e.g. red fluorescence/green fluorescence/transmitted light, so

variability between images in different treatment groups and at different time points should be expected. In analyzing a large image set, one must be assured that the set of operations is suitable across the data set (e.g., on dead or living cells). Traditional image analysis software does not offer the ability to assess a variety of images in an efficient manner, and thus typical live-cell microplate assays can be unwieldy, at best. Software must address the needs of the researcher by performing all the steps required to convert images to data at the scale of long-term time-lapse experiments, and at the rate of acquisition, in order to best understand biological processes while they are happening.

Chapter 3

Cell Culture Quality Control Assays

Real-Time Monitoring and Analysis of Cell Culture Conditions

The ultimate goal of *in vitro* cell culture is for the downstream analysis of cells for the characterization of their biological changes for deeper understanding as well as the development of novel therapeutics. However, the importance of careful analysis of cells during culture maintenance is often overlooked. With the advancement of cell models occurring rapidly and the promise of personalized medicine, the ability to monitor cells at every step of the cell culture workflow is necessary, as the quality of basic cell culture maintenance ultimately affects the quality of the subsequent data.

Many sources of cell culture variability are largely uncontrollable because they are inherent to the stochastic processes in biological systems. However, a large number of controllable environmental variables exist that can alter the growth and function of cells in culture. Some key controllable factors include:

- Poor CO₂ incubator performance due to lack of calibration and stability of temperature, humidity and CO₂ over time.
- Non-quantitative and/or inconsistent procedures for feeding and splitting cell cultures prior to running cell-based assays including inconsistent limits of cell density and feeding schedules, inconsistent cell density at the time of assay and changes to cell morphology.
- Alterations in media components due to lot-to-lot differences and alteration of concentrations over time due to degradation.
- Differences in cell culture growth surfaces such as variability among suppliers, vessel surface treatments and lot-to-lot variability.
- Biological issues resulting from growing cells in continuous culture for extended periods of time which in turn increases the risk of phenotypic drift,

contamination by infectious agents and cross contamination with other cell types.

Each of these controllable variables can adversely affect the results of data obtained from downstream analyses, leading to misinterpreted data, a waste of valuable resources and time, and ultimately delaying insight and the development of innovative therapies. A key element in controlling adverse variables is to standardize workflow and metrics, thereby eliminating human subjectivity and interpretation. Advantages of performing quality control of cell cultures via continuous monitoring The Incucyte® Live-Cell Analysis System provides a label-free, non-invasive method for monitoring cells directly in the incubator, for both cultures grown in two- and three-dimensional planes. In sharp contrast to manual monitoring of cell culture processes, quality control monitoring with real-time live cell analysis automates data capture and cell assessment (Figure 1). Cells can be

monitored around-the-clock and at precise, regularly scheduled sampling intervals. In addition to supporting decisions for current culture processes, historical information can be retrieved months or years later for comparison of cell lines and culture growth characteristics. Of significant importance, as cell models move to patient specific

samples and complex organoids, is the ability to monitor these cultures while they are maintained in a physiologically relevant environment. Combining unbiased analysis within a stable environment facilitates downstream assay reproducibility, through automated analysis of cells as they grow in culture.

Live-Cell Imaging and Analysis Approaches for Quality Control Assays

The Incucyte® Live-Cell Analysis System is compatible with multiple different types of cell culture vessels and can monitor multiple vessels and cell models at a time. Data

Manual Cell Culture Monitoring

Initial cell measurements—**subjective.**

Assessments made at random locations with variable frequencies— qualitative and operator dependent.

Cell utilization decisions including timing—**subjective.**

Initiate Culture

Monitor Growth

Utilize Cells

Time



Initial cell measurements—made for every well.

Assessments made at precise locations with scheduled sampling intervals—objective morphological and growth analysis support decisions.

Passage, treatment, harvest or assay imitation decisions based on data-driven, quantitative measurements.

Live-Cell Analysis

Figure 1. Comparison of cell culture monitoring methods. Vertical arrows represent interaction points with the cell culture using manual methods and real-time live-cell analysis. Subjective decisions made during manual monitoring result in variability for cell-based assays.

consists of objective, image-based growth metrics to capture transient and time-dependent events. Purpose built software is employed to identify cells, in both 2D and 3D cultures to accurately identify morphology and proliferation over time. Building on our knowledge of image acquisition and analysis, innovative image strategies were employed to accurately identify and quantify 3D organoids using the Incucyte® Organoid Analysis Software Module. Incucyte® Live-Cell Quality Control Assays allows for automatic analysis to enable real time decisions on culture status.

How Live-Cell Quality Control Assays Work

Cell Culture Quality Control (2D)

The Incucyte® Live-Cell Analysis System provides a label-free, non-invasive approach to long term monitoring of cell morphology and growth without removing cells from the incubator. Integrated analysis software provides phase segmentation metrics that track cell

growth over time using cell confluence curves. Using these basic confluence metrics or the more advanced Incucyte® Cell-by-Cell Analysis Software Module to individually identify label-free cells, non-adherent or adherent cultures can be accurately evaluated for changes in proliferation and morphology.

Organoid Quality Control

To monitor and make informed decisions about organoid culture status, the Incucyte® Organoid Analysis Software Module automatically locates and analyzes organoids within Matrigel® domes. The software uses image-based, kinetic analysis of count, size and morphology to enable informed decision on culture status to identify optimal culture conditions. Of critical importance is the ability to quantify and visualize the differentiation and maturation of organoids in 24- or 48-well plates, all while keeping these sensitive organoids within the stable environment of a tissue culture incubator.

3a

2D Cell Culture Quality Control

Introduction

In order to establish quality cell cultures and improve experimental outcomes in downstream assays, various aspects of cell culture need to be tightly controlled, optimized and documented.

- **Growth Conditions**

Prior to utilizing cells in quantitative assays, it is important to optimize and define cell culture regimens. Documenting variations in cell growth due to factors such as; lot-to-lot differences in cell culture media, changes in media component concentrations over time due to degradation, and inconsistent feeding schedules can all be identified using label-free phase image segmentation techniques that generate confluence measurements.

- **Documentation of Cell Morphology**

Changes in cell morphology due to cell seeding density or phenotypic drift can be identified using a range of magnifications to capture fine details of cells and spatial coverage of cell populations.

- **Accurate Assessment of Overall Monolayer**

By imaging multiple areas of your vessel or using a whole-well imaging mode, spatial variations in cell distribution can be quantified and then reduced.

- **Cell Seeding Densities**

To improve assay quality and consistency of kinetic assays, it is important to minimize variations in cell seeding densities due to pipetting errors during plate seeding which result in differential growth rates. Measuring confluence before utilizing assay plates eliminates assay variation, resulting in reproducible conditions.

- **Documenting Time-Dependent Variables**

Assessment of cell behavior and growth in association with cell treatment times can define experimental conditions to ensure consistent results.

With the Incucyte® Cell Culture Quality Control Assay, routine cell culture methods can be observed and monitored in a non-invasive, quantitative way that will lead improve the quality and consistency of cell based assays.

Incucyte® 2D Cell Culture Quality Control Assays at a Glance

The Incucyte® Live-Cell Analysis System and 2D Cell Culture QC Assay provide a label-free, non-invasive method in which researchers can optimize and define cell culture regimes. Conducted completely within the tissue culture incubator, HD phase contrast images are collected from the culture vessel of choice, such as microtiter plates, tissue culture flasks, and dishes, in order to visualize and quantify cell proliferation in various culture conditions. Multiple areas of the vessel can be imaged, or whole-well imaging can be used to highlight spatial variations and optimize cell distribution using quantitative metrics. With fully integrated software algorithms, label-free phase segmentation metrics track cell growth over time using cell confluence curves or direct label-free cell counts using the Incucyte® Cell-by-Cell Analysis Software Module. With the 2D Cell Culture QC Assay, cell-type specific culture conditions and growth characteristics can be defined.

Shortcomings of Traditional Assays	Live-Cell Imaging and Analysis Approaches
<ul style="list-style-type: none">▪ Lack of environmental control and physical movement of plate during analysis.	<ul style="list-style-type: none">▪ Uninterrupted environmental control provided by a tissue culture incubator, coupled with a label-free and automated image acquisition without needing to disturb cell.
<ul style="list-style-type: none">▪ Data obtained from a concatenated single time point yields minimal dynamic insight and causes variability in assay results.	<ul style="list-style-type: none">▪ Cells are measured continuously over time via repeated interrogation of the same well, providing insight into how conditions such as cell seeding artifacts impact cell growth.
<ul style="list-style-type: none">▪ Indirect detection methods are subject to artifacts that cannot be readily verified by eye.	<ul style="list-style-type: none">▪ True, direct measurements of cell confluence are generated non-invasively and visually verified via image and movies.

Table 1. Shortcomings of Traditional Assays vs Live-Cell Imaging and Analysis Approaches.

Cell Culture QC Assays

Measuring Proliferation to Optimize Growth Conditions and Seeding Densities

The Incucyte® Live-Cell Analysis System can be used to track cell proliferation over time from various regions within a tissue culture flask or plate, as shown in Figure 1. Integrated software provides label-free phase segmentation (confluence) metrics (Figure 2), allowing for the assessment of cell growth as well as monitoring cell culture and assay optimization.

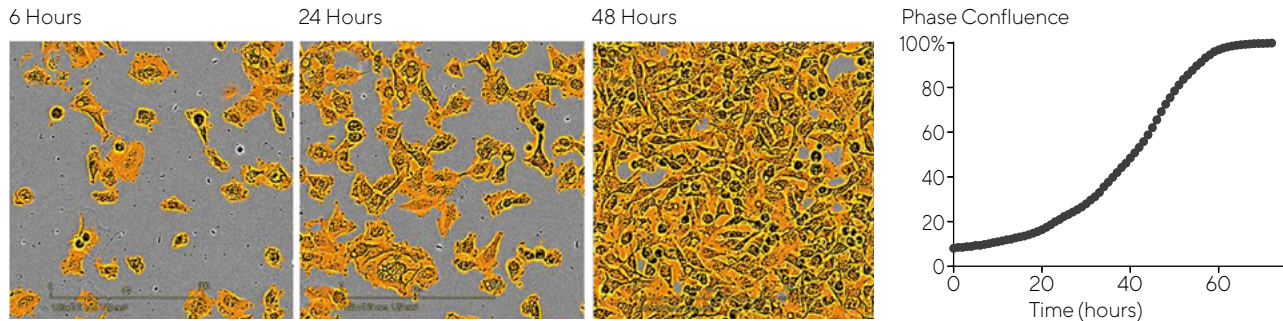
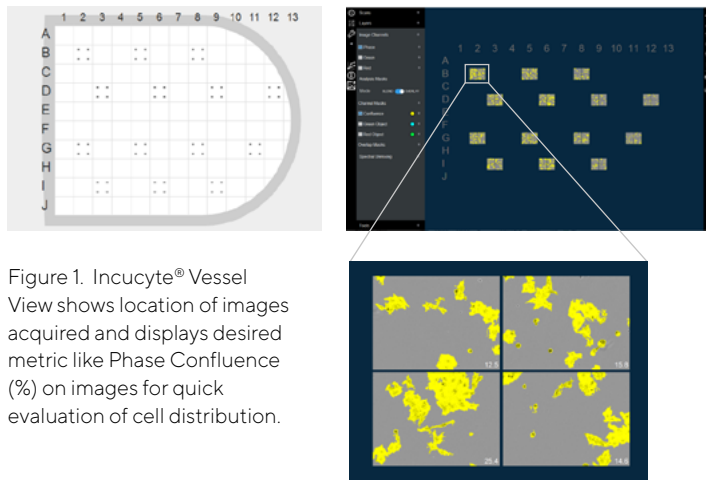


Figure 2. HD phase contrast images of HT-1080 human fibrosarcoma cells (confluence mask overlaid) with proliferation time-course.

In a study to assess different culture conditions (Figure 3), HUVEC cells were cultured in basal cell media supplemented with decreasing concentrations of fetal bovine serum (FBS). Additionally, HT-1080 cells were seeded at initial seeding densities ranging from 5000-30000 cells/well. Using Incucyte® integrated analysis software, images were automatically acquired and analyzed over time. In the HUVEC cells, a concentration dependent

effect on proliferation was found based on confluence curves. Additionally, HT-1080 cells exhibited different growth curves dependent on the initial seeding density. Gaining a better understanding of these culture conditions can help to optimize and define cell culture protocols.

Live-cell analysis can be used to accurately mask different morphologies and quantify label-free proliferation over time, as shown

in Figure 4. In 4A and 4B, the variation in cell seeding density-dependent proliferation in two different cell lines, A172 human glioblastoma and LNCap human prostate carcinoma, is exemplified. Understanding cell seeding variation and its effects on proliferation is important for controlling assay variability. As shown in 4C, images reveal accurate segmentation of cell types irrespective of morphology.

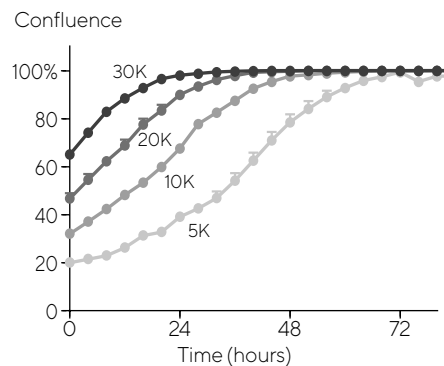
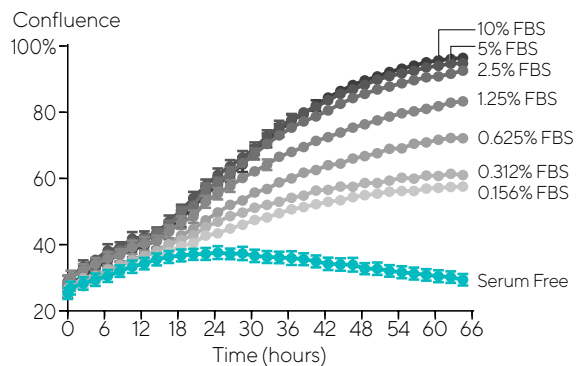
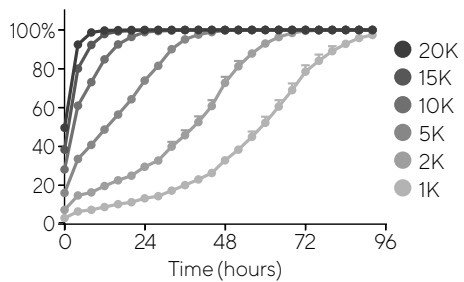
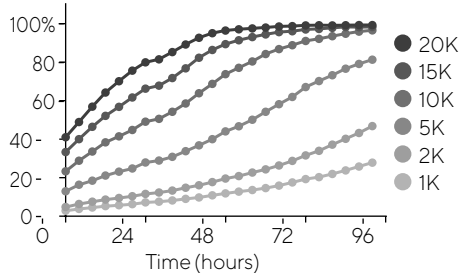


Figure 3. Human umbilical vein endothelial cells (HUVECs) cultured in basal cell media containing growth factors and supplemented with decreasing amounts of FBS. The optimal concentration of FBS for normal propagation was determined to be >2.5%. Different initial seeding densities were also tested and shown to have an effect on HT-1080 growth curves.

A Confluence**B** Confluence**C** A549 (6 hours)

HT-1080 (24 hours)

LNCap (72 hours)

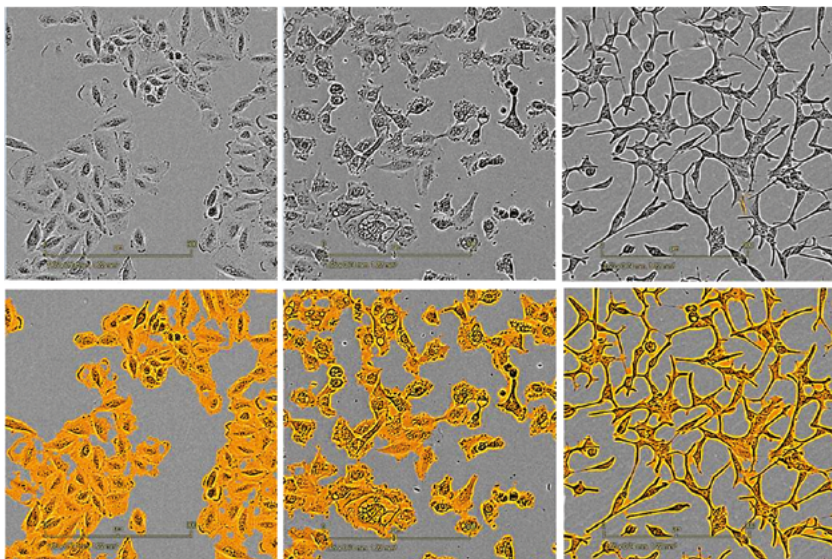


Figure 4. Quantification of A549 (A) and MCF-7 (B) growth curves using label-free confluence analysis. HD phase contrast images (C) of A549 human lung carcinoma, HT-1080 human fibrosarcoma and LNCap cells shown without and with confluence mask (orange). Images reveal accurate confluence masking of all three cell types of varied morphology.

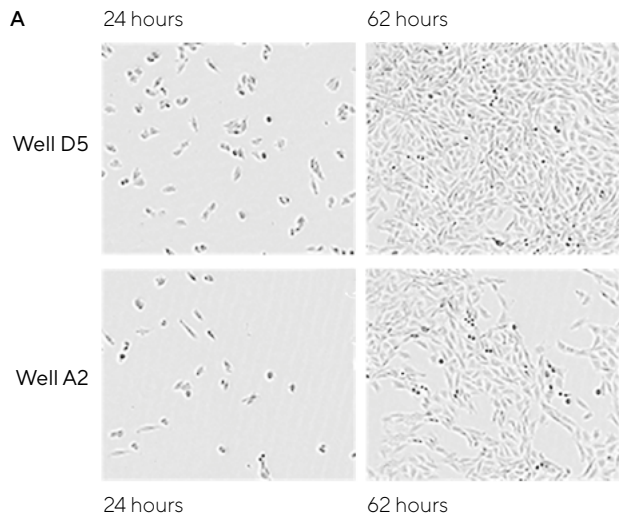
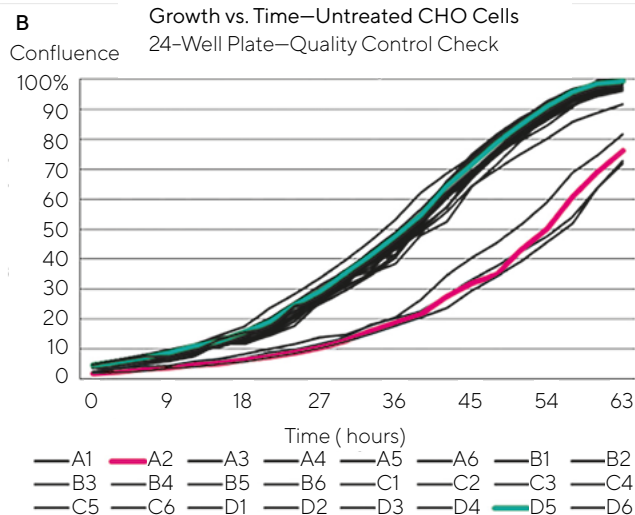


Figure 5. Images (A) and data (B) illustrating the effect of pipetting errors on growth. Wells were seeded at the same cell density and then checked prior to an endpoint assay for growth. Initial confluence for four wells were found to be ~50% that of the median initial confluence for the plate, a variable likely caused by pipetting errors.



Conclusions

With real-time live-cell analysis, it is possible to follow and quantify cell growth over time, effectively revealing both transient and time-dependent phenomena. This type of analysis is a powerful tool for cell culture quality control, providing a quantitative, objective, non-invasive and kinetic method of analyzing living cells, unperturbed in the incubator. Use of the Incucyte® Live-Cell Analysis System to document and monitor routine cell culture can improve cell-based assay quality and consistency.

3b

Organoid Culture Quality Control

Kinetic Analysis of Organoid Culture Status Within Matrigel® Domes


Introduction

In vitro 3D cultures have opened up new horizons for translational human disease research, disease modelling, regenerative medicine and predictive precision therapies. Significant progress has been made towards translational cell models and today, differentiated organ cell types can be generated *in vitro* from a variety of stem cells (SCs) to mimic complex tissues while retaining genomic stability and response to drug treatments. Conventional, two-dimensional cell cultures have been a fundamental tool for finding new medicines for decades. However, they have limited ability to generate the information needed to develop more complex 3D advanced cell models, study tumor microenvironment and determine when these cultures become functionally matured, used for further downstream assays. As such, organoids, which consist

of 3D collections of cells that resemble an organ or human tissues *in vivo*, have emerged as the ideal model. Advances in making and monitoring organoids have improved drug discovery workflow and disease modelling, leading to increased productivity and faster discovery of new treatments. In using *in vitro* organoid and spheroid culture methods, researchers are making the shift to more translational work that provides greater physiological relevance allowing for deeper insight into the characterization of patient-specific primary tissue and a better understanding of the biological pathways of pathological diseases. Organoids and spheroids, a less-complex but still 3D collection of cells, provide new opportunities in different therapeutic areas and may eliminate the need for longer term of animal studies.

Organoids have a distinct advantage over traditional 2D cultures and hold

unprecedented potential for various, innovative applications. However, in order to exploit these models for meaningful basic research, disease modelling and drug screening, specific and reliable culture and analysis methods are required. Currently, characterization and optimization of organoid cultures are limited in their ability to reproducibly form and monitor these 3D structures as they form and grow overtime. Traditional organoid culture techniques involve light microscopy, High Content Screening (HSC) or cytometers. However, these tools are limited in that they lack validated protocols for reproducible well-to-well organoid formation, are low throughput, involve manual, time-consuming image acquisition, and require the use of a third party software for analysis. Due to limited quantitative information and loss of environmental of control during acquisition of organoid images, a lot of variability can be observed throughout the assay.



In this chapter, we discuss how the Incucyte® Organoid Culture Quality Control (QC) Assay alleviates many of these challenges by providing a turnkey solution consisting of a validated protocol and software module for automated real-time visualization and label-free quantification to optimize organoid culture conditions. Along with the Incucyte® Live-Cell Analysis System and the Incucyte® Organoid Analysis Software Module, researchers are able to make informed decisions about organoid culture status and open a new world of analysis of advanced cell models.

Incucyte® Organoid Culture QC Assay at a Glance

To evaluate long-term organoid growth and formation Incucyte® Live-Cell Imaging and Analysis employs an end-to-end solution consisting of instrumentation and software utilized in a physiologically relevant environment. The Incucyte® Organoid Culture QC Assay can be used with a variety of tissue types to reliably culture and monitor their differentiation using label-free analysis of organoids in real time.

The Incucyte® Live-Cell Analysis System and Incucyte® Organoid Analysis Software Module captures these long-term growth,

morphological changes via continuous images or movie acquisition in every well of a 24- or 48-well microtiter plate. Acquired brightfield (BF) images are then analyzed to quantify the label-free growth, size, count or morphology over the course of the experiment, enabling continuous characterization of developing multiple cell lineages as they become functional and mature. This approach provides researchers the opportunity to continuously analyze the same population of organoids long-term from days to weeks to months, in order to gain insight into how and when organoids become mature and how their morphology changes over time.

Shortcomings of Traditional Assays	Live-Cell Imaging and Analysis Approaches
<ul style="list-style-type: none">▪ Data obtained from at a single point in time yields minimal insight as organoids develop and mature.	<ul style="list-style-type: none">▪ Long-term, kinetic evaluation shows morphological changes in organoid differentiation to determine optimal maturation and differentiation over time.
<ul style="list-style-type: none">▪ Measurement of growth and morphology from a limited number of organoids or by using concatenated single time point causes variability in assay results.	<ul style="list-style-type: none">▪ Tissue-derived organoids are automatically located and measured with high accuracy via continuous interrogation in the same Matrigel® dome over days, weeks, or month.
<ul style="list-style-type: none">▪ Non-validated, multiple protocols for organoid formation and growth with subjective analysis for passaging organoids.	<ul style="list-style-type: none">▪ Optimized protocol for standardized and reproducible organoid formation allows for optimization of organoid passaging or extension of cultures.
<ul style="list-style-type: none">▪ Complex instrumentation and image processing requires expert operation, 3rd parties software and training for data generation and analysis.	<ul style="list-style-type: none">▪ Automated acquisition of organoids with integrated, purpose-built software tools maximizes productivity.
<ul style="list-style-type: none">▪ Lack of environmental control and physical movement of plate during analysis disturbs sensitive stem cells, organoid structures and the biology of interest.	<ul style="list-style-type: none">▪ Uninterrupted environmental control provided by a tissue culture incubator, coupled with a label-free and automated image acquisition without physical movement of sample, protects sensitive stem cells and maintains integrity of data.

Table 1. Shortcomings of Traditional Assays vs Live-Cell Imaging and Analysis Approaches.

Sample Results

Automatic Evaluation of Tissue-Derived Organoids Using Image-Based, Kinetics Analysis

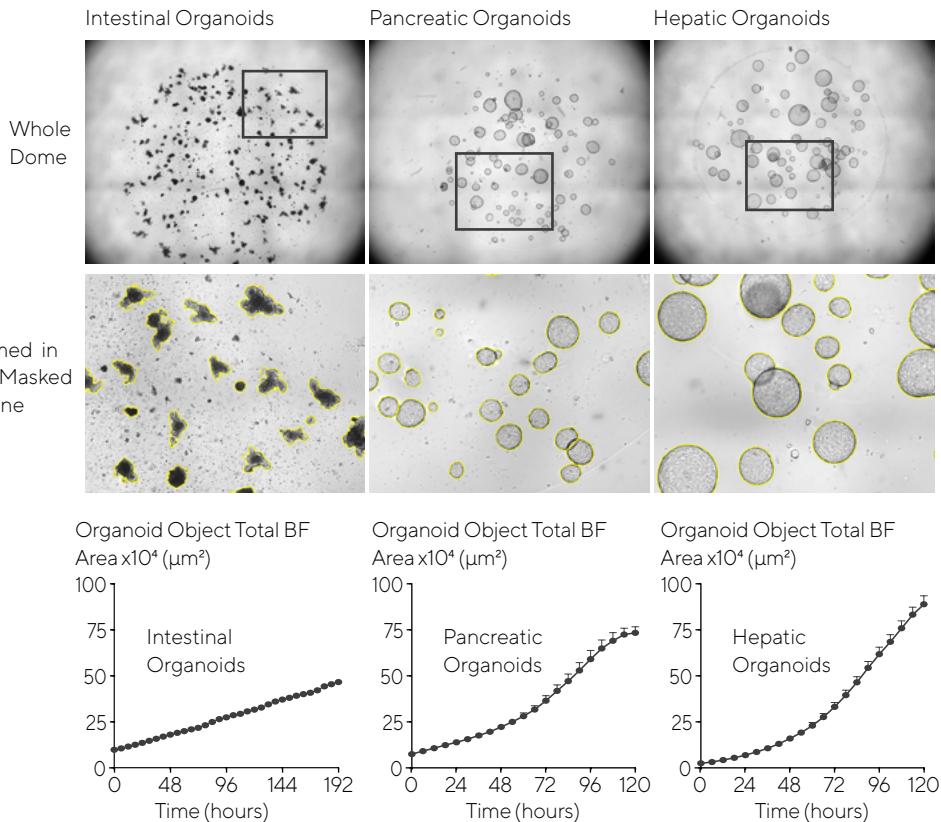
The Incucyte® Organoid Culture QC Assay offers a reliable approach for continuous visualization and label-free analysis of organoids in real time. Unlike other assays, we offer a turnkey solution using an established protocol for embedding organoids in Matrigel® domes and purpose-built software to image and analyze organoid growth, size, count and morphology in physiologically relevant conditions using repeated imaging and location of dome structures over time. In this experiment, three different types of organoids were evaluated over 6-8 days in culture to profile their growth and morphological changes (Figure 1). These included mouse intestinal organoids, mouse pancreatic organoids, and mouse hepatic organoids. Organoids were embedded in Matrigel® (10-50 µl and 50 or 100% Matrigel®) domes in 24- or 48-

well plates and imaged on an Incucyte® Live-Cell Analysis System. Using the Incucyte® Organoid Analysis Software Module, distinct organoid morphological changes were captured and quantified as shown. BF images of the whole dome were acquired using a 4X objective and are shown in the top row, while the bottom row shows zoomed in images of the same population of cells displaying the different organoid morphology and darkness correlating with organoid types.

Time-course profiles of BF area show cell-type specific organoid differentiation, morphology and growth respectively as indicated on representative graphs. The images also provide researchers with a qualitative assessment of morphology, size and count of organoids within whole domes over days and offer a great method to reproducibly form and accurately study organoid differentiation for pre-clinical downstream development. Scientists can understand the organoid forming capacity of stem cells to develop a quality

control standard protocol over time. Using the Incucyte® Organoid Culture QC established protocol and Incucyte® integrated analysis tools, we can define an optimal period for passaging or extension of cultures and visualize changes of morphology to exemplify differences in organoid culture.

Figure 1. Kinetically monitor and quantify organoid differentiation and growth in Matrigel® domes. Mouse intestinal (1:3 split, 50% Matrigel®), pancreatic (1:5 split, 100% Matrigel®) and hepatic organoids (1:40 split, 100% Matrigel®) were embedded in Matrigel® domes in 24-well plates. Brightfield (BF) images of the entire Matrigel® dome (top) show organoid maturation 6 days post seeding. Note accurate segmentation (yellow outline mask) and distinct phenotypes of mature organoids (bottom). Time-course plots showing the individual well total BF area (μm^2) over time (h) demonstrate cell type specific organoid growth. All images captured at 4x magnification. Each data point represents mean \pm SEM, $n = 4$ wells.



Monitor Organoid Formation Using Real-Time Kinetic Measurements

A key value of Incucyte® Live-Cell Imaging and Analysis is the ability to automatically analyze organoid growth and count of the entire Matrigel® dome over weeks or months to optimize culture conditions using the Incucyte® Organoid Analysis Software Module. This approach generates real-time kinetic measurements from multiple time-points and provides deeper biological insight by characterizing organoid forming

efficiency and comparing morphology from healthy and diseased tissues.

In Figure 2, mouse hepatic organoids were embedded in 10 μ l Matrigel® domes (100%) in 48-well plates at multiple seeding densities (1:10, 1:20 and 1:40 split). Optimizing the cell seeding density is critical and strongly recommended based on type of organoid to generate long-term viable organoid cultures and distinguish suitable conditions for maximal

culture expansion. Using BF images (5 d post seeding) and kinetic quantification of organoid count and area, we observed that organoid size and growth rate is directly proportional to cell number. Automated image processing identifies individual organoids in dome (yellow outline segmentation mask) and provides fully integrated kinetic analysis. Organoid growth was quantified by multiple label-free metrics, such as Organoid Total Area or Organoid Count.

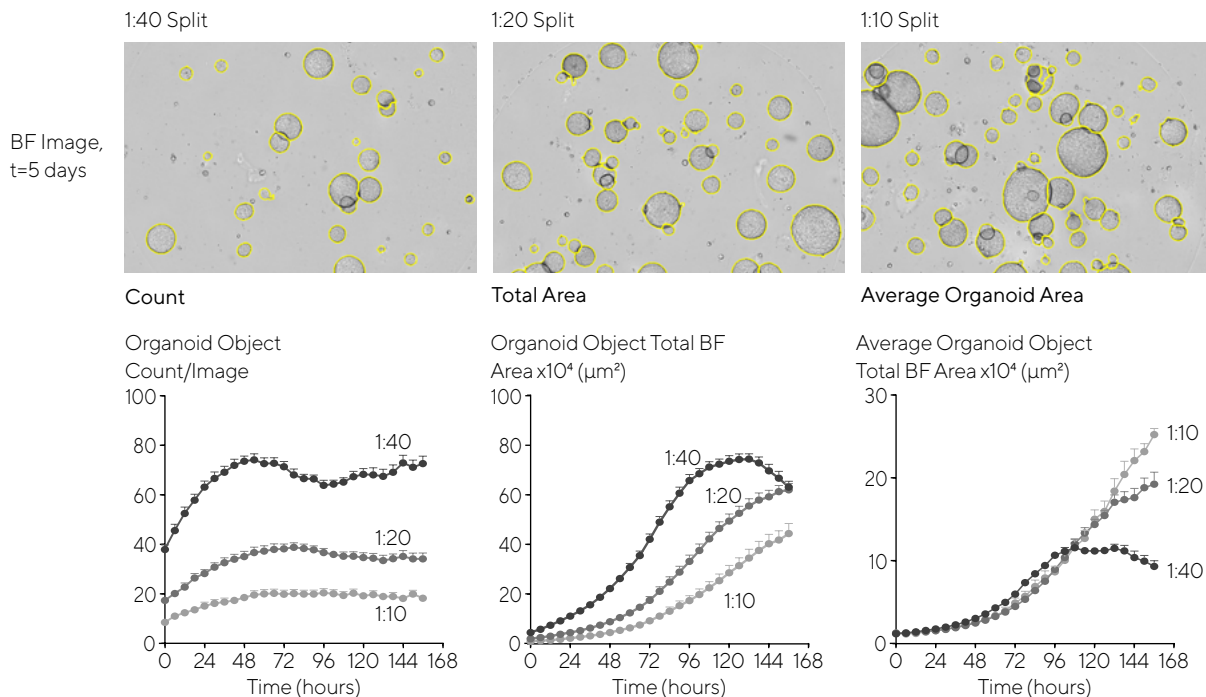


Figure 2. Determine optimal conditions for maximal organoid expansion using BF size measurements. Mouse hepatic organoids were embedded in Matrigel® domes (100%) in 48-well plates at multiple seeding densities. Images (5 d post seeding) and time-course data demonstrate that organoid size and growth rate is directly proportional to cell number.

Identify Maturation Phase of Organoid Cultures

Quantitative measurements of intestinal organoids could help scientists to define cell-type specific passing frequency and provide insight into the optimal period for passing or extending cultures using integrated morphology metrics. Intestinal organoid passing frequency is driven by indicators of maturation such as budding

and accumulation of debris within the lumen. Kinetically quantify these indicators using Incucyte® metrics such as Eccentricity for budding or Darkness for debris accumulation. These metrics can be used to define an optimal period for passing, e.g. when the majority of organoids have budded and a darkened lumen. Figure 3 shows how Eccentricity and Darkness were used to study the potential maturation

phase of mouse intestinal organoids using Incucyte® Organoid Analysis Software Module with integrated morphology metrics. Intestinal organoids exhibit a more irregular morphology and typically accumulate debris within the lumen over time, as seen in images and quantified by an increase in eccentricity and darkness.

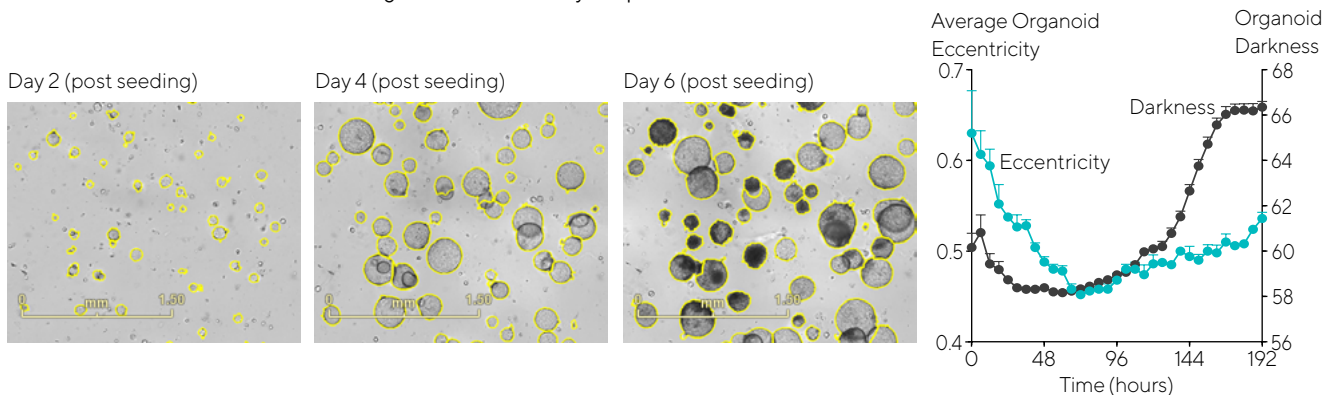


Figure 3. Define cell-type specific passing frequency using integrated morphology metrics. Mouse intestinal organoids were embedded in Matrigel® (50 µl and 50% Matrigel®) domes in 24-well plate using 1:3 split and imaged on an Incucyte® Live-Cell Analysis System. BF images captured distinct organoid morphology and changes in eccentricity or darkness were analyzed using the Incucyte® Organoid Analysis Software Module. Time-course data demonstrated that Organoid Eccentricity and Darkness increased over 10 days.

Track Organoid Differentiation and Growth Efficiency Through Passages

Under routine culture conditions, the growth capabilities and morphology of organoids are expected to remain consistent across multiple passages. In order to examine this, intestinal organoids were embedded in 50% Matrigel(%) domes for multiple passages (Figure 4). Measurements of Organoid Count, Area, Eccentricity and Darkness were used to evaluate organoid expansion and growth efficiency. When intestinal organoids were maintained at a consistent density across passages, they exhibited similar count, area, eccentricity and darkness measurements. Representative BF images from Passage 2, Passage 4, and Passage 6 also showed that a distinct budding phenotype was maintained across passages, further solidifying the amenability of this imaging and analysis approach to support robust and reproducible assessment of long-term organoid expansion.

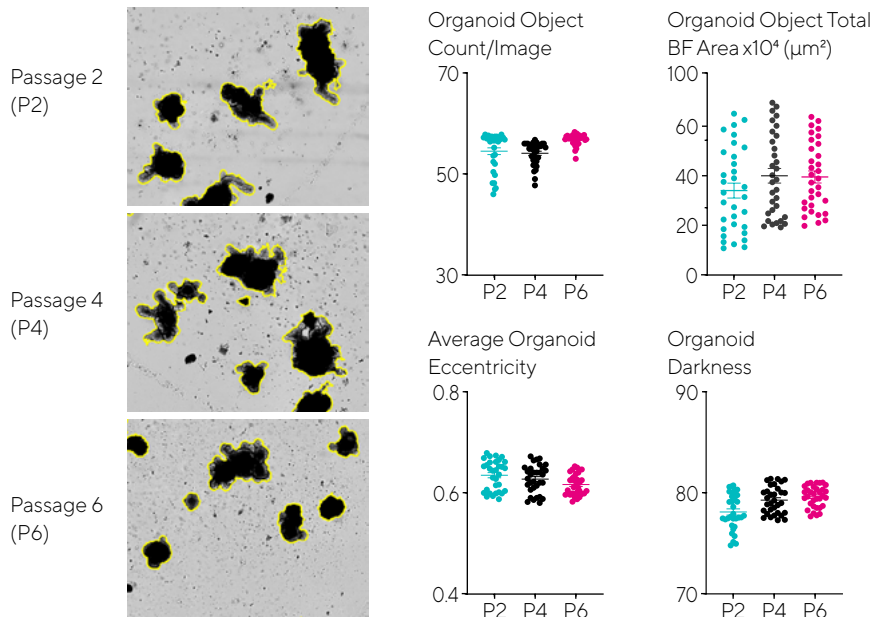


Figure 4. Assess growth and differentiation efficiency of organoids across multiple passages. Intestinal organoids were embedded in 50% Matrigel® domes (1:3 split, 24-well plate) over multiple passages and evaluated for growth and differentiation consistency over time. BF images (7 days post seeding) and corresponding plots show comparable morphology and growth across passages. Data were collected over 192 h at 6 h intervals. All images captured at 4x magnification. Each data point represents mean ± SEM, n=6 wells.

Conclusions

The Incucyte® Organoid Culture QC Assay, consisting of instrumentation, software, and protocol, provides access to complex, fully automated acquisition identification, and analysis of organoid culture progression throughout the entire Matrigel® dome. This assay achieves long-term evaluation in a variety of organoids to evaluate when they become mature and how their differentiation stage changes over time without removing cells from the physiologically relevant environment of a tissue culture incubator. Overall, live-cell analysis provides a valuable complement to established techniques, such as microscopy or HCS, for building and validating translational cell models for the discovery of novel advanced cell therapeutics.

- A non-invasive imaged-based approach allows quantitative monitoring of organoid maturation and multiple cell lineages develop; the need to select an arbitrary point in time to perform a single measurement or manually acquire and analyze images is alleviated.
- The Incucyte® Organoid Culture QC Assay offers a reliable, turnkey solution using an established Incucyte® Organoid Culture QC protocol for embedding organoids in Matrigel® domes and purpose-built software to image and analyze organoid size, count, and morphology using repeated imaging and location of dome structures over days, weeks or months.
- Easily make data-driven decision about organoid cultures and characterize their formation kinetically. Obtain continuous, label-free data to optimize culture conditions (for example media, growth factors), passaging frequency using the Incucyte® Organoid Analysis Software Module.
- Additional insights can be obtained when measurements of organoid differentiation stages and morphology are combined using Eccentricity to track degree of budding and Darkness to track lumen debris accumulation.
- Automated image acquisition and analysis tools provide a 'set up and walk away' experience. Visualize organoid differentiation and growth in 24-well or 48-well plates remotely to monitor experimental progress, increase productivity by scanning 6 microplates parallel and analyze them in real time.

Chapter 4

Kinetic Cell Health, Proliferation and Viability Assays

Real-Time Automated Measurements of Cell Health, Proliferation and Viability

Measurements of cell health are essential for studying the effects of drugs, culture conditions or genetic modifications on cell growth or viability. Such studies are used to rank compounds in drug discovery screens, identifying off-target toxic compounds, as well as to investigate the cellular changes that underlie disease pathologies.¹ In order to assess cell health and viability, a variety of end-point assays have been employed, such as ATP assays, LDH assays and vital dyes used in flow cytometry, but all fail to take into account the kinetics or have the capability to make simultaneous measurements in a single well. Understanding the biological time-dependence, along with the ability to evaluate multiple methods by which a cell dies, offers considerable advantages in the characterization of test compounds.²

Incucyte® Cell Health, Proliferation and Viability Assays allow for the kinetic evaluation of effective compound concentration and the time needed for the

compound to perturb the target, thereby discriminating if the test agent is fast acting or prolonged. Another advantage is the ability to perform multi-parametric analysis using non-perturbing reagents within a single well, enabling detection of the mechanism of cell death (e.g., apoptotic, cytotoxic, or mitotoxic) as well as monitoring cell viability utilizing reagents that label cell nuclei. These image-based detection methods can all be qualitatively validated with images to evaluate morphological changes associated with cell death.

Furthermore, these advantages of live-cell analysis are also ideally suited to meet the needs of more dynamic cellular models, such as co-culture immune cell killing assays, which require robust temporal and spatial quantitative measurements in physiologically-relevant conditions. Continuous live-cell imaging makes it possible to measure and visually validate the complex and dynamic interactions between

target and effector cells in co-culture for the reliable analysis of new potential immunotherapies.

Live-Cell Imaging and Analysis Approaches

The Incucyte® Cell Health, Proliferation and Viability Assays enable the detection and analysis of cell proliferation, viability, apoptosis, and cytotoxicity. Images of cell cultures in 96- or 384-well formats are automatically acquired and analyzed to generate time courses and reveal concentration-dependent responses that can be used to calculate EC₅₀ or IC₅₀ values.

How Live-Cell Health, Proliferation and Viability Assays Work

Proliferation and Viability Assays

Measure growth or growth inhibition in real time over several cell divisions using

label-free cell counts or confluence measurements in both adherent and non-adherent cell types. Additional assay strategies can be used to generate measurements of cell type-specific growth rates in co-cultures, including use of Incucyte® NuLight Reagents to fluorescently label nuclei and determine true counts of viable cells.

Cell Cycle Assays

To quantify cell cycle state, Incucyte® Cell Cycle Lentivirus Reagents are used to efficiently and homogeneously label living cells. The Cell Cycle Lentivirus Reagents are single-cassette, genetically encoded ubiquitination-based indicators that take advantage of cell cycle dependent changes in the expression patterns of Geminin and Cdt1. By linking fluorescent proteins TagGFP2 and mKate2 (green/red), or TagGFP2 and TagRFP (green/orange) to fragments of Geminin and Cdt1, the G1 and S/G2/M phases can be monitored in real time. Integrating these reagents with Incucyte® Live-Cell Imaging and Analysis enables the quantification of cell cycle progression over multiple cell divisions in the same population of cells.

Apoptosis Assays

Detect apoptosis in living cells and in real time using mix-and-read reagents that measure caspase-3/7 activity or phosphatidyl serine externalization.

Incucyte® Caspase-3/7 Dyes couple the activated caspase-3/7 recognition motif (DEVD) to a DNA intercalating dye and are ideally suited to the mix-and-read, real-time quantification of cells undergoing caspase-3/7 mediated apoptosis. When added to tissue culture medium, the inert, nonfluorescent substrate crosses the cell membrane where it is cleaved by activated Caspase-3/7 resulting in the release of the DNA dye and fluorescent staining of the nuclear DNA.

The Incucyte® Annexin V Dyes are specially formulated, highly-selective cyanine-based fluorescent dyes ideally suited to a simple mix-and-read, real-time quantification of apoptosis. Once cells become apoptotic, plasma membrane phosphatidylserine (PS) asymmetry is lost leading to exposure of PS to the extracellular surface and binding of the Incucyte® Annexin V Dye, yielding a bright and photostable fluorescent signal.

With the Incucyte® integrated analysis software, fluorescent objects can be quantified and background fluorescence minimized, to identify apoptosis as it occurs in real time.

Cytotoxicity Assays

Measure cell death upon loss of plasma membrane integrity over time using Incucyte® Cytotox Dyes. These reagents are inert, non-fluorescent and do not enter viable cells. As cells die and membrane integrity is lost, the Cytotox Dye enters the cell and fluorescently labels the nuclei. Dying cells are identified and quantified over time by the appearance of fluorescently labelled nuclei.

ATP Assay

For direct analysis of ATP, an end-to-end solution constituting hardware, reagent and software is employed. Transfection of live cells with the Incucyte® CytoATP Lentivirus Reagent Kit enables *in vitro* analysis of dynamic changes in cytoplasmic ATP. Integrated hardware and software capture, acquire and analyze dynamic changes in ATP binding independent of cell number.

References

1. Kepp, O., Galluzzi, L., Lipinski, M., Uan, J. and Kroemer, G. **Cell death assays for drug discovery.** *Nature Reviews* 2011 10:221.
2. Abassi, Y.A., Xi, B., Zhang, W., Ye, P., Kirstein, S.L., Gaylord, M.R., Feinstein, S.C., Wang, X. and Xu, X. **Kinetic Cell-Based Morphological Screening: Prediction of Mechanism of Compound Action and Off-target Effects.** *Chemistry & Biology* 2009 16:712.

Incucyte® User Publications

Balvers, *et al.*, investigated the therapeutic benefit of combination therapy in patient-derived glioma stem-like cells (GSC). The current standard of care for Glioblastoma Multiforme consists of radiation along with temozolomide (TMZ) chemotherapy. A possible strategy to increase the efficacy of TMZ is through interference with the DNA damage repair machinery, by poly(ADP-ribose) polymerase protein inhibition (PARPi). Proliferation assays consisted of longitudinal imaging of cell confluency in the Incucyte® Live-Cell Analysis System. Phase contrast images were acquired at 1-3hr intervals and confluence per well was calculated.

1. **ABT-888 enhances cytotoxic effects of temozolomide independent of MGMT status in serum free cultured glioma cells.** Balvers, R. K., Lamfers, M., Kloezeman, J. J., Kleijn, A., Berghauser Pont, L., Dirven, C. and Leenstra, S. *Journal of Translational Medicine* 2015 13:74.

Ong, *et al.*, evaluated PAK1 dysregulation (copy number gain, mRNA and protein expression) in breast cancer tissues. A novel small molecule inhibitor, FRAXIO36, and RNA interference were used to examine PAK1 loss of function and combination with docetaxel *in vitro*. The

Incucyte® Live-Cell Analysis System was used for caspase 3/7 activation apoptosis assays. Cells were treated with DMSO, FRAXIO36, and/or docetaxel. Caspase 3/7 reagent was added and cells imaged every 2 hours or 4 hours for 36 to 72 hours. Data was analyzed using Incucyte® analysis software to detect and quantify apoptotic cells.

2. **Small molecule inhibition of group I p21-activated kinases in breast cancer induces apoptosis and potentiates the activity of microtubule stabilizing agents.** Ong, C. C., Gierke, S., Pitt, C., Sagolla M., Cheng, C. K., Zhou, W., Jubb, A. M., Strickland, L., Schmidt, M., Duron, S. G., Campbell, D. A., Zheng, W., Dehdashti, S., Shen M., Yang, N., Behnke, M. L., Huang W., McKew, J. C., Chernoff J., Forrest, W.F., Haverty, P. M., Chin S., Rakha, E. A., Green, A. R., Ellis, I. O., Caldas, C., O'Brien, T., Friedman, L. S., Koepfen, H., Rudolph, J., Hoeflich, K. P. *Breast Cancer Research* 2015 17:59.

Barsyte-Lovejoy, *et al.* developed a protocol for measuring early toxicity/apoptosis response to chemical probes using the Incucyte® Live-Cell Analysis System.

3. **Methods in Enzymology, 2016. Chapter 4: Chemical Biology Approaches for Characterization of Epigenetic Regulators.** Barsyte-Lovejoy, D., Szewczyk, M.M., Prinos, P.

Novotny, *et al.* evaluated the ability of reversible HER2 inhibitors to inhibit signaling and proliferation in cancer cell lines driven by HER2-HER3 heterodimers activated via various oncogenic mechanisms. The Incucyte® Live-Cell Analysis System was used for real-time cell proliferation assays. CHL-1 cells were plated in clear-bottom black 96-well plates (Corning; 3904) and allowed to adhere overnight. The following day, media was changed to fresh media that contained either DMSO or compound. Confluence was measured every 2 h for 96 h using two bright-field images per well.

4. **Overcoming resistance to HER2 inhibitors through state-specific kinase binding.** Novotny, C.J., Pollari, S.,

Park, J.H., Lemmon, M.A., Shen, W., Shokat, K.M. *Nature Chemical Biology* 2016 12:923.

Skolekova, *et al.*, measured caspase-3/7 activity corresponding to the induction of apoptosis in human mesenchymal stromal cells (MSCs) cultivated in the presence of cisplatin using the Incucyte® Live-Cell Analysis System. Kinetic activation of caspase-3/7 was monitored and quantified using the Incucyte® FLR object counting algorithm. The authors showed that the secretory phenotype and behavior of mesenchymal stromal cells influenced by cisplatin differed from naive MSC. MSC were more resistant to cisplatin, which was cytotoxic for tumor cells.

5. **Cisplatin-induced mesenchymal stromal cells-mediated mechanism contributing to decreased antitumor effect in breast cancer cells.** Skolekova, S., Matuskova, M., Bohac, M., Toro, L., Durinikova, E., Tyciakova, S., Demkova, L., Gursky, J., and Kucerova, L. *Cell Communication and Signaling*. 2016 14:4.

Greenberg, *et al.*, studied whether Bcl-2-IP3R interaction is a potentially useful therapeutic target in small cell lung carcinoma (SCLC). The Incucyte® Live-Cell Analysis System was used to detect caspase activation and nuclear condensation in SCLC cell lines.

6. **Synergistic killing of human small cell lung cancer cells by the Bcl-2-inositol 1,4,5-trisphosphate receptor disruptor BIRD-2 and the BH3-mimetic ABT-263.** Greenberg, E. F., McCol, K. S., Zhong, F., Wildey, G., Dowlati, A., Distelhorst, C. W. *Cell Death and Disease* 2015 6:e2034.

Yang, *et al.*, describe characterization of a quadruplex dye (G4-REP; quadruplex-specific red-edge probe) that provides fluorescence responses regardless of the excitation wavelength and modality thus allowing for diverse applications and most imaging facilities. Authors demonstrated use via cell images and associated quantifications collected through use of the Incucyte® Live-

Cell Analysis System over an extended period, monitoring both non-cancerous and cancerous human cell lines.

7. **Real-time and quantitative fluorescent live-cell imaging with quadruplex-specific red-edge probe (G4-REP).** Yang, S. Y., Amor, S., Laguerre, A., Wong, J. M. Y., Monchaud, D. *Biochimica et Biophysica Acta (BBA) - General Subjects* <http://dx.doi.org/10.1016/j.bbagen.2016.11.046>.

Ano, et. al. sought to elucidate specific compounds that strongly suppress microglial inflammation by screening dairy products fermented with *Penicillium candidum*. Quantitative live cell imaging to assess apoptosis or neuronal cell-death was performed using an Incucyte® Live-Cell Analysis System. Images were obtained every 3 hour at 20x magnification in phase contrast mode. The number of cells that had undergone apoptosis or cell-death was determined using the object counting algorithm.

8. **Identification of a novel dehydroergosterol enhancing microglial anti-inflammatory activity in a dairy product Fermented with *Penicillium candidum*.** Ano, Y., Kutsukaka, T., Hoshi, A., Yoshida, A., Nakayama, H. *PLoS On 10*, e0116598, 201.

4a

Kinetic Proliferation Assays

Accurate and Reproducible Measurements in a Variety of Cell Culture Models

Introduction

Cell proliferation assays are a cornerstone of cancer therapeutic, developmental biology, and drug safety research.

Analysis of the sustained signaling pathways that underlie the progression of tumors, for example, accounts for >12,000 manuscripts in PubMed, the majority of which use cell proliferation analysis to evaluate tumor cell growth. Despite this, there has not been a direct, straightforward, scalable method for quantifying cell proliferation as a continuous event. Rather, the traditional approaches are endpoints or at best a series of concatenated endpoints to measure the time-course.

Challenges in monitoring cell proliferation via traditional single end point, non-image based assays that utilize plate readers or flow cytometers include:

- A single data point may not provide enough information to effectively distinguish impacts of conditions or treatments, (e.g. when comparing early or late acting compounds, or discerning cell-type dependent proliferative effects of drugs).
- Use of concatenated endpoints utilizes samples from different wells that are measured at different points in time. This potentially introduces artifacts, primarily due to variations in cell seeding densities.
- Many biochemical detection measures (e.g., MTT, LDH, ATP detection) are indirect, destroy the sample, and do not represent the true cell number.
- Measurements cannot be readily verified visually, and morphology changes due to treatment effects cannot be discerned.

- Proliferation rates of cells grown in co-cultures cannot be distinguished.

Live-cell imaging alleviates many of these challenges by allowing for non-destructive, repeated scanning of the same sample over time using either transmitted or fluorescent imaging modalities. However, there are challenges associated with adopting a live-cell approach for measuring proliferation, such as:

- Many biochemical detection measures (e.g., MTT, LDH, ATP detection) are indirect, destroy the sample, and do not represent the true cell number.
- Many fluorescent detection reagents perturb cell growth and morphology and are therefore unsuitable for kinetic analysis.

- Imaging more than one sample location requires movement of the sample, which is particularly problematic for non-adherent cells that can easily move to the edge of the well, or dish, and cause artifacts.
- Imaging over several cell divisions requires leak-free, environmental control systems for temperature, oxygen, and carbon dioxide that can both maintain the environment and enable access for the operator.
- Most live-cell imaging platforms require deep operator expertise and are not easily scaled to microplate throughput, either due to difficulty with set-up of image acquisition or ineffective workflow when viewing and analyzing large numbers of images.

A successful strategy for adoption of a scalable, live-cell approach for proliferation measurements must address the challenges described above. In this chapter, we illustrate how proliferation assays using the Incucyte® Live-Cell Analysis System in conjunction with fit-for-purpose software tools and non-perturbing reagents enable kinetic quantification of cell proliferation, at microplate scale, for both non-adherent and adherent cell cultures, both in mono- and co-culture. In addition, cell proliferation measurements can be multiplexed with cell health, morphology, or surface marker measurements.

Incucyte® Proliferation Assays
at a Glance

A variety of strategies for kinetic measurement of proliferation are possible using the Incucyte® Live-Cell Analysis System. Selection of label-free or fluorescent assays depends on the specific scientific question being asked and cell models studied. Continuous live-cell assays for both adherent and non-adherent cells are possible, as cells stay stationary inside a standard tissue culture incubator while the Incucyte® optics move. There is no sample or stage movement that can cause non-adherent cells to migrate to the edges of microplate wells and negatively impact data accuracy.

Incucyte® Live-Cell Imaging and Analysis enables non-invasive, label-free measurements of cell growth based on area (confluence) or cell number (count) metrics, both of which are generated via segmentation (masking) of high quality phase images. To resolve the challenge of quantifying low contrast cells that can be difficult to identify in phase contrast images, Incucyte® Nuclight Reagents for live-cell analysis can be used to

Shortcomings of Traditional Assays	Live-Cell Imaging and Analysis Approaches
<ul style="list-style-type: none">▪ Data obtained from a single, pre-defined time point yields minimal dynamic insight.	<ul style="list-style-type: none">▪ Continuous, real-time data can distinguish temporal differences in drug or treatment effects and enable decisions as experiments progress.
<ul style="list-style-type: none">▪ Concatenated end point experiments are subject to cell seeding artifacts.	<ul style="list-style-type: none">▪ Cells are measured continuously over time via repeated interrogation of the same well, without loss of environmental control.
<ul style="list-style-type: none">▪ Indirect detection methods are subject to artifacts that cannot be readily verified by eye.	<ul style="list-style-type: none">▪ True, direct cell counts are generated non-invasively and visually verified via image and movies.
<ul style="list-style-type: none">▪ Co-cultures cannot be studied as the entire population is analyzed indiscriminately.	<ul style="list-style-type: none">▪ Either label-free or fluorescent assays using non-perturbing reagents can be used for studying co-cultures.
<ul style="list-style-type: none">▪ Complex and dynamic insight (e.g., drug mechanism of action, characteristics of activation, heterogeneous populations) are not easily achieved.	<ul style="list-style-type: none">▪ Proliferation measurements of heterogeneous, adherent or non-adherent cells can be multiplexed with morphology, health, or functional readouts.

Table 1. Shortcomings of Traditional Assays vs Live-Cell Imaging and Analysis Approaches.

fluorescently label nuclei. Fluorescent Incucyte® images can then be acquired over time and analyzed to generate nuclear counts and derive doubling times in either mono- or co-cultures.

Additionally, Incucyte® Proliferation Assays can be multiplexed with Incucyte® fluorescent reagents for cell health assessments, including apoptosis (Incucyte® Caspase 3/7 Dye, Incucyte® Annexin V Dye), cytotoxicity (Incucyte® Cytotox Dye), or viability (Incucyte®

Nuclight Reagents). Cell boundaries can be identified using the Incucyte® Cell-by-Cell Analysis Software Module, and simultaneous assessment of cell death or viability achieved by measuring the fluorescence intensity originating from within the individual cell boundary.

Sample Results

Validation Data for Label-Free and Fluorescent Approaches

As mentioned, the choice of assay meth-

odology depends on the scientific question and cell model at hand. Depending on the level of rigor required, confluence assays can be a high value and valid approach. They are simple to implement and can distinguish concentration dependent effects on proliferation (Figure 1).

If a true cell count is required, label-free cell counting can be accomplished with Incucyte® Cell-by-Cell Analysis Software Module that utilize proprietary image acquisition strategies and algorithms to

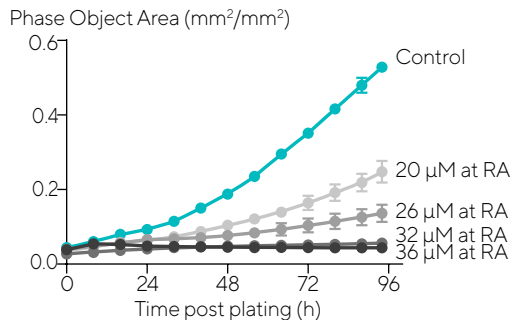
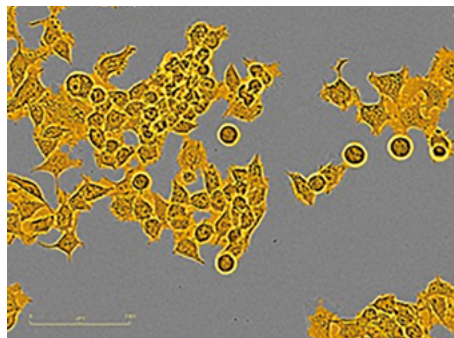
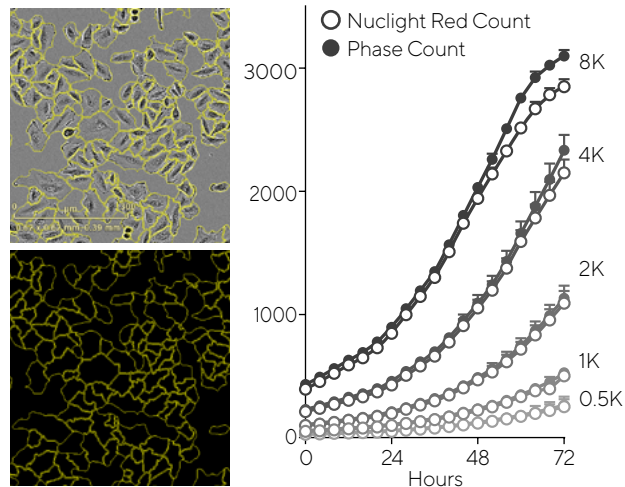


Figure 1. Proliferation is successfully measured by masking (segmenting) and analyzing Incucyte® HD phase images. An Incucyte® mask (orange) identifies the area of the image containing Neuro-2a cells. The proliferation of Neuro-2a cells decreases under increasing concentrations of all-trans retinoic acid.

identify individual cells in HD phase-contrast images. Figure 2 validates this approach, in both adherent and non-adherent cell modules, by comparing changes in cell number using phase-image segmentation versus fluorescent nuclei counting achieved

with Incucyte® Nuclight Lentiviruses (described further below). Throughout the duration of the experiment, the label-free and fluorescent nuclei cell count values tracked very closely, indicative of a robust segmentation algorithm and cell counting method.

Adherent Cells (A549)



Non-Adherent Cells (Jurkat)

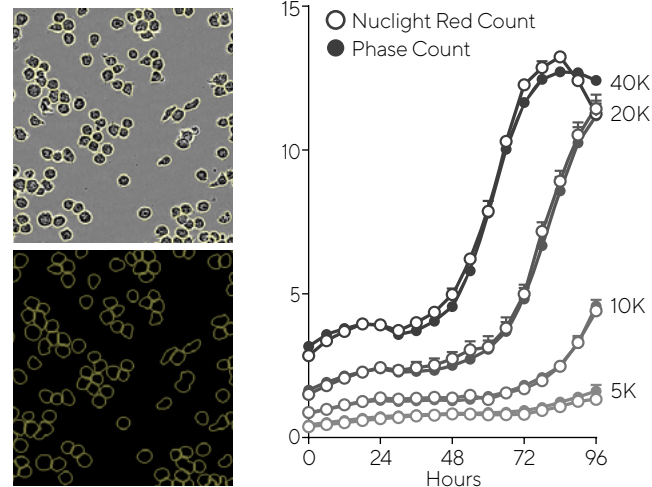
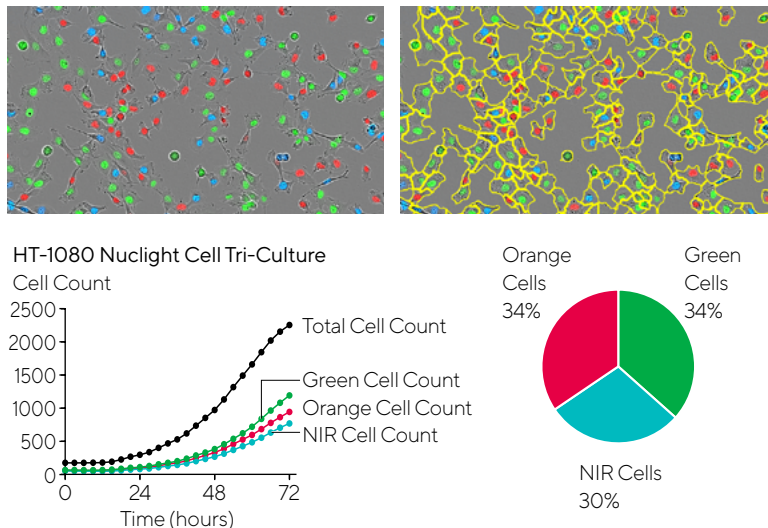


Figure 2. Label-free cell counting in adherent and non-adherent cell types using Incucyte® Cell-by-Cell Analysis – Various densities of adherent Nuclight Red A549 or non-adherent Nuclight Red Jurkat cells were analyzed over time with Incucyte® Cell-by-Cell Analysis Software Module and red object count was used to validate Incucyte’s label-free cell counting method. Images demonstrate individual cell masking using the Cell-by-Cell Software. Time course of phase count and red count across densities shows overlay of label-free and fluorescent data. This validation has been repeated across a range of cell types (data not shown). Values shown are mean \pm SEM of 4 wells.

If a label-free technique does not suffice, nuclear counts can be performed using Incucyte® Nuclight Reagents. These reagents are available in either dye (Incucyte® Nuclight Rapid Dye) or lentiviral (Incucyte® Nuclight Lentivirus) formats and are non-perturbing to cell health and morphology. Incucyte® Nuclight Rapid Dye is a cell permeable DNA stain that specifically stains nuclei in cells using a mix-and-read protocol. Incucyte® Nuclight Lentiviruses are compatible with convenient transduction protocols and provide homogenous expression of a nuclear-restricted fluorescent protein in your choice of primary, immortalized, dividing, or non-dividing

cells without altering cell function and with minimal toxicity. These reagents are ideal for generating stable cell populations or clones using puromycin or bleomycin selection. Fluorescent techniques have particular value when morphology of cells are flat and/or thin, and therefore Incucyte® Nuclight Lentiviruses can be utilized not only to determine nuclear counts in living cells as described in Figure 3, but also in combination with label-free cell identification methods to measure viability. Loss of viability is indicated by a loss in fluorescence, as fluorescent protein passes out of the nucleus as nuclear membrane integrity is lost.

Figure 3. HT-1080 fibrosarcoma cells stably expressing Incucyte® Nuclight Green, Orange, or NIR Lentivirus were monitored for 72 hours. Representative images taken at 48 hours, with and without the label-free Incucyte® Cell-by-Cell Analysis mask, automatically identify the entire population of cells and quantify percentages of green, orange, or NIR expressing cells.



Quantitative Measurement of Cancer Cell Proliferation in a Co-Culture Model

Certain cancers are resistant to chemotherapy due to the biological activity of their neighboring cells, or within the context of the tumor microenvironment. For example, stromal cells have been observed to rescue tumors from drug-induced toxicity by secreting growth factors that impede apoptotic pathways.¹ Such cell interactions may be illuminated by juxtaposing monocultures and co-cultures through *in vitro* assays. In this study, we conducted kinetic experiments to further examine and confirm previous reports of culture-dependent drug sensitivity in a commonly used breast adenocarcinoma cell line, SK-BR-3, that overexpresses HER-2. Previously, Konecny et al demonstrated that monocultures of SK-BR-3 cells were sensitive to the drug lapatinib, which induces cell death by inhibiting tyrosine kinase activity of the HER-2 and EGFR pathways.² However, a second study showed that when SK-BR-3 cells were co-cultured with normal skin fibroblasts (CCD-1068Sk), these stromal cells were

able to rescue the inhibitory effect of lapatinib. Interestingly, no such rescue effect was observed when SK-BR-3 cells grown in co-culture with normal human mammary fibroblasts (HMF).¹

In our study, the proliferation of SK-BR-3 cells in monoculture and co-culture were continuously monitored for more than 8 days in the presence of increasing concentrations of lapatinib (Figure 4). SK-BR-3 cells expressing Incucyte® Nuclight Red Lentivirus were cultured in the presence or absence of fibroblasts, and then quantified using Incucyte® integrated nuclear counting algorithm. This method allowed real-time cell counting based on nuclear restricted fluorescent protein expression. Kinetic graphs of nuclear counts per mm² show SK-BR-3 cells grown with CCD-1068Sk fibroblasts grow at a significantly higher rate than those grown alone or with HMF's in the presence of 500 nM lapatinib (Figure 4A). In addition, IC₅₀ values, calculated using the area under the curve (AUC) of nuclear counts per mm²/time, provide quantitative evidence for the differences in

drug response between monoculture and co-cultures in the presence of lapatinib. Specifically, SK-BR-3 cells grown with CCD-1068Sk fibroblasts are the least sensitive to lapatinib with an IC₅₀ value of 1.162 μM, followed by SK-BR-3 cells grown with HMF's with an IC₅₀ value of 0.581 μM (Figure 4B). Interestingly, SK-BR-3 cells grown in mono-culture remain effectively sensitive to lapatinib with an IC₅₀ value of 0.015 μM (Figure 4B) which is comparable to the published IC₅₀ value, 0.037±0.031 μM.² These striking data very clearly illustrate the difference in SK-BR-3 cell proliferation in the presence of stromal cells, thus highlighting the importance of considering the effect that the tumor microenvironment can have on drug resistance.

Comparison of SK-BR-3 Cells Treated with 555.56 nM Lapatinib

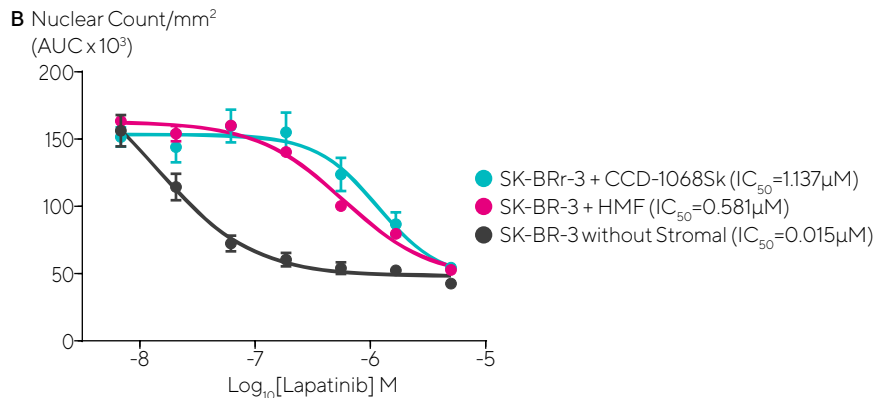
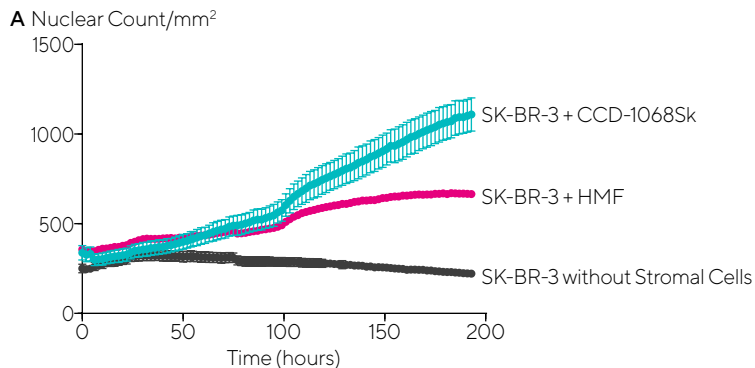


Figure 4. Proliferation of SK-BR-3 cells in co-culture and monoculture under lapatinib treatment. SK-BR-3 cells expressing Nuclight Red Lentivirus were grown with normal skin fibroblasts (CCD-1068Sk), human mammary fibroblasts (HMF), or in monoculture, and treated with varying concentrations of lapatinib for 8 days. (A) Nuclear counts per mm² of SK-BR-3 cells grown with or without stromal cells in the presence of 556 nM lapatinib illustrate the rescue effect of CCD-1068Sk fibroblasts compared to HMFs and mono-culture. (B) Area under the curve of nuclear counts per mm² over time for each concentration (n=4) was used to calculate and compare IC₅₀ values of SK-BR-3 cells grown with or without stromal cells.

High-Throughput Compound Testing Using Nuclight Green Labeled HT-1080s

High-throughput compound testing is essential for efficiently advancing promising drugs through the drug discovery pipeline. To examine the ability of the Incucyte® Live-Cell Analysis System to meet this need, cell proliferation was measured over time in a higher-throughput format. To assess many pharmacological agents simultaneously, 16 literature-standard compounds (Table 2) were applied to HT-1080 tumor-derived fibrosarcoma in a 384-well format (Figure 5). An 11-point concentration response curve was constructed for each compound (Figure 6). Of the 16 compounds tested, the rank order of potency for inhibition of cell proliferation was: doxorubicin = staurosporine = camptothecin > mitomycin C > cycloheximide = RITA > PD-98059 > FAK inhibitor 14 = cisplatin > 10-DEBC = Chrysin = Compound 401. The compounds TAME, PAC1, KU0063794 and FPA-124 had little or no effect on cell proliferation under the conditions of the experiment.

Drug	Description
Doxorubicin	Chemotherapy drug, intercalates DNA ³
Camptothecin	Alkaloid inhibits topoisomerase, causing DNA damage ³
Staurosporine	Potent alkaloid inhibitor of protein kinase ⁴
Mitomycin C	Chemotherapy drug, alkylates DNA ⁵
Cycloheximide	Protein synthesis, inhibitor ⁶
RITA	(Reactivation of p53 and induction of tumor cell apoptosis) a small molecule, binds p53 ⁷
PD-98059	MAPK1/2 inhibitor ⁸
Cisplatin	Chemotherapy drug acts through crosslinking DNA ⁹
FAK-inhibitor 14	Selective inhibitor of focal adhesion kinase ¹⁰
10DEBC	Selective inhibitor of Akt ¹¹
Chrysin	A flavonoid observed to inhibit growth in cancer cells ¹²
TAME	Tert-Amyl methyl ether; a gasoline additive with suspected toxic effects upon inhalation ¹³
PAC1	(Pro-caspase activating compound-1), a small-molecule activator of procaspase-3 to caspase-3 ¹⁴
KU0063794	Specific inhibitor of mTORC1/2 ¹⁵
FPA-124	Akt inhibitor ¹⁶
Compound 401	Inhibitor of DNA-dependent kinase and mTOR ¹⁷

Table 2. Drugs identified in literature as relevant to cell proliferation.

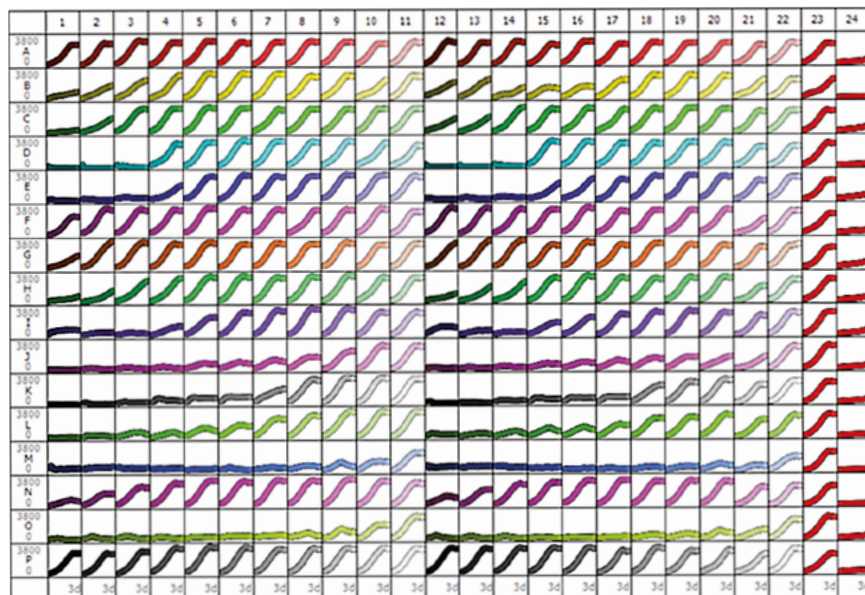


Figure 5. 384-well microplate view of Nuclight Green HT-1080 cell proliferation with 16 different compounds, 11-point concentration-response curves in duplicate (different colors, high to low concentrations left to right). Columns 15 and 16 are vehicle (0.5% DMSO) and CHX (3 μM) controls, respectively. Note the potent concentration-dependent inhibition of cell proliferation for certain compounds (e.g. Row J, Row M, Row O), and weaker effects/inactivity of others (e.g. Row A, Row P). Abscissa: time (0-72 hours), ordinate: fluorescent object count per well (0-3800).

Maximum object
count (1/mm²)

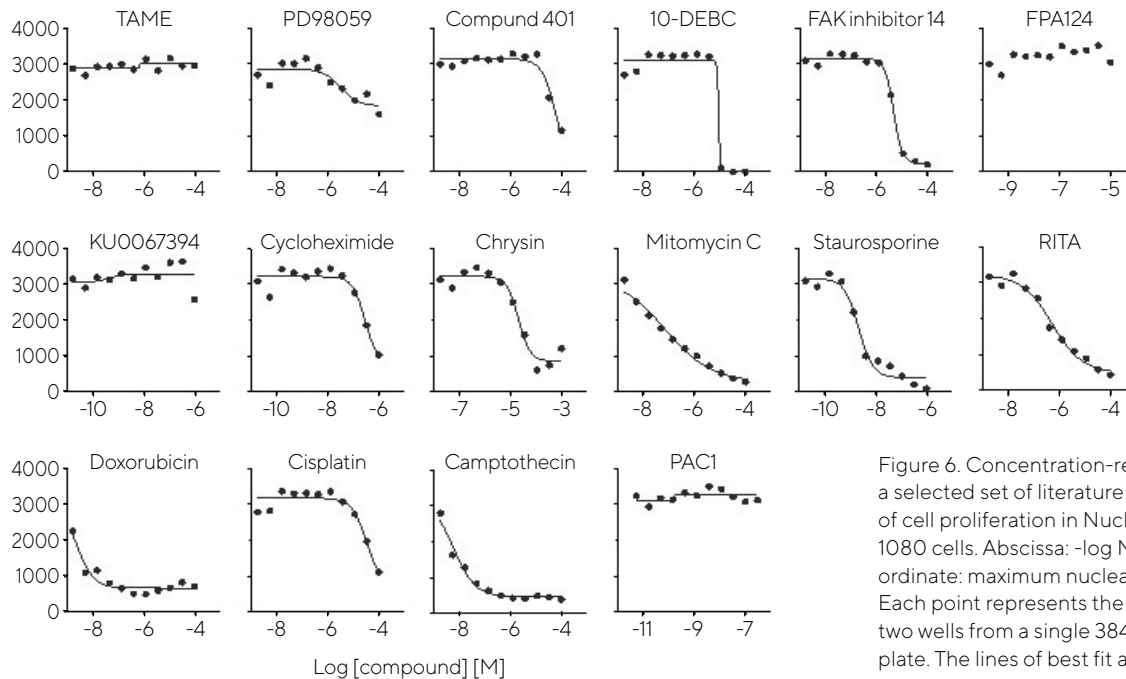


Figure 6. Concentration-response curves for a selected set of literature standard inhibitors of cell proliferation in Nuclight Green HT-1080 cells. Abscissa: $-\log M$ [compound], ordinate: maximum nuclear count (per mm²). Each point represents the average data from two wells from a single 384-well compound plate. The lines of best fit are a 4-parameter logistic equation and can be calculated using Incucyte® integrated analysis software.

To verify and extend these findings, representative images of the cells exposed to test compounds at selected concentrations were inspected (Figure 7). Following exposure to an IC_{80} concentration for 24h, staurosporine produced profound changes in cell morphology, with extensive branching

and condensation of the nucleus and cell body. The cells lost motility and there was clear evidence of cytotoxicity. In contrast, the inhibition of cell proliferation by RITA (also IC_{80} , 24h) was not accompanied by any obvious morphological changes. At anti-proliferative concentrations, both camptothecin and doxorubicin treated

cells appeared healthy with no evidence of cell death, suggesting that senescence had occurred. 10-DEBC (11 mM, 24h) produced overt cytotoxicity and complete cell lysis. These data show the potential of this kinetic and morphological approach to the screening, prioritization, and classification of compounds in drug discovery.

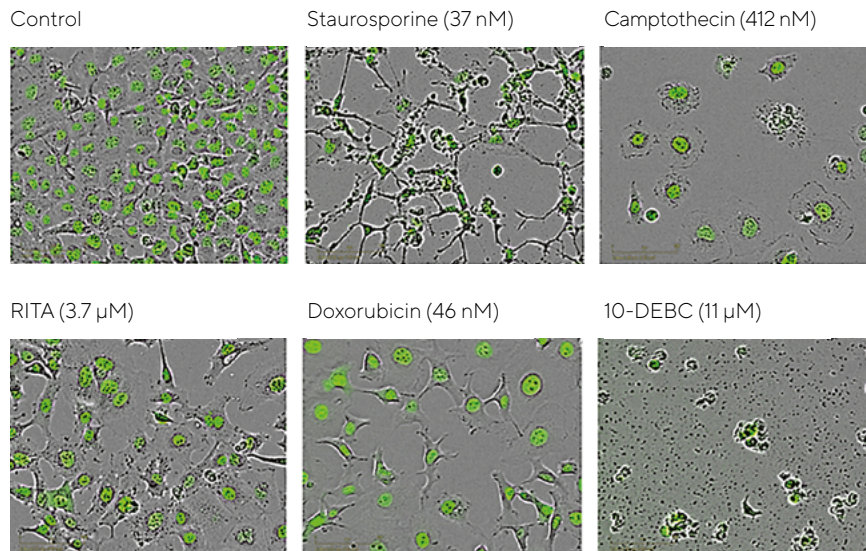


Figure 7. Representative 'blended' phase contrast/fluorescence images of Nuclight Green HT-1080 cells treated with different test compounds as labeled. Images shown were taken 24 h post compound treatment (10x). Note the reduction in total cell number for each treatment compared to the vehicle control, and the profound differences in cell morphology.

Label-Free Cell Counting and Immunophenotyping of Heterogeneous, Non-Adherent Cell Models

The experiment (Figure 8) illustrates label-free counting of live cells in a heterogeneous population of a mixed B cell/T cell culture, as well as the characterization of the CD surface markers. Specific antibodies to the leucocyte common antigen, CD45 and the B-lymphocyte specific antigen CD20 were labeled with Incucyte® Fabfluor-488, a fluorescently labeled antibody fragment. The Fabfluor/antibody conjugates were

then directly added to mixed cultures of Jurkat and Ramos B cells in full cell culture media. Incucyte® Opti-Green, a background fluorescence suppressing reagent, was included to minimize non-specific fluorescence from unbound Fab/ antibody complexes. Images were analyzed using Incucyte® Cell-by-Cell Analysis Software Module, then further classified based on CD45 positive and CD20 positive fluorescence (separate wells). In line with expectations, >95% of cells were labeled positive for CD45, irrespective of the proportion of Jurkat or Ramos cells added

to the mix. CD20 positive cells were only observed in Ramos containing cultures at the proportions expected. In the continued presence of the Fab/antibody, an increase in the number of fluorescently-labeled cells was observed over 48h as the cells proliferated. This simple proof-of-concept experiment demonstrates the ability to specifically label, count and quantify subsets of cells in mixed cultures and to subsequently track long-term changes in these subsets over time (see Chapter 7b - Kinetic Live-Cell Immunocytochemistry Assays for more details).

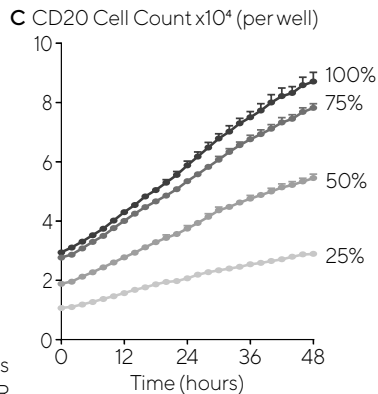
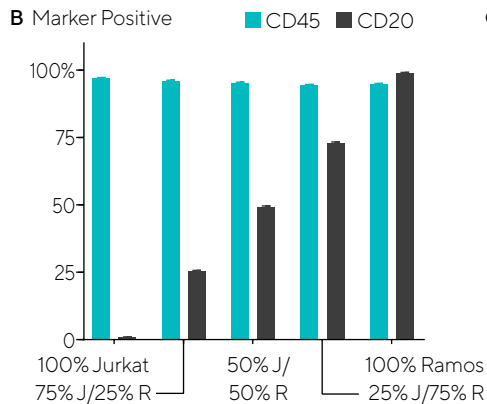
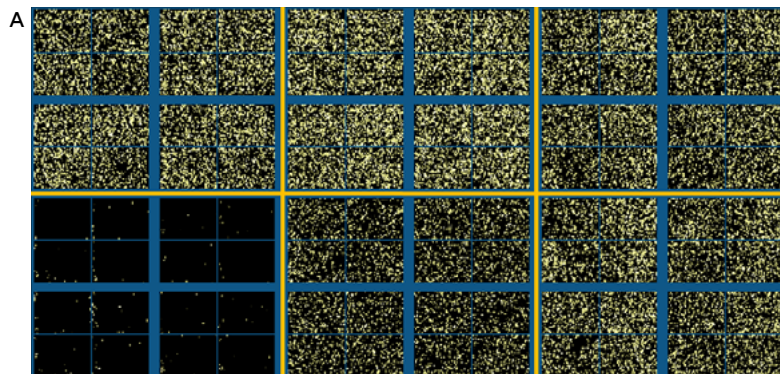


Figure 8. Label-free cell counting and characterization in heterogeneous non-adherent cultures. Characterization of a mixed B cell/T cell culture for the CD surface marker CD45 and CD20 using Incucyte® Fabfluor-488 labeled Abs. (A) Incucyte® Vessel View images (yellow = Ab-labeled cell) of mixed cell populations in the ratios shown. Note the greater proportion of CD20-labeled (Ramos) cells as the ratio of R:J increased in contrast to the CD45 that labels both cell types. (B) Cell-by-Cell quantification of the % expression in the mixed culture. (C) Time course of CD20+ cell count showing proliferation of CD20+ cells within the mixed culture. Values shown are mean \pm SEM of 4 wells.

Continuous Live-Cell Proliferation, Clustering and Viability Assays for T Cells

To investigate the effect of cell density on T cell proliferation and cluster formation, isolated human peripheral blood mononuclear cells (PBMCs) were seeded at various cell densities (20-50 K/well) on poly-L-ornithine (PLO) coated flat bottom 96-well plates (see Chapter 5a - Kinetic Assays for Immune Cell Activation and Proliferation for more details). Cells were grown in the absence or presence of T cell activators anti-CD3 (100 ng/mL), IL-2 (10 ng/ml) and HD phase contrast images were captured on an Incucyte® Live-Cell Analysis System over 144 hours. Images were analyzed for phase confluence (%) as a measure of cell proliferation and the number of phase objects above an area

threshold (cluster count/well) to define cluster formation. The kinetic graph (Figure 9A) demonstrates little or no proliferation under basal conditions (teal lines) but rapid proliferation in the presence of activators (grey lines), which is seeding cell density dependent. Following activation, T cells rapidly form clusters, which is displayed as a cluster count increase (Figure 9B) over time. Both data sets show an increase in the rate of proliferation or cluster formation with cell density (bar graphs, Figures 9A and 9B). The confluence in unstimulated PBMCs can be seen to drop over time due the possible presence of phagocytes. The Incucyte® Live-Cell Analysis System acquired HD phase-contrast images of IL-2/anti-CD3 activated PBMCs, confirming cluster formation as illustrated in Figure 9C.

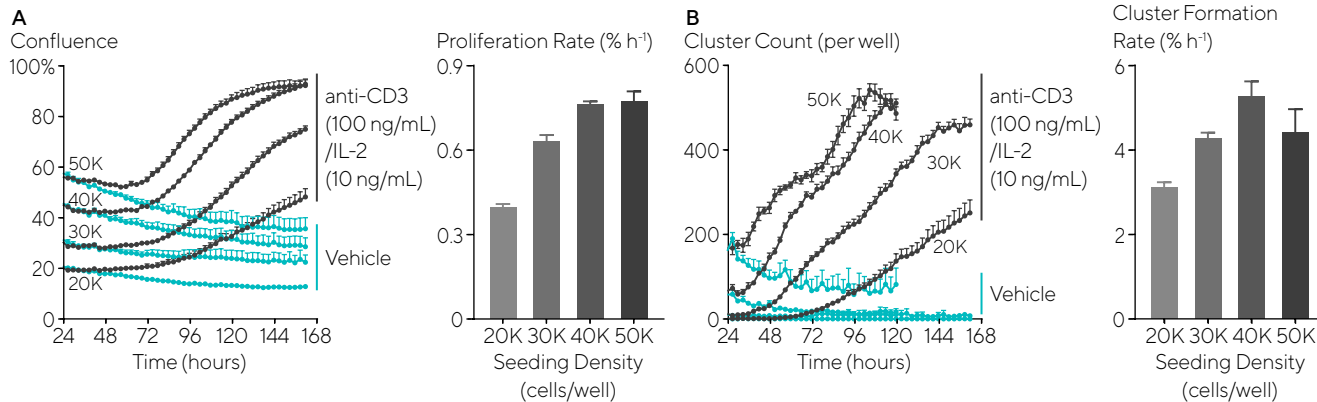
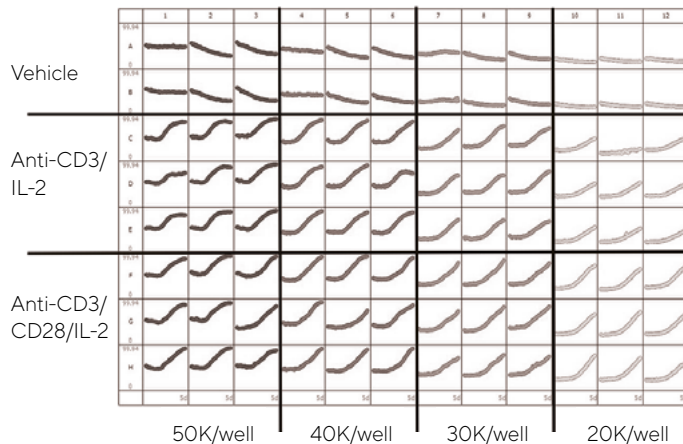



Figure 9. T cell proliferation and clustering is seeding-density dependent. T cells demonstrate little or no proliferation under basal conditions but rapidly proliferate (A) when activated (e.g. by IL- 2, anti-CD3, anti-CD28). Following activation, T cell clusters formed after activation (B) can be imaged, enabling quantification of this phenotype. Plate graph of time-courses reveals seeding-density differences under various activation regimes (C).

C Automated 96-Well Continuous Analysis





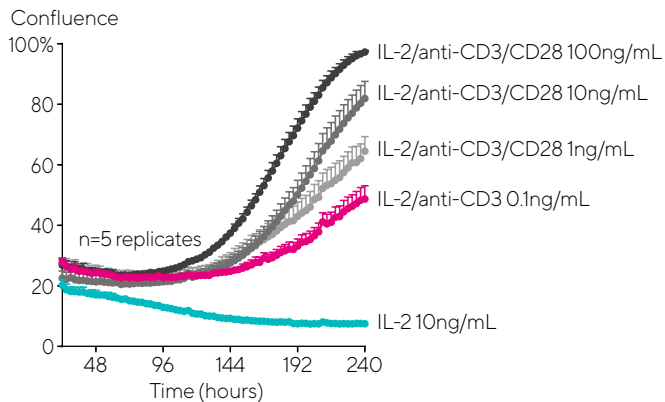
To capture the stimulus dependent effect on T cell proliferation and cluster formation, isolated human PBMCs were seeded (20 K/well) on a PLO-coated flat bottom 96-well plate and grown in the presence of various T Cell activator combinations, IL-2 (10 ng/ml), anti-CD3 (0.1 ng/ml) and/or anti-CD28 (1-100 ng/ml). HD phase contrast images were captured on the Incucyte® Live-Cell Analysis System over 240 hours and analyzed for phase confluence (%) as

a measure of cell proliferation and the number of phase objects above an area threshold (cluster count/well) to define cluster formation. As illustrated in Figure 10A on the following page, little or no cell proliferation was observed in the presence of IL-2 alone, however, moderate proliferation was observed with the addition of anti-CD3. T cell proliferation was further enhanced by the addition of anti-CD28, revealing a concentration dependent response (Figure 10A). A similar

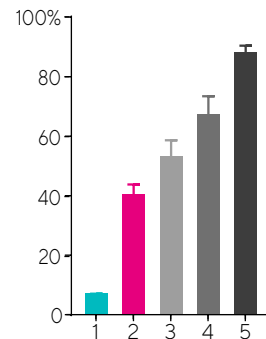
stimulus dependent cluster formation profile was also measured in the presence of various T cell activator combinations (Figure 10B). These data show the potential of this kinetic and morphological approach to evaluating immune cell activation.

Figure 10. T cell activation is stimulus and concentration-dependent. Data shown are for PBMCs treated with combinations of IL-2, anti-CD3, and anti-CD28.

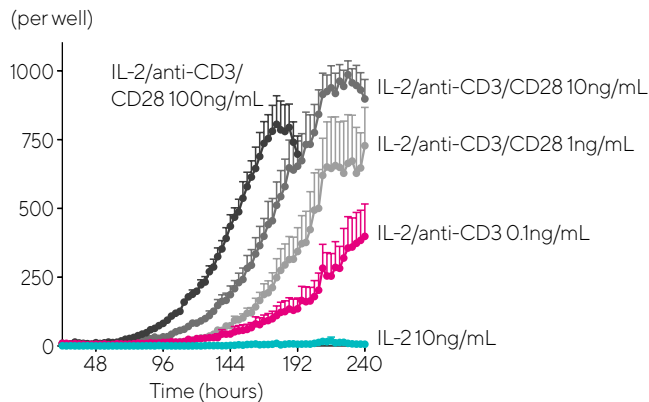
A Proliferation



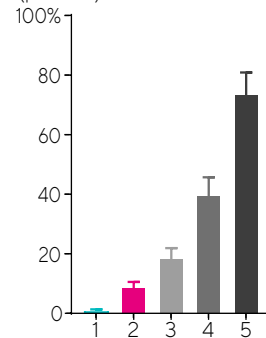
Confluence - 216h




B Cluster Count



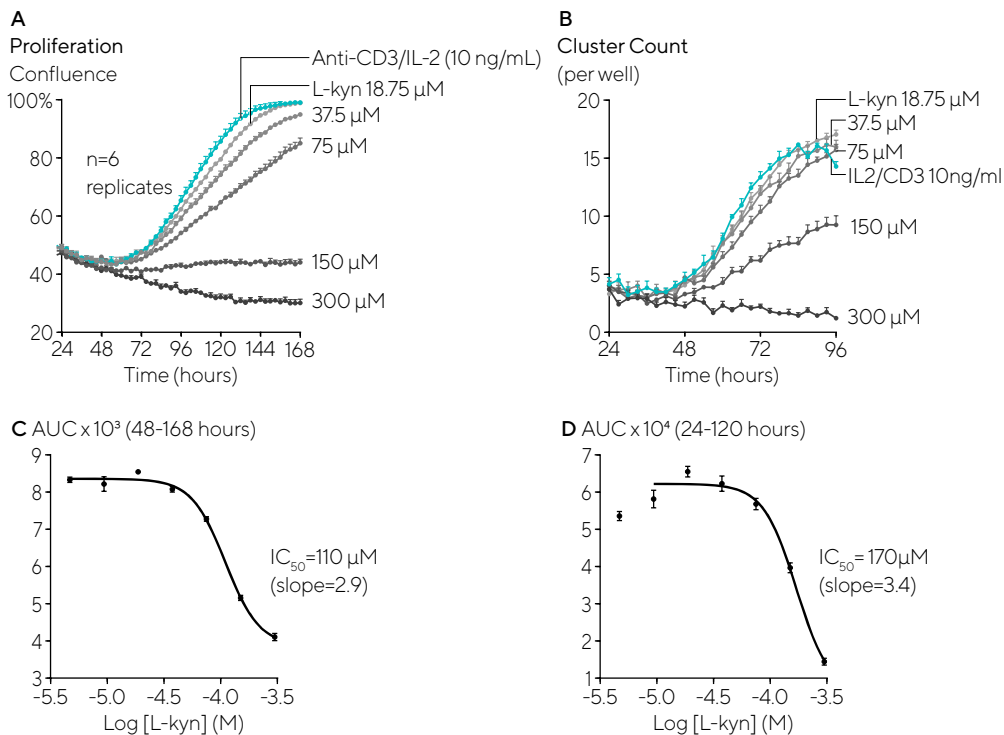
Cluster Count at - 168 h (per well)



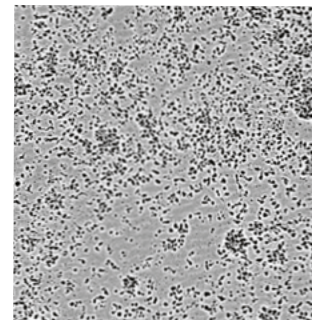


Additionally, the Incucyte® Live-Cell Analysis System was used to study effects of L-kynurenine (L-kyn) on T Cell proliferation and clustering. L-kyn is a metabolite formed from the catabolism of L-tryptophan by the enzymes indoleamine 2,3-dioxygenase (IDO) and tryptophan 2,3-dioxygenase (TDO). Some cancers increase L-kyn production in a bid to block

antigen-driven T Cell proliferation and induce T Cell death, thus allowing cancer cells to escape immune surveillance. Inhibitors of IDO and/or TDO are therefore promising therapeutic targets for the treatment of cancer. Figure 11 on the following page shows time-course results of L-kyn inhibition of T Cell proliferation and clustering.



E IL-2/anti-CD3



F + L-kyn (150 μ M)

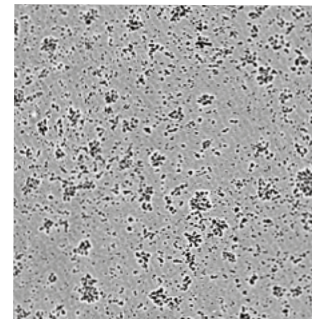


Figure 11. L-kynurenine inhibits T Cell proliferation and clustering. Data demonstrates a clear concentration-related inhibition of IL-2/anti-CD3 activated T Cell proliferation (A) and clustering (B) with the addition of exogenous L-kyn, over time. Time-course profiles enabled AUC analysis and generation of concentration-response curves from which IC₅₀ values for inhibition of proliferation (C) and clustering (D) were determined. Images reveal reduction of clustered morphology with addition of L-kynurenine (F) when compared to activated T Cells (E).

Conclusions

The Incucyte® Live-Cell Analysis System, in conjunction with proprietary software tools and Incucyte's Nuclight Reagents for live-cell nuclear labeling, provide a flexible assay platform for kinetic measurements of proliferation. These assays achieve quantitative and reproducible analysis of both adherent and non-adherent cells, in monoculture and importantly, co-culture, and without removing cells from the physiologically-relevant environment of a tissue culture incubator. Image-based methodologies give the user the ability to monitor morphological changes in parallel with quantification, the combination of which is a powerful and unique tool for detecting pharmacological or genetic manipulations that alter cell viability or function.

- Kinetic, label-free confluence or cell count measurements over several cell divisions can be generated using phase image segmentation and without using fluorescent labels– an ideal strategy for mono-culture analysis.
- Fluorescent reagents that label nuclei (e.g., Incucyte® Nuclight Reagents) can be used to measure proliferation of mono-cultures when cells are of low contrast and therefore difficult to identify via segmentation of phase contrast images. Nuclear-labeling strategies can also be used to differentiate the effects of supporting cells on the proliferation of a labelled cell population.
- Incucyte's kinetic label-free cell counting method can also differentiate between proliferation rates of subpopulations in co-cultures when individual cell types are of different size or shape (non-adherent cells only), or when the individual populations can be identified using cell surface markers (adherent or non-adherent cells), or when one population is fluorescently labelled with a nuclear marker (Incucyte® Nuclight Reagents).
- Proliferation assays can be run in microplates (96-well and 384-well) with high precision and reproducibility. In 384-well plates, a mix and read assay is exemplified whereby full concentration-response curves of 16 standard anti-proliferative agents were compared. In a single Incucyte® Live-Cell Analysis System, 6 x 384-well plates can be monitored providing >2000 wells of parallel data acquisition.
- All data and time points can be verified by inspecting individual images and/or time-lapse movies. Cell morphology observations provide additional validation and insight into mechanistic differences between treatments or conditions.
- Non-adherent cell proliferation and clustering can be visualized due to the non-perturbing nature of the Incucyte's optical design. Non-adherent cells stay stationary; there is no stage or sample movement, rather the optics move.

References

1. Strausman R, *et al.* Tumour micro-environment elicits innate resistance to RAF inhibitors through HGF secretion. *Nature* 2012, 487 (7408):500-504.
2. Konecny GE, *et al.* Activity of the dual kinase inhibitor lapatinib (GW572016) against HER-2-overexpressing and trastuzumab-treated breast cancer cells. *Cancer Res* 2006, 66(3):1630-1639.
3. Sappal, DS, *et al.* Biological characterization of MLN944: A potent DNA binding agent. *Molec. Cancer Ther.* 2004, 3(1):47.
4. Seynaeve, CM, *et al.* Differential inhibition of protein kinase C isozymes by UCN-01, a staurosporine analogue. *Mol. Pharmacol.* 1994, 45(6):1207-1214.
5. Palom, Y, *et al.* Bioreductive metabolism of mitomycin C in EMT6 mouse mammary tumor cells: cytotoxic and non-cytotoxic pathways, leading to different types of DNA adducts. The effect of dicumaro. *Biochem. Pharmacol.* 2001, 61(12):1517-1529.
6. Chang, TC *et al.* Effects of transcription and translation inhibitors on a human gastric carcinoma line. Potential role of Bcl-X(S) in apoptosis triggered by these inhibitors. *Biochem. Pharmacol.* 1997, 53(7):96-977.
7. Roh, JL *et al.* The p53-reactivating small-molecule RITA enhances cisplatin-induced cytotoxicity and apoptosis in head and neck cancer. *Cancer Let.* 2012, 325(1):35-41.
8. Aravena, C *et al.* Potential Role of Sodium-Proton Exchangers in the Low Concentration Arsenic Trioxide-Increased Intracellular pH and Cell Proliferation. *PLoS One* 2012, 7(12): e51451.
9. Hu, W. The anticancer drug cisplatin can cross-link the interdomain zinc site on human albumin. *Chem. Commun.* 2011, 47(21):6006-6008.
10. Cabrita, MA. Focal adhesion kinase inhibitors are potent anti-angiogenic agents. *Molec. Oncology* 2001, 5(6):517-526.
11. Janjetovic, K. Metformin reduces cisplatin-mediated apoptotic death of cancer cells through AMPK-independent activation of Akt. *Europ. J. Pharmacol.* 2011, 651(1-3):41-50.
12. Shao, J *et al.* AMP-activated protein kinase (AMPK) activation is involved in chrysin-induced growth inhibition and apoptosis in cultured A549 lung cancer cells. *Biochem. Biophys. Res. Comm.* 2012, 423(3):448-453.
13. Ahmed, FE. Toxicology and human health effects following exposure to oxygenated or reformulated gasoline. *Tox. Letters* 2001, 123(2-3):89-113.
14. Boldingh Debernard, KA. Cell death induced by novel procaspase-3 activators can be reduced by growth factors. *Biochem. Biophys. Res. Comm.* 2011, 413(2):364-369.
15. Garcia-Martinez, JM. Ku-0063794 is a specific inhibitor of the mammalian target of rapamycin (mTOR). *Biochem. J.* 2009, 421(1):29-42.
16. Strittmatter, F *et al.* Activation of protein kinase B/Akt by alpha1-adrenoceptors in the human prostate. *Life Sciences* 2012, 90(11-12):446-453.
17. Ballou, LM *et al.* Inhibition of Mammalian Target of Rapamycin Signaling by 2-(Morpholin-1-yl)pyrimido[2,1-a]isoquinolin-4-one. *J. Biol. Chem.* 2007, 282(33):24463-70.

Incucyte® User Publications

1. Balaban S, *et al.* **Adipocyte lipolysis links obesity to breast cancer growth: adipocyte-derived fatty acids drive breast cancer cell proliferation and migration.** *Cancer Metab.* 2017, Jan 5:1.
2. Blom M, *et al.* **The atypical Rho GTPase RhoD is a regulator of actin cytoskeleton dynamics and directed cell migration.** *Exp Cell Res.* 2017, Mar 15;352(2):255-264.
3. Blum W, *et al.* **Stem cell factor-based Identification and functional properties of in vitro-selected subpopulations of malignant mesothelioma cells.** *Stem Cell Reports.* 2017 Apr 11;8(4):1005-1017.
4. Bussian TJ, *et al.* **Clearance of senescent glial cells prevents tau-dependent pathology and cognitive decline.** *Nature.* 2018 Oct;562(7728):578-582.
5. Ihry RJ, *et al.* **p53 inhibits CRISPR-Cas9 engineering in human pluripotent stem cells.** *Nat Med.* 2018, Jul; 24(7):939-946.
6. Lau J1-, *et al.* **Tumour and host cell PD-L1 is required to mediate suppression of anti-tumour immunity in mice.** *Nat Commun.* 2017 Feb 21;8:14572.
7. McDonald AI, *et al.* **Endothelial regeneration of large vessels is a biphasic process driven by local cells with distinct proliferative capacities.** *Cell Stem Cell.* 2018 Aug 2;23(2):210-225.
8. Takigawa H, *et al.* **Mesenchymal stem cells induce epithelial to mesenchymal transition in colon cancer cells through direct cell-to-cell contact.** *Neoplasia.* 2017 May;19(5):429-438.
9. Zaretsky JM, *et al.* **Mutations associated with acquired resistance to PD-1 blockade in melanoma.** *N Engl J Med.* 2016 Sep 1;375(9):819-29.

Kinetic Apoptosis Assays

Quantitative Assays for Apoptotic Pathway Analysis for Both Drug Discovery and Basic Research

Introduction

Apoptosis, the biological process by which cells undergo programmed cell death, is required for normal tissue maintenance and development. However, aberrations in apoptotic signaling networks are implicated in numerous human diseases including neurodegeneration and cancer.¹ Apoptotic pathways are initiated by extrinsic factors that result in activation of pro-apoptotic receptors on the cell surface, or intrinsically by many different stimuli such as DNA damage, hypoxia, the absence of growth factors, defective cell cycle control, or other types of cellular stress that result in release of cytochrome C from mitochondria.

Stimulation of either the extrinsic or intrinsic apoptotic pathways triggers a signaling cascade that results in the activation of a family of proteins that play a major role in carrying out the apoptotic process called caspases.² Caspases (cysteiny l aspartate proteinases) cleave substrates following

an Asp (D) amino acid residue. Effector targets of caspases include caspase family members themselves, proteins involved in fragmentation of cellular DNA (caspase-activated DNases), nuclear lamins, as well as proteins that make up the cell cytoskeleton. Caspase proteins are traditionally separated into two groups, initiator caspases (caspase 2, 8, 9 and 10), and executioner or effector caspases (caspase 3, 6, and 7). As a primary executioner caspase in most systems, the activation of caspase-3 often results in the irreversible commitment of a cell to apoptosis. Therefore, the activation of caspase-3 is considered a reliable marker for cells undergoing apoptosis.

The regulated loss of plasma membrane phosphatidylserine (PS) symmetry is also a classical marker of apoptosis. Dying cells trigger the translocation of the normally inward-facing PS to the cellular surface, allowing for early phagocytic recognition of the dying cell by surrounding phagocytes.

Numerous enzymatic, plate-reader and flow-cytometric assays have been designed to measure caspase-3/7 activation or PS externalization. Most caspase-3/7 assays involve luciferase, colorimetric or fluorometric reagent substrates that incorporate a DEVD (Asp-Glu-Val-Asp) peptide motif³ which is recognized by the enzyme. Annexin V is a recombinant protein with a high affinity and selectivity for PS residues, allowing it to be used for the detection of apoptosis. Apoptosis assays using annexin V conjugated to a fluoroprobe have been optimized for detection of PS externalization and are most commonly measured by flow-cytometry.

In this chapter, we will examine kinetic approaches for measuring apoptosis using Incucyte® Caspase-3/7 and Annexin V fluorescent reagents. Unlike plate reader and flow-cytometric endpoint approaches, kinetic live-cell image-based analysis allows for the evaluation of time-dependent effects of treatments or cell-specific responses.

Incucyte® Apoptosis Assays at a Glance

The Incucyte® Caspase-3/7 Green and Incucyte® Caspase 3/7 Red Dyes are an inert, non-fluorescent substrates. When added to tissue culture growth medium, the substrate freely crosses the cell membrane where it is cleaved by activated caspase-3/7 resulting in the release of the DNA dye and fluorescent labeling of DNA.^{4,5} Incucyte® Annexin V Red, Green, Orange and NIR Dyes are specially formulated, highly-selective cyanine-based fluorescent dyes ideally suited to a simple mix-and-read, real-time quantification of apoptosis in living cells.

- The apoptotic signal relies on either the activation of Caspase-3/7, a primary and irreversible “executioner” pathway in most cell types, or using Annexin V conjugated to a fluoroprobe for detection of PS externalization.

Shortcomings of Traditional Assays

- Assays result in a **single, user-defined time point measurement** of caspase-3/7 activity.
- Techniques **require multiple wash steps or cell lifting** prior to data collection that may result in the loss of dying cells or lead to a loss in PS asymmetry.
- **Assays are not amenable to long-term measurements** due to increasing signal background over time.
- Manipulations can result in the **loss of cells or critical data** in experiments where cells undergo apoptosis at different rates according to treatment conditions.

Live-Cell Imaging and Analysis Approaches

- The assay provides a **full kinetic readout of apoptotic signaling over multiple days**, eliminating the need for determining a single, optimum, assay endpoint a-priori which can vary considerably for different cell types and for different compound treatment conditions.
- Cells can be simultaneously labeled with an Incucyte® apoptosis reagents and Incucyte® Nuclight Reagent for live-cell nuclear labeling to **measure apoptotic cell death, cell proliferation and kinetically monitor anti-proliferative effects of compounds**.
- Addition of Incucyte® apoptosis reagents to normal, healthy cells are **non-perturbing to cell growth or morphology** and yield little to no intrinsic fluorescent signal.
- IC₅₀ and EC₅₀ values can be calculated **using kinetic area under the curve** values of nuclear counts and Caspase-3/7 or Annexin V counts, respectively.

Table 1. Shortcomings of Traditional Assays vs Live-Cell Imaging and Analysis Approaches, continued on following page.

- Multiplexing the Caspase-3/7 and Annexin V Dyes detect and confirm apoptosis through two different pathways, verifying apoptosis as a mechanism of cell death.
- Multiplexing Incucyte® apoptosis reagents with a nuclear-labeling reagent such as Incucyte® Nuclight Lentivirus or Incucyte® Nuclight Rapid Dye enables differentiation between inhibition of cell growth and induction of cell death.
- High definition phase contrast images provide an additional qualitative validation of cell death based on morphological characteristics.
- Images are automatically acquired and analyzed to reveal concentration and time-dependent effects on biology.

Shortcomings of Traditional Assays

Live-Cell Imaging and Analysis Approaches

- 96- and 384-well assay using a homogeneous “mix and read” protocol which can be run over multiple days in full media. **No wash or lifting steps required**, negating the concern that cells are lost during the experiment or labeling process.
- The assay has **high statistical reproducibility** and can be used both for single-point screening or concentration response profiling.
- All data points and temporal data curves can be validated by individual images or time-lapse movies respectively. The kinetic readout of the Incucyte® Live-Cell Analysis System provides both **high definition (HD) phase as well as quantitative fluorescent imaging**.

Table 1. Shortcomings of Traditional Assays vs Live-Cell Imaging and Analysis Approaches, continued from previous page.

Sample Results

Quantitative Measurement of Caspase-3/7 Kinetic Activation

MDA-MB-231 cells, a human breast adenocarcinoma derived cell line, were treated with staurosporine (SSP) a well-known inducer of apoptosis. SSP was serially diluted in growth media containing 5 μ M Incucyte® Caspase 3/7 Dye in a 96-well plate. Once treated, the cells were immediately placed inside the Incucyte® Live-Cell Analysis System with a 10X objective in a standard cell culture incubator and both phase-contrast and fluorescent images were collected every 2-3 hours.

Alterations in cell morphology were evident within only a few hours of SSP treatment as illustrated in the phase image in Figure 1A. Using fluorescent images,

we positively identified cells containing fluorescently stained DNA indicating activation of caspase-3/7, cleavage of the DEVD moiety in the kinetic apoptosis reagent, and fluorescent labeling of cellular DNA (green image in Figure 1A). Using the object counting algorithm, we successfully quantified the number of fluorescent objects, shown in Figure 1A. The object counting criteria were then applied to all images in the experiment at each time point. The data in Figure 1B indicate that caspase-3/7 activation is detectable within a few hours of SSP treatment, with a maximal response triggered in the presence of 333 nM SSP.

Increasing concentrations of SSP also significantly affected cell proliferation. To demonstrate this on the Incucyte® Live-Cell Analysis System, we completed

an end point analysis at the 48 hour time point. Vybrant® DyeCycle™ Green DNA dye was added directly (no wash required) to the wells at a final concentration of 1 μ M in 50 μ L of PBS. After a 30 minute incubation, the total number of DNA containing objects was enumerated using the object counting algorithm. As expected, our data indicate an inverse correlation between the total number of objects and the apoptotic index as a function of increasing concentrations of SSP (Figure 1C). The data clearly indicate the ability of the Incucyte® Live-Cell Analysis System to accurately identify the activation of caspase-3/7, thus providing insight into the dynamics and timing of the apoptotic signaling pathway, thereby alleviating the need to pick an end-point for analysis prior to running the experiment.

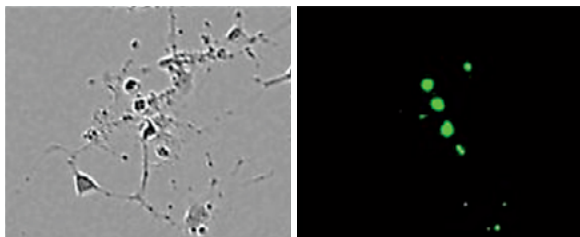
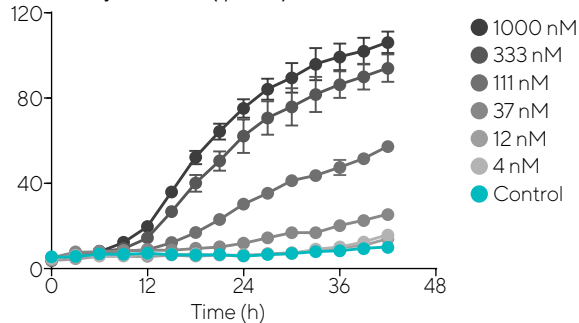
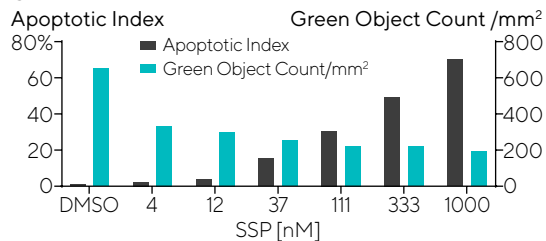
A

Figure 1. Staurosporine (SSP) induced caspase-3/7 activity in human breast adenocarcinoma cells (MDA-MB-231). (A) Representative phase contrast and fluorescent images reveal classical apoptotic cell morphologies and indicate activation of caspase-3/7, respectively. (B) Kinetic measures of the number of caspase-3/7 positive cells is recorded over time and plotted as fluorescent objects, n=3 wells per data point shown (C). At the 48 hour end point, the apoptotic index was calculated by dividing the number of caspase-3/7 fluorescent objects by the total number of DNA containing objects following staining with Vybrant DyeCycle Green.

BGreen Object Count (1/ mm²)**C**

Multiplexed, Kinetic Measurements of Proliferation and Apoptosis

The fluorescent channels on the Incucyte® Live-Cell Analysis System provide a way to kinetically measure caspase-3/7 activation in addition to proliferation (nuclear label) within the same well, eliminating the need for end-point analysis. In the next experiment, Nuclight Red HeLa cells were treated with SSP in the presence of 5µM Incucyte® Caspase-3/7 Green Dye and phase-contrast, red, and green images were

collected every 2 hours in the Incucyte® Live-Cell Analysis System using a 10x objective (Figure 2). These data illustrate typical results obtained using the Incucyte® Caspase-3/7 Green Dye multiplexed with Incucyte® Nuclight Red HeLa cells to measure the kinetic induction of apoptosis and proliferative effects of drug treatment (Figure 2B and 2C, respectively). Using all of the kinetic data in Figure 2B and 2C, area under the curve (AUC) values were plotted and EC₅₀ (apoptosis) and IC₅₀

(proliferation) values were calculated. This 2-color kinetic assay provides a multiplex way to analyze the apoptotic and anti-proliferative effects of various treatments.

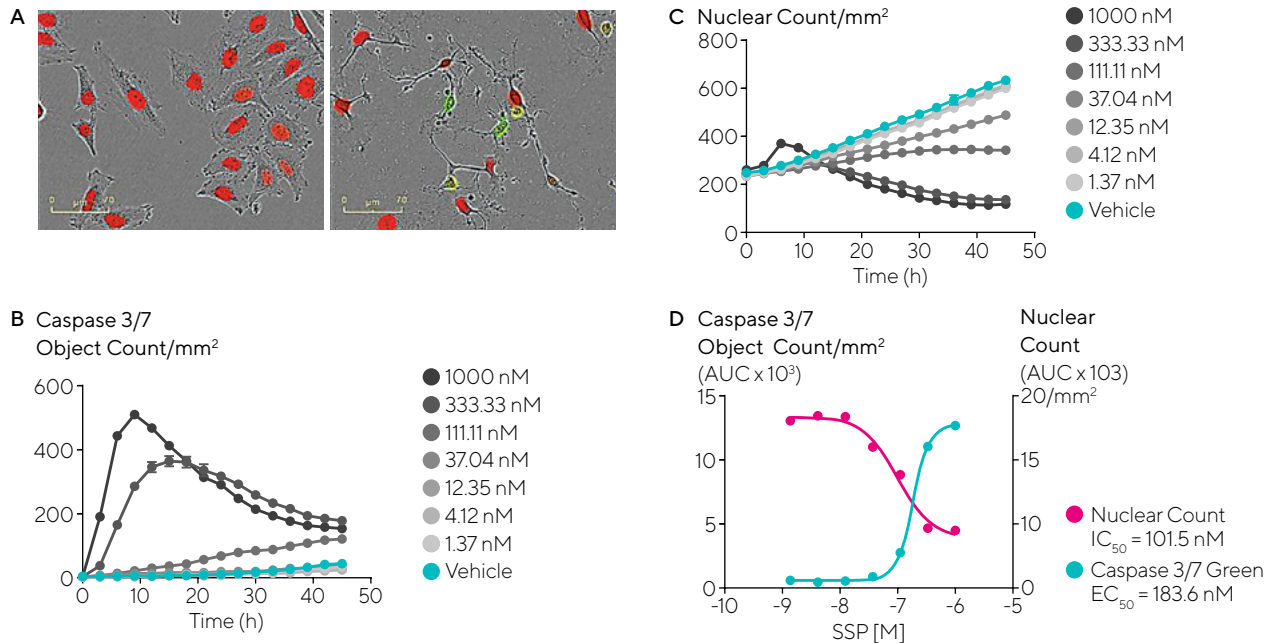


Figure 2. Pharmacological analysis of caspase-3/7 activation and nuclear counts in Nuclight Red HeLa cells treated with SSP. (A) Blended phase-contrast and red/green images taken at 20x show red nuclear signal and activation of caspase-3/7 as well as morphological differences in untreated cells (left) vs. cells treated with 300nM SSP (right). (B) Caspase-3/7 positive objects and (C) nuclear counts were measured over time in response to increasing concentrations of SSP. (D) Area under the curve (AUC) of nuclear counts/mm² and caspase object counts/mm² over time were measured and used to calculate IC₅₀ and EC₅₀ values, respectively.

Kinetic Measurement of Extrinsic Activation of Apoptosis

Depending on the cellular context, exposure of cells to tumor necrosis factor alpha (TNF- α) can induce either pro-survival, or cell death pathways. When used in isolation, TNF- α induces NF κ B activity and subsequent expression of pro-survival signaling molecules (e.g. FLIP, XIAP, A20). Alternatively, when used in conjunction with cycloheximide (CHX), itself an inhibitor of translation, TNF- α is a potent inducer of apoptosis through caspase 3 mediated signaling pathways. To demonstrate this using the Incucyte® Live-Cell Analysis System, A549 epithelial carcinoma cells were treated with increasing concentrations of TNF- α in the presence of 5 μ g/mL CHX. Caspase-3/7 was activated in a TNF- α concentration dependent manner (Figure 3A). The AUC values for caspase-3/7 positive objects over time were then used to calculate the EC₅₀ value of 0.676 nM TNF- α (Figure 3B).

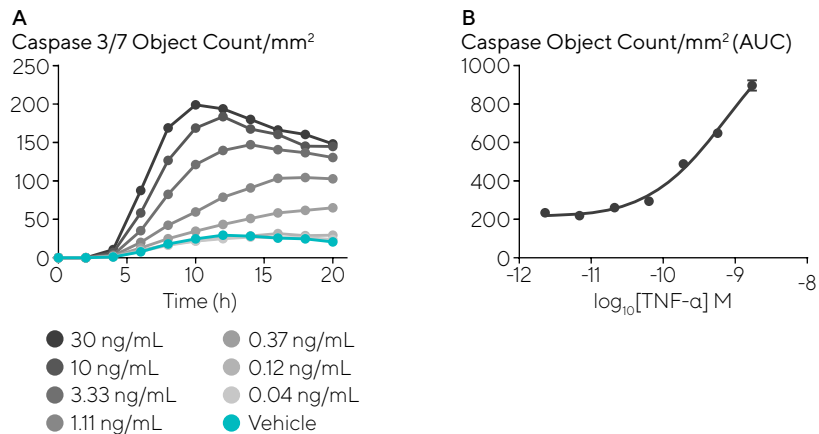


Figure 3. Extrinsic activation of caspase-3/7 in A549 lung epithelial cells. (A) Caspase-3/7 activation of A549 lung epithelial cells in response to varying concentrations of TNF- α in the presence of 5 μ g/mL cycloheximide (CHX). (B) The EC₅₀ value of TNF- α was calculated by using the area under the curve (AUC) of caspase-3/7 objects/mm² over time.

Using Images and Movies to Confirm Signaling

One of the major advantages of live-cell analysis is the ability to verify the quantified kinetic data with both phase contrast and fluorescent images. Classical morphological changes associated with apoptosis include: cell shrinkage, membrane blebbing, nuclear

condensation, and DNA fragmentation. The time lapse sequence presented in Figure 4 highlights this advantage, illustrating the ability to use phase contrast and fluorescent blended images to temporally correlate the activation of caspase-3/7 and the loss of red nuclei due to cell death with morphological changes in response to treatment with SSP. Using the Incucyte® Live-Cell Analysis System,

the temporal responses in every well can be supplemented with a “movie” of either a phase contrast, fluorescence or blended time-lapse sequence. This ability significantly enhances the confidence in the measured response and any subsequent conclusions drawn from quantitative image analysis.

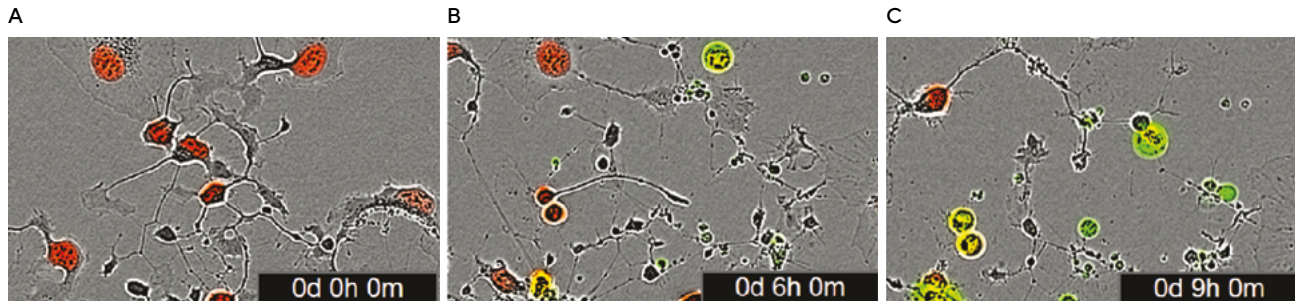
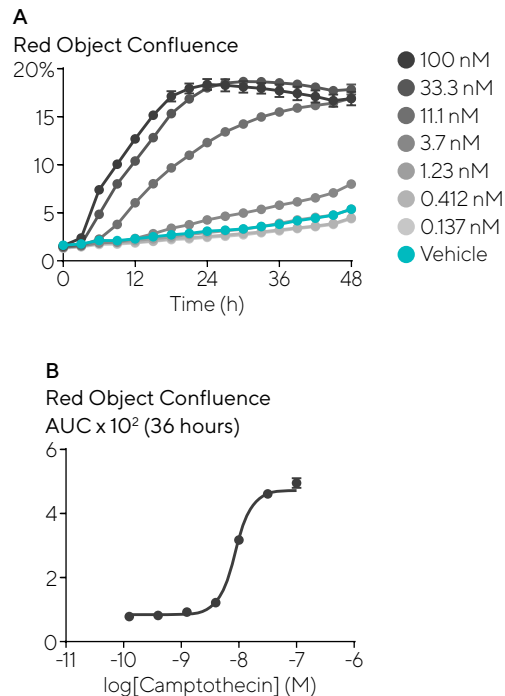


Figure 4. Time-lapse images and movies to detect SSP induced apoptosis in HT-1080 cells. Nuclight Red HT-1080 cells were treated with 300nM SSP in the presence of 5µM Caspase-3/7 Green Dye and imaged in Incucyte® Live-Cell Analysis System every 3 hours (A). Time-lapse images and movies monitor changes in morphology and confirm the activation of the green caspase-3/7 signal in (B) and the loss of the red nuclear signal (C).

Loss of Phosphatidylserine Asymmetry

Addition of the Incucyte® Annexin V Dye to normal healthy cells is non-perturbing to cell growth or morphology and yields little or no intrinsic fluorescent signal. Once cells become apoptotic, plasma membrane PS asymmetry is lost leading to exposure of PS to the extracellular surface and binding of the Incucyte® Annexin V Dye, yielding a bright and photostable fluorescent signal.

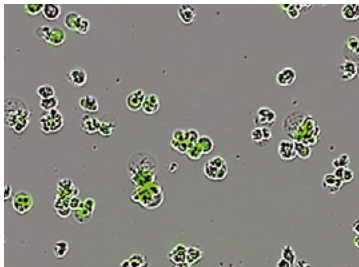
Figure 5. Concentration and time-dependent loss of PS asymmetry. Incucyte® Annexin V Red Dye was added to Jurkat human T cell leukemia cells treated with the topoisomerase inhibitor camptothecin. (A) Time-course for the effects of camptothecin on Jurkat cell death (Red Object Confluence (%)) presented as the mean \pm SEM, n=3 wells). (B) Concentration response curve to camptothecin. Area under the curve (AUC) values have been determined from the time-course shown in panel A (36 hours) and are presented as the mean \pm SEM, n=3 wells. Average AUC values were used to calculate pIC₅₀ values (camptothecin pIC₅₀ = 8.01).



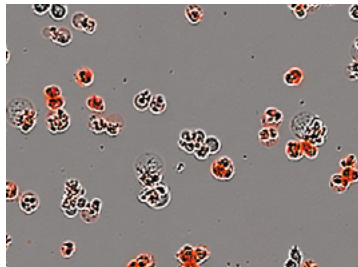
Multiplex Assays to Confirm Apoptotic Pathways

The Incucyte® Live-Cell Analysis System can be used to detect and confirm apoptosis through two different pathways by multiplexing Caspase-3/7 and Annexin V Dyes to verify apoptosis as a mechanism of cell death.

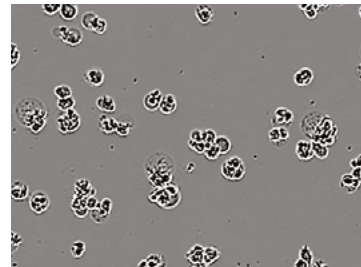
Caspase-3/7



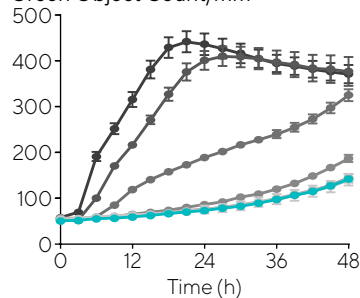
Annexin V



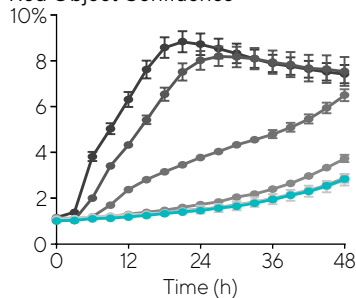
Label-Free Confluence



Green Object Count/mm²



Red Object Confluence



Phase Object Confluence

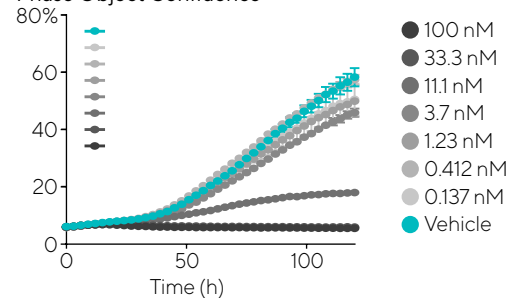


Figure 6. Detect both Caspase-3/7 and Annexin V signals in cultures. Automatically determine the time courses of apoptotic cell death and correlate with label free confluence measurements to provide an estimate of the proportion of apoptotic cells within the population (apoptotic index).

Assessment of Immune Cell Killing of Cancer Cells Using Caspase Signaling

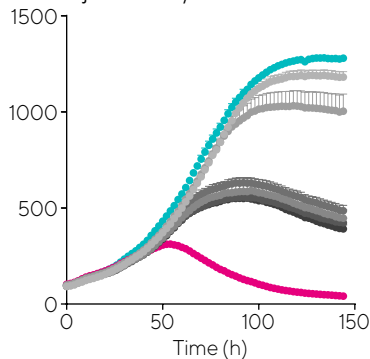
Caspase-3/7 was used to evaluate targeted tumor cell death in a co-culture Antibody-Dependent Cell-mediated Cytotoxicity (ADCC) assay to measure tumor cell apoptosis and for visual validation of tumor-immune cell interactions. To demonstrate the utility of this approach, ADCC cell death was measured via Caspase-3/7 induction in Her2-positive SKOV3 or negative Nuclight Red A549

cells (1.6K/well) co-cultured with PBMCs (8K/well) in the presence of trastuzumab, a clinically used monoclonal antibody for Her2-positive cancer cells. A concentration-dependent decrease in proliferation (IC_{50} 8.1 ng/mL) and increase in apoptosis (IC_{50} 4.6 ng/mL) was measured in Her2-positive SKOV3 cells. No response was seen in Her2-negative A549 cells (data not shown). These data

demonstrate that live-cell imaging and analysis can be used to discern the full-time course and specificity of immune cell killing, which are traditionally conducted as flow cytometry or biochemical readouts, requiring selection of end points and lack visual confirmation of cellular interactions (see Chapter 5b - Kinetic Assays for Immune Cell Killing for more details).

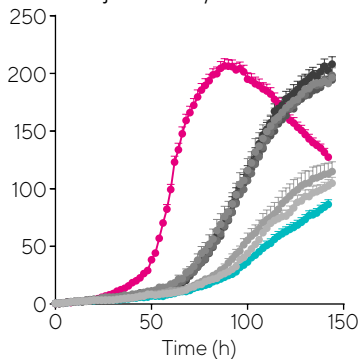
Proliferation

Red Object Count/mm²



Apoptosis

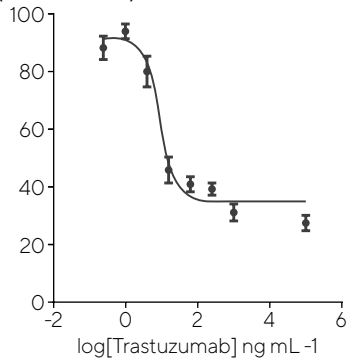
Green Object Count/mm²



- Vehicle
- Anti-CD3/IL-2
- 1000 ng ml⁻¹
- 250 ng ml⁻¹
- 63 ng ml⁻¹
- 16 ng ml⁻¹
- 4 ng ml⁻¹
- 1 ng ml⁻¹

Inhibition of Proliferation

(% of Controls)



Target Cell Death

(% of Controls)

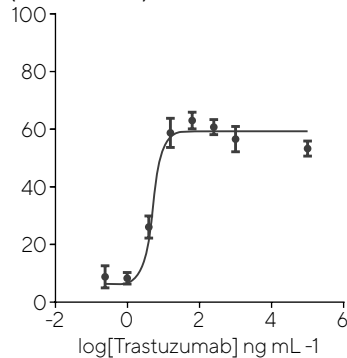


Figure 7. Trastuzumab induced ADCC in Her2-positive SKOV3 cells. SKOV3 cancer cells were seeded in combination with PBMCs in the presence of trastuzumab to induce ADCC. A concentration-dependent decrease in proliferation (IC₅₀ 8.1 ng/mL) and an increase in apoptosis (IC₅₀ 4.6 ng/mL) was seen.

Conclusions

Live-cell imaging and analysis is a powerful tool for the kinetic detection of apoptosis, demonstrating quantitative and reproducible data. This strategy of live-cell imaging and analysis gives the user the ability to monitor morphological changes in parallel with quantification, the combination of which is a powerful and unique tool for detecting pharmacological or genetic manipulations that alter cell health. In addition, Nuclight Reagents or cell lines, when used in conjunction with Incucyte® apoptosis reagents and the Incucyte® Live-Cell Analysis System, provide an additional parameter for measuring cytostatic (anti-proliferative) and apoptotic events. Together, these attributes provide new and unique assays for apoptotic pathway analysis for both drug discovery as well as basic cell biology research.

Key features of the apoptosis assays are:

- The irreversible “executioner” caspase-3/7 pathway or PS externalization can be kinetically monitored allowing for the detection of both short-term and long-term treatment effects.
- Non-perturbing Incucyte® Caspase-3/7 or Annexin V Dyes are added as mix-and-read reagents directly to the cultured cells in complete growth media, removing the need for fluid aspiration steps, thus eliminating cell disruption or loss of impaired cells.
- All data points can be validated by individual images or time-lapse movies to confirm processing metrics, significantly enhancing the confidence in the measured response.
- Live-cell imaging of apoptosis can be used to discern the full-time course and specificity of co-culture models such as immune cell killing, with visual confirmation of cellular interactions.

References

1. Cotter TG. **Apoptosis and Cancer: The Genesis of a Research Field.** *Nat Rev Cancer* 2009, 9(7):501-507.
2. Shi Y. **Mechanisms of Caspase Activation and Inhibition During Apoptosis.** *Mol Cell* 2002, 9(3):459-470.
3. Thornberry NA, Rano TA, Peterson EP, Rasper DM, Timkey T, Garcia-Calvo M, Houtzager VM, Nordstrom PA, Roy S, Vaillancourt JP, Chapman KT, Nicholson DW. **A Combinatorial Approach Defines Specificities of Members of the Caspase Family and Granzyme B. Functional Relationships Established for Key Mediators of Apoptosis.** *J Biol Chem* 1997, 272(29):17907-17911.
4. Daya S, Robets M, Isherwood B, Ingleston-Orme A, Caie P, Teobald I, Eagle R, Carragher N. **Integrating an Automated *in Vitro* Combination Screening Platform with Live-Cell and Endpoint Phenotypic Assays to Support the Testing of Drug Combinations.** SBS 16th Annual Conference and Exhibition 2010.
5. Cen H, Mao F, Aronchik I, Fuentes RJ, Firestone GL. **Devd-Nucview488: A Novel Class of Enzyme Substrates for Real-Time Detection of Caspase-3 Activity in Live Cells.** *FASEB J* 2008, 22(7):2243-2252.
6. Janicke RU, Sprengart ML, Wati MR, Porter AG. **Caspase-3 Is Required for DNA Fragmentation and Morphological Changes Associated with Apoptosis.** *J Biomol Screen* 1998, 273(16):9357-9360.
7. Zhang JH, Chung TD, Oldenburg KR. **A Simple Statistical Parameter for Use in Evaluation and Validation of High Throughput Screening Assays.** *J Biomol Screen* 1999, 4(2):67-73.

4c

Kinetic Cytotoxicity Assays

Real-Time, Live-Cell Assay to Quantify and Visualize Cytotoxic Events

Introduction

The cellular response to cytotoxic exposure is controlled by complex biochemical pathways, such as necrosis or apoptosis, which results in cell death. In apoptosis, morphological changes include pseudopodia retraction, reduction of cellular volume (pyknosis), nuclear fragmentation (karyorrhexis) and eventually loss of plasma membrane integrity.¹ Morphological changes that characterize necrosis include cytoplasmic swelling and early rupture of plasma membrane.² Compounds that have cytotoxic effects often compromise cell membrane integrity regardless of the pathway.

Assays designed to measure cytotoxicity *in vitro* are used to predict tissue-specific toxicity or to identify and classify leads for anti-cancer therapies. Multiplexed, high-throughput screening (HTS) *in vitro*

cytotoxicity assays measuring a variety of different readouts are being employed to assess the cytotoxicity of compounds in early drug development.³ Commonly used cytotoxicity assays evaluate a range of end-point parameters, such as the release of lactate dehydrogenase (LDH) and glutathione (GSH) following membrane rupture, generation of reactive oxygen species (ROS), cell proliferation, and disruption of mitochondrial transmembrane potential. Critical factors contributing to the predictive nature of these assays include compound concentration, and more importantly, the time allowed for the compound to elicit an effect.⁴ Although these multiplexed assays are able to simultaneously measure multiple indicators of *in vitro* cytotoxicity, they typically assess a single time point and are unable to assess the biological activity over time.

In this chapter, we will examine kinetic approaches for measuring cytotoxicity using reagents that fluorescently stain the nuclear DNA of cells that have lost plasma membrane integrity. Unlike traditional endpoint approaches, kinetic live-cell imaging allows for the analysis of time-dependent variation in treatment response as well as the ability to differentiate between cytostatic and cytotoxic effects.

Incucyte® Cytotoxicity Assay at a Glance

The Incucyte® Cytotoxicity Assay uses highly sensitive cyanine nucleic acid dyes ideally suited for mix-and-read kinetic measurements of cell membrane integrity overtime. Incucyte® Cytotox Red and Green Dyes are cell impermeant cyanine dimer nucleic acid stains that bind to dsDNA,⁵ and when added to the culture medium, these reagents fluorescently stain the nuclear DNA of cells that have lost plasma membrane integrity.

This Cytotoxicity Assay can be combined with Incucyte® Nuclight Reagents for live-cell nuclear labeling that incorporate a red or green nuclear label allowing for simultaneous measurement of proliferation and cytotoxicity in a single well. These reagents are available in either dye (Incucyte® Nuclight Rapid Dye) or lentiviral (Incucyte® Nuclight Lentivirus) formats and are non-perturbing to cell health and morphology and provide a means to quantify cell proliferation over time. Incucyte® Nuclight Rapid Dye is a cell permeable DNA stain that uses a simple,

Shortcomings of Traditional Assays

- Assays result in a **single**, user-defined time point measurement.
- **Lack of ability to assess biological activity over time** limits predictive nature.
- Manipulations can result in the **loss of cells or critical data in experiments** where cells undergo cell death at different rates according to treatment conditions.

Live-Cell Imaging and Analysis Approaches

- The assay provides a **full kinetic read-out** of cytotoxicity over multiple days, eliminating the need for determining a single, optimum, assay endpoint a-priori which can vary considerably for different cell types and for different compound treatment conditions.
- Addition of Incucyte® Cytotox Dyes to normal, healthy cells are **nonperturbing to cell growth and morphology**.
- Cells can be **simultaneously labeled with Incucyte® Cytotox Dyes and Incucyte® Nuclight Reagents for nuclear labeling to measure cytotoxicity and cell proliferation**.
- 96- and 384-well assay format follows a homogeneous **“mix-and-read” protocol** which can be run over multiple days in full media. **No wash or lifting steps** required, negating the concern that cells are lost during the experiment or labeling process.

Table 1. Shortcomings of Traditional Assays vs Live-Cell Imaging and Analysis Approaches, continued on following page.

mix-and-read protocol to specifically stain cell nuclei. Non-perturbing Incucyte® Nuclight Reagents provide a means to kinetically quantify cell proliferation over time. Incucyte® Nuclight Lentiviruses allow for the expression of a nuclear-restricted GFP (green fluorescent protein), mKate2 (red fluorescent protein), TagRFP (orange fluorescent protein) or iRFP713 (Near-IR fluorescent protein) in mammalian cells without altering cell function and with minimal toxicity. Incucyte® Nuclight Lentiviruses allow for the creation of stable cell populations or clones.

Phase-contrast images can be used to qualitatively monitor associated morphological changes in the same cells over the same time course.

Sample Results

Quantitative Measurement of Cytotoxicity Using Incucyte® Cytotox Dye Staurosporine (SSP) and camptothecin (CMP) are compounds that are known to cause cell death due to cytotoxicity. SSP is a high affinity, non-selective, ATP-competitive kinase inhibitor and

Shortcomings of Traditional Assays

Live-Cell Imaging and Analysis Approaches

- All data points and temporal data curves can be **validated by individual images or time-lapse movies** respectively. The kinetic readout of the Incucyte® Live-Cell Analysis System provides both high definition (HD) phase as well as **quantitative fluorescent imaging**.

Table 1. Shortcomings of Traditional Assays vs Live-Cell Imaging and Analysis Approaches, continued from previous page.

is classically used as a research tool to induce caspase-3 mediated apoptosis.^{6,7} CMP causes cell death by inhibition of the DNA enzyme, topoisomerase I (topo I), resulting in double strand breaks during S-phase and triggering the apoptotic program.⁸ These two compounds were used to illustrate the ability of the cell impermeant DNA dye based Cytotoxicity Assay to measure cell death over-time using two different cell lines, HT-1080

(human tumor derived fibrosarcoma) and MDA-MB-231 (human tumor derived breast adenocarcinoma). In addition, we also measured the response of these same two cell types to the protein synthesis inhibitor, cycloheximide (CHX), a cytostatic compound which was predicted to inhibit cell proliferation while not affecting cell viability (Figure 1).

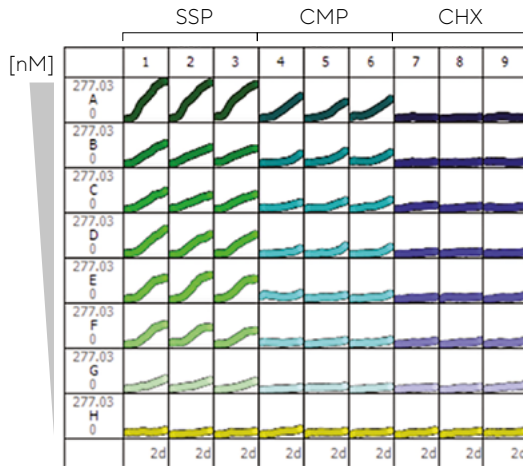
A 7-point concentration curve of each compound clearly illustrated that in both cell types, SSP and CMP induced a concentration-dependent cytotoxic response. Specifically, we observed a

statistical induction of cytotoxicity in MDA-MB-231 cells at 16 and 26 hours for SSP and CMP treatments, respectively (Figure 1A). In identically treated HT-1080 cells, there was a more rapid induction of

the cytotoxic responses correlating to 12 and 22 hours for SSP and CMP treatments, respectively, which illustrates a slight cell type dependent difference (Figure 1B).

A MDA-MB-231

Fluorescent Objects/mm²



B HT-1080

Fluorescent Objects/mm²

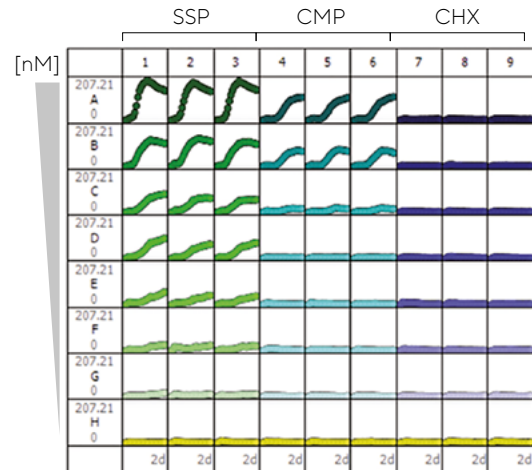


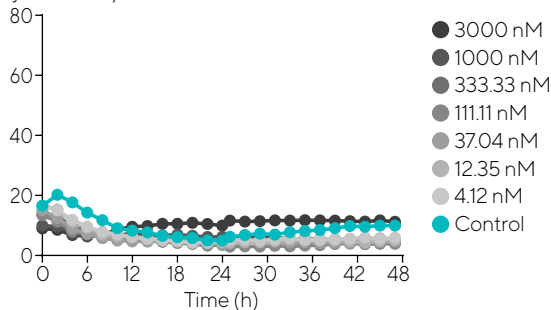
Figure 1. Discrimination of cytotoxic and cytostatic compounds. 96-well microplate graph showing the kinetic measurement of cell death as determined by Cytotox Green staining in response to several concentrations of SSP, CMP, and CHX in MDA-MB-231 cells (A) and HT-1080 cells (B).

In contrast, no statistical induction of cytotoxicity was observed when either cell type was treated with any of the tested concentrations of CHX (Figure 1A, 1B). However, a clear concentration-dependent inhibition of cell proliferation was

observed as measured by the Incucyte® Nuclight Red fluorescent signal (Figure 2). Moreover, end-point normalization, which corrects for differences in proliferation within treatment groups, revealed a concentration-dependent cytotoxic index

for both SSP and CMP in MDA-MB-231 and HT-1080 cells, whereas no cytotoxic response was induced by treatment with CHX (Figure 3).

Membrane Permeability Cytotox Green Object Count/mm²



Proliferation Nuclear Count/mm²

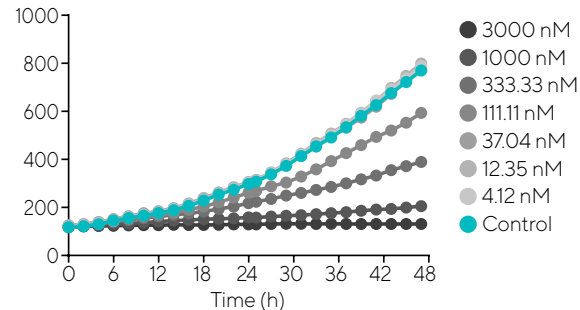
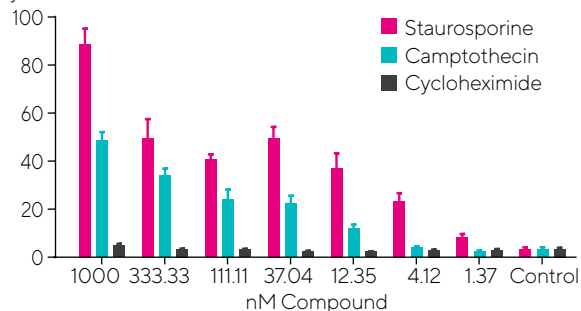


Figure 2. Cytostatic effect of cycloheximide (CHX). Nuclight Red HT-1080 cells were treated with several concentrations of cycloheximide in the presence of Cytotox Green Dye. Graphs illustrate no induction of cytotoxicity as measured by green fluorescence staining of DNA (A) however, inhibition of cell proliferation (B) as measured by fluorescent nuclear counts is observed. Cell morphology did not significantly differ from untreated cells as illustrated in Figure 5. Each data point represents the mean \pm SE in N=3 wells.

A MDA-MB-231 Cytotoxic Index



B HT-1080 Cytotoxic Index

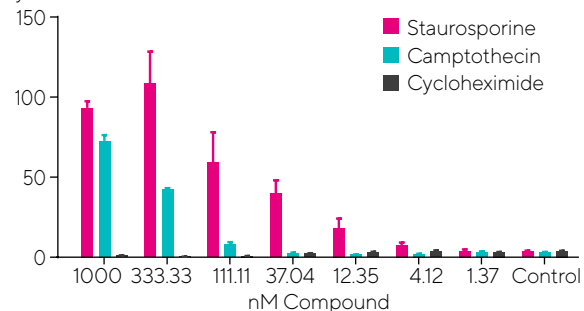


Figure 3. End-point normalization of cytotoxic and cytostatic compounds. At the 72-hour end-point, Triton X-100 at a final concentration of 0.0625% was added to allow nuclear dsDNA staining by Cytotox Green Dye of all cells present/well. The cytotoxic index was calculated by dividing the number of Cytotox Green fluorescent objects by the total number of DNA containing objects (fluorescent objects counted post Triton X-100 treatment).

SSP

CMP

CHX

Control

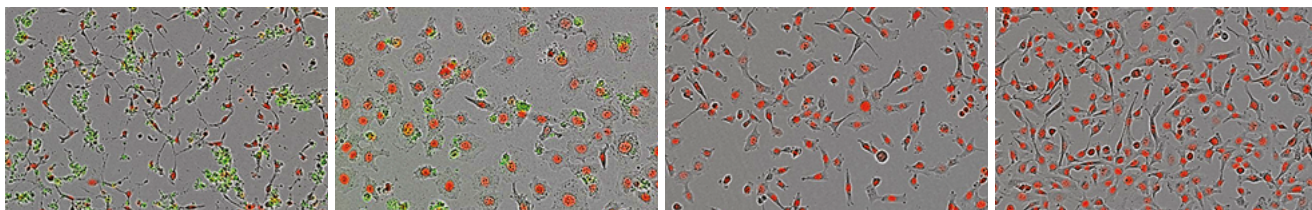



Figure 4. Morphological images. Phase-contrast and fluorescent images of Nuclight Red HT-1080 cells 24hrs post-treatment, showing morphological changes in response to SSP, CMP and CHX.



The Incucyte® Live-Cell Analysis Systems acquired phase-contrast and fluorescent images of HT-1080 cells, under all three compound treatments, confirmed fluorescent object count data as illustrated in Figure 4 (similar results were observed with MDA-MB-231 cells). These data show the potential of this kinetic and morphological approach to the screening, prioritization, and classification of compounds in drug discovery.

In order to evaluate the accuracy and reproducibility a series of experiments using MDA-MB-231 and HT-1080 cell lines and two known cytotoxic compounds (SSP and CMP) were used.

To assess intra-assay reproducibility, each well of a 96-well plate was seeded with 5,000 HT-1080 or MDA-MB-231 cells. Each row of cells was treated with 2-fold decreasing concentrations of CMP (2000 nM to 62.5 nM; n=12 wells per

condition) in the presence of Cytotox Green Dye and kinetic measurements of fluorescent objects were analyzed. As illustrated in the microplate graph view in Figure 5A, we obtained a highly reproducible kinetic measure of cell viability. In addition, using end-point data, we were able to demonstrate an inverse relationship between total DNA object count and cytotoxic index (Figure 5B, 5C) in both cell lines analyzed.

A Cytotox Green Fluorescent objects/mm² (HT-1080)

Fluorescent Objects/mm²

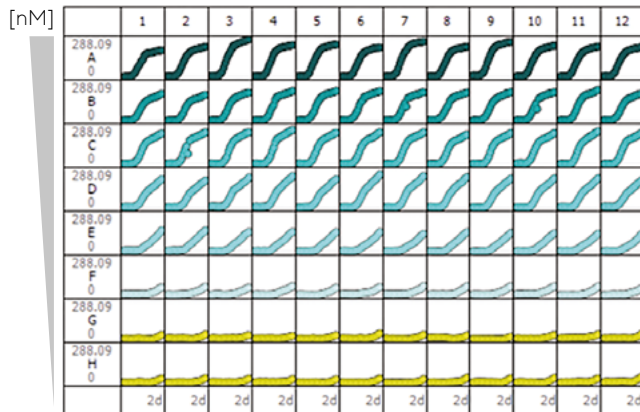
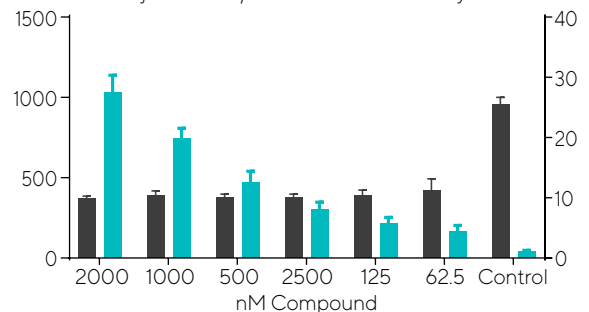


Figure 5. Intra-assay reproducibility of HT-1080 and MDA-MB-231 cells in response to CMP. 96-well microplate graph showing reproducibility of concentration response to CMP (A). After the 48-hour end-point, the cytotoxic index was calculated by dividing the number of Cytotox Green fluorescent objects by the total number of DNA containing objects (fluorescent objects counted post Triton X-100 treatment) (B and C).

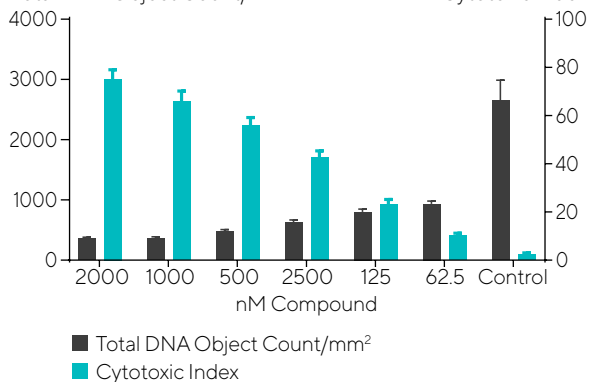
B MDA-MB-231

Total DNA Object Count/mm²



C HT-1080

Total DNA Object Count/mm²

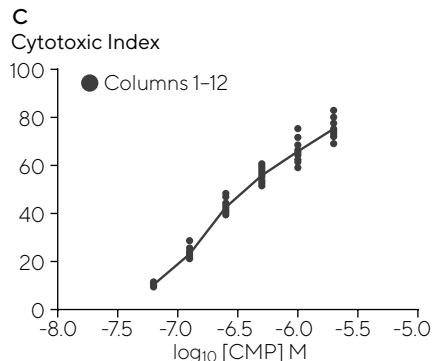


A

[CMP]	Cytotoxic Index (Mean)	SD	$z' = 0.82$
2000 nM	75.280	3.805	
1000 nM	65.895	4.397	
500 nM	55.943	3.293	
250 nM	42.595	2.846	
125 nM	23.063	2.265	
62.5 nM	10.441	0.773	
Control	2.641	0.657	

B

[CMP]	Cytotoxic Index (Mean)	SD	$z' = 0.64$
2000 nM	27.443	2.941	
1000 nM	19.829	1.768	
500 nM	12.636	1.826	
250 nM	8.080	1.234	
125 nM	5.690	1.102	
62.5 nM	4.338	1.078	
Control	0.984	0.264	



Column	pEC ₅₀
1	7.078
2	6.681
3	6.578
4	6.741
5	6.61
6	6.747
7	6.738
8	6.817
9	6.594
10	6.791
11	6.621
12	6.651
MEAN pEC ₅₀	6.721
MEAN 95% CI	6.501 to 6.933
Geometric Mean (Antilog Converted)	
EC ₅₀	190.4 nM
95% CI	116.7 to 315.5 nM

Figure 6. Statistical analysis of intra-assay reproducibility. Calculated cytotoxic index of HT-1080 (A) and MD-MB-231 (B) cells to decreasing concentrations of CMP. (C) EC₅₀ values determined from HT-1080 plate described in Figure 5A.

Assay Z' factors of 0.82 (HT-1080) and 0.64 (MD-MB-231) were calculated, indicating that this assay platform is amenable to screening protocols (Figure 6A, 6B). In addition, using the end-point cytotoxic index from the HT-1080 data, we were able to calculate remarkably consistent pEC₅₀ values from each column of the microplate with a total geometric mean of 198 nM (Figure 6C).

In order to determine inter-assay reproducibility and accuracy, HT-1080 cells were seeded in two 96-well plates at a density of 5,000 cells/well. Random wells of each plate were spiked with independently prepared stocks of CMP at 1000, 500, 200 and 50 nM ($n=6$ per concentration), as illustrated in Figure 7A. The data from both plates were then plotted on different axes and analyzed using linear regression

(Figure 7B). The resulting R^2 value of 0.9588 demonstrates a strong correlation between identically treated wells on separate plates. Additionally, the Z' factors of 0.72 and 0.62 are again indicative of a high quality assay (Figure 7C).

A

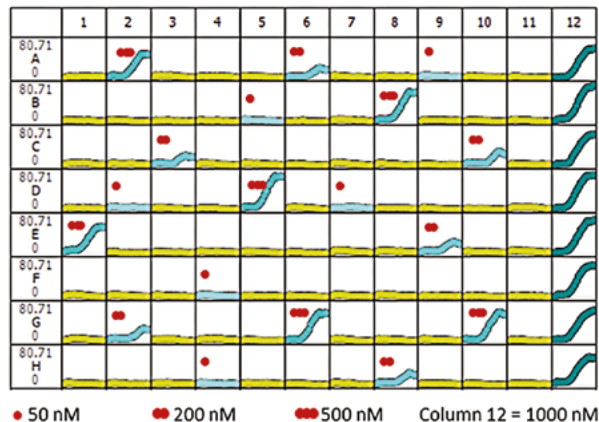
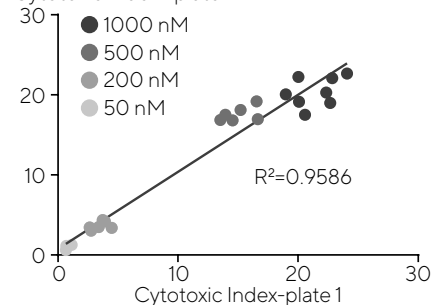


Figure 7. Inter-assay reproducibility of HT-1080 response to CMP. At the 72-hour end-point, Triton X-100 at a final concentration of 0.0625% was added to allow nuclear dsDNA staining by Cytotox Green Dye of all cells present/well. The cytotoxic index was calculated by dividing the number of Cytotox Green fluorescent objects by the total number of DNA containing objects (fluorescent objects counted post Triton X-100 treatment). (A) A 96-well microplate graph showing reproducibility of single-well responses to various concentrations of CMP on HT-1080 cells. (B) Replicate plates of HT-1080 were spiked with identical concentrations of CMP and results were graphed to show correlation. (C) Statistical measurements from the same plates showing Z' factors exceeding 0.60.

B

Inter-Assay Reproducibility

Cytotoxic Index—plate 2



C

Plate 1: N=6 per Treatment

[CMP]	Cytotoxic Index (Mean)	SD	$z' = 0.72$
50 nM	1.09	0.238	
200 nM	3.65	0.514	
500 nM	17.57	0.936	
1000 nM	20.37	1.829	

Plate 2: N=6 per Treatment

[CMP]	Cytotoxic Index (Mean)	SD	$z' = 0.62$
50 nM	0.84	0.224	
200 nM	3.48	0.703	
500 nM	15.06	1.309	
1000 nM	21.45	1.772	

Differentiating Cytotoxic and Cytostatic Treatments

A multiplexed assay capable of measuring cytotoxicity in addition to cell proliferation was created. Nuclight Red HT-1080 cells were seeded at 5,000 cells/well and treated with serially diluted concentrations of SSP, CMP or CHX in the presence of 0.1 μ M Cytotox Green Dye (all data not shown). The Incucyte® Live-Cell Analysis System was used to mask the green fluorescent nuclear signal to quantitate cell death as well as the red fluorescent nuclear signal to monitor cell proliferation kinetic dose response curves for both Cytotox Green positive events as well as nuclear counts of Nuclight Red HT-1080 cells were exported to GraphPad Prism.

Statistical analysis of the area under the curve (AUC) was calculated for time points within the kinetic curves. Replicate AUC values, at peak response, were used to calculate EC_{50} and IC_{50} values. Figure 8 shows the inverse relationship between cell proliferation (nuclear count) and membrane permeability (Cytotox Green positive objects) over time in the presence of SSP. The AUCs were then used to statistically determine at which concentration SSP

exhibited purely cytostatic effects. The concentration at which the AUC of Cytotox Green Object Count/ mm^2 over time was different from the control group was termed cytotoxic and/or cytostatic. Concentrations where the AUC of Cytotox Green Object Count/ mm^2 over time was

not different from that of the control, but the AUC of Nuclear Count/ mm^2 over time was significantly different from the control was termed purely cytostatic. These data show the potential of this kinetic and multiparametric approach to the classification of compounds in drug discovery.

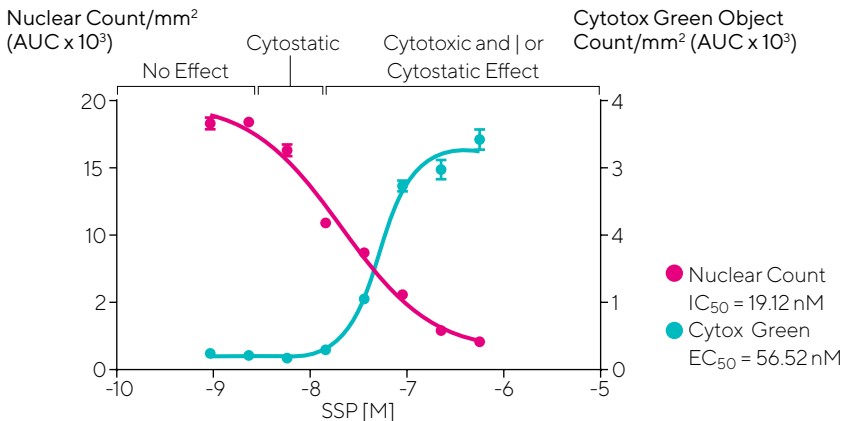


Figure 8. Inter-assay reproducibility of HT-1080 response to CMP. HT-1080 cells were treated with varying concentrations SSP. Dual fluorescent images were used to calculate the area under the curve (AUC) of cell death (Cytotox Green Object Cnt/ mm^2) and cell proliferation (Nuclear Cnt/ mm^2) over time. Average AUC values were then used to calculate EC_{50} and IC_{50} values, respectively. Dunnett's Multiple Comparison Test was used to compare the differences between AUCs at each concentration.

Conclusions

Using the Incucyte® Live-Cell Analysis System in conjunction with the Incucyte® Cytotox Green or Red Dyes as a live-cell, kinetic assay for the measurement of cytotoxicity has demonstrated quantitative and reproducible detection of cell permeability, a hallmark of cell death. This strategy also gives the user the ability to monitor morphological changes in parallel with quantification, the combination of which is a powerful and unique tool for detecting pharmacological or genetic manipulations that alter cell viability. In addition, Nuclight reagents or cells lines, when used with Incucyte® Cytotox Green or Red Dyes and the Incucyte® Live-Cell Analysis System, provide an additional parameter for measuring cytostatic (anti-proliferative) and cytotoxic events.

Key features of the Cytotoxicity Assay are:

- Non-perturbing cytotoxicity reagents are added directly to the cultured cells, removing the need for fluid aspiration steps, thus eliminating cell disruption or loss of impaired cells.

- Data generated using live-cell multi-parametric analysis of cytotoxicity and proliferation delivers more reliable data and allows for differentiation between cytosatic and cytotoxic effects of treatments as well as detection of both short-term and long-term alterations.
- All data points can be validated by individual images or time-lapse movies to confirm processing metrics, significantly enhancing the confidence in the measured response.

References

1. Kepp O, Galluzzi L, Lipinski M, Yuan J, Kroemer G. **Cell death assays for drug discovery.** *Nat Rev Drug Discov* 2011, 10(3):221-237.
2. Kroemer G, Galluzzi L, Vandenabeele P, Abrams J, Alnemri ES, Baehrecke EH, Blagosklonny MV, El-Deiry WS, Golstein P, Green DR, et al. **Classification of cell death: recommendations of the Nomenclature Committee on Cell Death 2009.** *Cell Death Differ* 2009, 16(1):3-11.
3. Abraham VC, Towne DL, Waring JF, Warrior U, Burns DJ. **Application of a high-content multiparameter cytotoxicity assay to prioritize compounds based on toxicity potential in humans.** *J Biomol Screen* 2008, 13(6):527-537.
4. Abassi YA, Xi B, Zhang W, Ye P, Kirstein SL, Gaylord MR, Feinstein SC, Wang X, Xu X. **Kinetic cell-based morphological screening: prediction of mechanism of compound action and off-target effects.** *Chem Biol* 2009, 16(7):712-723.
5. Becker B, Clapper J, Harkins KR, Olson JA. **In situ screening assay for cell viability using a dimeric cyanine nucleic acid stain.** *Anal Biochem* 1994, 221(1):78-84.
6. Chae HJ, Kang JS, Byun JO, Han KS, Kim DU, Oh SM, Kim HM, Chae SW, Kim HR. **Molecular mechanism of staurosporine-induced apoptosis in osteoblasts.** *Pharmacol Res* 2000, 42(4):373-381.
7. Karaman MW, Herrgard S, Treiber DK, Gallant P, Atteridge CE, Campbell BT, Chan KW, Ciceri P, Davis MI, Edeen PT, et al. **A quantitative analysis of kinase inhibitor selectivity.** *Nat Biotechnol* 2008, 26(1):127-132.

4d

Kinetic Assays for Studying Cell Cycle

Real Time Quantification and Visualization of the Events Leading to Cell Arrest, Senescence and Death

Introduction


The cell cycle is a series of growth and development steps that is critical in maintaining cellular homeostasis through signaling pathways, which that control the frequency of DNA duplication and ultimately cell division. Without this regulation, cells can divide in an uncontrolled manner leading to uncorrected mutations and avoidance of programmed cell death. As such, the cell cycle and its tightly regulated checkpoints are targets for cancer therapies aimed at arresting unchecked cell division and promoting apoptosis. Cell cycle regulation also plays a key role in stem cell pluripotency and cell differentiation, being evaluated for enhanced reprogramming efficiency, which holds great promise in regenerative medicine therapies.¹ Analysis of the cell cycle thus holds

significant importance for both cancer and regenerative medicine research, as developing novel, targeted therapies for treating cancer as well as targeting the cell cycle for novel regenerative medicines are both being explored.

Traditional methods to study cell cycle progression are often challenging. Such methods provide only a single time-point or concatenated time-points from either a small number of cells or from cells that are fixed or exhausted during evaluation. Further, they are unable to study the cell cycle over multiple cell divisions within the same cell. Rather, they combine independent, non-integrated solutions for cell cycle labeling, data acquisition and analysis, and complex data analysis is required for evaluation of stages of the

cell cycle. Live-cell imaging and analysis is uniquely suited to providing temporal information on the cell cycle through real-time, automated quantification and visualization of the events leading up to cell arrest, senescence or death. This enables users to generate kinetic, image-based measurements to capture and quantify cell cycle progression over time in a physiologically-relevant context with microplate throughput in living cells.

This chapter demonstrates how the Incucyte® Cell Cycle Assay allows users to quantify cell cycle progression continuously over multiple cell divisions, inside their own incubator, for deeper insights into treatment effects on cell cycle dynamics. This assay features the non-perturbing Incucyte® Cell Cycle

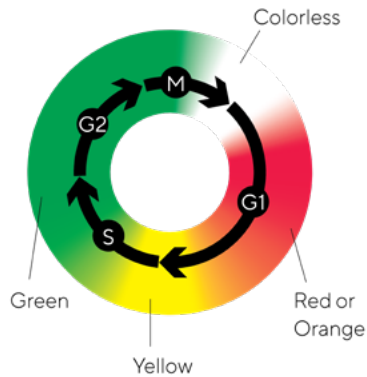
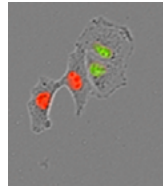


Green | Red Lentivirus or the Incucyte® Cell Cycle Green | Orange Lentivirus for cell cycle labeling. The Incucyte® Cell Cycle Assay also uses simple, validated protocols, easy-to-learn automated image acquisition, and integrated analysis of 96- or 384-well plates to examine cell cycle progression. Additionally the Incucyte® Cell-by-Cell Analysis Software Module enables multiplexing with label-free cell counts with total cell population quantification to determine percentage of cells within each cell cycle phase. Taken together, this system allows users to gain deeper insight into treatment effects on cell cycle dynamics or link cell cycle arrest to morphology and function using unique and accessible approach to live-cell imaging and analysis.

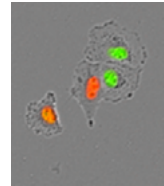
Incucyte® Cell Cycle Assays at a Glance

The Incucyte® Cell Cycle Lentivirus Reagents (Green | Red or Green | Orange) have been developed to distinguish between cells in the G1 and S | G2 | M cell cycle phase without altering cell function. These fluorescent ubiquitination-based cell cycle indicators (FUCCI) provide a homogeneous expression of two fluorescent proteins to distinguish between cells in the interphase or the mitotic phase to enable the visualization of cell cycle progression. These proteins are used to target fluorescence proteins for degradation during certain cell cycle phases, therefore cells will fluoresce green during S | G2 | M and red or orange during G1; cells are colorless during

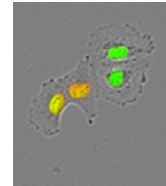
the transition from M to G1 and yellow (expressing green and red, or green and orange, simultaneously) in transition from G1 to S phase. Images of cells expressing Incucyte® Cell Cycle Lentivirus can be acquired and analyzed automatically in the Incucyte® Live-Cell Analysis System to identify phases of cell cycle in individual cells for real-time measurements of cell cycle dynamics. The schematic in Figure 1 shows the expression of green and red, or green and orange, fluorophores across the cell cycle, and the time course of images demonstrate the change in fluorescence as the cell divides. The indicated cell with red fluorescence is in G1 phase at 0 hours. By 4 hours, the cell is transitioning from G1 to S, and at 7 hours, the cell is green indicating S | G2 | M phase. At 9 hours, the cell is mitotic, and by 11 hours daughter cells in G1 are observed.

A**B** 0 h

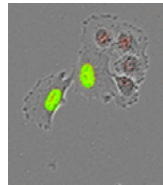
2 h



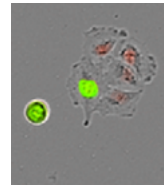
4 h



7 h



9 h



11 h

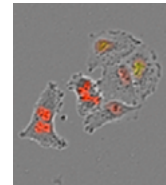


Figure 1. Incucyte® Cell Cycle Lentivirus. Schematic displays the fluorescence expressed at each stage of the cell cycle (A). Cells expressing Incucyte® Cell Cycle Lentivirus will exhibit green fluorescence during S | G2 | M and red or orange fluorescence during G1. Transition from M – G1 is non-fluorescent, and transition from G1 – S displays yellow fluorescence, i.e., both green and red, or green and orange. Images of HeLa cells were acquired on the Incucyte® Live-Cell Analysis System (B). Sequential images show a cycling cell over time starting in G1 at 0 h with red fluorescence.

Incucyte® Cell-by-Cell Analysis enables individual cells in the field of view to be segmented in the phase contrast image, and metrics can be extracted per cell relating to fluorescence within the segmented boundary. Using the integrated analysis software, cell populations can be classified based on fluorescence characteristics. In combination with the Incucyte® Cell Cycle Lentivirus, this enables the percent cells in each phase to be rapidly quantified. Users can visually verify classifications, analyze, and graph to identify trends and generate new insights.

Shortcomings of Traditional Assays	Live-Cell Imaging and Analysis Approaches
<ul style="list-style-type: none">▪ Use single or concatenated time-points from a small number of cells that may be fixed or exhausted.	<ul style="list-style-type: none">▪ Continuous imaging and analysis over time of non-perturbed cells in incubator to study cell cycle dynamics and quantify progression.
<ul style="list-style-type: none">▪ Inability to study multiple cell divisions in the same cell.	<ul style="list-style-type: none">▪ Tracks individually identified phases of the cell cycle in individual cells.
<ul style="list-style-type: none">▪ Challenging to link cell cycle arrest to changes in morphology and function, and drug effects.	<ul style="list-style-type: none">▪ Can readily link changes in cell cycle to concomitant changes in morphology and function to study effects of drugs on regulation.
<ul style="list-style-type: none">▪ Data acquisition and complex analysis complicated by limited throughput and use of non-integrated methods.	<ul style="list-style-type: none">▪ Automated image acquisition and integrated analysis of 96- and 384-well plates in one platform.

Table 1. Shortcomings of Traditional Assays vs Live-Cell Imaging and Analysis Approaches

Sample Results

Quantification of Cell Cycle Phase

The Incucyte® Cell-by-Cell Analysis Software Module enables individual cells in the field of view to be segmented in the phase contrast image so that metrics can be extracted per cell relating

to fluorescence within the segmented boundary. With this integrated analysis software, various cell populations can be classified based on fluorescence characteristics. In combination with the Incucyte® Cell Cycle Lentivirus, this enables the percent of cells in each cell cycle phase to be rapidly quantified, as

demonstrated in Figure 2. Cells expressing high green fluorescence (S | G2 | M) can be studied separately from those expressing high red fluorescence (G1), and transition phases can also be identified with high red and green (G1 – S) or low red and green (M – G1). Both adherent and non-adherent cells can be quantified with this method.

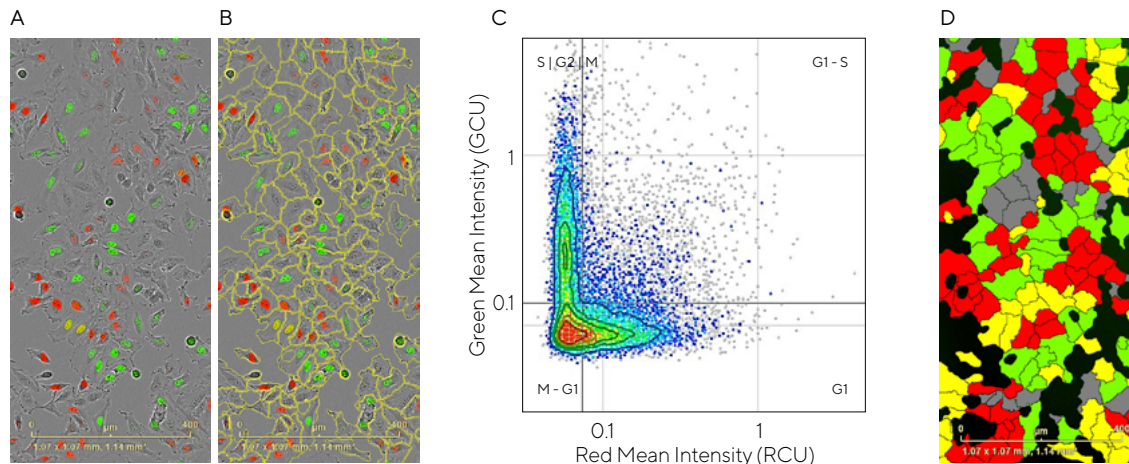


Figure 2. Cell cycle quantification. Images acquired using Incucyte® Cell-by-Cell Analysis Software Module, which allows individual cells to be segmented (A, B). Cells can be classified according to red and green fluorescence intensity (C). Classification mask shows cells identified as red, green, yellow or non-fluorescent (D).

Additionally, cells expressing Incucyte® Cell Cycle Lentivirus can be monitored by counting the number of green and red objects (or green and orange objects, depending upon the lentivirus used) using basic fluorescence segmentation. Cells transitioning from G1 – S appear yellow and can also be quantified by measuring objects with overlapping green and red fluorescence; these objects should be subtracted from the green object and red object counts to avoid over-estimation of these objects. This method enables evaluation of alterations in cell cycle progression in co-culture models, however information on the M – G1 phase is not available as these cells will be non-fluorescent and cannot be distinguished from a secondary non-labelled cell type.

Cell Cycle Synchronization

Cell cycle synchronization is often required to study cell cycle specific mechanisms and regulation. Synchronization results in populations of cells in the same phase which can be examined and quantified using the Incucyte® Cell-by-Cell Analysis Software Module. The DNA synthesis inhibitor Thymidine, is commonly used for synchronization, as it blocks progression beyond the S phase. As seen in Figure 3, HeLa cells expressing Incucyte® Cell Cycle Lentivirus were treated with Thymidine for inhibition of DNA synthesis and cell cycle arrest in the S | G2 | M phase, and a prominently green cell population was observed at 24 h. Immediately following block removal, synchronized cells progressed past the S phase as evidenced by a decrease in the percent green cells followed by sequential peaks in non-fluorescent cells (M – G1 transition), red

cells (G1), yellow cells (green and red, G1 – S transition). As the figure illustrates, the time between peaks of the same color can be considered one full cell cycle, shown by a second peak of green fluorescence at 17 h after block removal as cells returned to S | G2 | M phase. This temporal profiling provides insight into cell proliferation. Additional cell lines synchronized with Thymidine displayed variation in peak-to-peak time (i.e., MDA-MB-231 cells at 16 h, SKOV-3 was 24 h). Comparison of the HeLa non-fluorescent population time course with label-free cell count revealed that the transition between M and G1 is associated with a sharp rise in cell number as cells divide (Figure 3C). This validates that mitosis is occurring during the non-fluorescent M – G1 phase.

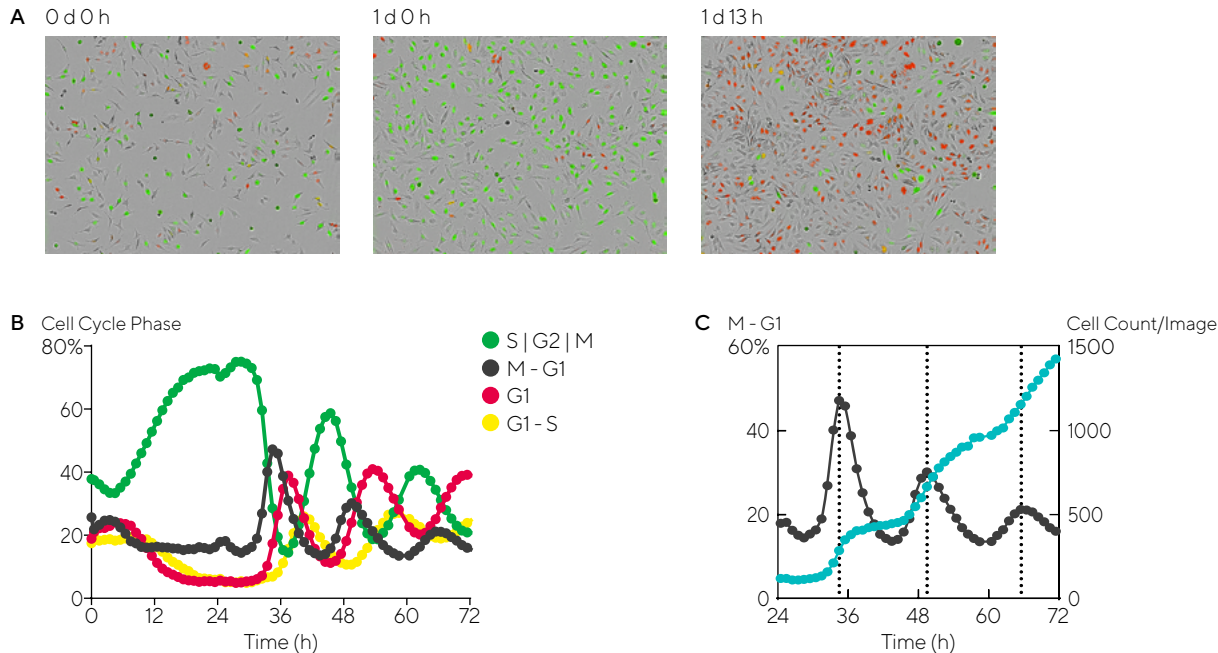


Figure 3. Synchronization of cell cycle phase. (A) Image at 0 h shows unsynchronized cells expressing a mix of red and/or green fluorescence. After 1 day treatment with arresting agent, Thymidine (2.5 mM, 24 h), cells have arrested in S | G2 | M and are prominently green. Thymidine block was released at 1 d and 13 h later, a peak in red fluorescence is observed as synchronized cells reach G1. (B) Quantification was achieved using Incucyte® Cell-by-Cell Analysis. Time course of cell cycle phase shows cells accumulating in S | G2 | M during the first 24 h of Thymidine treatment. When the block is removed, consecutive peaks in M - G1, G1, and G1 - S are observed. (C) Overlay of cells in M - G1 (dark gray) with cell count (teal) show increase in cell number during this transition period consistent with cell division.

Cell Cycle Modulation

Modulation of the cell cycle is a target for new therapies and can be induced *in vitro* through serum starvation or the addition of chemical agents, such as the anti-cancer therapeutic 5-fluorouracil (5-FU). Incucyte® Live-Cell Imaging and Analysis was used to examine targeted cell cycle therapies using 5-FU and cisplatin. 5-FU acts through depletion of nucleotides for

DNA synthesis while cisplatin acts as a DNA intercalator, causing checkpoint activation and cell cycle arrest in the S | G2 | M phase. HT-1080 fibrosarcoma cells expressing Incucyte® Cell Cycle Lentivirus were treated with 5-FU (0–50 μ M), which increased the percent of cells in G1 over 24 h, indicating cell cycle arrest. In contrast, treatment with cisplatin (0–50 μ M) reduced the percent cells in G1 as cells arrested in S | G2 | M. As

seen in Figure 4, these effects were both time- and concentration-dependent for cell cycle arrest. Figure 4A shows a temporal 96-well plate overview of percent cells in G1 phase, providing insight into compound effects, assay robustness, and well-to-well reproducibility. EC₅₀ values were calculated with Incucyte® integrated software to quantify compound potency.

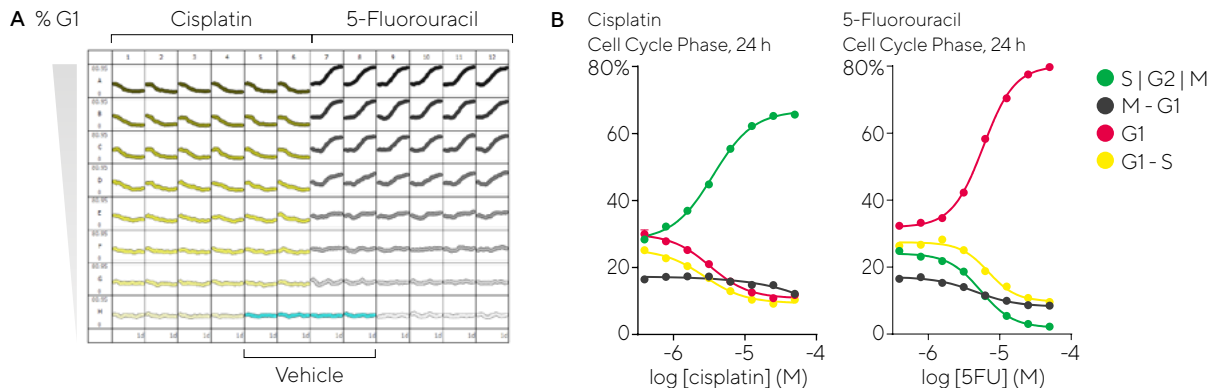


Figure 4. (A) Concentration dependence of cell cycle modulators. HT-1080 cells expressing Incucyte® Cell Cycle Lentivirus were treated with cisplatin (0–50 μ M) or 5-FU, (0–50 μ M). Plate view shows the time course of percentage of cells in G1 phase in each well of a 96-well plate, over 1 day treatment with cisplatin or 5-FU. (B) Concentration response curves indicate the efficacy of cisplatin and 5-FU at 1 d and percent change in each population over the concentration ranges tested (B).

Distinguishing Cell Cycle Arrest from Apoptosis

Along with the Incucyte® SX5 Live-Cell Analysis System, which uses three fluorescent channels (green, orange, and Near IR) the Incucyte® Cell Cycle Green/Orange Lentivirus can be multiplexed with the Incucyte® Annexin V NIR Dye to study the effect of experimental treatments on cell cycle arrest and cell viability. Figure 5 illustrates the effect of different compound effects on the temporal relationship between cell cycle arrest and apoptosis. Phase and fluorescence images acquired three days post-treatment showed the change in cell number and fluorescence induced by each compound.

AU565 and MDA-MB-231 cells treated with vehicle control showed a mixture of green and orange fluorescent cells, and a small dip in the percent of orange fluorescent cells corresponded to a small peak in the percent of green fluorescent and vice versa. A very low number of cells were apoptotic (Annexin V NIR positive) since these cells were healthy and proliferating.

Next, AU565 and MDA-MB-231 cells were treated with carboplatin, which is a non-selective DNA intercalator that induces rapid arrest in S | G2 | M via a similar mechanism to cisplatin.⁴ A rapid increase in the percentage of green cells in both cell types was observed within 48 h, remained stable until approximately 72 h, at which point the cells began to undergo apoptosis. Carboplatin was also found to have a strong morphological effect on MDA-MB-231 cells as shown by phase contrast images.

Cells were also treated with lapatinib, a dual HER2/EGFR inhibitor that targets receptors expressed by AU565.⁵ Lapatinib caused AU565 cells to undergo cell cycle arrest in G1 which increased the percent of orange cells over time while decreasing other populations. This was not observed in MDA-MB-231 cells, which lack the cell surface receptors targeted by lapatinib. Rather, MDA-MB-231 cells continued to proliferate in the presence of lapatinib.

Finally, the cytotoxic DNA synthesis inhibitor camptothecin was seen to

cause a transient increase of AU565 in the G1 phase that peaked at 48h before diminishing. Additionally, while the apoptotic cells increased over the course of the assay, the percentage of S | G2 | M cells was dropped. In MDA-MB-231 cells, the percent of S | G2 | M cells decreased along with an increase in the percent of apoptotic cells, and the percent of G1 cells plateaued 8 h post treatment. These studies revealed that camptothecin had a cell cycle-dependent toxicity and demonstrated an increased potency on cells in S | G2 | M as compared to those in G1. This correlated with the camptothecin mechanism of action of S (DNA synthesis) phase inhibition and aligns with previous reports that apoptotic population cells treated with camptothecin is derived from cells in S phase.

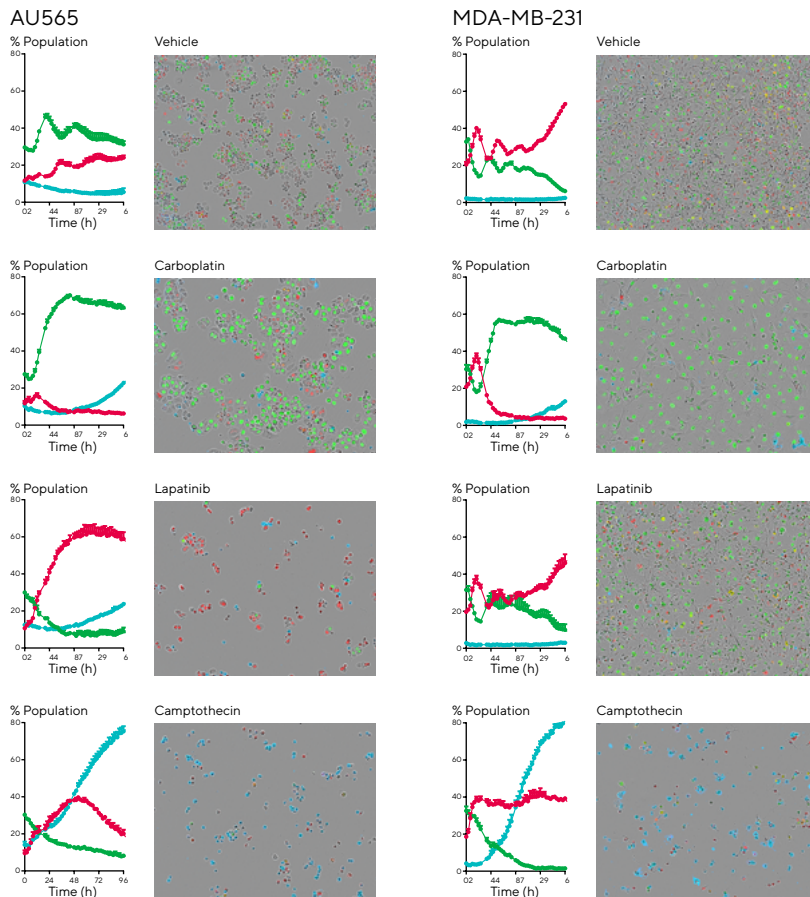


Figure 5. Combining Incucyte® Cell Cycle Lentivirus and Incucyte® Annexin V NIR Dye enables added insight into compound mechanism. AU565 and MDA-MB-231 cells expressing Incucyte® Cell Cycle Green/ Orange Lentivirus were treated with carboplatin (100 μ M), lapatinib (0.1 μ M) and camptothecin (10 μ M) in the presence of Incucyte® Annexin V NIR Dye (1:200). Scans were acquired and analyzed in the Incucyte® SX5 using the Incucyte® Cell-by-Cell Analysis Software Module. Time-courses show the populations of cells in S | G2 | M (green) or G1 (red) overlaid with the population of Annexin V positive objects (teal). Carboplatin arrests cells in S | G2 | M. Lapatinib targets specific cell receptors and is, therefore, effective on AU565 but not MDA-MB-231. Camptothecin induces apoptosis in both cell lines. Phase and fluorescence (green, orange, NIR) blended images show AU565 or MDA-MB-231 cells at 3 d post treatment.

Effect of Differentiation on Cell Cycle and Function

Incucyte® Live-Cell Imaging and Analysis and Incucyte® Cell Cycle Lentivirus Reagents can be used to quantify cell cycle phase by determination of percentage of cells in each phase of the cell cycle. Non-fluorescent metrics can also be derived from the HD Phase channel relating to cell count, area, and eccentricity. Combining these data with the reagent provides insight into morphological changes and cell behavior during differentiation (refer to Chapter 5 – Kinetic Assays for Immune Cell Models for more details).

THP-1 cells are a common *in vitro* model of human monocyte function and differentiation into macrophages.^{7,8} The relationship between cell differentiation and cell cycle was explored using THP-1 cells expressing Incucyte® Cell Cycle

Lentivirus (Figure 6). Cells were stimulated with PMA (100 nM) or LPS with IFN γ (both 100 ng/mL). Cell cycle phase studies revealed that both stimulants arrested cells in G1, evidenced by increased expression of red fluorescence. Morphological differences between cells activated with PMA vs. LPS | IFN γ were also observed, in which cells changed from a non-adherent to an adherent morphology following PMA treatment, with increased cell area and eccentricity. However, cells treated with LPS | IFN γ exhibited a mixed phenotype with small, rounded, star-like shapes. Despite cell cycle arrest, cell function remained intact and stimulated cells (PMA and LPS | IFN γ) were able to phagocytose bioparticles. To determine phagocytic activity, the total phase channel confluence of pHrodo® Zymosan bioparticles was compared in the presence and absence of cells treated

with PMA or LPS | IFN γ . Without cells, bioparticles settled to the bottom of the well within 12 h and the confluence remained constant for the remainder of the assay, whereas Bioparticles were engulfed when in the presence of functionally active cells were present as shown by decrease in confluence. Cells differentiated with PMA were found to be highly phagocytic (30% bioparticle clearance), while LPS | IFN γ treatment were found to be less phagocytic (15% bioparticle clearance). From this study, it was concluded that LPS | IFN γ stimulation increases the phagocytic capacity of THP-1 cells, while PMA treatment produces a macrophage-like phenotype with greater phagocytic potential.^{8,7}

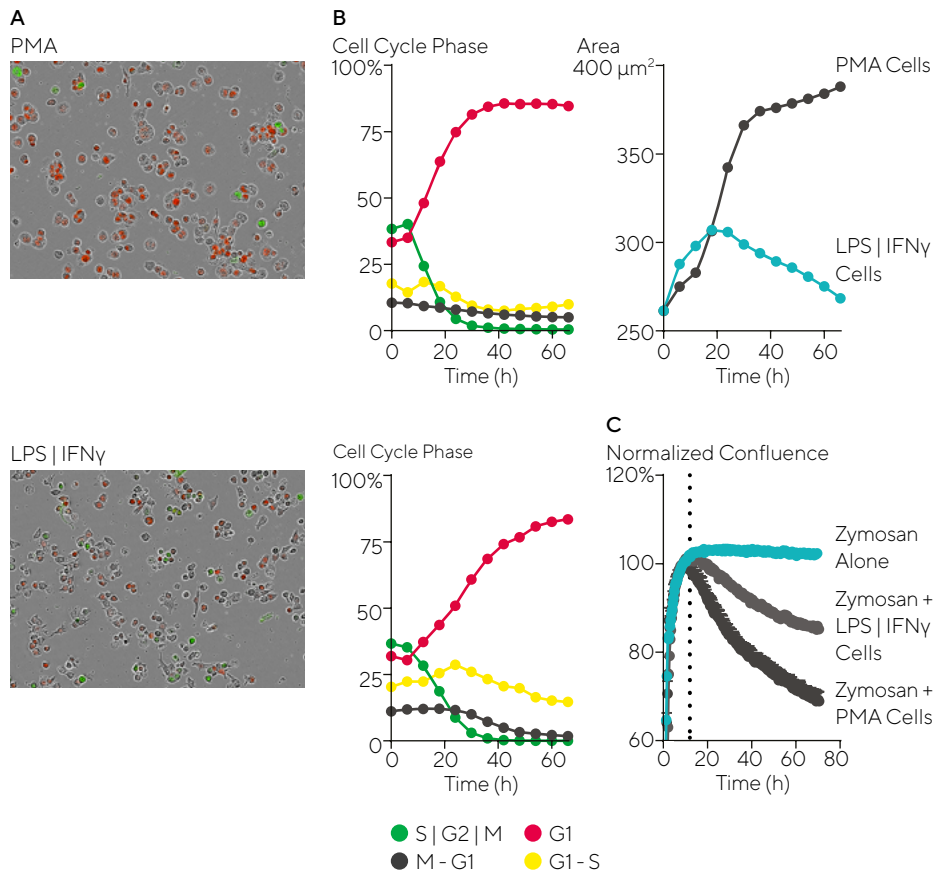


Figure 6. Differentiation of THP-1 arrests cell cycle, alters morphology, and results in phagocytic cells. THP-1 cells expressing Incucyte® Cell Cycle Lentivirus were differentiated by treatment with PMA (100 nM) or LPS | IFN γ (100 ng/mL each) for 62 h (A). Blended phase and fluorescence images show cells with altered morphology and a high proportion of red cells. Time courses of cell cycle phase indicate that both treatments induce arrest in G1, with PMA acting more rapidly than LPS | IFN γ . Average cell area shows a rapid increase in the size of PMA treated cells while LPS | IFN γ -treated cells become slightly enlarged before returning to approximately 260 μm^2 . To assess functional capacity, stimulated cells were washed with media to remove non-adherent and dead cells, and Zymosan bioparticles (1.5 μg per well) were added (B). Total confluence was measured using basic phase segmentation, and once the bioparticles had settled (confluence of bioparticles alone reaching a maximum value at 12 h), confluence was normalized to 100%.

Immune Cell Killing and Cell Cycle Arrest

Complex co-cultures can also be evaluated using the Incucyte® Cell Cycle Assay, which is especially useful for studying the interactions between tumor cells and immune cells *in vitro* and the mechanism through which immune cells induce cell death or suppress tumor cell growth (refer to Chapter 5 – Kinetic Assays for Immune Cell Models for more details). Figure 7 illustrates the dynamic interaction between peripheral blood mononuclear cells (PBMCs) that were co-cultured with target tumor cells expressing Incucyte® Cell Cycle Lentivirus. Basic fluorescence masking and analysis of green and red objects was used to continuously monitor the tumor cell cycle status as activated immune cells induced apoptotic cell death over the course of the assay. T47D cells

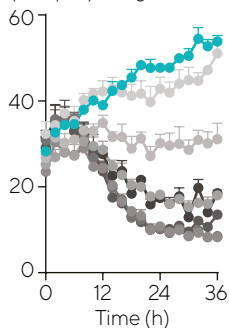
expressing Incucyte® Cell Cycle Lentivirus were cultured with increasing densities of activated, freshly isolated PBMCs. Based on the drop in green object count, it was determined that cells in the S | G2 | M phase were preferentially targeted while PBMCs affected cells in the G1 phase less. Red object count decreased only when T47D cells were cultured with the two highest PBMC densities and at a slower rate than the green objects. The red object count continued to increase at the lower PBMC densities, suggesting that cells were arresting.

However, compared to the T47D cells the MDA-MB-231 cells exhibited a different behavior in the presence of PBMCs. The green object count did not decrease, but rather plateaued, and the red object

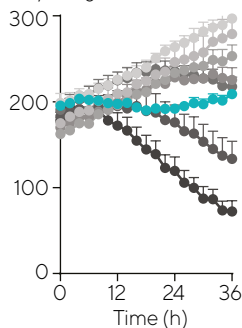
count was unaffected by the immune cells' presence. Taken together, this suggested a cytostatic mechanism that is consistent with reports that T cells can use via IFN γ -mediated cell cycle arrest to suppress tumor cell growth.⁹

T47D

S | G2 | M / image

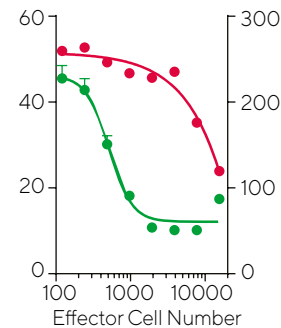


G1 / image



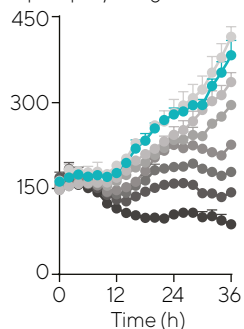
S | G2 | M

at 36 h

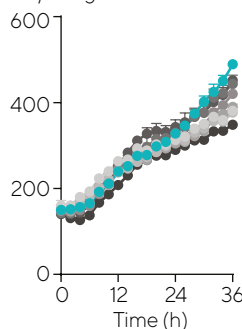


MDA-MB-231

S | G2 | M / image



G1 / image



S | G2 | M

at 36 h

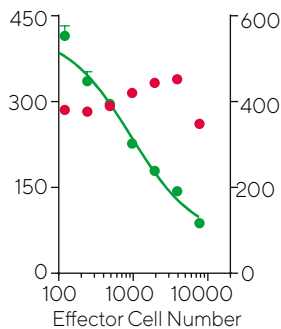
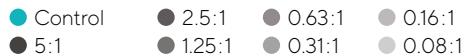


Figure 7. Incucyte® Cell Cycle Lentivirus illustrates mechanism of T cell interactions with tumor cells. T47D and MDA-MB-231 breast cancer cells expressing Incucyte® Cell Cycle Lentivirus were incubated with increasing ratio of pre-activated PBMCs (anti-CD3, 72 h). Phase and fluorescence images were acquired over 3 days and green and red fluorescent objects were counted using basic fluorescence segmentation. S | G2 | M cells were quantified by subtracting overlap (yellow) object count from green object count. G1 cells were similarly quantified. Time courses for T47D cells (top row) show a density-dependent decrease in S | G2 | M and G1 cells, with cells in S | G2 | M (green objects) being affected more rapidly and at lower PBMC density than cells in G1 (red objects). This is highlighted by the data showing cell populations at 36 h, which show a reduction of cells in S | G2 | M at low PBMC densities, while loss of cells in G1 is only observed at the two highest PBMC densities. Time courses for MDA-MB-231 show that only cells in S | G2 | M are affected by the presence of activated PBMCs while the number of cells in G1 is unaffected. This is confirmed by data showing populations at 36 hours.



Conclusions

The Incucyte® Live-Cell Analysis System, Incucyte® Cell Cycle Lentivirus, and Incucyte® Cell-by-Cell Analysis Software Module provide a complete, turnkey solution for analyzing cell cycle progression. Taken together, this system offers a number of important advantages over other methods:

- The system enables the study cell cycle progression in living cells over multiple cell divisions, in a variety of cell types, within the physiologically relevant environment of the incubator.
- The non-perturbing Incucyte® Cell Cycle Lentivirus provides homogeneous expression of fluorescent proteins to distinguish between cells in the interphase or the mitotic phase, and to enable the visualization of cell cycle progression.
- Acquisition and analysis of cell cycle data is continuous, requiring no fixing or lifting, and can be performed in 96- and 384-well plates to enable high-throughput study of drug-induced treatment effects on cell cycle transitions or linking cell cycle modulation to function.
- The Incucyte® Cell-by-Cell Analysis Software Module, combined with the Cell Cycle Lentivirus, enables direct quantitative measurement of cell cycle progression, which is useful for the evaluation of drug treatment effects, or link drug-induced cell cycle arrest to cell differentiation.
- Combining cell cycle data with cell morphology, function and cell health readouts enable multiple aspects of a treatment or culture conditions to be considered in a single well, distinguishing between events such as cell cycle arrest and apoptosis.
- More advanced cell models, such as co-cultures with immune cells, can also benefit from the information yielded by the Incucyte® Cell Cycle Lentivirus, under physiologically relevant conditions for greater understanding of temporal patterns of cell cycle progression.
- Perform multiplexing studies to understand the effects of differentiation on cell cycle and impact on cell functions, such as phagocytosis.

The Incucyte® Cell Cycle Assay enables users to overcome many of the limitations imposed by other methods, and provides new insights into growth, development, and dysregulation of cells during cell cycle for enhanced understanding cell cycle regulation and assessment of drug effects.

References

1. Hindley C, Philpott A. **The cell cycle and pluripotency.** *Biochem J.*,2013, 451(2):135-143. doi:10.1042/BJ20121627
2. Yoshikawa R, et al. **Dual antitumor effects of 5-fluorouracil on the cell cycle in colorectal carcinoma cells: a novel target mechanism concept for pharmacokinetic modulating chemotherapy.** *Cancer Research*, 2002, 61(3):1029 – 1037/
3. Basu A and Krishnamurthy, S. **Cellular Responses to Cisplatin-Induced DNA Damage.** *Journal of Nucleic Acids*, 2010, 1 – 16.
4. Dasari S, and Tchounwou P. **Cisplatin in cancer therapy: molecular mechanisms of action.** *European Journal of Pharmacology*, 2014, 364 – 378.
5. 9. Tang L, et al. **Lapatinib induces p27Kip1-dependent G1 arrest through both transcriptional and post-translational mechanisms.** *Cell Cycle*, 2013, 12(16):2665 – 2674.
6. Johnson N, Tony TC, and Parkin JM. **Camptothecin causes cell cycle perturbations within T-lymphoblastoid cells followed by dose dependent induction of apoptosis.** *Leukemia Research*, 1997, 21(10):961 – 972.
7. Park EK, et al. **Optimized THP-1 differentiation is required for the detection of responses to weak stimuli.** *Inflammation Research*, 2007, 56:45 – 50.
8. Widdrington JD, et al. **Exposure of Monocytic Cells to Lipopolysaccharide Induces Coordinated Endotoxin Tolerance, Mitochondrial Biogenesis, Mitophagy, and Antioxidant Defenses.** *Frontiers in Immunology*, 2018, 9:2217
9. Kakimi K, et al. **CTLs regulate tumor growth via cytostatic effects rather than cytotoxicity: a few T cells can influence the growth of many times more tumor cells.** *Onc Immunology*, 2014, 4(3):e970464.

Kinetic ATP Metabolism Assays

Direct, Real-Time Visualization and Measurement of ATP in Living Cells

Introduction

A key discovery by Warburg and Cori decades ago began a new era of investigation into the metabolic changes that occur in cancer. Their finding that cancer cells consume glucose in the presence of oxygen and secrete lactate, termed “the Warburg effect”, has since been documented in a variety of cancers¹. Since then, altered tumor metabolism observed in different types of tumors, and even the subpopulations of cells within them, has been established as a hallmark for cancer. These cellular bioenergetics and metabolic reprogramming have been extensively studied as the means through which tumor development and progression are supported via increased energetic, biosynthetic, and redox demands. Following numerous studies across a various tumor types, it was discovered that one of the common

metabolic requirements for cancer cells has been the dependence on glucose and glutamine, both of which can be used for the production of adenosine triphosphate (ATP). Characterizing ATP metabolism continues to hold promise for identifying and exploiting this process for the development of new therapeutic approaches.

A variety of traditional reagents and methods have been used to assess metabolic perturbation, such as mass spectrometry, biochemical detection methods, and the detection of by-products of metabolism. These methods, however, are not without their limitations. Traditional end-point assays provide only limited kinetic information at best, and results can be compromised due to varying cell densities within wells, requiring normalization for accurate data analysis. These assays also prevent

morphological assessment of changes that accompany metabolic perturbations, either by damaging the cells or due to the lack of integrated cell imaging and analysis. End-point assays are unable to provide long-term temporal information, missing key mechanistic insight to changes in ATP production over time, and may be unable to differentiate the generation of ATP from either glycolytic or oxidative phosphorylation. Further, they are not able to identify metabolic changes from specific cell types or populations in co-culture models, which are now a commonplace model for *in vitro* translational research. This speaks to the need for a practical, consistent method to assess metabolic changes without perturbation, concurrent assessment for phenotypic change, and the ability to separate changes in more complex translational models such as co-cultures or those that include stromal components.

In this chapter, we will examine how the Incucyte® ATP Assay presents a solution for the challenges to assess metabolic change *in vitro* that are imposed by traditional methods. The cornerstone of the assay is the non-perturbing Incucyte® CytoATP Lentivirus which encodes an ATP binding indicator. Expression of this reagent enables detection of cell-type specific changes in complex co-culture models, and along with optimized protocols, allows for the direct measurement of cytosolic ATP and the ability to differentiate between glycolytic and oxidative phosphorylation pathway usage. When used in conjunction with the Incucyte® SX5 Live-Cell Analysis System (configured with the Incucyte® SX5 Metabolism Optical Module) and the Incucyte® ATP Analysis Software Module, this assay enables measurement of metabolic changes in physiologically relevant conditions, allowing for long-term, temporal monitoring of changes in ATP, coupled with the ability to qualitatively monitor associated changes in cell morphology in living cells, in real time.

Furthermore, due to direct, ratiometric ATP measurements, data generated is independent of cell number or indicator expression level, thus alleviating any need for secondary normalization. In contrast to other methods, this assay is able to distinguish cell-type specific changes in ATP in mono- and co-cultures,

Incucyte® ATP Assays at a Glance

In order to study changes in cytosolic ATP, Incucyte® Live-Cell Imaging and Analysis utilizes an end-to-end solution, consisting of instrumentation, software and reagents. The Incucyte® CytoATP Lentivirus Kit includes a novel, non-perturbing ATP-binding indicator (Incucyte® CytoATP Lentivirus) and the ATP nonbinding control (Incucyte® CytoATP Non-binding Control Lentivirus) for direct measurement of ATP in cancer cell lines. Both of these reagents are identical, single cassette, dual fluorescent reporters comprised of two fluorescent proteins tethered by an ATP binding domain, with the exception of two mutations that prevent ATP binding

in the Incucyte® CytoATP Non-binding Control. Both lentiviruses are driven by an EF-1 α promoter with puromycin selection to allow generation of cell lines or clones which stably express their respective single cassette, genetically encoded, dual fluorescent (cpmEGFP and mKO κ) indicators. Use of the Incucyte® CytoATP Non-binding Control Lentivirus enables calculation of the Corrected ATP Ratio, minimizing the effect of experimental artifacts that can affect fluorescence output (e.g. pH) and setting the detection limit. The Incucyte® SX5 configured with the Incucyte® SX5 Metabolism Optical Module and the Incucyte® ATP Analysis Software Module captures and analyzes ATP-dependent fluorescent changes over time. Images of cells expressing the dual fluorescent CytoATP indicators are acquired at a fixed emission of 578 nm for both the 485 nm and 535 nm excitation wavelengths. The ratio of fluorescence intensity of those images (485X | 578M) | (535X | 578M) is used to evaluate dynamic population changes in ATP over time. This approach allows for reliable intra- and

inter-assay data generation which is not affected by changes in cell number and allows for evaluation of complex cancer co-cultures models.

Shortcomings of Traditional Assays	Live-Cell Imaging and Analysis Approaches
<ul style="list-style-type: none">▪ Use single or concatenated time-points requiring cell lysis or short-term analysis of live cells for a few hours.	<ul style="list-style-type: none">▪ Continuous, automated live-cell imaging and analysis for over 72 h with continuous incubation in a physiologically relevant environment.
<ul style="list-style-type: none">▪ May use indirect, byproduct measurements of metabolism.	<ul style="list-style-type: none">▪ Novel, non-perturbing Incucyte® CytoATP Lentivirus for direct measurement of cytosolic ATP in live cells.
<ul style="list-style-type: none">▪ Unable to distinguish cell-type specific metabolic changes in complex co-cultures, ATP measured for entire culture.	<ul style="list-style-type: none">▪ Can distinguish cell-type specific metabolic changes in co-cultures using a genetically encoded sensor expressed in a single cell type.
<ul style="list-style-type: none">▪ Cannot simultaneously assess morphology changes associated with ATP changes.	<ul style="list-style-type: none">▪ Captures HD phase contrast images at every time point for simultaneous temporal assessment of morphology changes and direct measurement of ATP.

Table 1. Shortcomings of Traditional Assays vs Live-Cell Imaging and Analysis Approaches

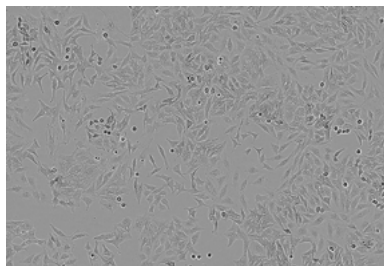
Sample Results

Non-Perturbing, Direct Measurement of ATP Modulation in Living Cells

As detailed previously, the Incucyte® CytoATP Lentivirus Kit is compatible with a variety of cells types and can be used for direct measurement of ATP in living cells grown in either mono- or co-cultures. Both glycolysis and oxidative phosphorylation (OXPHOS) generate cellular ATP. To verify the assay's ability to track ATP dynamics in living cells, the experiment in Figure 1 was performed to illustrate the efficient, non-perturbing labeling of living HeLa cells and direct

measurement and tracking of cytosolic ATP. The Incucyte® CytoATP Lentivirus Kit was used to label the cells, followed by puromycin selection to produce a stable, expressing population. Images were acquired and analyzed at 20 min intervals in dual excitation, single emission Ratio Mode. Two baseline scans were performed, which showed equal starting ratios across each treatment condition before the addition of compounds. As shown in Figure 1A and 1B below, the Incucyte® SX5 Live-Cell Analysis System captured the morphology and proliferation respectively of parental and CytoATP HeLa cells, which was unchanged due to

the non-perturbing nature of the reagent. Figure 2C shows the effect of combined treatment with 2-deoxy-D-glucose (2-DG) and potassium cyanide (KCN), illustrating a concentration-dependent depletion of ATP when glycolysis and oxidative phosphorylation were simultaneously blocked.

A Parental

CytoATP

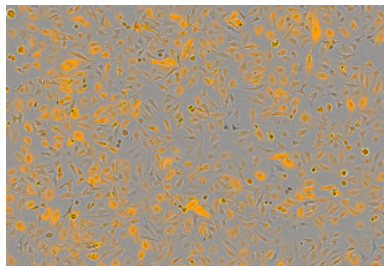
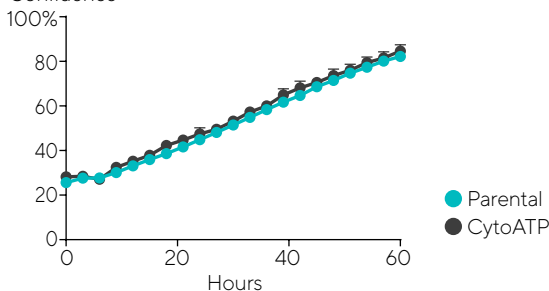
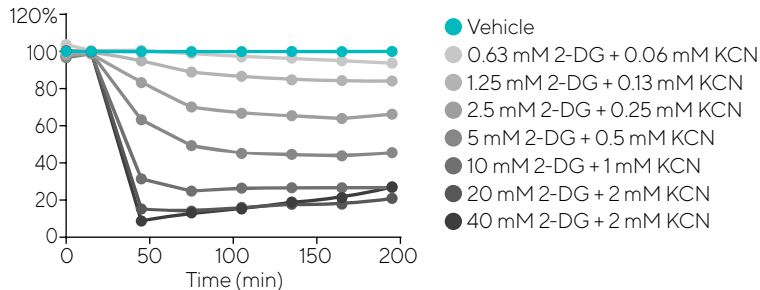
**B** Confluence**C** ATP Relative to Vehicle

Figure 1. Non-perturbing labeling of living cells enables direct measurement of cytosolic ATP/ HeLa cells were infected with Incucyte® CytoATP Lentivirus and subjected to puromycin selection to generate a stably expressing population. Morphology (A) and proliferation (B) of CytoATP-expressing cells were unchanged compared to parental cells. (C) HeLa cells stably expressing CytoATP seeded at 4,000 cells/well in a 96-well microplate were exposed to a combined treatment of 2-deoxy-D-glucose (2-DG) and potassium cyanide (KCN). Quantification of CytoATP fluorescence images captured over 3 hours reveals a rapid, concentration-dependent depletion of ATP resulting from concurrent glycolysis and oxidative phosphorylation blockade.

In another pharmacological blockade of both glycolysis and oxidative phosphorylation, A549 cells stably expressing Incucyte® CytoATP Lentivirus were treated with a combination of 2-DG (0.6 – 40 mM) and KCN (0.06 – 4 mM). A rapid concentration-dependent depletion of ATP was observed, with the highest concentrations dropping ATP close to the limit of detection within 20 min of treatment

(Figure 2B). A small, transient increase in the CytoATP readout was, observed at the first time point following treatment due to a temperature-dependent decrease in the CytoATP Lentivirus K_d . Color-scaled ratio images within the Incucyte® ATP Analysis Software Module were also used to examine the treatment-induced effects on ATP. In the vehicle-treated wells at the top of the plate, the cells appear bright yellow while

2-DG + KCN treated cells have lower ATP levels as depicted by progressively dimmer yellow signal with increasing concentration down the plate (Figure 2C). This assay was repeated across seventeen cell lines (data not shown), confirming the ability of the CytoATP Lentivirus and CytoATP Non-Binding Control Lentivirus to provide direct, live-cell measurements of rapid ATP changes.

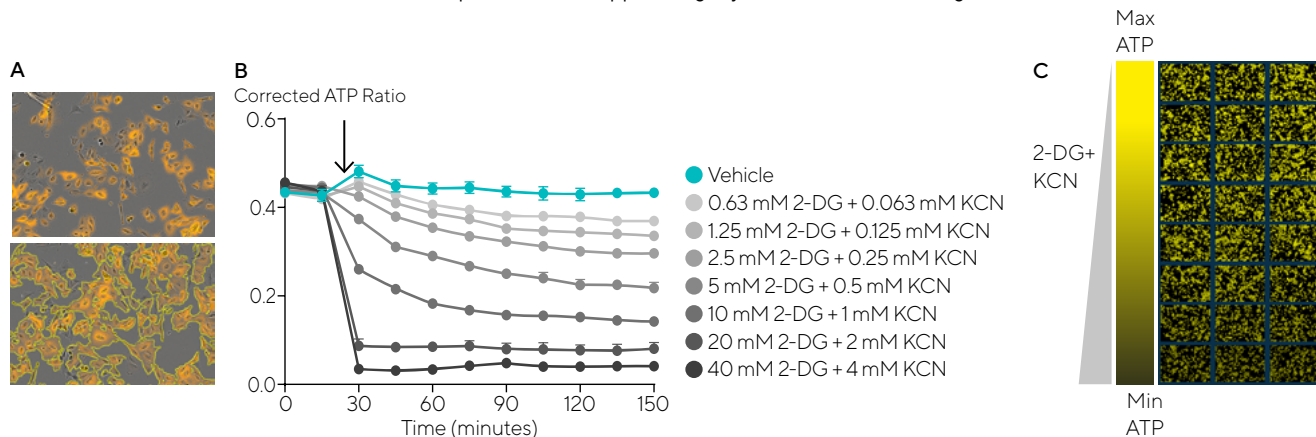


Figure 2. Direct measurement of ATP in live cells. Images of A549 cells stably expressing Incucyte® CytoATP indicators are segmented (yellow outlines, bottom half of image) based on 535X | 578M fluorescence (A). Analysis demonstrates a rapid, concentration-dependent decrease in ATP following combined 2-DG and KCN treatment blockade of glycolysis and OXPHOS, respectively (B). Color-scaled ratio images provide visualization of concentration-dependent ATP depletion in cells treated with 2-DG + KCN compared to vehicle (C).

ATP Measurement Independent of Cell Number

Unlike many standard metabolic assays, the CytoATP Lentivirus enables direct ratiometric ATP measurements independent of cell number and indicator expression levels, which can be altered with metabolic perturbations that affect cellular growth. To demonstrate this capability, HeLa cells stably expressing CytoATP Lentivirus or Non-binding Control Lentivirus were seeded at 4,000 cells/well and 8,000 cells/well in a 96-well microplate. To induce ATP depletion, cells were treated with both 2-DG (0.6 - 40 mM) and KCN (0.06 - 4 mM) and then monitored in the Incucyte® SX5 Live-Cell Analysis System over the next 2 hours. After this time, the same plate of cells

was used for comparative measurement of ATP via CellTiter-Glo® (CTG), as CTG measurements were previously confirmed to be comparable between parental cells and those stably expressing CytoATP indicators (separate study, not shown). As shown in Figure 3A, the color-scaled ATP Ratio images demonstrated similar cytoplasmic ATP levels between the two plating conditions. At both seeding densities, vehicle-treated cells appeared a brighter yellow than 2-DG+KCN treated cells. Concentration-response curves were generated using data collected at 2 hours. The overlay of curves generated from the two plating densities confirmed that CytoATP measurements were independent of cell number (Figure 3B). Additionally, across all treatment conditions, the CTG

measurements taken from the 8,000 cells/well density were consistently about 2-fold higher than those taken from the 4,000 cells/well density (Figure 4C) which was as expected given the cell density dependence of CTG. Notably, there was a minimal difference in confluence between the treatment groups across wells seeded with the same cell density. The slight decrease in confluence observed at the highest treatment concentration was most likely due to a change in morphology as opposed to cell death. As such, the differences in CTG values between treatments corresponded to lower ATP levels within the cells, which was supported by the Incucyte® ATP Assay.

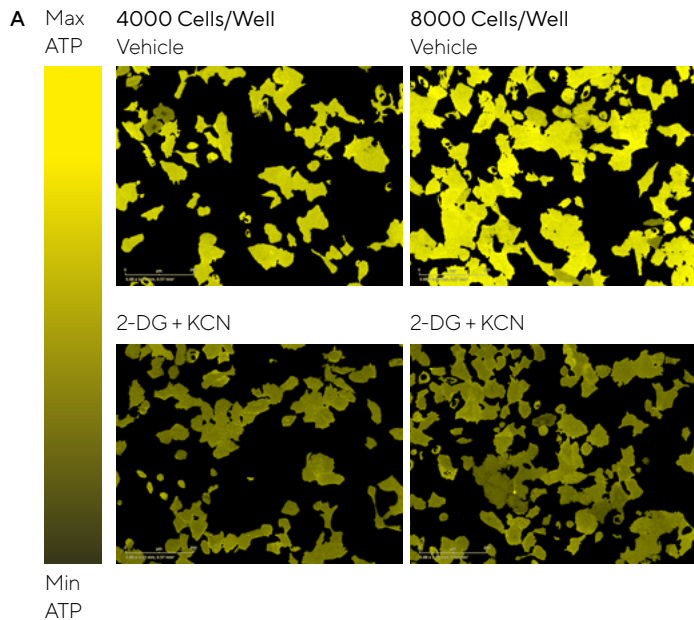
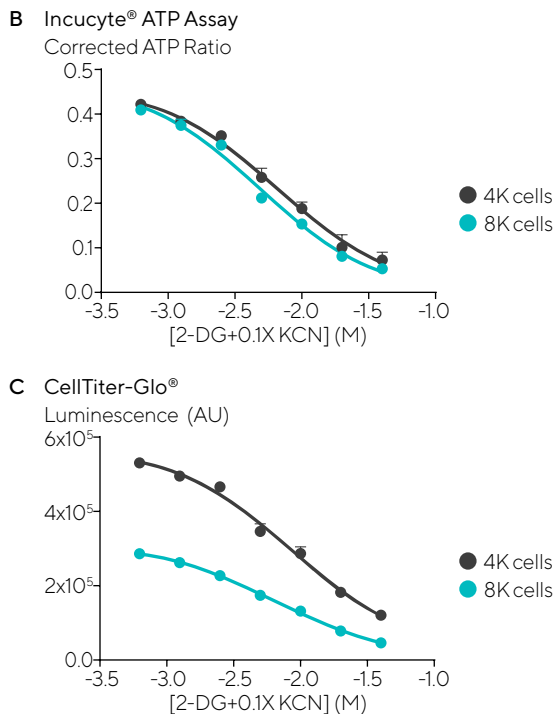


Figure 3. Ratiometric output enables measurement of ATP independent of cell number. Color-scaled ratio images of HeLa cells stably expressing CytoATP seeded at 4,000 or 8,000 cells per well and exposed to vehicle or 2-DG (20 mM) and KCN (2 mM) (A). End-point (2 h) measurement of ATP ratio using Incucyte® ATP Assay is independent of cell number (B) while CellTiter-Glo® luminescence signal from the same cells depends on cell density (C).



Effect of GLS-1 Inhibition on ATP in Mono- and Co-Culture Models

One limitation of traditional approaches is the inability to distinguish cell-type specific metabolic changes in complex co-cultures, as they often measure ATP for the entire culture. To demonstrate this capability, the effect of the glutaminase inhibitor CB-839 on ATP was characterized in both mono- and co-culture models using the Incucyte® ATP Assay (Figure 4). For this experiment, panels of four triple-negative breast cancer (TNBC) cell lines (BT-20, HCC38, HCC1806, and MDA-MB-231) and four receptor-positive breast cancer (MCF-7, ZR-75-1, AU565, and SK-BR-3) cell lines stably expressing the CytoATP indicators were generated. Cells were cultured alone or in co-culture with CCD14086SK fibroblasts to model stromal-tumor cell nutrient exchange and treated with CB-839 (1.4 nM–1 μ M) CB-839 treated cells in monoculture displayed a concentration-dependent depletion

of ATP in the TNBC line HCC38 that was maintained throughout the 72 h time course. All TNBC lines tested were found to display similar results. Alternatively, there was little to no effect on ATP in the the majority of receptor-positive cell lines treated with CB-839, with the exception of MCF-7 cells, which demonstrated a pronounced, transient depletion of ATP and full recovery within 48 h. This insight would have not been possible with traditional assays that lack the capability to capture kinetic live-cell ATP measurements in long-term experiments (Figure 4B).

In co-culture with CCD14086SK fibroblasts, HCC38 cells demonstrated a reduced response to CB-839, an effect which was observed in all TNBC lines tested (Figure 4C). Data collected at 72 h was used to generate concentration-response curves, showing a similar separation between monoculture (solid lines) and co-culture responses (dashed

lines) in all TNBC cell lines tested (Figure 4D). MCF-7 cells, however, showed no difference between mono- and co-culture conditions (compare the right graphs in Figures 4B and 4C). As expected, CB-839 was still observed to have no effect in other receptor-positive lines, even in the presence of CCD14086SK cells. Figure 4E shows 72 h concentration-response curves for receptor-positive cell lines. For the MCF-7 cells, the 15 hour time point was better suited to highlight the overlapping mono- and co-culture concentration-response curves, which is important as it shows that the differences observed in TNBC mono- and co-cultures was not the result of drug buffering. Instead, this effect maybe be due to metabolic exchange or other biological interaction with stromal cells that specifically promotes resistance to CB-839 in TNBC cells.

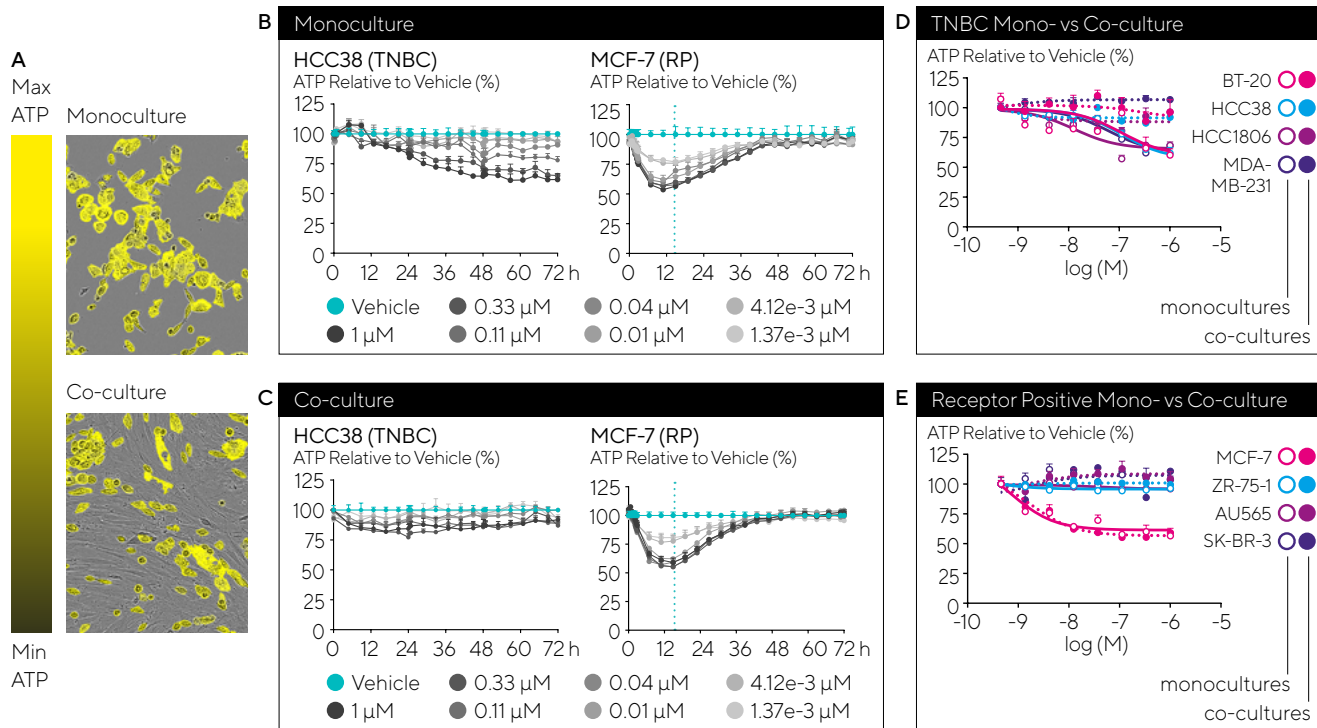


Figure 4. Differential effect of GLS-1 inhibition on breast cancer cells in mono- and co-culture. Color-scaled images provide visualization of ATP in HCC38 cells treated with 330 nM CB-839 in monoculture and in co-culture with CCD14086SK cells (A). Kinetic measurement of ATP in HCC38 (TNBC cell line) and MCF7 (receptor positive cell line) in monoculture (B) and co-culture with CCD14086SK cells (C). Comparison of CB-839 concentration-response curves between a panel of TNBC (D) and receptor-positive breast cancer cell lines (E) in monoculture and co-culture. Data represent 72 h time point except where indicated. CytoATP Lentivirus ratio values were normalized to vehicle controls at each time point.

Assessment of Compound Effects on Mitochondrial Function

ATP is produced by both glycolytic and mitochondrial OXPHOS pathways, which can contribute to the pool measured by the Incucyte® CytoATP Lentivirus. Mechanism of action studies often includes assessment of mitochondrial bioenergetics to examine mitochondrial dysfunction. Mitochondrial-driven toxicity may be missed by traditional assays. To explore the use of CytoATP Lentivirus for this purpose, compounds with known toxicity profiles were evaluated using a live-cell adaptation of the glucose-galactose switch.

NIH 3T3 cells stably expressing Incucyte® CytoATP or Non-binding Control Lentivirus were adapted to media that contained galactose in lieu of glucose. Cells grown in galactose media were seeded in the same plate as cells grown in glucose media to directly compare compound-induced effects on CytoATP measurements between the media conditions. Baseline scans confirmed equal starting ATP values across treatment conditions, after which cells were then treated with compounds previously shown

in literature to be nontoxic, cytotoxic, or mitotoxic (0.4-100 μM for all compounds). Images were acquired and analyzed with the Incucyte® SX5 Live-Cell Analysis System every 20 min at early time points to capture early changes in ATP. Thereafter, images were obtained every hour from 3 – 24 h following compound addition in order to monitor recovery, stability, or progressive depletion of ATP.

Figure 5 displays representative datasets from each category. Unsurprisingly, the nontoxic compound ambrisentan did not affect ATP in any of the tested cell culture media conditions (left column). Chlorpromazine, an antipsychotic compound, induced a rapid, concentration-dependent depletion of ATP in cells grown in both glucose (top middle) and galactose (middle). Data from the 24 h time point was used to generate concentration-response curves (bottom row). The overlapping curves between glucose or galactose grown cells indicate a cytotoxic profile. Interestingly, the antidepressant nefazodone, which has been known to induce mitochondrial toxicity, showed increased potency in cells grown in galactose. In glucose grown cells,

only the highest concentration (100 μM) of nefazodone induced sustained and progressive ATP depletion over time (top right). At 50 μM of nefazodone, a small and transient depletion and recovery was also observed. However, in galactose grown cells, the same concentrations of nefazodone resulted in an immediate, pronounced ATP depletion that continued to decrease over the course of the assay to nearly undetectable levels. At lower concentrations (12.5-25 μM), galactose-grown cells displayed rapid decreases in ATP that were followed by partial recovery, reversal, and then progressive depletion over the course of the assay (middle right). As seen in the concentration-response curves, the responses from glucose and galactose media conditions varied at different time points (bottom right). In either condition, nefazodone EC_{50} values of cells cultured in glucose were > 4 -fold higher than those grown in galactose. This is consistent with profiles of mitotoxic compounds and validates the use of the Incucyte® ATP Assay for the characterization of compound effects on OXPHOS.

Qualitative assessment of cell morphology

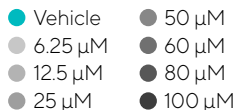
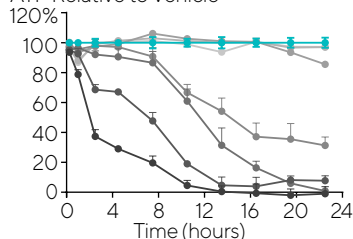
Unlike perturbing, traditional techniques that measure changes in ATP and metabolites, Incucyte® Live-Cell Imaging and Analysis can monitor alterations in cell growth and morphology along with ATP measurement without additional technology or concatenated end points. Automated Incucyte® HD phase contrast images are collected throughout the time course of the Incucyte® ATP Assay, enabling quantification of confluence and qualitative assessment of images to reveal morphological changes that accompany changes in ATP. To demonstrate this capability, HeLa cells stably expressing CytoATP indicators were treated with compounds that exhibiting various mechanisms of action. These included chlorpromazine

(6.25 – 100 μ M, a dopamine D₂ receptor antagonist), etoposide (1.4 nM – 100 μ M, a topoisomerase II inhibitor), and the combined treatment of 2-DG (63 μ M – 40 mM) + KCN (6.3 μ M – 4 mM). Baseline scans were collected prior to drug treatment, following which all of the compounds were found to cause a concentration-dependent decrease of ATP. However, the time of ATP depletion varied, ranging from with the first 20 minutes to > 24 h post treatment (Figure 6, top row). HD phase contrast images (Figure 6, bottom row) were collected for each compound at concentrations and time points where ATP < 20% of vehicle-treated values. Cells treated with chlorpromazine displayed a small, rounded phenotype that suggested apoptosis, consistent with its known cytotoxic profile. Alternatively, while some

cells treated with etoposide had a rounded morphology similar to chlorpromazine, many others demonstrated an enlarged and flattened morphology, indicative of a senescence phenotype. This mixed morphology is consistent with previous studies in which etoposide was shown to induce both apoptosis and senescence. Cells treated with 2-DG + KCN, however, had a morphology similar to that of vehicle treated cells at this particular time point and concentration. Regardless of the similar treatment induced ATP depletions, marked differences in morphology were observed between compounds with varying mechanisms of action.

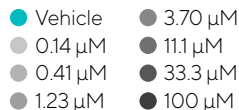
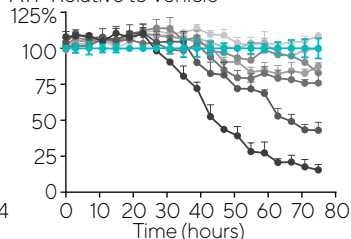
Chlorpromazine

ATP Relative to Vehicle



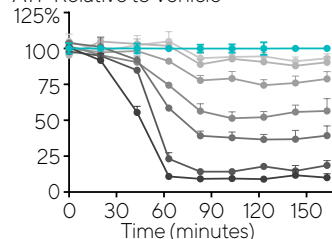
Etoposide

ATP Relative to Vehicle

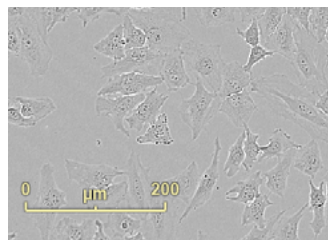


2-DG + KCN

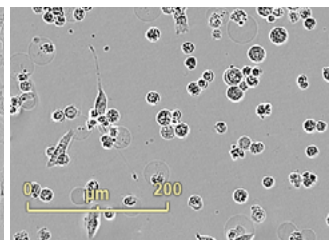
ATP Relative to Vehicle



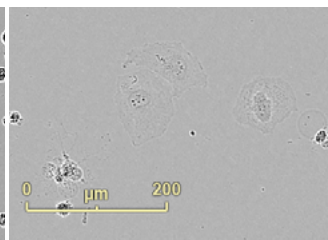
Vehicle



Chlorpromazine



Etoposide



2-DG + KCN

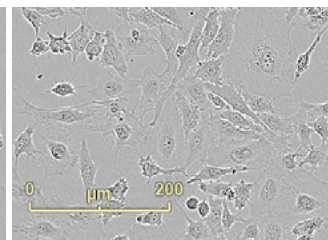


Figure 6. Qualitative inspection of cell morphology with HD phase contrast images. Top: Kinetic measurement of ATP in HeLa cells following chlorpromazine, etoposide, or 2-DG + KCN treatment at the concentrations indicated. Bottom: HD phase contrast images of HeLa cells acquired under vehicle control conditions or during ATP depletion induced by chlorpromazine (60 μM , 23 h), etoposide (100 μM , 75 h), or 2-DG (20 mM) + KCN (2 mM) (180 minutes).

Conclusions

The experiments outlined above highlight both the utility and value of the Incucyte® ATP Assay. The novel, non-perturbing and genetically-encoded Incucyte® CytoATP Lentivirus and Incucyte® CytoATP Non-binding Control Lentivirus are combined with the quantitative power of ratiometric readouts with the use of the Incucyte® SX5 Metabolism Optical Module and Incucyte® ATP Analysis Software Module. This assay affords researchers the following advantages over traditional end-point methods, these being:

- Direct, long-term cytosolic ATP measurements in living cells using the non-perturbing Incucyte® CytoATP Lentivirus and can be used in a variety of cancer cell lines to analyze dynamic changes in ATP over time; alleviates the need to select a single end-point measurement for characterizing changes in ATP.

- Data generated is independent of cell number or reporter expression, ensuring appropriate interpretation of data, which is critical for the analysis of metabolic perturbations that rapidly alter cancer cell growth.
- Ability to capture and analyze cell-type specific metabolic changes in relevant co-cultures to study metabolic exchange or biological interactions within complex models.
- The ability to capture HD phase contrast images at every time point throughout the course of the experiment to correlate changes in morphology with changes in ATP, providing new insight into compound effects, efficacy, and selectivity.
- The ability to explore to the glucose-galactose switch paradigm in living cells, which can be useful for screening for mitochondrial toxicity liabilities or for mechanistic studies of compounds.

This assay fills a critical need for improved tools to examine the influence of nutrient exchange and cell-cell interactions on therapeutic efficacy. The Incucyte® ATP Assay provides researchers with the enhanced capacity and throughput needed to address key metabolomics questions in the search for new therapeutics.

References

1. Potter M, Newport E, and Morten KJ. **The Warburg effect: 80 years on.** *Biochem Soc Trans.* 2016 Oct 15; 44(5):1499-1505.
2. Li H, *et al.* **The landscape of cancer cell line metabolism.** *Nature Medicine.* 2019 May; 25(5):850-860

Chapter 5

Kinetic Assays for Studying Immune Cell Models

Live-Cell Assays for Dynamic Monitoring of Immune Cell Proliferation, Function and Morphology

The importance of understanding immune responses continues to grow in the areas of infectious disease, immunotherapy, and personalized medicine. Exciting advancements in immune cell manipulation, such as CRISPR technology, allows for the greater understanding of health and disease through precision therapy. However, at the core of this revolutionized research is still the basic requirement to monitor and quantify immune cell activation, proliferation, health and function to identify phenotypic and morphological changes in cell biology.

Assessments of immune cell activation, proliferation, health, and function are typically performed using various technologies such as flow cytometry, plate readers, or microscopes. These assays typically are endpoint assays (e.g. immunocytochemistry) require laborious workflows, and are performed

while the cells are in isolation and not in a stable environment. As immune cells have a complex response, it is essential to characterize their response kinetically in a physiologically relevant environment for improved immunomodulatory therapeutics and vaccine development.

Live-cell imaging and analysis approaches are advantageous over traditional immune cell assays in that they can provide critical, missing pieces of information by documenting and analyzing the kinetics of immune cell proliferation, health and function in real time in response to treatments, as well as their interactions with surrounding cells. The Incucyte® Live-Cell Analysis System incorporates automated image acquisition and analysis, all while maintaining physiologically relevant conditions within the researcher's incubator. Dynamic changes can be quantified in real time for hours, days,

or weeks using non-perturbing image acquisition and analysis as the cells sit stationary. The Incucyte® Live-Cell Analysis System provides support for multiple applications with the ability to multiplex using non-perturbing reagents and integrated software to increase time-to-result for assessment of cell health, function, and morphology while minimizing operator exposure to potential pathogens via remote access. This helps to maximize the data obtained from each sample for more complete analysis and deeper biological insight. The chapters that follow will illustrate how Incucyte® Live-Cell Imaging and Analysis can be readily used for studying immune cell health, proliferation, morphology, movement, and function.

Live-Cell Imaging and Analysis

Approached for Studying Immune Cells

The automated Incucyte® Live-Cell Analysis System enables users to study the kinetic changes in immune cell health, morphology, movement, and function in long-term cultures and co-cultures as cells respond to immune challenge, treatment, cellular interactions, or other experimental manipulations. This flexible platform includes instrumentation, applications, protocols, and non-perturbing reagents. Purpose-built software identifies immune cells, label-free in heterogeneous cultures, to assess proliferation and morphological changes associated with activation. The study of immune cell killing and cellular interactions are enabled with non-perturbing labeling strategies and cell health indicators for the identification of different cell populations in co-culture models. Users may also multiplex to assess other functional outputs such as phagocytosis, efferocytosis, and chemotaxis (see Chapter 6b - Kinetic Chemotaxis Assays for additional details). Even complex immune responses such as NETosis can be monitored and quantitated

in real time for deeper insights into this important early immune response. Multiplex analysis is possible in both 2D and more complex 3D *in vitro* immune models. The 96- and 384-well, multi-vessel capacity enables the throughput needed pharmacological screening, immune therapeutic target identification, study of early host/pathogen interactions, and determinations of potential cytotoxicity from therapeutic intervention. Users can perform comprehensive analysis of many immune system parameters from a small sample, providing complete portrait of the immune response than could be achieved by traditional methods.

How Incucyte® Live-Cell Assays for Immune Cell Models Work

Activation and Proliferation Assays

To measure changes in cell activation and proliferation, non-invasive, label-free image acquisition and integrated analysis is employed. Quantification of cell proliferation are performed using integrated software which evaluates cell area (confluence) or cell number (count)

metrics via segmentation (masking) of high-quality phase images. The Incucyte® Cell-by-Cell Analysis Software Module is employed to assess label-free proliferation, but can also be implemented along with associated Incucyte® reagents to accurately evaluate changes in heterogeneous populations or co-cultures. Fluorescent images can be automatically acquired over time and analyzed to generate information alongside label-free counts in mono- or co-cultures. These assays can also be multiplexed with other Incucyte® fluorescent reagents for additional assessments including apoptosis, cytotoxicity, or viability.

Immune Cell Killing Assays

Incucyte® Immune Cell Killing Assays enables users to perform direct, multiplexed measurements of immune cell-mediated killing of tumor cells by combining real-time, automated analysis with the use of non-perturbing, live-cell reagents to study events such as cytotoxic T cell killing, antibody-dependent cell-mediated cytotoxicity (ADCC), and immune cell killing in either 2D or complex 3D tumor spheroid models. The protocols require no washing, cell lifting, or radioactive labels. Target tumor cells may be co-cultured with the user's immune cells of choice. Tumor cell death is measured directly and in real-time through the addition of mix-and-read, non-perturbing Incucyte® Caspase-3/7 Green or Red Dyes or Incucyte® Annexin V Red, Green, Orange or NIR Dyes to the culture. Users may also multiplex using three colors to label both target and effector cells, supplemented with a third-color cell health readout. Automated image analysis enables the selective quantitation of tumor cell death. Users may also perform simultaneous tumor cell

counts by labeling target cells with a range of Incucyte® Nuclight Reagents. Cells that are difficult to label may also be identified using Incucyte® Cytolight Rapid Dyes. Users can employ the Incucyte® Cell-By-Cell Analysis Software Module to quantify both the labeled target cell population and the non-labeled effector cell population (proliferation and death). For adherent target cells, the software enables the tracking of effector cell populations in the presence of target cells.

NETosis Assays

The Incucyte® Live-Cell Analysis System and the Incucyte® Cytotox Green Dye allows for automatic quantification of neutrophils undergoing NETosis in real-time. Users can capture swelling and decondensation of nuclei, followed by NET release, which can be measured for validation of these distinct NETosis morphological changes. Incucyte® Cytotox Green Dye enables rapidly visualization and quantification of NETosis as extracellular DNA is released and undergoes fluorescence enhancement. Incucyte® Annexin V Red Dye can also be

used with the Incucyte® Cytotox Green Dye for multiplexed measurements to distinguish between apoptosis and NETosis.

Differentiation, Phagocytosis, and Efferocytosis Assays

The Incucyte® Live-Cell Analysis System, integrated analysis software, and non-perturbing reagents can also be used for long-term monitoring of morphology and growth associated with cellular differentiation and accompanied by functional changes, such as phagocytosis and efferocytosis. Morphological changes associated with differentiation can easily be visualized, confirmed, and tracked in long-term cultures in the incubator with minimal disturbance. Cell surface markers can be labeled using Incucyte® Fabfluor-488 Antibody Labeling Dyes and then analyzed using the Incucyte® Cell-by-Cell Analysis Software Module. This enables users to temporally classify cells into subsets based on CD antigens without cell lifting or fix/wash protocols. Changes in surface protein expression can be associated with cell function

and morphology to reveal informative, temporal changes in functional behavior following cellular differentiation. Incucyte® Phagocytosis Assays enable automated assessment of phagocytosis over the entire assay time course in the incubator and use simple mix-and-read protocols without washing, fixing, or lifting. These assays provides real-time visualization and analysis of the internalization of sterile

bioparticles using pH sensitive-conjugated probes, and are ideal for monitoring phagocytosis of bacterial Gram- positive, Gram-negative or yeast-derived pathogens by immune cells. The Incucyte® pHrodo® Bioparticles® are phagocytosed and, on entering the acidic environment of the phagosome, increase in fluorescence. Phagocytosis can be validated with both images and movies for studying the effect

of treatments throughout the full time course of an assay to create phagocytosis profiles. Users may also investigate efferocytosis and antibody mediated cellular phagocytosis (e.g. anti-CD47/ADCP) and label their choice of target cells using the Incucyte® pHrodo® Cell Labeling Kit.

References

1. Giordano-Attianese G, Gainza P, Gray-Gaillard E, *et al.* A computationally designed chimeric antigen receptor provides a small-molecule safety switch for T-cell therapy. *Nat. Biotechnol.*, 2020, 38(4):426-432.
2. Pavesi A, Tan AT, Koh S, *et al.* A 3D microfluidic model for preclinical evaluation of TCR-engineered T cells against solid tumors. *JCI Insight*. 2017, 2: e89762.
3. Zaretsky JM, Garcia-Diaz A, Shin DS, *et al.* Mutations associated with acquired resistance to PD-1 blockade in melanoma. *N. Engl. J. Med.*, 2016, 375: 819–829.
4. Chen MB, Lamar JM, Li R, Hynes RO, Kamm RD. Elucidation of the roles of tumor integrin $\beta 1$ in the extravasation stage of the metastasis cascade. *Cancer Res.*, 2016, 76: 2513-2524.
5. Sahin U, Derhovanessian E, Miller M, Kloke BP, *et al.* Personalized RNA mutanome vaccines mobilize poly-specific therapeutic immunity against cancer. *Nature*, 2017, Jul 13; 547(7662):222-226.
6. Roth TL, *et al.* Reprogramming human T cell function and specificity with non-viral genome targeting. *Nature*, 2018 Jul; 559(7714):405-409.
7. Ihry RJ, Worringer KA, Salick MR, *et al.* p53 inhibits CRISPRCas9 engineering in human pluripotent stem cells. *Nat. Med.*, 2018; 24: 939–946.
8. Rothan HA, Zhong Y, Sanborn MA, Teoh TC, Ruan J, Yusuf R, Hang J, Henderson MJ, Fang S. Small Molecule grp94 Inhibitors Block Dengue and Zika Virus Replication. *Antiviral Res.*, 2019 Nov; 171:104590
9. Zander R, Schauder D, Xin G, *et al.* CD4+ T Cell Help Is Required for the Formation of a Cytolytic CD8+ T Cell Subset that Protects against Chronic Infection and Cancer. *Immunity*, 2019, 51(6):1028-1042.e4.
10. Barr FD, Ochsenbauer C, Wira CR, Rodriguez-Garcia M. Neutrophil Extracellular Traps Prevent HIV infection in the Female Genital Tract. *Mucosal Immunol.*, 2018, 11(5):1420-1428.
11. Smith CA, Tyrell DJ, Kulkarni UA, *et al.* Macrophage migration inhibitory factor enhances influenza-associated mortality in mice. *JCI Insight*. 2019, 4(13):e128034. Published 2019 Jul 11. doi:10.1172/jci.insight.128034
12. Gupta S, Chan DW, Zaal KJ, Kaplan MJ. A High-Throughput Real-Time Imaging Technique to Quantify NETosis and Distinguish Mechanisms of Cell Death in Human Neutrophils. *J Immunol.*, 2018, 200(2):869-879. doi:10.4049/jimmunol.1700905

5a

Kinetic Assays for Immune Cell Activation and Proliferation

Continuous Quantification and Visualization of Immune Cell Proliferation and Morphology

Introduction

The regulation of immune cell activation, proliferation, and differentiation is the foundation of an appropriately gauged immune response, and these events may be further complicated by individual genetics affecting cellular immune responses and underlying inflammatory status. Performing assessments of these events, against the backdrop of individual variance, can provide critical clues and new insights for the treatment of disease, response to infectious pathogens, and autoimmune dysfunction. Kinetic, comprehensive analysis can uncover key information on the timing and intensity of this dynamic, complex story, providing clues to functional differences that can be leveraged for personalized medicine approaches as well as pharmacological development. The activation and proliferation of immune may change throughout the course of response to treatment, cellular therapy, or vaccine.

Traditionally, *in vitro* methods such as flow cytometry, PCR, and various forms of ELISA have been used by immunologists to better characterize the cells of the immune system. While these techniques provide insight of different cell populations at a molecular and functional level, they may not allow for measurements of morphology and of how immune cells interact with each other, especially within complex co-cultures and 3D models. Combined with end-point analysis and concatenated endpoint experiments, these assays are further limited by their inability to capture and characterize the dynamics of the complex, underlying biology behind the immune response which is especially problematic for today's fast-paced demands for target identification, therapeutic screening, and vaccine development.

In this chapter, we will illustrate the kinetic approaches for measuring immune cell activation, and proliferation using the Incucyte® Live-Cell Analysis System, Incucyte® reagents, and Incucyte® integrated software. Unlike traditional end-point approaches, kinetic live-cell image-based analysis allows users to better examine the sequential steps and timing of the events surrounding the immune response. A more complete understanding provided by kinetic insight from live-cell analysis can be crucial to the development of appropriate interventions for disease management. Incucyte® assays for proliferation and activation offer non-invasive, measurement of cell growth based on confluence or cell count. Movable optics allow the culture plate remain stationary while high-quality images of cells are captured.

Incucyte® Immune Cell Activation and Proliferation Assays at a Glance

With Incucyte® Live-Cell Imaging and Analysis, users can readily study changes in morphology, phenotype, and cell number, generate long-term growth curves or growth inhibition for a wide variety of cell types, including T cells, B cells, NK cells, macrophages, and microglia (refer to Chapter 9c - Kinetic Neuroimmune Assays for more information on microglia). The quantification of cell growth based on confluence or cell count can be performed using Incucyte® integrated software. Detailed insight into dynamic changes in activation and true label-free cell counts can be accomplished using Incucyte® Cell-by-Cell Analysis Software Module. Users may also multiplex proliferation assessments with Incucyte® Caspase 3/7 Dyes, Incucyte® Annexin V Dyes, or Incucyte® Cytotox Dyes for quantification of apoptosis or cytotoxicity. Cellular identification and immuno-phenotyping can also be performed using Incucyte® Fabfluor-488 Antibody Labeling Dyes. These immune cell activation and

Shortcomings of Traditional Assays	Live-Cell Imaging and Analysis Approaches
<ul style="list-style-type: none">▪ Data obtained from a single, pre-defined time point provides minimal dynamic insight as key events may be undetected.	<ul style="list-style-type: none">▪ Continuous, real-time monitoring and data collection enables detection of temporal differences in drug or treatment effects to better guide experimental decision making.
<ul style="list-style-type: none">▪ Concatenated end point experiments lack environmental control.	<ul style="list-style-type: none">▪ Cells are measured continuously over time in a controlled environment via repeated interrogation of the same well.
<ul style="list-style-type: none">▪ Indirect detection methods are subject to artifacts that cannot be readily verified visually.	<ul style="list-style-type: none">▪ True direct counts can be generated non-invasively and are verified with image collection and movies.
<ul style="list-style-type: none">▪ Studying the responses of cell subsets among heterogeneous populations is not possible as the entire population is analyzed indiscriminately.	<ul style="list-style-type: none">▪ Proliferation measurements of heterogeneous, adherent or non-adherent cells can also be multiplexed with morphology, health, or functional readouts.

Table 1. Shortcomings of Traditional Assays vs Live-Cell Imaging and Analysis Approaches

proliferation assays yield full time-course data, provide crucial morphological insight, and can be miniaturized to 96- and 384-well plates for sufficient throughput.

Sample Results

T Cell Activation and Clustering

During an immune response, activated cells of the immune system, such as T cells, undergo rapid expansion to better fight infection or disease. Following early activation events surrounding the interaction between the T cell antigen-specific receptor (TCR) and antigen-major histocompatibility complex (MHC), activated cells undergo clonal expansion and upregulation of activation markers on the T cell surface. As T cells are critical in

adaptive immunity, understanding T cell activation and clustering is fundamental in order to characterize the effect and extent of the immune response. Incucyte® Live-Cell Imaging and Analysis can be used to capture and analyze the activation and clustering of T cells, as well as the expression of surface markers in real time to generate new kinetic insights. Label-free, high-definition, phase-contrast imaging can be used to monitor morphological changes, such as cell size and eccentricity, between activated and non-activated cells. Users may also use fluorescence surface

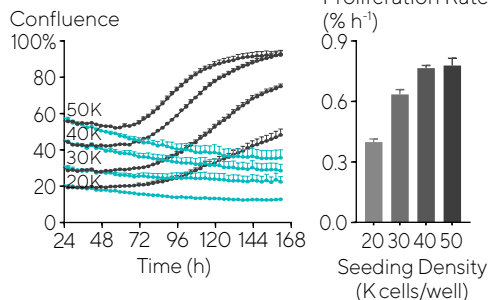
labeling to assess markers of interest (refer to Chapter 7b - Kinetic Live-Cell Immunocytochemistry Assays for more on cell marker analysis).

Figure 1 (below) illustrates the assay's ability to assess T cell proliferation and clustering under basal conditions as compared to activation with IL-2, anti-CD3, and anti-CD28 when seeded at different densities. Following activation, T cell cluster formation was captured and quantified over time using the Incucyte® Live-Cell Analysis System, which demonstrated the ability of the platform

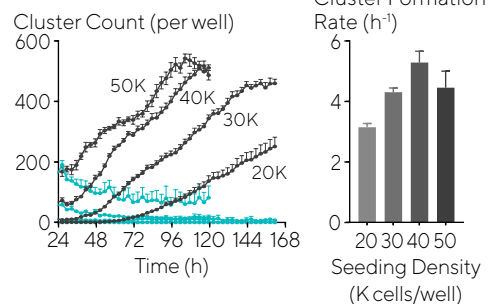
Figure 1. T cell proliferation & clustering is seeding density-dependent. T cells demonstrate little or no proliferation under basal conditions but rapidly proliferate when activated (e.g. by IL-2, anti-CD3, anti-CD28). Following activation, T cells also form cell clusters; Incucyte® Live-Cell Imaging and Analysis enables quantification of this phenotype.

● anti-CD3 (100 ng/mL)/IL-2 (10 ng/mL)
● Vehicle

Proliferation



Cluster Formation



and software to capture and quantitate a seeding density dependent response on proliferation and cluster formation.

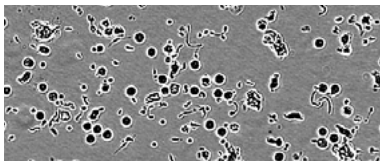
Combining phase-contrast imaging with fluorescent surface labeling can enable

users to monitor the dynamic changes of cell activation and associated morphological changes over time. As shown in Figure 2, we were able to observe an increase in PBMC cell size and eccentricity in response to activation with anti-CD3 and IL-2 versus

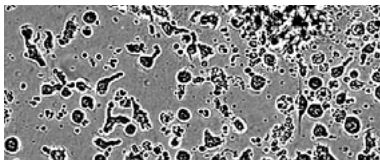
when treated with a vehicle control. By multiplexing with the Incucyte® Fabfluor-488 Antibody Labeling Dye, we were able to also observe an upregulation of cell surface makers thus providing a more complete characterization of activation.

A

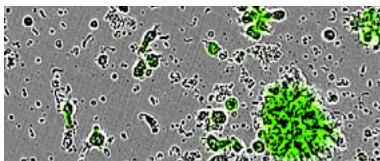
Non-Activated



Activated



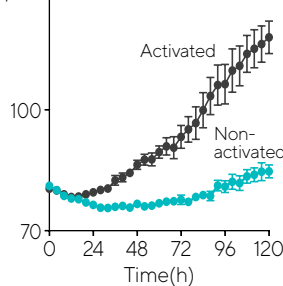
Activated, CD71



B

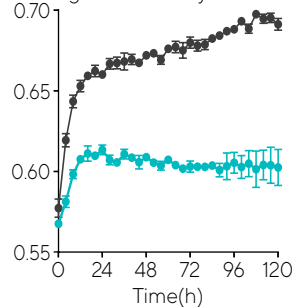
Cell Size

Average Area
130 μm^2



Cell Shape

Average Eccentricity



%CD71+ Expression in Subsets

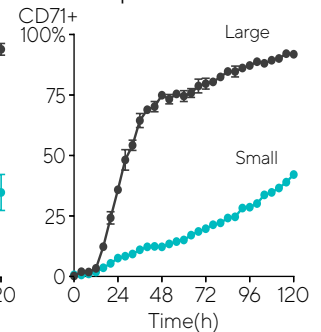


Figure 2. Visualization of PBMC activation using phase-contrast imaging and live-cell immunocytochemistry (Fabfluor-488- anti-CD71). PBMCs (30K/ well) were treated with anti-CD3 and IL-2, or vehicle control, and labeled using Fabfluor-488- anti-CD71. (A) Label-free phase-contrast imaging detects morphological differences between non-activated and activated PBMCs. Note the change in eccentricity preceded the increase in area. Phase-contrast imaging coupled with live-cell ICC shows upregulated CD71+ in activated cells. (B) Activation induces increased cell size, increased cell eccentricity and upregulation of CD71+ in larger vs smaller subsets of cells.

To better understand the heterogeneous populations that arise following activation the Incucyte® Cell-by-Cell Analysis Software Module enables identification and quantification of cellular subsets based on cell size, shape (eccentricity), or fluorescent intensity. In this same study, Cell-by-Cell Analysis was used to perform label-free characterization of

heterogeneity and dynamics within the culture following activation. Figure 3 shows the area distribution graph and density plots that were generated, illustrating the emergence of separate populations over time following activation and highlighting the increased heterogeneity. In particular the emergence of a population of large cells with high eccentricity was observed.

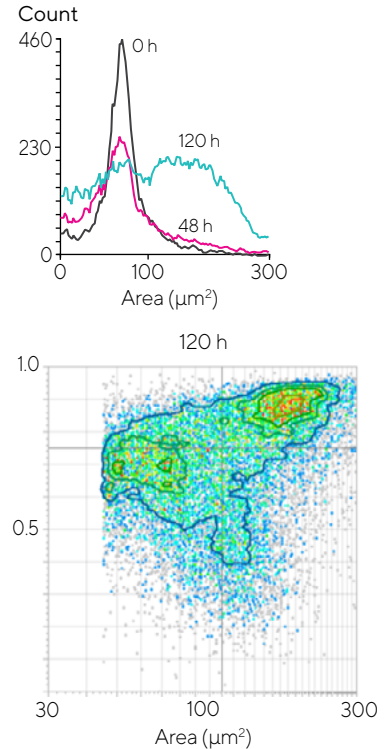


Figure 3. PBMCs were treated with anti-CD3 and IL-2, or vehicle control, and monitored over time with the Incucyte® Live-Cell Analysis System. The cell-by-cell area distribution and density plots highlight the increased heterogeneity over time following activation, and the appearance of a population of large cells with high eccentricity. Values shown are the mean \pm SD of 4 wells.

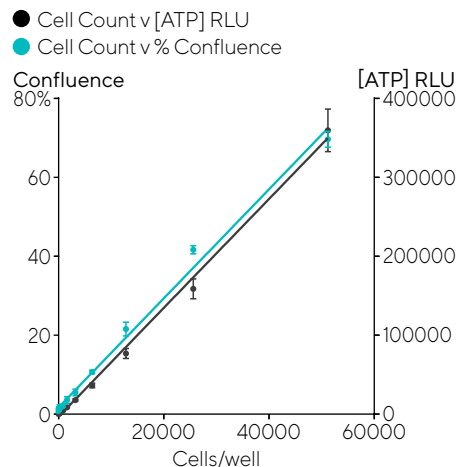
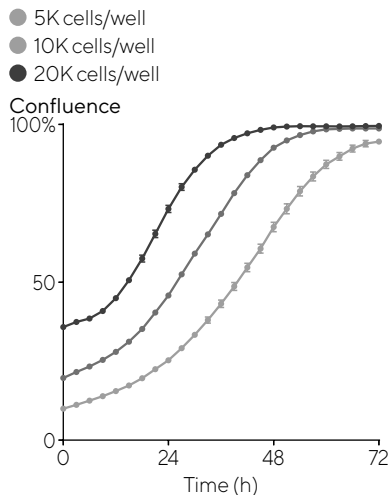
B Cell Activation and Proliferation

In addition to T cells, Incucyte® Live-Cell Imaging and Analysis of proliferation and activation can be assessed in other immune cell types, such as B cells. As B cells are at the center of the adaptive immune response, B cell activation and proliferation are crucial for the secretion of antibodies, but continuous stimulation

can also lead to the survival and growth of B cell leukemias and lymphomas. As shown in Figure 4, Incucyte® Live-Cell Imaging and Analysis was used to capture proliferation in the non-adherent B cell line WIL-2NS using phase contrast imaging, followed by a downstream, secondary assessment of ATP content from harvested, permeabilized cells to obtain

additional data. Not only can the Incucyte® Live-Cell Analysis System assess B cell proliferation, activation, and clustering, but also additional functional outputs such as B cell death and antibody internalization (refer to Chapter 7a - Kinetic Antibody Internalization Assays for more details).

Figure 4. Proliferation of a non-adherent B cell line. The proliferation of WIL-2NS cells, a B cell line, quantified from phase contrast images. The starting confluence is seeding density dependent. Validation of the confluence measurement was achieved by seeding known amounts of cells per well, allowing settling and then quantifying using the phase contrast algorithm. Cells were subsequently permeabilized and the ATP content determined to provide a secondary readout. A very strong correlation between % confluence and cell number or ATP determination was observed.



Neutrophil Activation and Proliferation

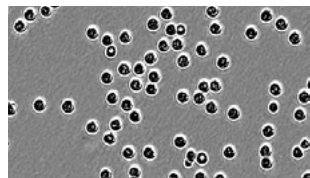
In the innate immune system, neutrophils are the first line of defense and are critical in early immune responses as well as tissue damage that may occur during immune challenges, such as bacterial infection. Primed, activated neutrophils can contribute to manifestations of dysregulated

activation such as organ damage and ARDS of severe sepsis following infection. Characterizing neutrophil activation, proliferation, and differentiation can be key to identifying potential therapeutic interventions. In the study shown in Figure 5, PMNs were seeded in Matrigel® and treated with increasing concentrations of CXCL8. Using Cell-by-

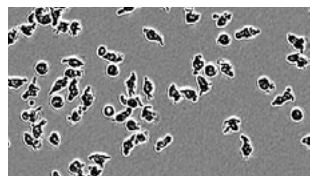
Cell Analysis, we were able to identify and quantify changes in cell shape (eccentricity) over the course of the experiment and observe a concentration dependent response of cell shape to CXCL8. We determined an EC_{50} of 0.63 nM and also observed an inhibition of CXCL8 with the addition of anti-CXCL8.

Phase Image, 1 h

Vehicle

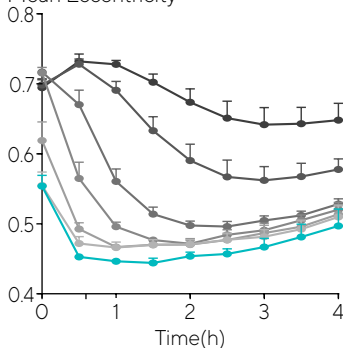


CXCL8 (1nM)

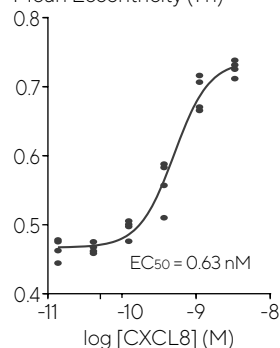


● 3.33 nM ● 0.12 nM ● Vehicle
● 1.11 nM ● 0.04 nM
● 0.37 nM ● 0.01 nM

Response to CXCL8
Mean Eccentricity



Response to CXCL8
Mean Eccentricity (1 h)



Inhibition of CXCL8
Mean Eccentricity (1 h)

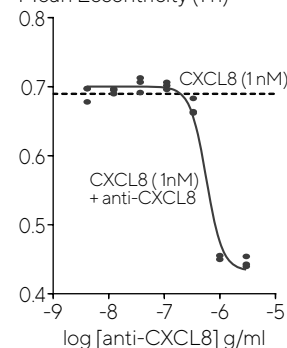


Figure 5. Changes in cell shape (eccentricity) of PMNs. PMNs from whole blood seeded in Matrigel with increasing concentration of CXCL8. Images were captured in Incucyte® Live-Cell Analysis System and the Incucyte® Cell-by-Cell Analysis Software Module was used to quantify changes in cell shape over time.

Conclusions

As new and exciting methods emerge for today's immunologists, the need to understand immune cell activation, proliferation and differentiation remains the essential core of immunology research. As outlined throughout this chapter, the Incucyte® Live-Cell Analysis System, portfolio of non-perturbing reagents, and purpose-built, integrated software provide the flexibility and throughput to accommodate the demand for thorough, comprehensive evaluation of the immune cell response. Most importantly, Incucyte® Immune Cell Activation and Proliferation Assays provide the user with capabilities that cannot be found using more traditional endpoint analysis, among these being:

- Flexible assay platform that enables label-free or fluorescently labeled analysis of immune cell proliferation in mono- or co-culture applications
- Continuous, real-time, automated monitoring and analysis of immune cell activation, proliferation, and differentiation in a physiologically relevant environment, using a mobile optical train to collect data from each well of a 96- or 384-well plate, thus minimizing interference with cell biology
- Minimize troubleshooting and produce reproducible, well-to-well kinetic data using lab tested protocols, high quality images, and unbiased analysis
- Verify all data points through inspection of individual images and/or time-lapse movies
- Multiplexed measurements for additional insights into cell morphology, health, and function using non-perturbing reagents. This allows for maximizing sample use and minimizing time-to-result.

Incucyte® User Publications

1. Balaban S, Shearer RF, Lee LS, *et al.* **Adipocyte lipolysis links obesity to breast cancer growth: adipocyte-derived fatty acids drive breast cancer cell proliferation and migration.** *Cancer Metab.*, 2017, 5:1.
2. Foster AE, Mahendravada A, Shinnars NP, *et al.* **Regulated Expansion and Survival of Chimeric Antigen Receptor-Modified T Cells Using Small Molecule-Dependent Inducible MyD88/CD40.** *Mol Ther.*, 2017, 25(9):2176-2188.
3. Duong MT, Collinson-Pautz MR, Morschl E, *et al.* **Two-Dimensional Regulation of CAR-T Cell Therapy with Orthogonal Switches.** *Mol Ther Oncolytics*, 2018,12:124-137.

5b

Kinetic Assays for Immune Cell Killing

Quantification and Visualization of Immune Cell Killing

Introduction

The rapid advancement of immunotherapy and personalized medicine incorporates a variety of strategies including the development of genetically engineered immune cells to enhance tumor killing, therapeutic antibodies, and checkpoint inhibitors.¹ In response to these advancements, *in vitro* models are becoming increasingly complex in order to better recapitulate the *in vivo* microenvironment, with the inclusion of more cell types, cell-to-cell contact, and stromal elements.^{2,3} This is especially true for *in vitro* models of immune cell killing, which attempt to mimic the complex interactions between immune cells and their targets. These models require a deeper understanding of model performance and cellular interaction, often in heterogeneous cultures, and co-cultures with 2D and 3D models, for activities such as toxicity screening following

cellular reprogramming, development of therapeutic antibodies and cancer vaccines, exploring drug mechanisms of action, overcoming immune cell exhaustion, and the eradication of infected cells during infection.

Answering such questions through traditional endpoint analysis of immune cell killing poses significant challenges. Traditional approaches such as flow cytometry and biochemical readouts give only limited insights on the dynamics of cellular interaction between targets and effector cells. They often utilize time consuming, 'end-point' fix and stain protocols that only provide a single image per time-point, which does not adequately capture the full biological story. Protocols may also involve multiple washing steps with radioactivity or antibody labeling for quantification, as well as cell lifting. Assays may be performed on multiple instruments,

resulting in a lack of environmental control. Further, traditional *in vitro* assay methods may be unable to determine cell-specific cytotoxic signals in co-culture models due to global well measurements. Even with the use of ⁵¹Cr release assay can be employed to isolate cell specific signals. However, background signals can still limit the conclusions drawn from this assay as many cancer cells do not effectively take up or retain the chromium label.^{4,5} Traditional end-point methods may also concatenate data from different samples in order to construct a time course, which may inadvertently introduce artifacts.

Incucyte® Live-Cell Imaging and Analysis provides a solution for many of the challenges associated with traditional endpoint analysis methods for the assessment of immune cell killing. The Incucyte® Live-Cell Analysis System enables quantification of real-time

dynamic interactions and functional activity in both 2D and 3D cultures. The instrument resides in the user's own incubator for greater environmental control, and automatically captures and analyzes images of tumor cell death and viability for long-term studies. Users may readily study of immune cell killing in their choice of cells, using flexible assay format, multiplexing assessments of cell health, function, and activity using mix-and-read non-perturbing reagents and optimized cell-sparing protocols. The instrument accommodates 384-well plates for greater throughput. Analysis can be quickly performed using integrated analysis software, including the Incucyte® Cell-By-Cell Analysis Software Module, which allows the quantification of both labeled target cell populations and non-labeled effector cell populations (proliferation and death) in heterogeneous and complex co-cultures, providing researchers with a versatile platform that maximizes the amount of information-rich data from each sample.

Incucyte® Immune Cell Killing Assays at a Glance

In order to measure immune cell killing in multiple model types and accurately assess target cell death and immune cell health, Incucyte® Immune Cell Killing Assays use real-time, automated analysis combined with non-perturbing, live-cell reagents and purpose-built software. This flexible assay is ideal for the assessment of cytotoxic cell killing, antibody-dependent cell-mediated cytotoxicity (ADCC), and immune cell killing in both 2D and 3D models in either 96- or 384-well plates, all from within a physiologically relevant environment.

In order to study targeted tumor cell death and viability, non-perturbing, labeling reagents are employed. Incucyte® Nuclight Lentivirus Reagents, are used to provide homogenous expression of nuclear-restricted fluorescent protein for long-term analysis of cell proliferation and viability, as loss of the nuclear label is indicative of cell death. Multiplexed measurements of cell death are accomplished using mix-and-read Incucyte® Caspase-3/7 Dyes (green/red) or Incucyte® Annexin V Dyes (green/red/orange/NIR) that are added directly

to cultures. The Incucyte® Caspase-3/7 Dyes are inert, non-fluorescent (DEVD) substrates cross the cell membrane, and upon cleaving by activated caspase-3/7, release a either a green or red DNA-binding fluorescent label, appearing as fluorescently labeled nuclei within the cells. The Incucyte® Annexin V Dyes employ bright, photo-stable dyes that emit a fluorescent signal when they bind to exposed phosphatidylserine in cells undergoing early apoptosis. Cell death via cytotoxicity can be measured using a cell impermeant dye, Incucyte® Cytotox Dyes (green/red), which only labels cells when the cell membrane has been compromised. In order to study immune cell location and interactions with target cells, Incucyte® Cytolight Rapid Dyes (green/red) are typically employed, enabling simple and efficient labeling of cells for use in advanced immune cell killing models. The flexibility of this assay format also allows for the use of Incucyte® Fabfluor-488 Antibody Labeling Reagents to study changes in surface marker expression over time as cells interact and respond to external stimuli.

The Incucyte® Cell-By-Cell Analysis Software Module allows for the quantification of both labeled target cell populations and non-labeled effector cell populations (proliferation and death) in heterogeneous and complex co-cultures. This approach allows users to fully evaluate target cell death and viability, as well as track effector cell populations, in order to continuously interrogate these complex interactions over time.

Shortcomings of Traditional Assays	Live-Cell Imaging and Analysis Approaches
<ul style="list-style-type: none"> Data obtained from a single, pre-defined time point provides minimal dynamic insight into cell killing as key events may be undetected. 	<ul style="list-style-type: none"> Continuous, real-time monitoring and data collection enables quantification of dynamic interaction in real-time.
<ul style="list-style-type: none"> Concatenated end point experiments and lack of environmental control. 	<ul style="list-style-type: none"> Kinetic data on immune cell killing and interactions is collected in the controlled environment of the user's own incubator.
<ul style="list-style-type: none"> Protocols may also involve multiple washing steps with radioactivity or antibody labeling for quantification and cell lifting, perturbing cells. 	<ul style="list-style-type: none"> Non-perturbing reagents and image analysis tools for selectively quantification of apoptosis and cell proliferation.
<ul style="list-style-type: none"> Studying the responses of cell subsets among heterogeneous populations is not possible as the entire population is analyzed indiscriminately. 	<ul style="list-style-type: none"> Incucyte® Cell-by-Cell Analysis Software Module enables the classification of effector and target populations, and quantification of cellular interactions in 2D and 3D models, heterogeneous cultures.

Table 1. Shortcomings of Traditional Assays vs Live-Cell Imaging and Analysis Approaches

Sample Results

Immune Cell Killing in 2D Models

The Incucyte® Live-Cell Analysis System, along with mix-and-read reagents and integrated software, can quickly perform analysis of immune cell killing in 2D *in vitro*

models. Real-time images capture morphological changes and cellular interactions, while tumor cell proliferation and apoptosis can be quantified using image analysis. In the experiment shown in Figure 1, Incucyte®

Nuclight Red A549 tumor cells were cultured in combination with PBMCs at a target: effector (T:E) ratio of 1:10. All wells contained Incucyte® Caspase 3/7 Green Dye to measure apoptosis, and anti-CD3

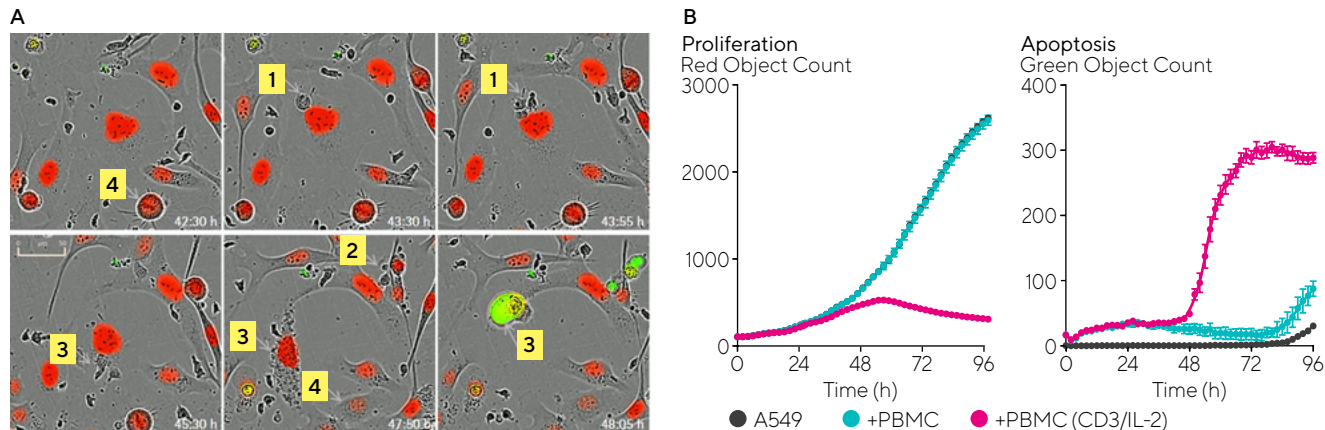


Figure 1. The use of live-cell analysis to assess immune cell killing in a simple 2D co-culture model. (A) Visualization of the interplay between immune cells and tumor cells. Images were captured in an Incucyte® Live-Cell Analysis System every 2 h over the course of 4 days.


1 Physical contact between a small cytotoxic T cell and a larger labeled tumor cell (red).

2 Tumor cells under attack from a cytotoxic T lymphocyte: The "kiss of death".

3 Tumor cell cytoplasmic granulation immediately followed by Caspase 3/7 labeling (green), nuclear condensation and cell death.

4 Tumor cell mitosis: One cell becomes two.

(B) Quantification of tumor cell proliferation (Red Object Count) and death (Green Object Count) in real-time.

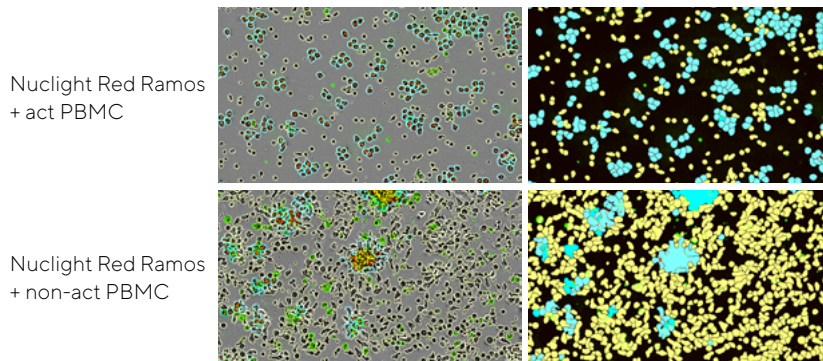


and IL-2 were added to select wells to activate the PBMCs. Wells in which PBMCs were activated showed increased target cell death (Green Object Count) and reduced proliferation (Red Object Count). This study illustrates the use of live-cell analysis to obtain aggregate measures of tumor cell proliferation and apoptosis, and to provide valuable qualitative data showing the interplay between cell types. This type of analysis can also be valuable for troubleshooting and quality control (QC) to monitor cell cultures for cell health and function for greater consistency and reproducibility.

Unlike other traditional assays for immune cell killing, Incucyte® integrated analysis software can perform automated detection and selective quantitation of cell death in real time in mixed cultures. This is achieved by Incucyte® Cell-By-Cell Analysis Software Module masking, which recognizes all cells within the image based on fluorescence. This allows the quantification of both labeled target cell populations and non-labeled effector cell populations (proliferation and death) in heterogeneous and complex co-cultures. With adherent target cells, the software enables the user to track effector cell populations in the presence of target cells. To illustrate the use of cell masking software in non-adherent cultures, Nuclight Red Ramos cells (10,000 cells/well) were mixed with

an increasing ratio of pre-activated or non-activated PBMCs in the presence of Incucyte® Annexin V Green Dye as a marker of apoptosis (Figure 2). Advanced image processing algorithms within the Incucyte® Cell-by-Cell Analysis Software Module were used to mask individual cells, which could then be classified into target and effector cell populations based on the presence or absence of red fluorescence. The target cell population (red) displayed a decrease in proliferation and an increase in apoptosis in the presence of increasing numbers of effector cells. In contrast, the effector cell population (non-red) displayed proliferation over time, but only for activated cells.

A Effector Cells (Yellow Mask) | Target Cells (Blue Mask)



B Classification of Populations

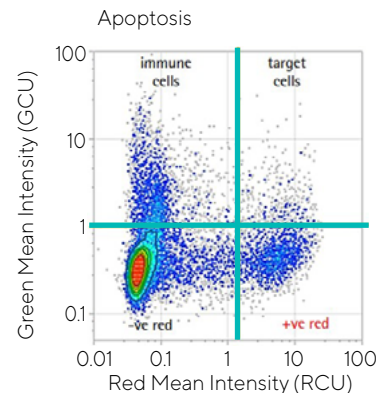
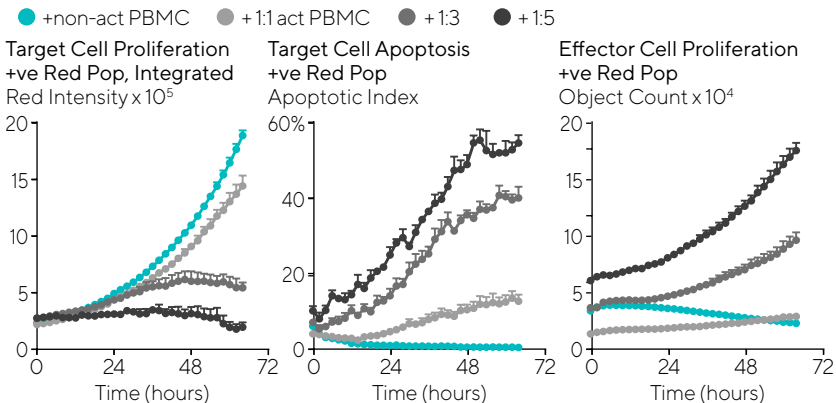


Figure 2. Enhanced image quantification using Incucyte® Cell-by-Cell Analysis Software Module.

(A) Images show individual cell masking of the total population with the Cell-by-Cell Analysis Software. Target (blue) and effector (yellow) sub-populations were distinguished based on red fluorescence. (B) Sub-populations were classified based on red and green fluorescence. (C) Quantification of proliferation and apoptosis over time. The target cell population (positive red cells) shows a decrease in proliferation and increase in apoptosis (% of red cells also green) in the presence of increasing numbers of effector cells. The effector cell population (non-red cells) shows proliferation when activated. Data shown as mean \pm SEM, $n=4$ wells.

C



An additional analysis challenge is the ability to visualize and quantify the kinetics of interactions between immune cells and their tumor targets. Figure 3 demonstrates the ability of the Incucyte® Cell-By-Cell Analysis to quantify the coincidence or overlay of two cell masks to analyze immune and target cell interactions. In this study, A549 cells labeled with Incucyte® Cytolight Rapid Red were cultured with either pre-activated or non-activated PBMCs (T:E ratio of 1:5) in the presence of Incucyte® Fabfluor-488- α -CD45 and Incucyte® Opti-Green background suppressor to label the total lymphocyte population. Two hours after PBMC addition, the image processing software was used to mask the cells, enabling the quantification of spatial information from target and effector cells to be quantified. Activated PBMCs showed significantly greater interaction with target cells, aligning with cell engagement and increased immune cell killing (ICK).

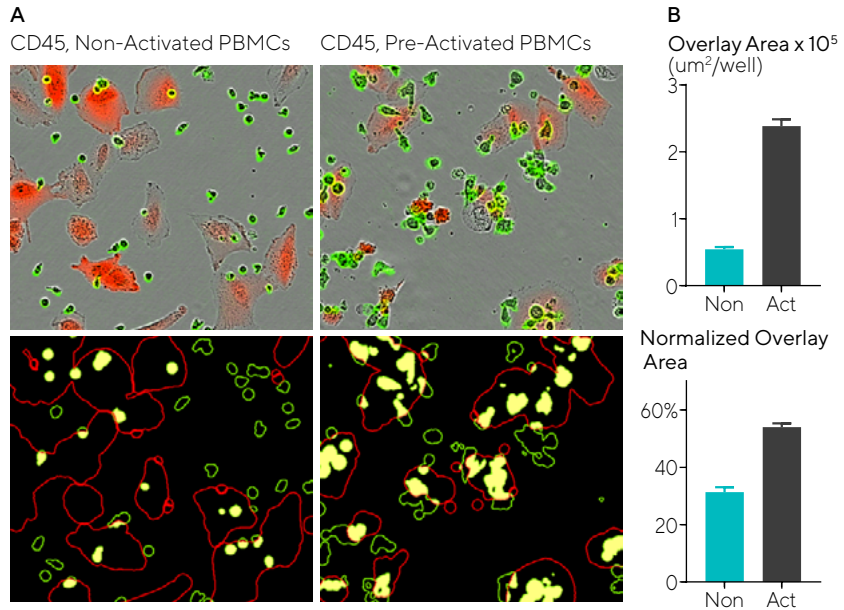




Figure 3. Visualization and quantification of immune and tumor cell interactions. (A) Images at two hours after PBMC addition show interactions between CD45+ cells (green) and A549 cells (red). The overlay between the two cell types is shown with the yellow mask. (B) Quantification of the overlay reveals a markedly higher interaction for activated compared to non-activated effector cells.



Another limitation of some traditional assays is the lack of flexibility to measure immune cell killing in both adherent and non-adherent cell cultures. As shown in Figure 4, Incucyte® Nuclight NIR A549 cells were co-cultured with increasing numbers of activated or non-activated PBMCs. Incucyte® Annexin V Orange Dye, Incucyte® Fabfluor-488- α -CD45 antibody complex and Incucyte® Opti-Green

background suppressor were also added to the wells to measure apoptosis and enable subpopulation analysis. Count of NIR (blue) nuclei was used to quantify target cell proliferation, and the area of orange fluorescence, corresponding to Annexin V Orange, was used to calculate target cell death. The Incucyte® Cell-by-Cell Analysis Software Module was used generate total effector cell numbers label free and in

the presence of tumor cells. Additionally, quantification of the Fabfluor-488-CD45 signal confirmed that >80% of the PBMCs were CD45 positive immune cells.



The Incucyte® Cell-by-Cell Analysis Software Module can also be used to quantitate non-adherent target and effector cell proliferation, death and perform subpopulation analysis. As shown in the experiment in Figure 5, activated or non-activated PBMCs were added to cultures of Nuclight Orange Ramos cells in the presence of Incucyte® Annexin V

NIR Dye, Incucyte® Fabfluor-488- α -CD8 antibody complex and Incucyte® Opti-Green background suppressor. In the presence of activated PBMCs, reduced target cell proliferation (orange-red) and increased target cell death (blue) was observed. The Incucyte® Cell-by-Cell Analysis Software Module also used the total target and effector cell numbers to

calculate the apoptotic index of target cells. Additionally, with the use of the Fabfluor- α -CD8 enabled subpopulation analysis of the PBMCs to determine the percentage of total effector cells that were CD9 positive.

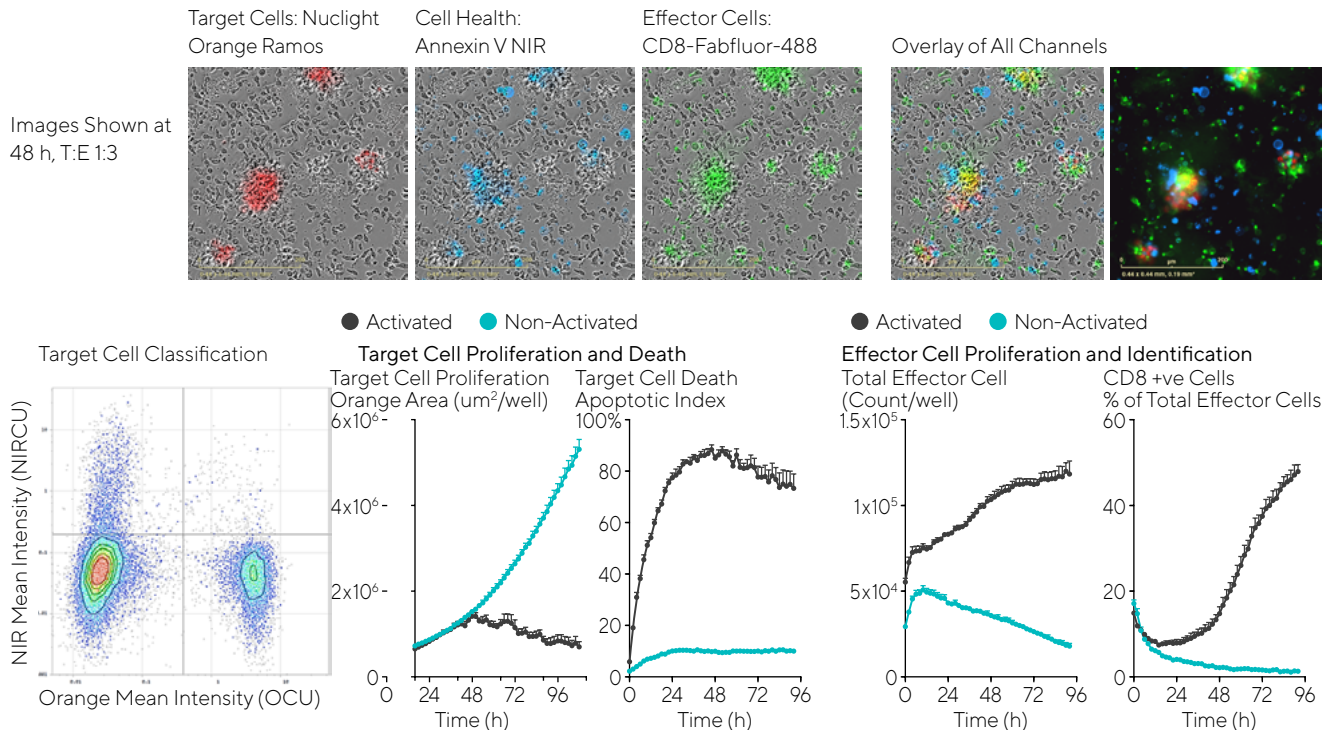


Figure 5. Measurement of non-adherent target and effector cell proliferation, death and subpopulation analysis using Incucyte® Cell-by-Cell Analysis Module. Ramos cells, transduced with Incucyte® Nuclight Orange Lentivirus were co-cultured with activated or non-activated (using anti-CD3/IL-2) PBMCs in the presence of Incucyte® Annexin V NIR Dye, Incucyte® Fabfluor-488- α -CD8 antibody complex and Incucyte® Opti-Green background suppressor. Quantification of Orange (red) nuclei indicate target cell proliferation and area of NIR (blue) fluorescence the target cell death. Using Incucyte® Cell-by-Cell Analysis Software Module total target and effector cell numbers, apoptotic index of target cells can be quantified and graphed over time.

3D Immune Killing

The use of advanced 3D *in vitro* models continues to increase in the quest for greater translational relevance, particularly in the fields of cancer biology, immunology and hepatotoxicity² (See Chapter 8 - Kinetic Assays for Complex Cell Models for more details). The Incucyte® Live-Cell Analysis System enables the study of 3D single spheroid analysis in real-time. Brightfield (BF) imaging, in combination with phase contrast imaging, enables label free study of 3D spheroid morphology, growth, and shrinkage in 96- and 384-assay formats. Incucyte® HD phase images facilitate comprehensive visualization of spheroid morphological features (shape, size) and intercellular compaction (loose aggregates vs. compact spheroids) characteristic for each cell type. BF provides the means for objective spheroid kinetic quantification and cell dependent growth rate profile assessment for diverse type of spheroids.

As shown in Figure 6 on the next page, Nuclight Red A549 tumor cells were seeded in a round-bottom 96-well plate and allowed to form spheroids over three days. Once formed, spheroids were co-cultured with PBMCs at a T:E ratio of 1:2.5 in the presence or absence of activating cytokines (anti-CD3 and IL-2). Incucyte® HD phase and fluorescence images were then used to monitor the spheroids over several days. Results show a marked loss of fluorescence intensity for spheroids in the presence of activated PBMCs, which reflects an increased death of tumor cells and is used to quantify cytotoxicity.

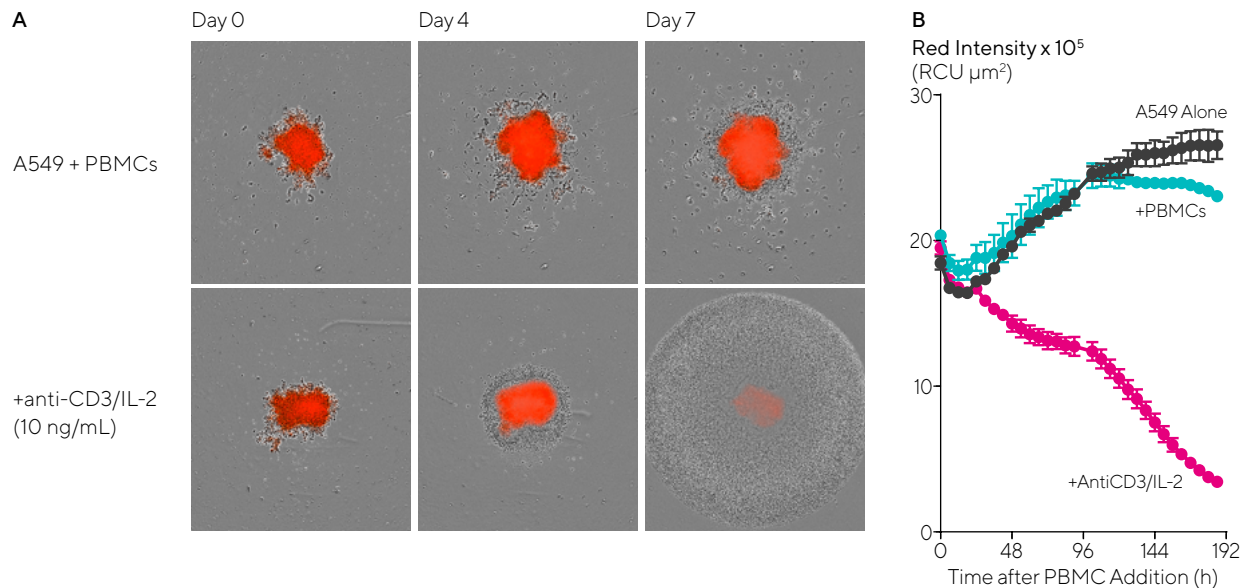


Figure 6. Impact of activated PBMCs on tumor spheroid proliferation. (A) HD phase and fluorescence images compare the effect of PBMCs on spheroid proliferation in the absence (top panel) and presence (bottom panel) of activating cytokines. A marked loss of fluorescence intensity can be seen in the presence of activated PBMCs. (B) Time-course plot shows spheroid cytotoxicity quantified as a loss of fluorescence intensity over time. Data was collected over seven days at six-hour intervals. Data shown as mean \pm SEM, $n=3$ wells.

Additionally, Incucyte® Live-Cell Imaging and Analysis can be used to measure antibody dependent cell mediated cytotoxicity (ADCC), as seen in Figure 7. First, Nuclight Red SKOV-3 spheroids were cultured alone or with increasing densities

of activated PBMCs. As seen in the images, red fluorescence intensity decreased over time in the spheroids cultured with increasing concentrations of PBMCs. Next, spheroids were cultured treated with Herceptin (0.08 – 50 $\mu\text{g/mL}$) in the

presence or absence of activated PBMCs, and a Herceptin-induced concentration dependent inhibition of SKOV-3 spheroid growth was observed and quantified via kinetic and AUC data.

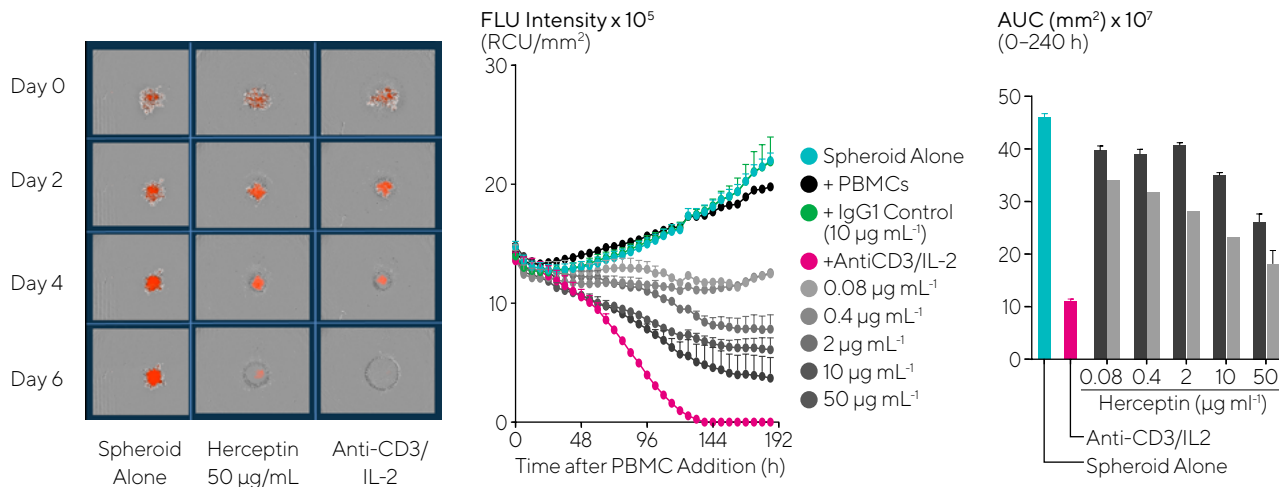



Figure 7. Measurement of ADCC in tumor spheroids. Blended phase and fluorescent images of Nuclight Red SKOV-3 spheroids in the presence or absence of immune cells, either untreated or in the presence of anti-CD3 (10 ng/ml)/IL-2 (10 ng/ml) or Herceptin (0.08 – 50 $\mu\text{g/mL}$). Cytotoxicity was quantified based on the red fluorescent intensity. Kinetic and AUC data demonstrate destruction of tumor spheroids by the activated PBMCs and a Herceptin-induced cell cytotoxicity.



In addition to single spheroid analysis, the versatile Incucyte® Live-Cell Analysis System can perform quantitative analysis of immune cell killing in more complex, 3D multi-spheroid models, overcoming a significant restriction of other analysis methods and platforms. Shown in figure 8, the ADCC Herceptin on Her2 positive cells was assessed. Her2 negative Nuclight Red MCF-7 cells or Her2 positive Cytolight Green BT-474 cells were seeded on

Matrigel® and multi-spheroids formed over three days. Herceptin was added in either the presence or absence of PBMCs (T:E ratio of 1:5) and the spheroids were monitored over several days via BF and fluorescence imaging. A concentration-dependent loss of fluorescence in the presence of Herceptin was observed only in the Her2 positive BT-474 cells, but not the Her2 negative MCF-7 cells. However, following activation of the T cell

populations (anti-CD3/IL-2), increased cytotoxicity was observed in both cell types as seen by a loss of fluorescence intensity

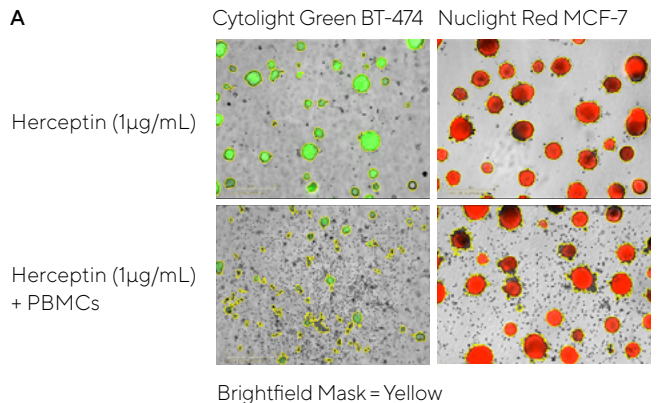
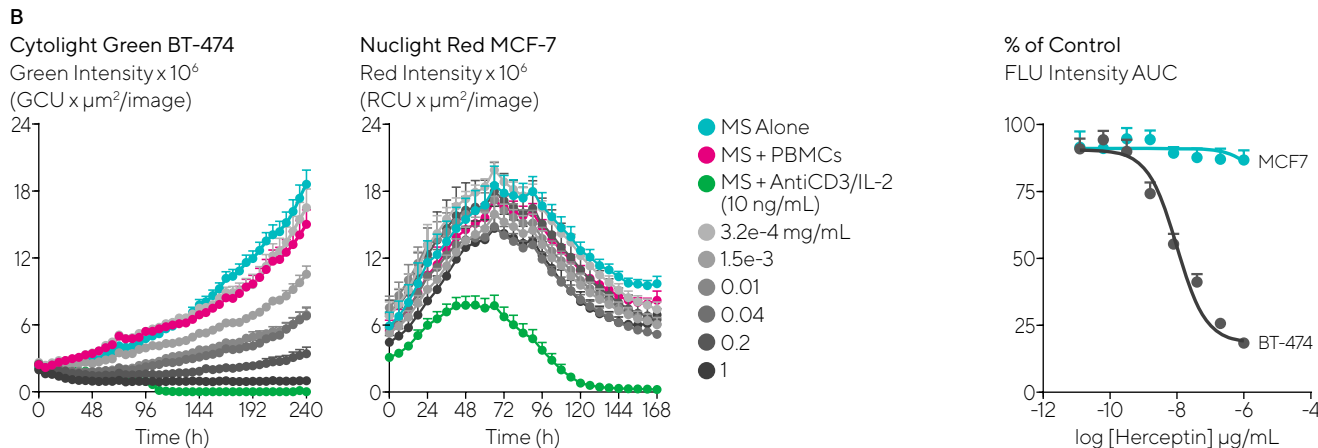


Figure 8. Impact of Herceptin-induced PBMCs on multi-spheroid proliferation. (A) Incucyte® BF and fluorescence images taken at seven days (Nuclight Red MCF-7) or ten days (Cytolight Green BT-474) show the effect of Herceptin on spheroid proliferation in the absence (top panel) and presence (bottom panel) of PBMCs. The brightfield outline mask is shown in yellow. (B) Time-courses show multi-spheroid death quantified as a loss of fluorescence intensity within the spheroid brightfield object. Increased cytotoxicity was seen with the addition of treatments activating T cell populations (anti-CD3 and IL-2). Data was collected over ten (BT-474) or seven (MCF-7) days at six-hour intervals. Data shown as mean \pm SEM, $n=4$ wells.



Conclusions

The immune cell studies show above highlight how Incucyte® Live-Cell Analysis System, Incucyte® Cell-by-Cell Analysis Software Module, and non-perturbing Incucyte® reagents work harmoniously to provide an end-to-end solution to many of the challenges of traditional immune cell killing assays. The comprehensive collection and analysis and immune cell killing, cellular interactions, in both 2D and complex 3D models, represents a significant step forward in the analysis of these critical interactions, maximizing the amount of data collected from each sample to provide new insights with greater translational relevance. This flexible platform provides the following benefits for the assessment of immune cell killing:

- Incucyte® Live -Cell Imaging and Analysis captures the kinetics of immune cell killing and cellular interactions allowing for tracking time-dependent biological interactions, critical for personalized immunotherapies.
- Specific and robust multiplexed measurements of cell proliferation, viability, death as well as protein expression can be performed in every well at every time point to generate data rich information.
- Non-perturbing reagents and environmentally controlled conditions maintain greater physiological relevance, and cells may be harvested for select downstream analysis, maximizing the data obtained from each sample.
- Incucyte® Cell-by-Cell Analysis Software Module and masking enables the classification of effector and target populations and quantification of cellular interactions for detailed information into each cell population within the complex co-culture model.
- The Incucyte® Immune Cell Killing Assay is amenable to both 2D- and 3D- cultures using 96- or 384-well throughput, which is ideal for pre-clinical research and pharmacological screening activities.

References

1. Bernards R, et al. **A roadmap for the next decade in cancer research.** *Nature*, 2020 *Cancer*, Vol. 1:12-17.
2. Elliott NT and F YUAN. **A review of three-dimensional in vitro tissue models for drug discovery and transport studies.** *Pharmaceutical Science*, 2011, 100:59-74.
3. Costa EC et al. **3D tumor spheroids: an overview on the tools and techniques used for their analysis.** *Biotechnol Adv.*, 1026 Dec ;34(8):1427-1441.
4. L. Zaritskaya, M. R. Shurin, T. J. Sayers, and A. M. Malyguine, **New flow cytometric assays for monitoring cell-mediated cytotoxicity.**, *Expert Rev. Vaccines*, 2010, Jun, vol. 9, no. 6, pp. 601-16.
5. D. L. Nelson, C. C. Kurman, and D. E. Serbousek, **51 Cr Release Assay of Antibody-Dependent Cell-Mediated Cytotoxicity (ADCC)**, in *Current Protocols in Immunology*, 2001, vol. 8, no. 1, Hoboken, NJ, USA: John Wiley & Sons, pp. 7.271-7.278

IncuCyte® User Publications

1. Griffiths, G.M. et al. **Loss of ARPC1B impairs cytotoxic T lymphocyte maintenance and cytolytic activity.** *J Clin Invest*, 2019, 129(12):5600-5614.
2. Adams, KJ et al. **The use of induced pluripotent stem (iPS) cells for the safety testing of enhanced affinity TCR-transduced T cells.** *Cancer Research*, AACR, 2014, April 5-9, San Diego, CA.
3. Adams, K. **Redirected T cell activity by high affinity TCR-Anti-CD3 Bispecific candidate therapeutics.** 2013. [PhD Dissertation, Cardiff University]
4. Roth TL et al. **Reprogramming human T cell function and specificity with non-viral genome targeting.** *Nature*.2018, Jul; 559 (7714): 405-409.
5. Shifrut E., et al. **Genome-wide CRISPR screens in primary human T cell reveal key regulators of immune functions.** *Cell*, 2018, Dec 13; 175(7):1958-1971.
6. Fry TJ, et al, **CD22-targeted CAR T cells induce remission in B=ALL that is naive or resistant to CD19-targeted CAR immunotherapy.** *Nat Med.*, 2018, Jan; 24(1):20-28.
7. Lanigan TM, Rasmussen SM, Weber DP, et al. **Real time visualization of cancer cell death, survival and proliferation using fluorochrome-transfected cells in an IncuCyte® imaging system.** *J Biol Methods.* 2020.;7(2):e133. Published 2020 Jun 12.

Kinetic Assays for NETosis

Quantification and Visualization of NETosis

Introduction

Neutrophils are the first line of defense at the site of an infection, playing an essential role in the innate immune system, employing multiple strategies to degrade and kill microbes. One of these strategies is programmed neutrophil cell death known as NETosis, during which neutrophils corner and destroy the invading pathogens and abnormal cells through the formation of neutrophil extracellular traps (NETs). These NETs contain DNA from neutrophils, nuclear chromatin, antimicrobial and oxidant enzymes. NETs are produced when enzymes within the neutrophil are transported to the nucleus, followed by chromatin decondensation which causes the internal cellular membranes break down and NETs are released. The formation of NETs by neutrophils has been implicated in the pathogenesis of diseases such as thrombosis and stroke, preeclampsia, malaria, cancer, sepsis, and

autoimmune disease, among others. Most recently, NETosis has gained attention for its possible role in the immunothrombosis and ARDS of COVID-19 infection, with NETosis biomarkers of cell-free DNA, myeloperoxidase DNA (MPO-DNA), and citrullinated histone H3 (Cit-H3) in COVID-19 patient serum samples.^{1,2}

Studying NETosis *in vitro* with standard end-point methods such as microscopy (immunofluorescence, TEM, and SEM) or indirect, biomarker detection by methods such as flow cytometry, ELISA, or cell-free DNA detection kits is challenging. These approaches involve technically laborious, time-consuming protocols that lack environmental control as cells are removed from the incubator for analysis of cells or collection of supernatant samples. These protocols may use stains, reagents, and cell lifting protocols that perturb normal cellular physiology. Studies are often performed as end-point assays that miss important kinetic events of NET formation and release.

Further, standard microscopy approaches can be subject to bias. Standard end-point assays may also be unable to distinguish between NETosis and other cell death mechanisms, such as apoptosis.

This chapter examines how the Incucyte® NETosis Assay addresses many of the challenges imposed by standard end-point methods by enabling real time, automated, direct visualization and quantification of NETosis throughout the time-course of NET formation and release. Using live cell imaging and analysis and the non-perturbing mix-and-read Incucyte® Cytotox Green Dye, the various stages of NETosis involving swelling and decondensation of nuclei followed by NET release can be observed and measured easily and in a physiologically relevant environment. Unlike tedious microscopy methods, the Incucyte® Live-Cell Analysis System and integrated software analysis tools enable the throughput necessary to comprehensively study the dynamics of NET formation and

release, in real time, making it well-suited for pharmacological screening.

Incucyte® NETosis Assays at a Glance

The Incucyte® NETosis Assay combines the use of Incucyte® Cytotox Green Dye and live-cell imaging and analysis for visualization and quantification of neutrophils undergoing NETosis. Captured HD phase and fluorescent images are automatically analyzed in the physiologically controlled environment of the user's own incubator allowing to track NETosis in real-time as well as identify the distinct morphological changes associated with NETosis, including loss of multi-lobulated nuclei, nuclear decondensation, and membrane compromise. The mix-and-read Incucyte® Cytotox Green Dye, can be used to rapidly visualize and quantify NETosis as extracellular DNA is released and undergoes fluorescence enhancement. Multiplexing the Incucyte® Cytotox Green Dye with Incucyte® Annexin V Red Dye can supply mechanistic insights, as users can readily discriminate between NETosis and apoptosis. The NETosis Assay allows for multiplexing with other

Shortcomings of Traditional Assays	Live-Cell Imaging and Analysis Approaches
<ul style="list-style-type: none">▪ Data obtained from a single, pre-defined time point provides minimal dynamic insight as key events may be undetected.	<ul style="list-style-type: none">▪ Continuous, real-time monitoring and data collection enables detection of morphological and functional temporal differences for NETosis validation and response to treatment effects.
<ul style="list-style-type: none">▪ Concatenated end point experiments with standard methods lack environmental control.	<ul style="list-style-type: none">▪ Cells remain unperturbed in the incubator, and are visualized and quantitated in real-time via repeated interrogation of the same well.
<ul style="list-style-type: none">▪ Tedious staining protocols and reagents that may perturb cell physiology.	<ul style="list-style-type: none">▪ Non-perturbing reagents and simple mix-and-read 96-well protocols enable throughput suitable for pharmacological screening.
<ul style="list-style-type: none">▪ Additional experimentation may be needed to distinguish NETosis from other cell death mechanisms such as apoptosis.	<ul style="list-style-type: none">▪ Ready discrimination between NETosis and cell death events, such as apoptosis, using multiplexing with non-perturbing reagents and apoptotic readouts.

Table 1. Shortcomings of Traditional Assays vs Live-Cell Imaging and Analysis Approaches

reagents to distinguish NETosis from other cell death mechanisms and examine events such as ROS formation, externalization of phosphatidylserine, and caspase activation.

Sample Results

The Incucyte® Live-Cell Analysis System enables the live-cell visualization of NETosis in real-time throughout the

course of NET formation. This is enabled by combining phase and fluorescence imaging to visualize and quantitate NET formation. In the experiment shown in Figure 1 below, HL-60 cells were differentiated to neutrophil-type using DMSO and ATRA, generating multinuclear HL-60 cells, which were stimulated with PMA. At approximately t=2h post-stimulation, the nuclei began

to decondense. As the cytoplasm mixed with karyoplasm, the nuclei were no longer visible in phase contrast images. The nuclear contents then moved to the plasma membrane and were released. External DNA bound to the Incucyte® Cytotox Green Dye and fluorescence enhancement (green) was observed, appearing approximately t=2h post-stimulation.

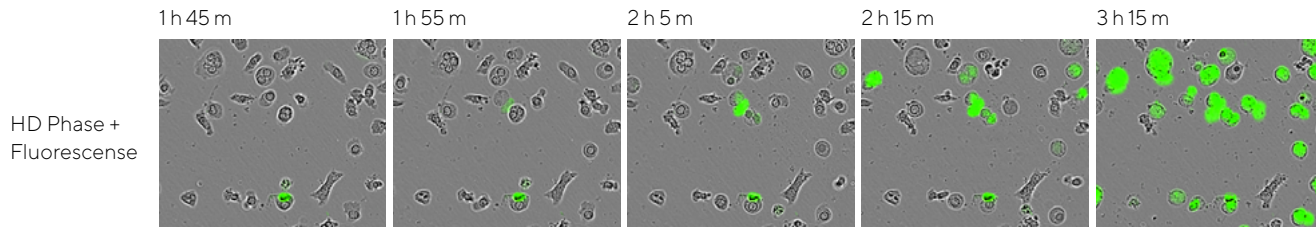


Figure 1. Incucyte® live-cell visualization of NETosis. Differentiated HL-60 cells imaged with phase and fluorescence imaging, demonstrating visualization of neutrophil extracellular trap (NET) formation.

Multiplexing Incucyte® Cytotox Green Dye with other fluorescent reagents can enable deeper assessment and observation and quantification of other cellular events in real-time. Figure 2 shows how the Incucyte® Live-Cell Analysis System was used to capture NET formation in primary human neutrophils, along with reactive oxygen species (ROS) formation. Primary human neutrophils were extracted from blood and seeded in serum-free media onto an Incucyte® Imagelock 96-well Plate,

which enabled the collection of high-quality image registration for time-lapse imaging. This experiment was performed in the presence of Incucyte® Cytotox Green Dye and CellROX™ Deep Red. Cells were then stimulated with PMA (100 nM) and placed into Incucyte® Live-Cell Analysis System, and HD phase contrast and fluorescence images were acquired. Morphology changes were observed, and as the cells flattened and became adherent, ROS formation was visualized

and quantified using the CellROX™ Deep Red reagent. At $t=1\text{h}$ post-stimulation, ROS formation peaked, and intracellular membranes began to permeabilize. At $t>2\text{h}$ post stimulation, many of the nuclei were no longer visible in phase and nuclear contents were expelled into extracellular space as visualized by the green fluorescence.

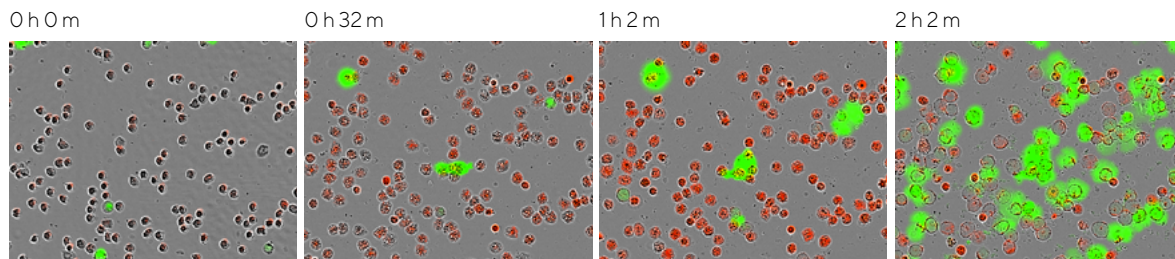


Figure 2. Incucyte® live-cell visualization of NET formation in primary human neutrophils stimulated with PMA and assessed for NETosis using Incucyte® Cytotox Green Dye and ROS formation using CellROX™ Deep Red.

The power of the Incucyte® Live-Cell Analysis System lies not only in the HD imaging, but also with the integrated software and fluorescence masking capabilities. Figure 3 below details how this adds value to the analysis. As shown below, PMA-stimulated cells generated NETs, which were visualized as large asymmetric clouds of extracellular DNA which fluoresce in the presence of Incucyte® Cytotox Green Dye. These cells were found to have the largest average object area. CMP-treated cells undergoing apoptosis demonstrate permeabilization of the plasma membrane, which enabled nuclear staining that resulted in small round objects (green). Untreated vehicle (VEH) cells in culture contained a small number of dead cells, which were similar to apoptosis-induced, but fewer in number. Fluorescent masking algorithms (yellow outline) yielded average fluorescent object size (top right graph) which clearly separated NETosing (PMA-stimulated) and apoptotic (CMP-treated) cells. Additionally, using a size exclusion filter to remove smaller objects, such as dead cells, from the analysis allows for direct quantification of the NETosis signal (bottom right graph).

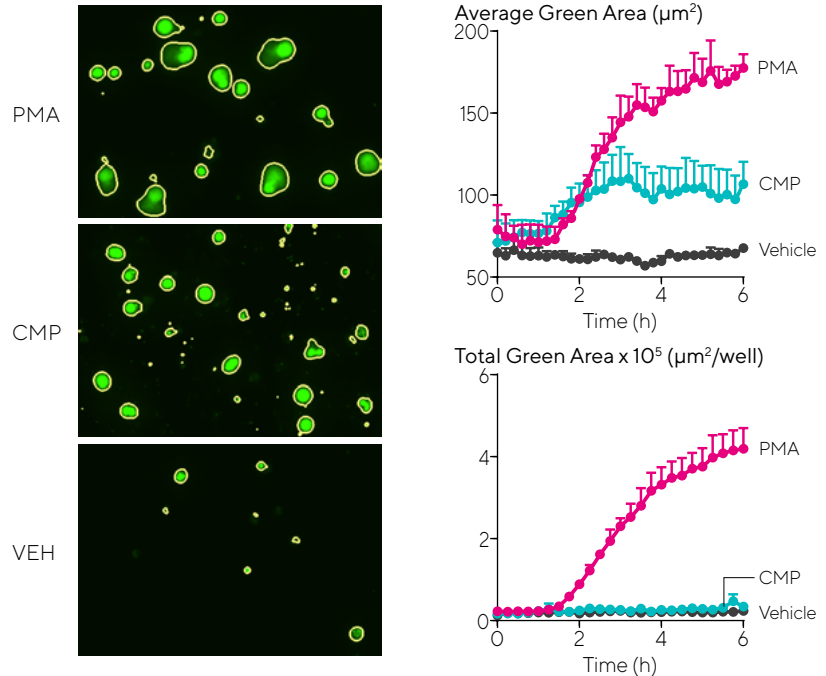


Figure 3. Quantification of NETs by fluorescence masking with Incucyte® Live-Cell Analysis System. NET formation following PMA, CMP or vehicle treatment is visualized using the Incucyte® Cytotox Green Dye. Kinetic time course graphs of Average Green Area and Total Green Area allow for separation of cells undergoing NETosis (PMA-stimulated) and cells undergoing apoptosis (CMP-treated).

Kinetic data, generated by the Incucyte® Live-Cell Analysis System and analyzed with integrated, user friendly software, can provide additional mechanistic insights. Figure 4 shows the examination

of temporal events surrounding the nature of the PMA-induced ROS formation. As shown, ROS formation occurs precedes NET release, and DPI was found to inhibit the NADPH oxidation activation,

inhibiting PMA induced NET release for up to 6 hours. This comprehensive analysis revealed that the PMA-induced NETosis was ROS-dependent.

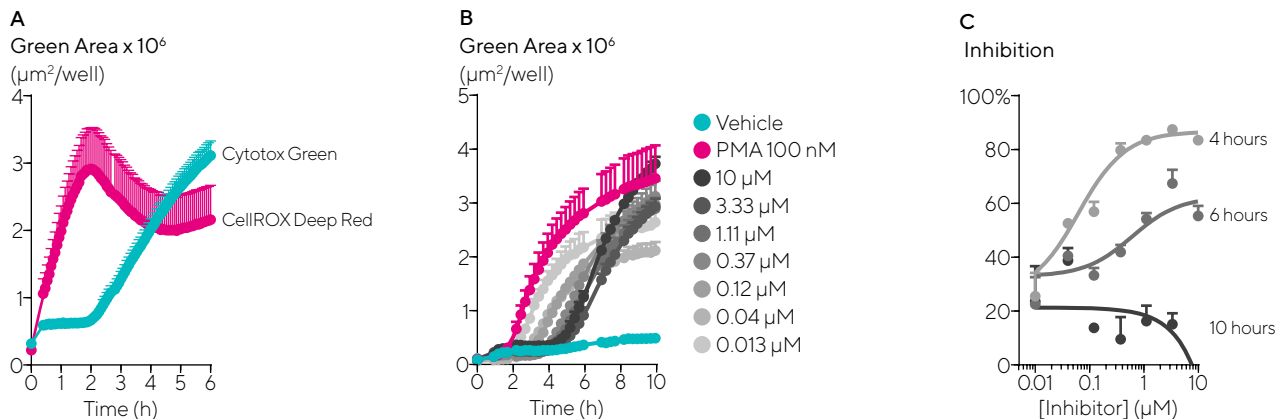


Figure 4. PMA-induced NETosis is ROS-dependent. (A) Overlay of ROS (pink) and NET release (teal) response: ROS burst (0-1h) precedes NET release (>2h) (B) DPI inhibits NADPH oxidase activation (respiratory burst) for up to 6h and therefore NET release is inhibited. (C) PMA-induced NETosis is inhibited in the presence of DPI up to 6h.

Incucyte® Live-Cell Imaging and Analysis can also differentiate between different mechanisms of NETosis, as shown below in Figure 5. Using the Incucyte® Cytotox Green Dye (Green Area), it was found that ionomycin induced rapid formation of NETs, while PMA induced NETosis

began about 2 h post stimulation. Additionally, Incucyte® Annexin V Red Dye was used to show how cells treated with ionomycin were found to externalize phosphatidylserine (PS) rapidly, during which time PMA and CMP treatment both showed lower and slower increases

in PS externalization (early indicator of apoptosis). However, it was found that PMA stimulates rapid ROS production (0-1h), preceding NET release which indicates that ionomycin induces NETosis via a ROS independent mechanism.

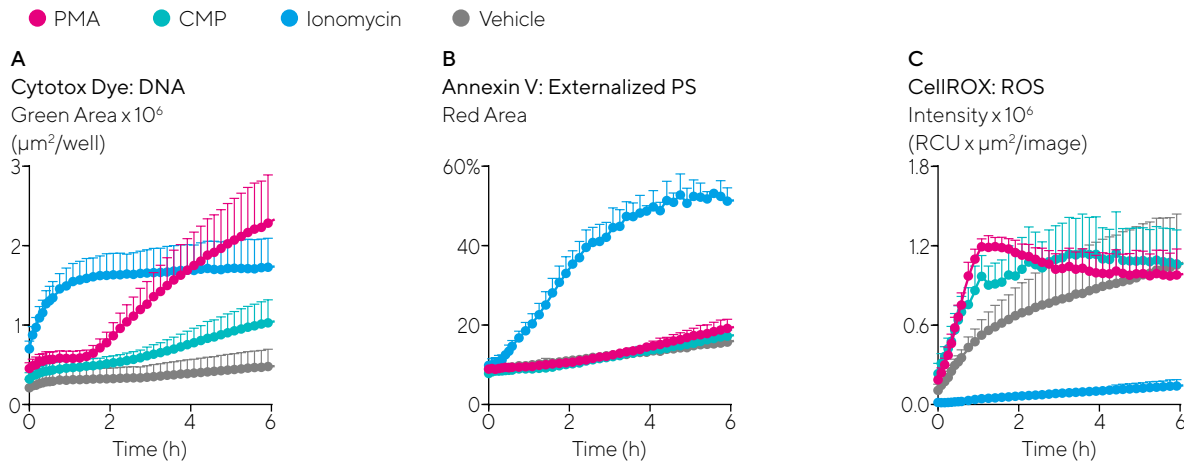


Figure 5. Differentiation of NETosis mechanisms. (A) Kinetic time-course graphs showing increases in Green Area (Incucyte® Cytotox Green Dye) in cells treated with ionomycin (blue), PMA (pink), and CMP (teal). (B) PS externalization following treatment of ionomycin, PMA and CMP was quantified with Incucyte® Annexin V Red over 4 h. CellROX™ Deep Red was used to show the time-course of ROS production in cells treated with ionomycin, PMA and CMP.

Verifying NET formation using biomarkers is often a part of clinical diagnostic assessment. The experiment shown in Figure 6 below demonstrates the validation of an *in vitro* Incucyte® NETosis Assay using the NETosis biomarkers of myeloperoxidase (MPO) and neutrophil elastase (NE). Following an 18 h kinetic

analysis, cells in a 96-well microplate were removed from Incucyte® Live-Cell Analysis System. Supernatant samples were removed and cells were fixed and immunofluorescence staining for myeloperoxidase (MPO) and neutrophil elastase (NE) was conducted. With a PicoGreen™ Assay, it was determined

that PMA-induced NETosis resulted in a high concentration of cell-free DNA. Additionally, immunofluorescence analysis confirmed a high presence of extracellular MPO and NE from PMA treated cells as opposed to lack of MPO and little NE released by untreated cells.

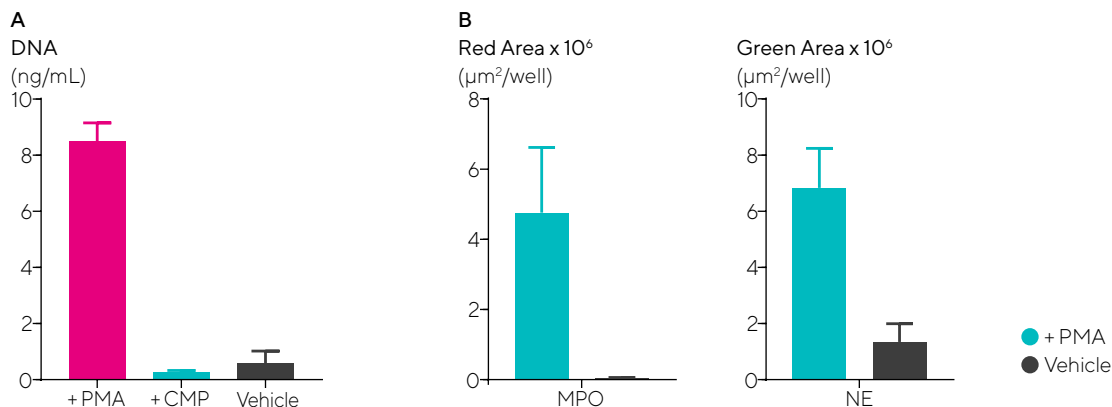


Figure 6. (A) PicoGreen™ Assay for quantification of cell-free DNA following PMA, CMP and vehicle control treatment (B) Total fluorescence area was observed after immunofluorescence with anti MPO or anti-NE antibodies and appropriate conjugated secondary Ab. It was found that PMA-treated cells released of MPO and NE into extracellular space while untreated cells released no MPO and little NE.

Conclusions

As outlined in the studies above, the Incucyte® NETosis Assays and Incucyte® Live-Cell Analysis System overcome many of the challenges of studying NETosis *in vitro* encountered when using standard end-point methods (microscopy, flow cytometry, ELISA, or cell-free DNA detection), providing users with:

- Incucyte® Live-Cell Analysis System, integrated software, non-perturbing reagents and mix-and-read protocols enable real time, automated, direct visualization and quantification of NETosis throughout the time course of NET formation and release for greater insight.
- Assays are performed within the physiologically controlled environment of the incubator for minimal perturbation.
- Flexibility to use HD phase contrast or fluorescent time-lapse imaging to capture the distinct morphological changes associated with NETosis.
- Ability to multiplex with other reagents and staining to distinguish NETosis from other cell death mechanisms, and to examine events such as ROS formation, externalization of phosphatidylserine, and caspase activation, among others.
- Throughput needed to simultaneous comparison of different sample types and treatment kinetics to better understand the underlying mechanisms of NETosis, ranging from early events to NET release.

Taken together, the Incucyte® Live-Cell Analysis System, software analysis tools, and non-perturbing reagents provide an end-to-end solution for the rapid, real-time visualization and quantification of NETosis, making this platform ideally suited for pharmacological screening.

References

1. Middleton EA, He XY, Denorme F, *et al.* **Neutrophil Extracellular Traps (NETs) Contribute to Immuno-thrombosis in COVID-19 Acute Respiratory Distress Syndrome** [published online ahead of print, 2020 Jun 29]. *Blood*. 2020.
2. Yalavarthi S, Shi H, *et al.* **Neutrophil extracellular traps in COVID-19.** *JCI Insight*, 2020,5(11):138999. Published 2020 Jun 4
3. Gupta S, Chan DW, Zaal KJ, Kaplan MJ. **A High-Throughput Real-Time Imaging Technique To Quantify NETosis and Distinguish Mechanisms of Cell Death in Human Neutrophils.** *J Immunol*. 2018;200(2):869-8.

Incucyte® User Publications

1. Barr FD, Ochsenbauer C, Wira CR, Rodriguez-Garcia M. **Neutrophil extracellular traps prevent HIV infection in the female genital tract.** *Mucosal Immunol.*, 2018, 11(5):1420-1428.
2. Chirivi, R.G.S., van Rosmalen, J.W.G., van der Linden, M. *et al.* **Therapeutic ACPA inhibits NET formation: a potential therapy for neutrophil-mediated inflammatory diseases.** *Cell Mol Immunol*, 2020,10.1038/s41423-020-0381-3.
3. Brown AC, Reddy VRAP, Lee J, Nair V. **Marek's Disease Virus Oncoprotein Meq Physically Interacts with the Chicken Infectious Anemia Virus-encoded Apoptotic Protein Apoptin** *Oncotarget*, 2018, Jun 22;9(48):28910-28920.
4. Cubas-Gaona LL *et al.* **Exacerbated Apoptosis of Cells Infected with Infectious Bursal Disease Virus upon Exposure to Interferon Alpha.** *J Virol.*, 2018, May 14;92(11).

5d

Kinetic Assays for Immune Cell Differentiation, Phagocytosis and Efferocytosis

Monitor Differentiation and Quantify Phagocytosis and Efferocytosis

Introduction

Following activation, immune cells differentiate to carry out functional activities, such as phagocytosis, for the elimination of invading pathogens, and efferocytosis for the elimination of apoptotic or abnormal tumor cells. The ability of immune cells to carry out appropriate phagocytic responses can be key for identifying new therapeutic targets and studying their efficacy, or for detecting possible impairment of functional phenotypes.

Common methods to assess differentiation, phagocytosis and efferocytosis in immune cell models may fail to distinguish between phagocytosis and the artifacts arising from non-specific cellular uptake and/or surface-bound, non-internalized fluorophores. Further, such

assays are often unable to directly visualize and monitor morphological changes in cellular differentiation, and temporally couple these with functional changes such as cell engulfment and quantitation of internalization. Traditional methods may involve laborious protocols, cell lifting (e.g. flow cytometry) or washing/quenching of the labeled pathogen (e.g. fluorescein labeling), and often provide only a single time point (e.g. High Content Analysis (HCA) which fails to capture key dynamic cellular changes.

Live-cell imaging and analysis alleviates these challenges by providing morphological and phenotypic analysis that can be measured over the long term (hours to weeks). Unlike traditional assays, users may profile and quantitate real-time functional changes that occur as cells differentiate and respond to immune

challenge, providing greater insight into cell behaviors with greater accuracy and sensitivity¹. Live-cell imaging and analysis also minimizes cell perturbation through acquisition of data from within the stable environment of the tissue culture incubator as the optical train moves to the wells to collect images for analysis, thus reducing artifacts that are typically introduced during cell manipulation and handling. In this chapter, we will discuss how Incucyte® Differentiation, Phagocytosis and Efferocytosis Assays can be used to in real-time throughout the course of the experiment to better understand how differentiation impacts immune cell function.

Incucyte® Differentiation,
Phagocytosis, and Efferocytosis
Assays at a Glance

Analysis of immune cell differentiation is accomplished through automated analysis of morphological and phenotypic changes as detected by HD phase and fluorescence imaging. Changes in immune cell shape (eccentricity), for cell types such as PMNs, can be monitored using HD phase image analysis, while tracking phenotypic markers is accomplished by using Incucyte® Fabfluor-488 Antibody Labeling Dye (refer to Chapter 7b - Kinetic Live-Cell Immunocytochemistry Assays for more details). Additional phenotypic insights can be generated using Incucyte® Cell-by-Cell Analysis Software Module, which allows users to gain dynamic insight into the phenotypic biology of cell subsets through identification and classification of individual adherent or non-adherent cells with advanced software algorithms.

Incucyte® reagents and mix-and read protocols streamline analysis, by offering flexible options to evaluate and validate phagocytosis. For studying the immune

Shortcomings of Traditional Assays	Live-Cell Imaging and Analysis Approaches
<ul style="list-style-type: none">▪ Data obtained single time point assays provide minimal morphological and dynamic insight as key phenotypic and functional events may be undetected.	<ul style="list-style-type: none">▪ Automated real-time monitoring and continuous data collection enables visualization of morphological changes and quantification of cell function such as phagocytosis and efferocytosis.
<ul style="list-style-type: none">▪ Concatenated end point experiments and lack of environmental control.	<ul style="list-style-type: none">▪ Visualize and capture temporal morphological and functional changes in the controlled environment of the user's own incubator.
<ul style="list-style-type: none">▪ Protocols may also involve fixation, staining, blocking, permeabilization, lifting, for quantification that may perturb cells.	<ul style="list-style-type: none">▪ Non-perturbing reagents, mix-and read protocols and image analysis tools for capturing and quantifying differentiation, phagocytosis, and efferocytosis.
<ul style="list-style-type: none">▪ Use of multiple instruments and software slow time-to-result for target identification and pharmacological screening.	<ul style="list-style-type: none">▪ User friendly instrumentation, integrated software, and flexible vessel formats allow complete profiling at higher throughput to speed time-to-result.

Table 1. Shortcomings of Traditional Assays vs Live-Cell Imaging and Analysis Approaches

response to pathogens, users have their choice of Incucyte® pHrodo® E. coli Bioparticles® (green/red), Incucyte® pHrodo® S. aureus Bioparticles® (green/

red) or the Incucyte® pHrodo® Zymosan Bioparticles® (green/red) which, on entering the acidic environment of the phagosome, increase in fluorescence.

Images and movies enable confirmation of signal and provide insight into the dynamic morphological changes (e.g. formation of phagocytic cups) associated with phagocytosis. To study phagocytosis in mammalian cells, the surface membranes of the target cells (e.g. dying neutrophils or tumor cells) can be labeled with the Incucyte® pHrodo® Cell Labeling Kit (red/orange). Upon engulfment, an increase in fluorescence can be measured. In the absence of phagocytes, the fluorescence intensity of the labeled cells remains low. These reagents enable real-time evaluation of phagocytic regulation by pharmacological agents as well as genetic and environmental factors.

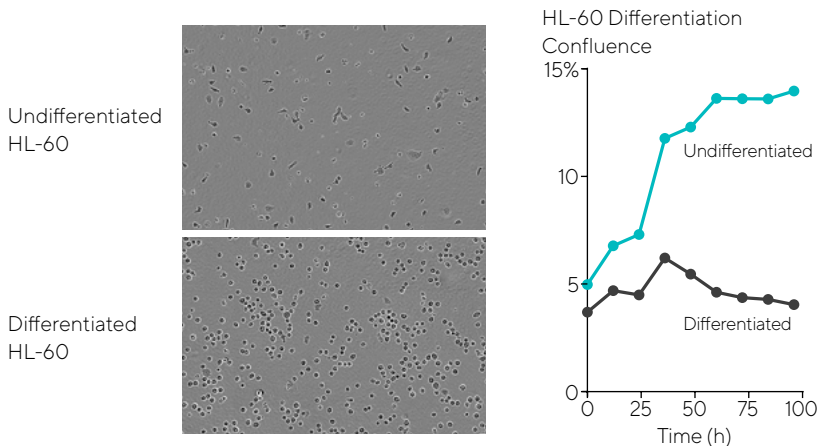
Figure 1. Use of Incucyte® HD phase confluence imaging to track differentiation. Phase images show differences in morphology of undifferentiated HL-60 cells and HL-60 cells differentiated to neutrophil-like cells by adding 1.25 % DMSO and 1 μ M ATRA to RPMI + 10% FBS media. Kinetic data shows differences in cell proliferation as detected by HD phase confluence.

Sample Results

Neutrophil Differentiation and Phagocytosis

The differentiation and functional responses of neutrophils are critical for early immune defense and may become dysregulated, resulting in tissue or organ damage that may occur during acute respiratory distress syndrome (ARDS) and cytokine storms. Studying this process may hold important clues for the identification of new therapeutic targets,

or re-purposing of existing therapeutics. Figure 1 below shows how Incucyte® HD phase confluence images were used to capture morphology changes in HL-60 cells that were differentiated into neutrophil-like cells by addition of DMSO and ATRA to the culture media. Additionally, kinetic time course data of phase confluence showed how differentiation could be determined by differences in cell proliferation.



Assessment of changes in functional phenotype during differentiation can also be captured, as shown during a study in which Incucyte® pHrodo® Green E. coli Bioparticles were used to monitor and quantify the phagocytic capabilities of differentiated cells. As seen in Figure 2A, an increase in Green Object Area was observed in differentiated HL-60 cells, illustrating the differences in functional phenotype between naïve and differentiated cells, with the differentiated cells yielding a substantial increase in fluorescence area, indicative of phagocytosis. Figure 2B shows the phagocytic capabilities of primary neutrophils following the addition of Incucyte® pHrodo® Green E. coli Bioparticles. Primary neutrophils are highly phagocytic and readily engulfed the Bioparticles, leading to an increase in fluorescent signal.

The Incucyte® Cell-by-Cell Analysis Software Module can also be used to monitor changes in PMN eccentricity in response to cytokines, as well as expression of CD11b over time. As shown in Figure 3 below, time- and concentration

dependent changes in area, shape (eccentricity) and the surface expression of CD11b in response to CXCL8 were captured through phase and fluorescent imaging and analysis. Cell-by-Cell Analysis

showed a rapid, concentration dependent increase in eccentricity with CXCL8 with an EC_{50} of 0.63 nM, in combination with an increase in CD11b expression with an EC_{50} of 0.22 nM.

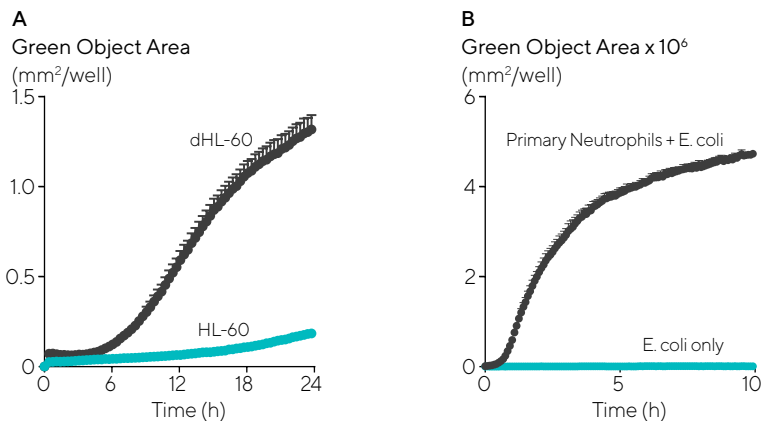


Figure 2. (A) HL-60 cells were differentiated into neutrophils by exposing the cells to 0.1 μ M ATRA and 1.2% DMSO for 5 days. Cells were then seeded and Incucyte® pHrodo® Green E. coli Bioparticles were added. The phagocytic capability of differentiated HL-60 cells was assessed using Green Object Area. (B) Primary neutrophils extracted from peripheral blood were then seeded and Incucyte® pHrodo® Green E. coli Bioparticles were added. Phagocytic activity was monitored by the increase of Green Object Area following bioparticle engulfment.

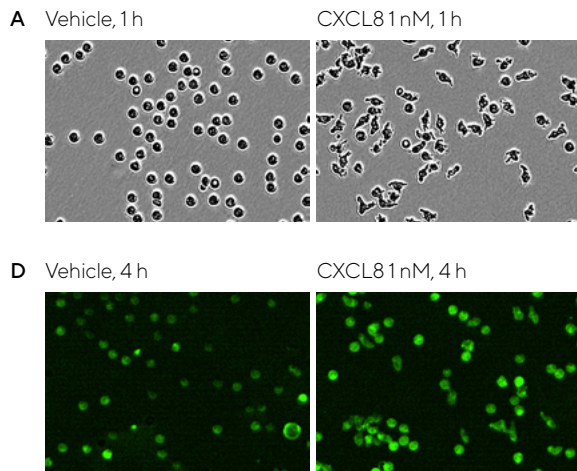
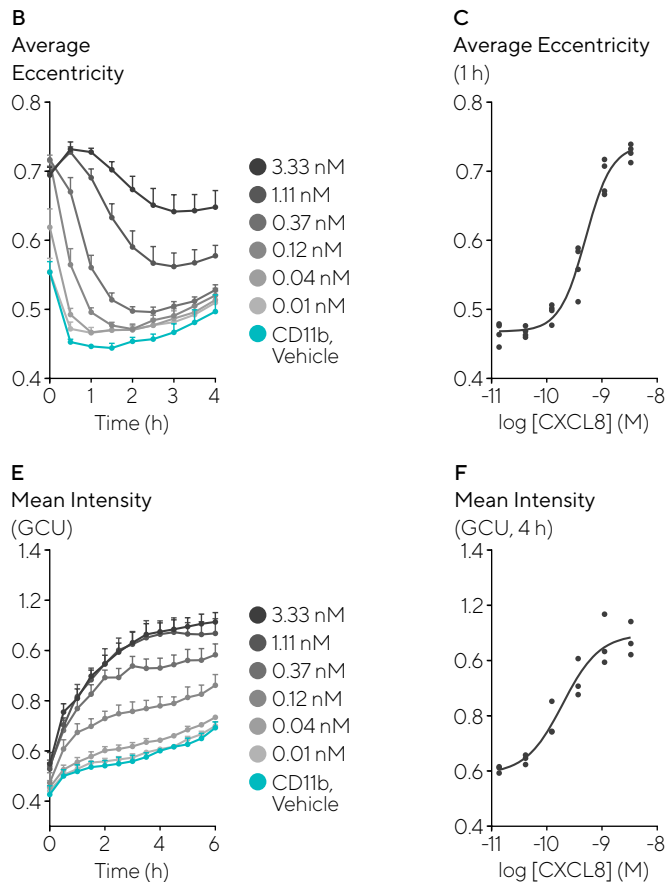


Figure 3. Freshly isolated human neutrophils were seeded (40K/well) in Matrigel® (50 µg/mL) coated 96-well plates and treated with increasing concentrations of CXCL8 in the presence of Incucyte® Fabfluor-488 labeled CD11b antibody (1 µg/mL). Images were captured every 30 min (20x) and analyzed using Incucyte® Cell-by-Cell Analysis. Images (A and D) show the change in morphology and CD11b expression induced by CXCL8 (1 nM). Morphology was quantified as a change in eccentricity and CD11b expression as mean intensity. Data shown as mean of at least 3 separate donors \pm SEM.



Macrophage Differentiation, Phagocytosis, and Efferocytosis

Macrophage phenotypic polarization from M1 (pathogen killing, inhibition of proliferation, phagocytosis) to M2 (repairing, increased proliferation) phenotypes in response to stimuli is of intense interest for studies of macrophage plasticity during immune responses during disease and inflammatory states.² Incucyte® Live-Cell Imaging and Analysis is particularly useful for *in vitro* studies examining this important balance, due to its ability to capture morphological changes associated with differentiation and multiplex of functional outputs such as proliferation, activation, phagocytosis, and wound repair. As discussed above for neutrophils, phagocytosis is a functional output that can be readily measured with Incucyte® integrated software and validated with images and movies to best capture the kinetics of phagocytosis.

The video below shows how time-lapse phase contrast and fluorescence images, acquired using the Incucyte® Live-Cell Analysis System, enable the real-time visualization of Incucyte® pHrodo® Green E. coli Bioparticles® engulfment by the mouse macrophage cell type J774A.1. The bioparticles are phagocytosed and enter the acidic environment of the phagosome resulting in increased fluorescence of the pHrodo® label. Incucyte® integrated image analysis tools enabled detection and measurement of the

green fluorescent signal over the entire assay time-course and eliminate the impact of background fluorescence.

Additionally, the Incucyte® Live-Cell Analysis System can be used to quantify efferocytosis. In this second video, real-time analysis of the engulfment of apoptotic Jurkats labeled with the Incucyte® pHrodo® Red Cell Labeling Kit by macrophages was observed. As the engulfed cells entered the acidic environment of the phagosome, an increase in red fluorescence was seen. The Incucyte® Live-Cell Analysis System and integrated image analysis tools enabled the detection and measurement of the red fluorescent signal over the entire time-course of the assay and minimized the impact of background fluorescence. Note the clearance of apoptotic Jurkats by macrophages over time, while non-apoptotic Jurkats, which lacked externalized phosphatidylserine, were not engulfed.

In a proof of concept experiment, T-lymphoblast CCRF-CEM were incubated with 5 µg/ml anti-CD47 for 1 hour then cultured with bone-marrow derived macrophages. These treated

cells were then added into a 96-well microplate containing bone marrow derived macrophages and imaged within an Incucyte® Live-Cell Analysis System. Figure 4 shows representative images

collected from the Incucyte® Live-Cell Analysis System, which validates anti-CD47 Ab induced phagocytosis of CCRF-CEM cells.

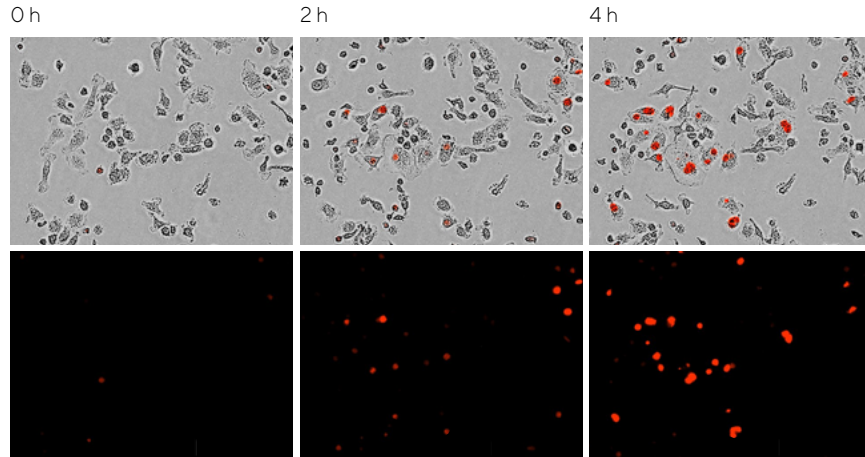


Figure 4. Phase and red fluorescent images demonstrating induction of phagocytosis by of labeled CCRF-CEM cells treated with anti-CD47 antibody at t=0, 2, and 4hrs. Images were captured every 15-30 minutes at 20x magnification in an Incucyte® Live-Cell Analysis System.

Evasion of phagocytosis is one mechanism that tumors use to escape clearance by host macrophages. Figure 5 below demonstrates the use of Incucyte® Live-Cell Imaging and Analysis to examine CD47 antibody-induced engulfment of human leukemic T cells (CCRF-CEM) by

bone-marrow macrophages. CCRF-CEM cells were labeled with the Incucyte® pHrodo® Red Cell Labeling Dye, treated with increasing concentrations of anti-CD47 antibody, and cultured with human bone marrow-derived macrophages. As shown, a concentration dependent

increase in Red Object Area was observed, correlating to an increased phagocytic activity at higher concentrations of anti-CD47 antibody. This assay is amenable to many cell types and enables researchers to screen for small molecules or antibodies that enhance or inhibit phagocytosis.

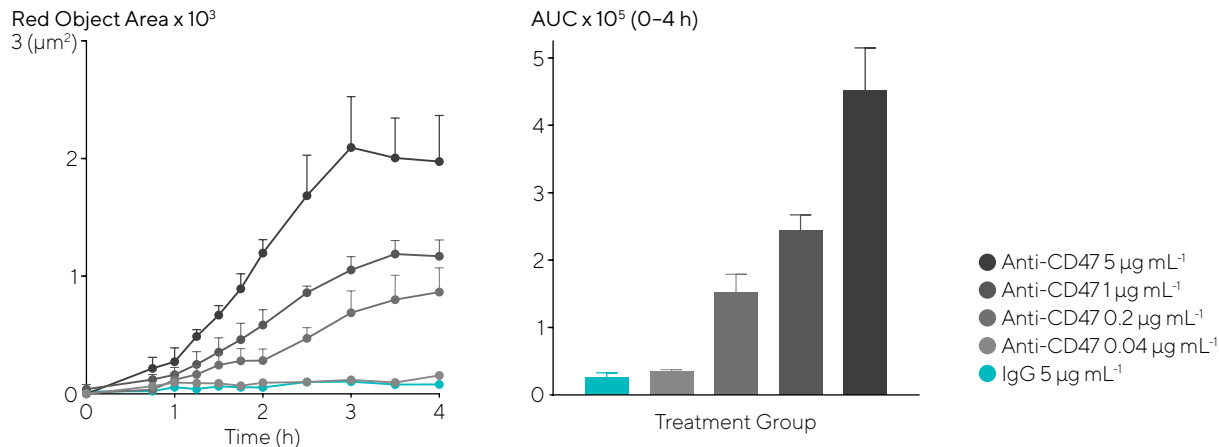



Figure 5. Labeled CCRF-CEM cells were treated with increasing concentrations of anti-CD47 antibody and added to human bone marrow-derived macrophages (BMDM; values shown are mean ± SEM, n=4).



Incucyte® Live-Cell Imaging and Analysis can also be used to study macrophage differentiation and study cell surface markers and multiplexed with other functional outputs. Figure 6 illustrates Incucyte® analysis and multiplexing capacity to study differentiation of THP-1 monocytes that were exposed to various treatments in the presence of Incucyte® Fabfluor-488 Antibody Labeling Dye complexed to CD11b, CD14 or CD40. The kinetic graphs generated by Incucyte® integrated image analysis

software highlight differential and time-dependent surface protein expression in response to the treatments. PMA, but not media or vitamin D3, yielded a decrease in cell proliferation (confluence) and concordant increase in phagocytic potential as measured by efferocytosis of apoptotic Jurkat cells labeled with Incucyte® pHrodo® Red Cell Labeling Kit. Additionally, differences in cell surface marker expression in response to various treatments were visualized and quantified via green fluorescent area measurements

(Incucyte® Fabfluor-488-Ab complexes). Multiplexing of cell surface markers, phagocytic activity, and proliferation measurement enables the visualization of morphology associated with functional changes. This ability maximizes the amount of data that can be obtained from each sample for greater insight, speeding time-to-result. These features make such assays well suited for pharmacological screening activities.

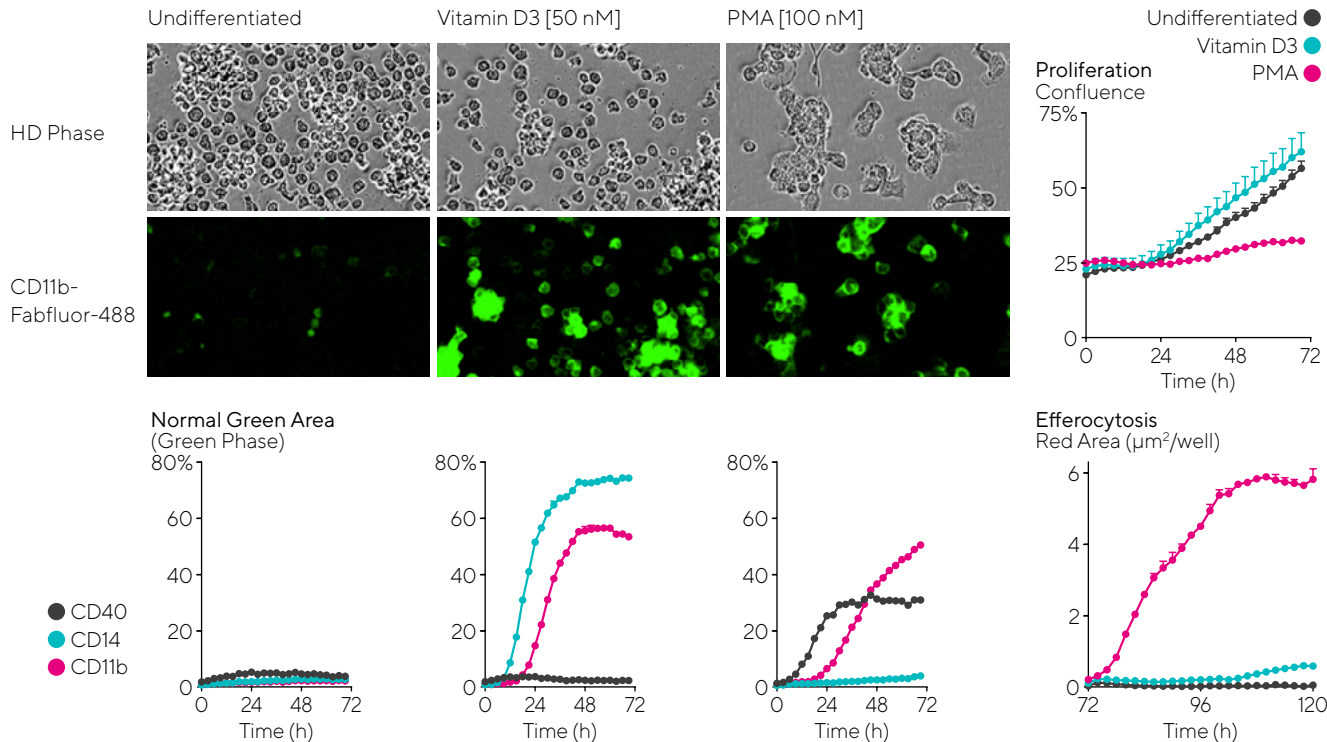


Figure 6. THP-1 monocytes were left undifferentiated or exposed to PMA or Vitamin D3 treatments in the presence of Incucyte® Fabfluor-488 Antibody Labeling Dye complexed to CD11b, CD14 or CD40. HD phase images and kinetic graphs reveal a marked change in cell morphology and proliferation in PMA treated cells, but not Vitamin D3 or media alone. This is concordant with an increase in phagocytic potential measured by an increase red fluorescent area indicating efferocytosis of pHrodo® labeled apoptotic Jurkats. Surface marker expression was also studied via green fluorescent imaging and quantification of green object area (Incucyte® Fabfluor-488-ab complexes).

Analysis of differentiation can also be combined with other functional outputs such as chemotaxis, using Incucyte® Clearview 96-well Plates (refer to Chapter 6b - Kinetic Chemotaxis Assays for more details). Figure 7 shows the

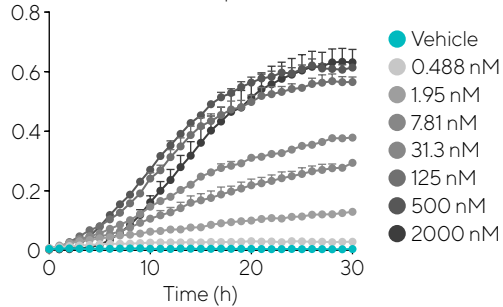
pharmacological response of naïve or PMA differentiated THP-1 cells (human acute monocytic leukemia) seeded on Incucyte® Clearview Plates coated with fibronectin and exposed to a C5a gradient. Differentiated macrophage-like THP-1 cells

had a strong concentration-dependent response towards C5a, as shown by increases in total cell area on the bottom of the plate where cells had migrated. Little or no response was observed in THP-1 cells prior to differentiation.

Differentiated THP-1 Cells (M0)

Total THP-1 Area (Bottom)

Normalized to Initial Top Value



Total THP-1 Area (Bottom)

Normalized to Initial Value (30 h)

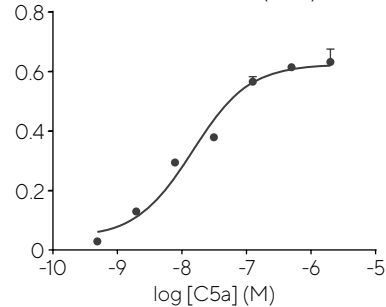


Figure 7. Biological significance of monocyte maturation. THP-1 cells, either naïve or PMA differentiated M0 were seeded on Incucyte® Clearview 96-well Plates coated with fibronectin, followed by C5a gradient exposure and imaging every hour using the Incucyte® Live-Cell Analysis System. Analysis of pharmacological response was performed at t=30 hr.

Chemotaxis may also be studied in the context of specific macrophage differentiation states. Figure 8 illustrates the importance of using kinetic monitoring to uncover new insights. Primary blood monocytes were differentiated into M2-like phenotype with 50 ng/mL M-CSF

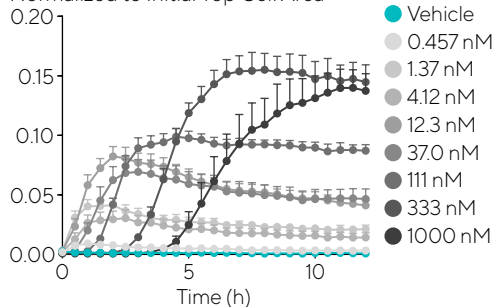
for 6 days followed by 20 ng/mL IL-4 for a further day. Macrophages were seeded on Matrigel® coated membranes of the Incucyte® Clearview 96-well Plate, then exposed to a C5a gradient. Bottom-side phase analysis was performed to quantify cell migration through the membrane

and EC_{50} values were calculated at to be 10.6 nM and 86.8 nM at 4 and 11 hrs, respectively. This analysis detected a substantial time dependent C5a potency shift due to delay in response at higher concentrations.

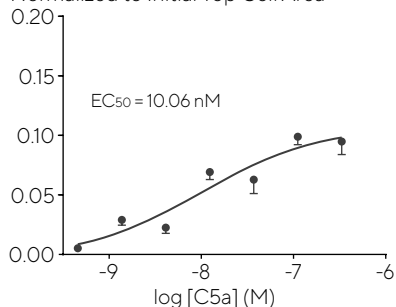
Differentiated Primary Macrophages (M2)

Total Macrophage Area (Bottom)

Normalized to Initial Top Cell Area



Total Macrophage Area [Bottom] (4.5 h)
Normalized to Initial Top Cell Area



Total Macrophage Area [Bottom] (11 h)
Normalized to Initial Top Cell Area

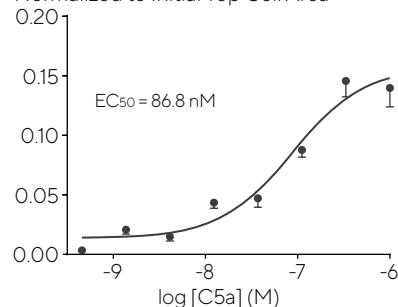


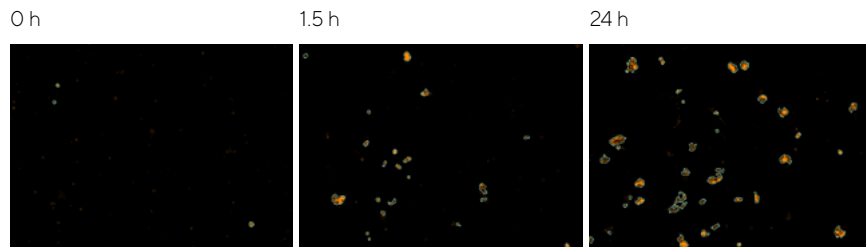
Figure 8. Primary blood monocytes were differentiated into M2-like phenotype with a time-dependent C5a potency shift due to delay in response at higher concentrations. Images were acquired every 2 hours within an Incucyte® Live-Cell Analysis System and bottom-side metrics were used to quantify chemotaxis and determine pharmacological response at 4.5 and 11 hours.

Microglia Phagocytosis and Efferocytosis

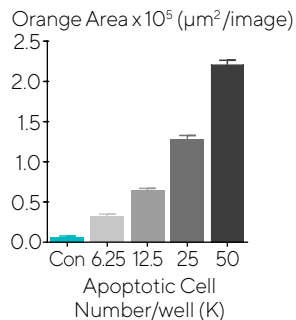
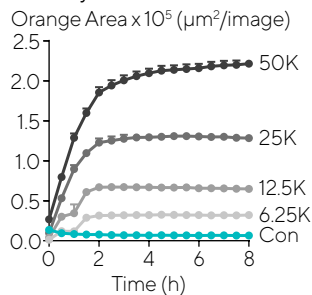
Immune cells can play a pivotal role in the modulation of neuronal networks, for example, synaptic pruning by microglia is a key component of neural plasticity. Injury, infection or loss of homeostasis can lead to neuroinflammation and activation of microglia, which in turn phagocytose dead or dying neurons and infective agents. Chronic neuroinflammation is believed to underlie a number of neurodegenerative disorders, such as Alzheimer's disease, where prolonged activation of microglia is detrimental to neuronal networks (refer to Chapter 9c - Kinetic Neuroimmune Assays for more details).

The Incucyte® Live-Cell Analysis System enables extensive morphological and functional characterization of microglia, including quantification of phagocytosis

and efferocytosis in real time. As shown in Figure 9, apoptotic Neuro-2a cells were labeled with the Incucyte® pHrodo® Orange Cell Labeling Kit and cultured with iPSC-derived microglia. As seen in the fluorescent images, engulfment of the pHrodo® labeled apoptotic Neuro-2a cells by microglia was observed and masked for quantification (orange fluorescence, blue outline). As the apoptotic Neuro-2a cells were internalized into acidic phagosomes, intracellular orange fluorescence increased. In a similar experiment, pHrodo® labeled amyloid beta (A β) was cultured with microglia, and an increase in orange fluorescence was observed as the A β was phagocytosed. Efferocytosis of pHrodo® labeled Neuro-2a cells was found to be cell number-dependent, while phagocytosis of pHrodo® labeled A β aggregates was both time- and concentration-dependent.



Efferocytosis



Phagocytosis

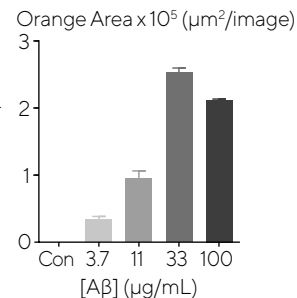
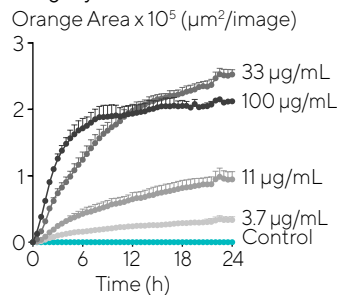


Figure 9. Real-time quantification of efferocytosis and phagocytosis by microglia. Representative fluorescent images of iPSC-derived microglia (Axol Bioscience) engulfment of pHrodo® labeled apoptotic neurons (Neuro-2a); the segmentation mask is shown as the cyan outline. pHrodo® labeled Aβ aggregates were also cultured with microglia at various concentrations. An increase in intracellular orange fluorescence was observed as target cells or Aβ aggregates were internalized into acidic phagosomes. Cell-dependent efferocytosis of the Neuro-2a cells was observed, while Aβ aggregates phagocytosis was found to be time- and concentration dependent.

Conclusions

As illustrated in the studies above, Incucyte® Differentiation, Phagocytosis and Efferocytosis Assays captures morphological changes associated with differentiation in real time, correlating these changes with temporal functional assessments such as phagocytosis and efferocytosis. Unlike more laborious traditional approaches, these assays feature mix-and-read protocols to reduce time spent on washing, non-perturbing reagents, and are performed in the controlled environment of the user's own incubator for greater physiological relevance. Incucyte® Live-Cell Imaging and Analysis offers the following advantages:

- Continuous, automated, real-time HD phase and fluorescent analysis of morphology changes in immune cells during differentiation, phagocytosis, and efferocytosis to capture time-dependent biological effects.

- Data is acquired from within the user's own incubator as the cells sit stationary, thus reducing artifacts traditionally introduced through cell handling and movement.
- Validated assays for differentiation, phagocytosis and efferocytosis using non-perturbing reagents enabling specific and robust data without the need for extended optimization of assays.
- All data points can be validated by individual images or time-lapse movies to confirm biological changes.
- Capability to pair phagocytosis assessments with Incucyte® Live-Cell Immunocytochemistry and Chemotaxis Assays to couple protein dynamics with temporal changes in cell function and behavior.

Taken together, these assays enable the study of differentiation and corresponding temporal assessment of phagocytosis, efferocytosis, and other functional outputs in real-time with enhanced throughput to capture greater biological insights from each sample, making this platform ideal for the identification of new therapeutic targets.

References

1. Kapellos TS, Taylor L, Lee H, et al. **A novel real time imaging platform to quantify macrophage phagocytosis.** *Biochem Pharmacol.* 2016; 116:107-119
2. Wang N, Liang H, Zen K. **Molecular mechanisms that influence the macrophage m1-m2 polarization balance.** *Front Immunol.*, 2014, 5:614.

Incucyte® User Publications

1. Barkal AA, Brewer RE, Markovic M, et al. **CD24 signalling through macrophage Siglec-10 is a target for cancer immunotherapy.** *Nature.* 2019;572(7769):392-396.
2. Haney MS, et al. **Identification of phagocytosis regulators using magnetic genome-wide CRISPR screens.** *Nat Genet.*, 2018, Dec;50(12):1716-1727. Epub 2018 Nov 5
3. Pluvinae JV, Haney MS, Smith BAH, et al. **CD22 blockade restores homeostatic microglial phagocytosis in ageing brains.** *Nature*, 2019, 568(7751):187-192.

Chapter 6

Kinetic Cell Migration and Invasion Assays

Real-Time Automated Measurements of Cell Motility

Cell migration and invasion play a role in many normal and pathological processes including immune responses, embryonic development, angiogenesis, regeneration, tumor metastasis, and wound healing.¹ A wide variety of assays can be used to monitor and analyze cell migration and invasion in vitro, from very simple assays to very complex. The scratch assay permits velocity measurements of wound closure and is dependent upon a cell density gradient, whereas methods to study chemical factors that regulate migration and invasion of cells typically employ modifications of Boyden chamber assays. Scratch assays are typically performed by manually creating scratches in multiple well plates (e.g., 6-, 12-, 24-or 48-well) and then acquiring images using a microscope at defined time-points. This approach leads to variation in scratch uniformity, as well as disrupting the assay environmental control during image acquisition. Current chemotaxis assay approaches have inherent drawbacks such

as non-linear gradients, inability to observe cell morphology and validate cell movement, are technically challenging and have cumbersome quantification steps. In order to drive development of novel therapeutics, a deeper understanding of these processes is required to gain valuable insights.

Incucyte® Cell Migration and Invasion Assays allow continuous visualization and analysis of cell motility and kinetics. This approach addresses the inherent shortcomings of traditional assays that deliver a user-defined time points or a single end-point measurement and don't allow visualization of cells as they move in response to their environment. The Incucyte® Scratch Wound Assay is a method that utilizes the Incucyte® 96-well Woundmaker Tool to create precise scratches within a cell monolayer, eliminating assay variability that is inherent in "home-brew" methods.² The Incucyte® Chemotaxis Assay is a kinetic and visual chemotactic driven method, that alleviates hurdles such

as laborious end point measurements, high cell usage, and non-linear gradient that is common in traditional transmembrane assays. These image-based detection methods offer simple and reliable assays which deliver new biological insights into cell migration and invasion.

Live-Cell Imaging and Analysis Approaches

The Incucyte® Cell Migration and Invasion Assays enable the detection and analysis of live-cell movement in 96-well formats. Incucyte® Scratch Wound and Chemotaxis Assays allow users to kinetically monitor and analyze migration and invasion with or without a chemotactic gradient, and associated images allow for the ability to observe cell morphology.

How Live-Cell Migration and Invasion Assays Work

Incucyte® Scratch Wound Assay

The Incucyte® Scratch Wound Assay is a 96-well, high throughput wound assay that measures cell density-dependent migration and invasion. Utilizing the Incucyte® 96-well Woundmaker Tool, 96 precise, uniform, cell-free zones are

created in cell monolayers and wound closure is visualized and analyzed in real-time with the Incucyte® Live-Cell Analysis System and integrated software.

Incucyte® Chemotaxis Assay

The Incucyte® Chemotaxis Assay enables real-time visualization and quantification of cell migration and invasion in response to a chemotactic gradient. Using an

optically clear membrane insert that contains optimally spaced 8-micron pores, cell migration and invasion are automatically imaged and analyzed as the cells move through the pores, generating a chemotactic signal.

Scratch Wound Assays

Migration

Cell Density
Dependent
(no gradient)

Can my cells move across
a surface in response to
cell density changes?

Invasion

Can my cells break down a
matrix and invade in response
to cell density changes?

No Matrix

Matrix (ECM)

Chemical
Gradient

Can my cells move across
a surface in response to a
chemical gradient?

Can my cells break down a
matrix and invade in response
to a chemical gradient?

Chemotaxis Assays

References

1. **Cell Migration: integrating signals from front to back.** Ridley, A.J., Schwartz, M.A., Burridge, K., Firtel, R.A., Ginsberg, M.H., Borisy, G., Parsons, J.T. and Horwitz, A.R. *Science* 302:1704.
1. **Cell Migration and Invasion Assays as Tools for Drug Discovery.** Hulkower, K. I and Herber, R. L. *Pharmaceutics* 2011 3:107

Incucyte® User Publications

Scratch Wound Assay

Drebert, *et al.*, used the Incucyte® Scratch Wound Assay to assess HUVEC migration in response to conditioned medium from solvent- (CMS) and dexamethasone (Dex)-treated (CMD) colon cancer-derived myofibroblasts. In the HUVEC scratch assay, CMS-induced acceleration of wound healing was blunted by CMD treatment.

1. **Colon cancer-derived myofibroblasts increase endothelial cell migration by glucocorticoid-sensitive secretion of a pro-migratory factor.** Drebert, Z., MacAskill, M., Doughty-Shenton, D., De Bosscher, K., Bracke, M., Hadoke, P.W., Beck, I.M. *Vascul. Pharmacol., Vascu Pharmacol.* 2016 Oct 4. pii: S1537-1891(16)30137-9. doi: 10.1016/j.vph.2016.10.004. [Epub ahead of print], 2017.

Härmä, *et al.*, cultured prostate cancer cells on Incucyte® Imagelock Plates from Sartorius until fully confluent and scratched with the Incucyte® 96-well Woundmaker Tool. Wound closure was monitored and quantified with the Incucyte® Live-Cell Analysis System. Study results suggest that some betulin-derivatives may specifically target cell motility and invasion by affecting the organization of filamentous actin fiber network at low nanomolar concentrations.

2. **Optimization of invasion-specific effects of betulin derivatives on prostate cancer cells through lead development.** Härmä, V., Haavikko, R., Virtanen, J., Ahonen, I., Schukov, H. P., Alakurtti, S., Purev, E., Rischer, H., Yli-Kauhaluoma, J., Moreira, V. M., Nees, M., Oksman-Caldentey, K. M. *PLoS ONE* 05/2015 10(5):e0126111.

Moody, *et al.* conducted scratch wound assays using the Incucyte® Live-Cell Analysis System to assess the functional consequence of growth arrest specific 6 (Gas6) neutralization in lung cancer cells. Gas6 is a vitamin-K dependent, 75 kDa growth factor-like protein involved in the regulation of a wide array of cellular activities, including adhesion, migration, mitogenesis, aggregation, stress-response, differentiation, immune activation, efferocytosis and apoptosis. A Gas6 neutralizing antibody was also tested for its ability to inhibit Gas6-induced proliferation using the same platform.

3. **Antibody-mediated neutralization of autocrine Gas6 inhibits the growth of pancreatic ductal adenocarcinoma tumors *in vivo*.** Moody, G., Belmontes, B., Masterman, S., Wang, W., King, C., Murawsky, C., Tsurda, T., Liu, S., Radinsky, R., Beltran, P. *Int J of Cancer.* 2016 139:1340.

This review article explores how advances in time-resolved imaging contributes to the characterization of distinct modes of invasion and molecular mechanisms. The author highlights the latest advances in kinetic imaging instrumentation applicable to *in vitro* and *in vivo* models of tumor invasion.

4. **Profiling distinct mechanisms of tumor invasion for drug discovery: imaging adhesion, signalling and matrix turnover.** Carragher, N. *Clinical & Exp Metastasis.* 2009 April 26(4).

Chemotaxis Assay

Taylor, *et al.*, used the Incucyte® Chemotaxis Assay to study netrin-1, a cellular guidance signal. The authors demonstrated that netrin-1 inhibits human monocyte and

murine macrophage migration towards C5a, a complement peptide with potent chemotactic and anaphylatoxic properties that upregulate endothelial adhesion molecules, increase vascular permeability, and localize leukocytes and inflammatory molecules at sites of infection.

5. **Netrin-1 reduces monocyte and macrophage chemotaxis towards the complement component C5a.** Taylor, L., Brodermann, M. H., McCaffary, D., Iqbal, A. J., Greaves, D. R. *PLoS ONE*, 2016 Aug 10; 11(8).

A study by Pasqualon, *et al.*, demonstrated that syndecan-1, a surface-expressed proteoglycan on epithelial tumor cells, promotes macrophage migration inhibitory factor (MIF) binding and MIF-mediated cell migration. Invasion studies showed that MIF induced the chemotactic migration of A549 tumor cells, wound closure and invasion into Matrigel without affecting cell proliferation. These MIF-induced responses were abrogated by silencing of syndecan-1. The authors conclude that this may represent a relevant mechanism through which MIF enhances tumor cell motility and metastasis.

6. **Cell surface syndecan-1 contributes to binding and function of macrophage migration inhibitory factor (MIF) on epithelial tumor cells.** Pasqualon, T., Lue, H., Groening, S., Pruessmeyer, J., Jahr, H., Denecke, B., Bernhagen, J., Ludwig, A. *BBA-Mol Cell Res.* 2016 Apr; 1864 (4).
7. **Orphan G protein-coupled receptor GPRC5A modulates integrin β 1-mediated epithelial cell adhesion.** Bulanova, D.; Akimov, Y.; Rokka, A.; Laajala, T.; Aittokallio, T.; Kouvonon, P.; Pellinen, T.; Kuznetsov, S. *Cell Adhesion & Migration.* 2016 Oct.
8. **Potent EMT and CSC phenotypes are induced by oncostatin-M in pancreatic cancer.** Smigiel, J.; Parameswaran, N.; Jackson, *MMol Can Res.* 2017 Jan.

Kinetic Scratch Wound Assays

Real-Time Assays to Assess Migration and Invasion Potential

Introduction

Cell migration is a multistep process that is a fundamental component of many biological and pathological processes such as embryonic development, tissue re-organization, angiogenesis, immune cell trafficking, chronic inflammation and tumor metastasis. Cell migration is initiated by a stimulus that activates a set of signaling pathways leading to cellular polarization and a rapid reorganization of actin filaments and microtubules. Cells advance by protruding their membrane at their leading cell border, which is followed by dynamic substrate adhesion via integrin adherence to the substrate. Membrane retraction at the lagging cell edge finishes the cycle, which is then repeated in rapid succession. The summation of this process results in cell migration.

In this section, we will review how the Incucyte® Scratch Wound Assay provides real-time visualization and analysis of cell movement that is driven by changes in cell density. Unlike traditional assays, which require repeatedly removing cells from an incubator to perform manual image acquisition and have variability in scratch width and uniformity, this live-cell assay approach enables continuous analysis and eliminates assay variability with the use of the Incucyte® 96-well Woundmaker Tool to create precise scratches in the cell monolayer.

Incucyte® Scratch Wound Assay at a Glance

The Incucyte® Scratch Wound Migration and Invasion Assay can be used to quantitatively assess both cellular

migration and cell invasion potential in the presence of experimental agents. The 96-well Incucyte® 96-well Woundmaker Tool creates cell-free zones in cell monolayers cultured on Incucyte® Imagelock 96-well Plates with the use of precision engineered pins, without disrupting the underlying biomatrix or damaging the tissue culture treated plastic. After wounding, the Scratch Wound Assay is initiated by simply adding media to the cells for the migration assay or by overlaying the cells with an optimized concentration of a biomatrix material for the invasion assay. Incucyte® Scratch Wound Analysis Software Module enables real time, automated measurement of label-free or dual fluorescence of cell migration and invasion.

- Visualize cell migration and invasion, and assess morphological changes in real time with the scratch wound method.
- Assays are flexible, quantitative and easily reproducible with the Incucyte® 96-well Woundmaker Tool.
- Monitor and quantify cell movements across a substrate (migration) or through a gel matrix (invasion) in the same plate, up to six 96-well plates at once.
- Validated with a wide range of adherent primary, immortalized and tumor cell types.

Shortcomings of Traditional Assays	Live-Cell Imaging and Analysis Approaches
<ul style="list-style-type: none"> ▪ Assays result in a single, user-defined time point measurement or requires manual intervention to generate multiple time points. ▪ Lack of precision and reproducibility in creating the wound and capturing data. 	<ul style="list-style-type: none"> ▪ Real-time, direct visualization and automated analysis of migration and invasion. ▪ 96-well Imagemock Plates enable precise, scan to scan repeat imaging of the same field of view. ▪ Reproducible kinetic data supported by images and time-lapse movies. ▪ Spatio-temporal, label-free format provides data on both the rate and the extent of migration and invasion for a given set of experimental variables. ▪ Explore time-dependent pharmacology, in order to enhance assay sensitivity. ▪ Measure migration without fixing or staining steps.

Table 1. Shortcomings of Traditional Assays vs Live-Cell Imaging and Analysis Approaches

Sample Results

Assessing Wound Closure Rates and Morphology

The differences in wound closure rates and cell morphology between migrating and invading HT-1080 cells are shown in Figure 1. Migrating HT-1080 cells (odd numbered columns) closed the wound region at a significantly faster rate with

complete wound closure detected by 10-12 hours post wounding. In contrast, HT-1080 cells invading 8 mg/ml Matrigel® reached 80% wound closure within 48 hours as measured by the Relative Wound Density metric. Morphological differences were also noted. Migrating cells maintained a fibroblastic morphology, had rounded lamellipodia, and advanced as a uniform population of cells. Invading HT-1080

cells adopted a mesenchymal phenotype displaying extended cell bodies and, in some cases, “spike-like” lamellipodia as the cells advanced into the Matrigel matrix in an irregular manner. The clear morphological differences between migrating and invading HT-1080 cells can be used to select the optimum condition for the invasion assay.

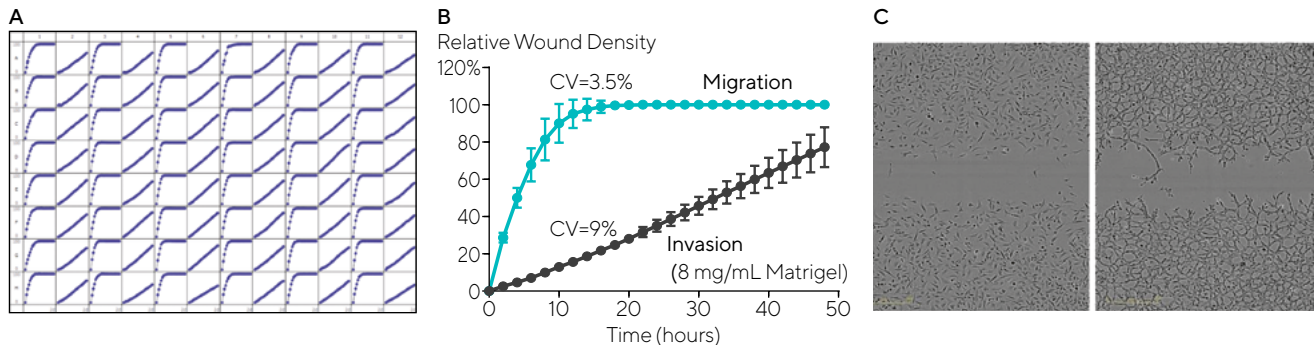


Figure 1. Measurement of the reproducibility the migration and invasion assay in the same microplate. HT-1080 cells were plated at 2×10^4 cells per well on 100 μ g/ml Matrigel coated Imagelock plates. The cells in odd numbered columns had only media added after using the 96-well Woundmaker representing cell migration. The cells in even numbered columns were overlaid with 8 mg/mL Matrigel representing invasion. (A) Temporal progression of wound closure in each well with time using RWD as the metric to measure migration or invasion. (B) Time course of means of each condition. The respective coefficients of variation for each assay were averaged. (C) Representative images of HT-1080 cells migrating on Matrigel (left) and invading through 8mg/mL.

Differentiating Between Invasive and Non-Invasive Cells

Both MDA-MB-231 and HT-1080 cells are highly invasive cell types. In contrast, MCF-7 cells are relatively non-invasive. All three cell types were tested in invasion and migration assays as indicated in Figure 2. As previously shown, HT-1080

cells migrated on collagen 1 coated plates and invaded collagen 1, with the rate of invasion slowing as the concentration of collagen 1 matrix was increased from 1-3 mg/ml. MDA-MB-231 cells also migrated on collagen 1-coated plates, but invaded collagen more slowly than HT-1080 cells. Interestingly, the rate of invasion

of MDA-MB-231 cells was similar at all concentrations of collagen 1 tested.

MCF-7 cells, like the other two cells types, migrated on collagen 1-coated plates, but in contrast to the other two cells types, MCF-7 cells did not have the capacity to invade collagen 1 at the concentrations tested.

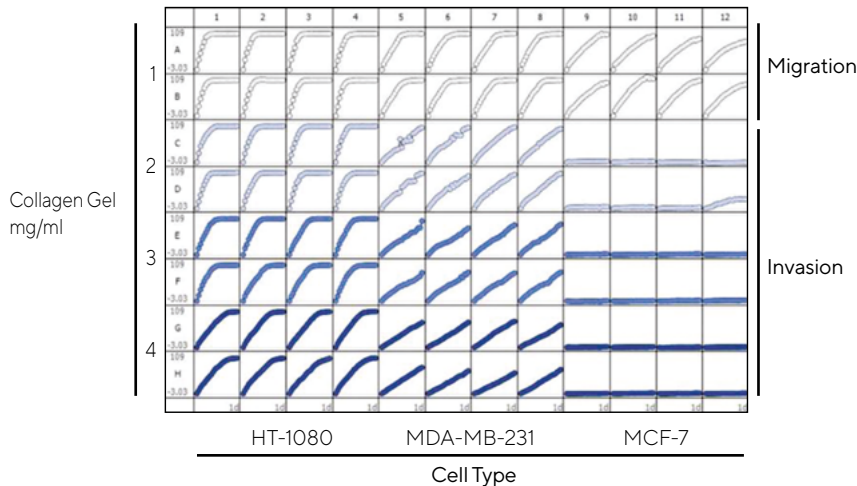


Figure 2. 96-well microplate graph of three cell types in the cell migration and invasion assay. All wells were coated with 300 $\mu\text{g}/\text{mL}$ collagen 1. HT-1080 (2×10^4 cells per well) are in column 1-4, MDA-MB-231 (2.5×10^4 cells per well) are in column 5-8 and MCF-7 (5×10^4 cells per well) are in column 9-12. Rows A and B show the cell migration data for the three cell types. The same cells in the invasion assay are shown in rows C-D (1 mg/ml collagen 1), rows D-E (2 mg/ml collagen 1) and rows G-H (3 mg/ml collagen 1). The plate map graph shows the progression of each well with time using the RWD metric to measure migration or invasion.

Pharmacology Applications

Blebbistatin is a pharmacological agent that is known to inhibit myosin by binding to the ATPase intermediate with ADP and phosphate bound at the active site, slowing the release of phosphate and inhibits locomotion of cells.¹ Previous studies have suggested that blebbistatin may be more effective at inhibiting cell invasion as compared to cell migration.² With the 96-well format, it is easy to set up an experiment to measure migration and invasion concurrently within the same microplate. Using this approach, the effect of blebbistatin on migration and invasion using HT-1080 cells was studied. The plate map in Figure 3A demonstrates a convenient way to set up this experiment. Three columns of cells were used for migration, and three were used for invasion. A 7-point concentration curve of blebbistatin was carried out

as depicted in rows A-G. Row H was used a solvent control. The microplate graph in Figure 3B demonstrates the reproducibility of the assay and shows the effect of each concentration of drug in both assay formats. By inspection, it appeared that blebbistatin had a larger effect on invasion compared to migration. Plotting the data as the average of the treatment group for migration and invasion made it clear that blebbistatin had a much larger effect on invasion (Figure 3 C and D, respectively). Figure 3E shows the concentration response analysis at the 24-hour time point for both assays. From these data, the calculated IC_{50} of blebbistatin for migration and invasion is 92 and 5.2 μ M, respectively. The Z' for this data set is 0.77.

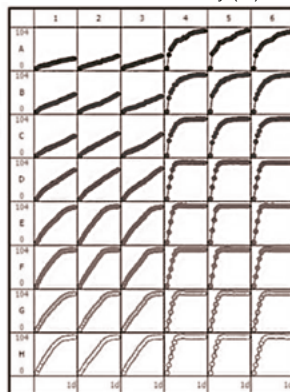
Matrix metalloproteinases (MMPs) are zinc-dependent endopeptidases that

degrade collagen 1 and other basement membrane materials and are expressed at increased levels by many highly metastatic tumor derived cells. GM6001 is a broad MMP inhibitor that has been shown to inhibit the invasion of HT-1080 cells into collagen 1.³ The Incucyte® Migration and Invasion Assay was configured in order to test the effect of this drug on invasion and migration on the same microplate. As shown in Figure 4A, GM6001 had no effect on the migration of HT-1080 cells. In contrast, as shown in Figure 4B, GM6001 inhibited invasion into collagen 1 in a concentration-dependent manner. Interestingly, the addition of a protease cocktail containing E-64 (25 μ M) pepstatin A (100 μ M), leupeptin (2 μ M) and aprotinin (2 μ M) had no measurable effect on cell migration or cell invasion (data not shown).

A

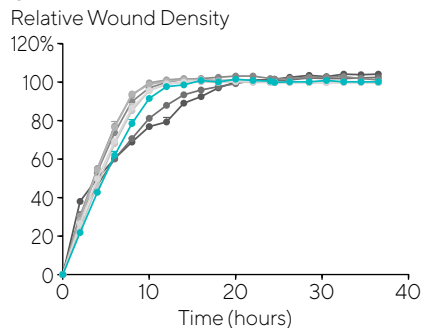
	1	2	3	4	5	6
A	Blebbistatin 60 μ M HT 1080 (25) 20K / well Collagen gel, 3 mg/ml			Blebbistatin 60 μ M HT 1080 (25) 20K / well		
B	Blebbistatin 30 μ M HT 1080 (25) 20K / well Collagen gel, 3 mg/ml			Blebbistatin 30 μ M HT 1080 (25) 20K / well		
C	Blebbistatin 10 μ M HT 1080 (25) 20K / well Collagen gel, 3 mg/ml			Blebbistatin 10 μ M HT 1080 (25) 20K / well		
D	Blebbistatin 3.33 μ M HT 1080 (25) 20K / well Collagen gel, 3 mg/ml			Blebbistatin 3.33 μ M HT 1080 (25) 20K / well		
E	Blebbistatin 1.11 μ M HT 1080 (25) 20K / well Collagen gel, 3 mg/ml			Blebbistatin 1.11 μ M HT 1080 (25) 20K / well		
F	Blebbistatin 0.37 μ M HT 1080 (25) 20K / well Collagen gel, 3 mg/ml			Blebbistatin 0.37 μ M HT 1080 (25) 20K / well		
G	Blebbistatin 0.12 μ M HT 1080 (25) 20K / well Collagen gel, 3 mg/ml			Blebbistatin 0.12 μ M HT 1080 (25) 20K / well		
H	DMSO 0.6% HT 1080 (25) 20K / well Collagen gel, 3 mg/ml			DMSO 0.6% HT 1080 (25) 20K / well		

B Relative Wound Density (%)

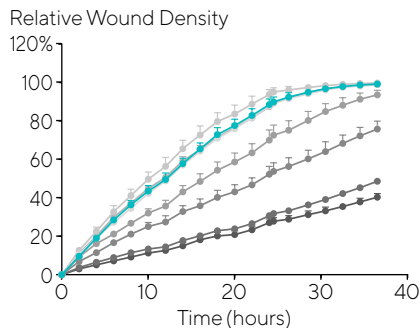


● 60 μ M ● 10 μ M ● 1.11 μ M ● 0.12 μ M
 ● 30 μ M ● 3.33 μ M ● 0.37 μ M ● Vehicle

C



D



E

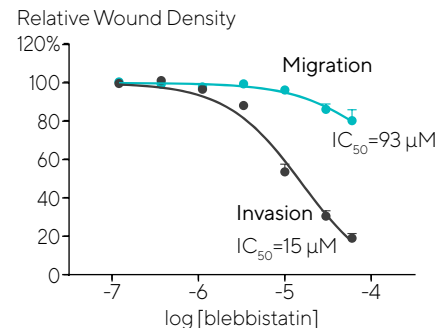


Figure 3. Effect of blebbistatin on the migration and invasion of HT-1080 cells. HT-1080 cells were plated at 2×10^4 cells per well on 300 μ g/mL collagen 1 coated plates. Panel A shows the plate map for the experiment. The cells in columns 1-3 were overlaid with 3 mg/mL collagen 1 containing blebbistatin or solvent control. The cells in columns 4-6 were given complete growth media with blebbistatin or the solvent control. Panel B shows the microplate graph of the experiment. Panel C and D show the means of each treatment group for migration and invasion, respectively. Panel E shows the concentration response analysis of blebbistatin on cell migration and invasion. The IC₅₀ calculation for each assay is included next to the concentration response curve.

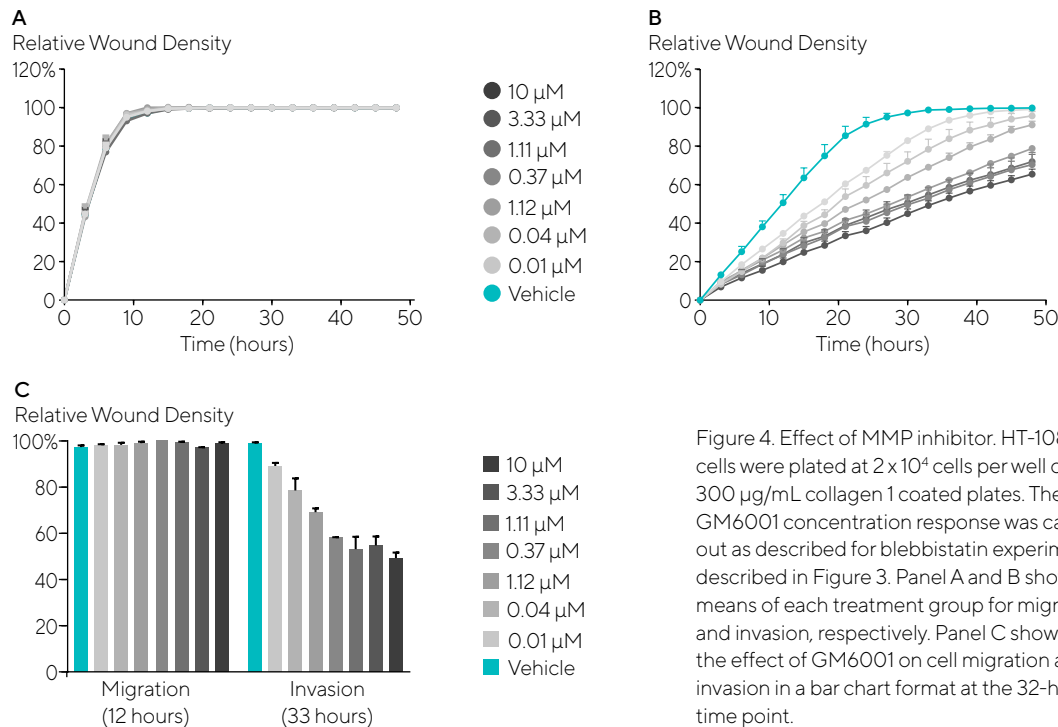


Figure 4. Effect of MMP inhibitor. HT-1080 cells were plated at 2×10^4 cells per well on 300 μ g/mL collagen 1 coated plates. The GM6001 concentration response was carried out as described for blebbistatin experiment described in Figure 3. Panel A and B show the means of each treatment group for migration and invasion, respectively. Panel C shows the effect of GM6001 on cell migration and invasion in a bar chart format at the 32-hour time point.

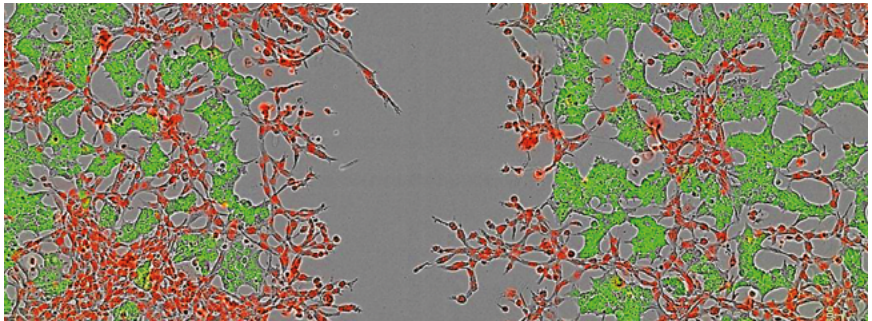
Two-Color Fluorescent Scratch Wound Experiments

In addition to phase contrast images, two-color images can be collected using Incucyte® fluorescent labeling reagents. This allows study of the interactions between several cell types in a mixed

culture, and how each affects migration, invasion, and proliferation of the other, all within one well of a 96-well plate. As shown in Figure 5, the non-invasive MCF-7 cells were labeled with Incucyte® Nuclight Green Lentivirus, and the HT-1080 cells labeled with Incucyte® Nuclight Red Lentivirus

were mixed in co-culture, and plated for an invasion assay through 8 mg/ml Matrigel®. Imaging in phase, red, and green channels revealed the HT-1080 cells efficiently invaded the Matrigel® matrix whereas MCF-7 remained non-invasive.

Figure 5. Two color fluorescent scratch wound. The ability to image cells in both wavelengths in addition to phase contrast allows users the ability to explore cell-cell interactions as it pertains to cell migration and invasion. In this example, Nuclight Red HT-1080 cells were plated with Nuclight Green MCF-7 cells and invasion through 8 mg/ml Matrigel® was monitored over time (Image shows the 24 hour time point).



Conclusions

Incucyte® Scratch Wound Migration and Invasion Assays are flexible, quantitative, and reproducible. The unique tip design of the 96-well Incucyte® Woundmaker is a critical part of these assays, as it creates a cell-free zone from a confluent monolayer of cells making the biology consistent and reproducible. Both assays utilize Incucyte's innovative high definition optics and integrative analysis algorithms to make quantitative measurements without the need for labeling cells. Having high-quality images at every time point gives an investigator access to both the kinetics and morphological changes occurring in migration and invasion experiments, enabling additional insight into the effects test agents have on cells undergoing these processes. Key features and benefits include:

- Investigators can measure migration and invasion on the same microplate. This provides the best opportunity for determining the specificity of drugs and the utility of potential drug targets.

- The spatio-temporal, label-free format of both the Incucyte® Migration and Invasion Assays allows investigators to follow both the rate and the extent of migration and invasion for a given set of experimental variables. This feature can be used to explore time-dependent pharmacology, in order to enhance assay sensitivity.
- After the experiment is initiated, phase contrast and/or fluorescence images are collected and processed automatically, yielding un-biased results.
- Precise wounding ensures that results are quantitative and reproducible.
- Incucyte® high definition optics eliminates the need to label the cells.
- HD images are acquired at every time point and can be automatically assembled into time-lapse movies for convenient visualization of morphology and wound closure.

References

1. Kovacs, M., Toth, J., Hetnyi, C., Malnasi-Csizmadia, A and Sellers, J.R. **Mechanism of action of Blebbistatin inhibition of Myosin II.** *J. Biol. Chem.* 279(34) 35557 (2004)
2. Poincloux, R., Collina, O., Lizárraga, F., Romao, M., Debray, M., Piel, M. and Chavrier, P. **Contractility of the cell rear drives invasion of breast tumor cells in 3D Matrigel.** *PNAS* 108 (5):1943 (2011)
3. Fischer, K.E., Pop, A., Koh, W., Anthis, N.J., Saunders, W.B. and Davis, G.E. **Tumor cell invasion of collagen matrices requires coordinate lipid agonist-induced G-protein and membrane-type matrix metalloproteinase-1-dependent signaling.** *Mol Cancer.* 5:69 (2006)

Kinetic Chemotaxis Assays

Powerful Assays for Quantification and Visualization of Chemotactic Cell Migration and Invasion

Introduction

Chemotactic migration and invasion play an essential role in many normal and pathological processes including immune response, cell differentiation and tumor metastasis. Methods to study factors that regulate the directional migration of cells typically employ modifications of Boyden chamber assays. Boyden chamber assays consist of an upper and lower chamber separated by a porous filter, allowing for the diffusion of a chemotactic agent. Although these assays offer insight into the chemotactic response of cells, they have inherent drawbacks including the inability to visualize active cell migration and the requirement for a large number of cells, typically 50,000 to 100,000 cells per well. Most importantly, perhaps, Boyden chamber assays “only afford the measurement of cell migration at a single time point, and as the kinetics of cell migration vary markedly depending on the

cell type studied and the chemoattractant used, this limits the utility of this type of assay.”¹

In this chapter, we will review how Incucyte® Chemotaxis Cell Migration and Invasion Assays accurately measure and visualize cell movement in response to a chemical gradient. This approach allows for the assay to be completed in a physiologically relevant environment, supports a stable gradient, and automatically analyzes images, alleviating technically challenging and cumbersome quantification steps in traditional approaches.

Incucyte® Scratch Wound Assay at a Glance

The Incucyte® Chemotaxis Assay is conducted in an Incucyte® Clearview 96-well Plate consisting of an optically clear membrane insert and reservoir

that allows for direct visualization of cell migration and morphological changes using phase contrast and/or fluorescent imaging. The plate is placed in the Incucyte® Live-Cell Analysis System, a fully automated live-cell analysis system with integrated image analysis tools that is placed inside a standard tissue culture incubator. With the Incucyte® Chemotaxis Analysis Software Module, integrated metrics precisely quantify the chemotactic response using 1,000 to 5,000 cells per well, a significant advantage when using rare primary hematopoietic cells from the blood. This assay method is sensitive to surface-integrin signaling, and sustains a linear gradient over several days. The result is 96 wells of reproducible kinetic data supported by images and movies, requiring very few cells and minimal hands-on time.

Shortcomings of Traditional Assays	Live-Cell Imaging and Analysis Approaches
<ul style="list-style-type: none"> ▪ Inability to visualize active cell migration. 	<ul style="list-style-type: none"> ▪ Real-time, direct visualization and automated analysis of chemotactic migration, invasion in a 96-well assay format.
<ul style="list-style-type: none"> ▪ Requirement for a large number of cells, typically 50,000 to 100,000 cells per well. 	<ul style="list-style-type: none"> ▪ Reproducible kinetic data supported by images and movies.
<ul style="list-style-type: none"> ▪ Measurement of cell migration at a single time point. 	<ul style="list-style-type: none"> ▪ Requires only 1,000 to 5,000 cells per well, a significant advantage when using rare primary hematopoietic cells from the blood.
	<ul style="list-style-type: none"> ▪ Assay is sensitive to surface-integrin signaling allowing the study of migration on biologically-relevant surfaces.
	<ul style="list-style-type: none"> ▪ Sustains a linear gradient over several days.
	<ul style="list-style-type: none"> ▪ Measure label-free or labeled cell migration without fixing or staining steps.
	<ul style="list-style-type: none"> ▪ Flexibility to study adherent and non-adherent cell chemotaxis, in mono- or co-culture, with or without fluorescent labels.

Table 1. Shortcomings of Traditional Assays vs Live-Cell Imaging and Analysis Approaches.

Sample Results

Automated Analysis and Visualization

Whole-well images of cells on both the bottom and the top of the Incucyte® Clearview Plate membrane are captured at user-defined intervals. All images are processed using automated algorithms to quantify cell area on each side of the membrane (Figure 1). Directed cell migration can be reported as either an increase in area on the bottom side of the membrane for adherent cells, or a decrease in area on the top side of the membrane for non-adherent cells that migrate down the pore and fall off of the membrane.

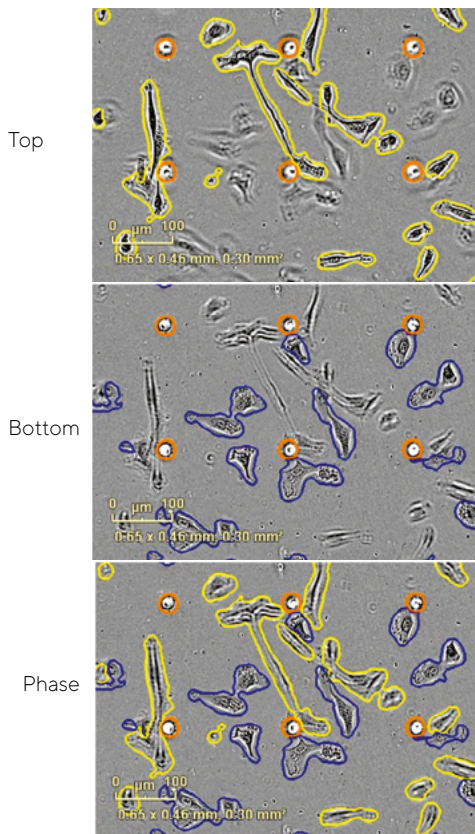


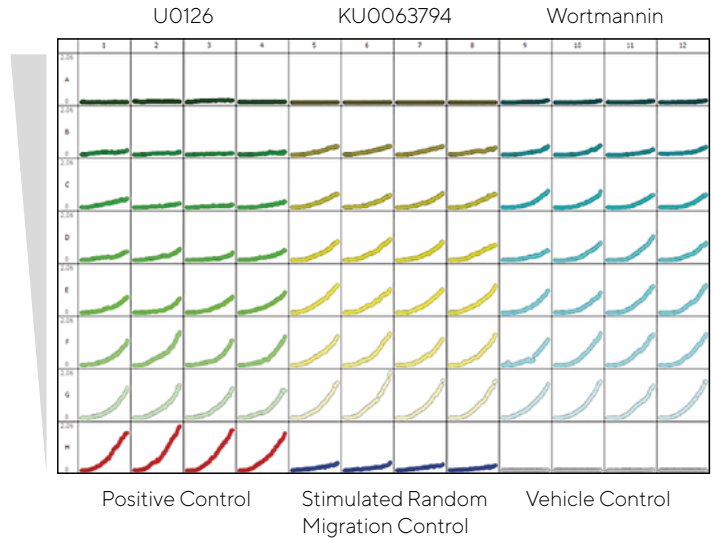
Figure 1. Chemotaxis quantification. HT-1080 fibrosarcoma cells were plated in the top chamber of the Incucyte® Clearview 96-well Plate at a density of 1000 cells/well. 10% FBS was added to the bottom chamber as a chemoattractant. Images represent the top and bottom side of the membrane at the 36-hour time point. Automated image processing separates cells located on the top (outlined in yellow) and the bottom (outlined in blue) surface of the membrane. Pores are outlined in orange. Images are processed as they are acquired, and data can be plotted in real time.

Cancer Cell Chemotactic Migration—Adherent Cells

The pharmacological effect of traditional signaling pathway inhibitors on the directed migration of HT-1080 fibrosarcoma cells toward fetal bovine serum (FBS) was investigated (Figure 2).

We observed concentration-dependent inhibition of directed cell migration with each of the three inhibitors tested: KU0063794 (Akt pathway), U0126 (MEK/ERK MAPK pathway), and Wortmannin (PI3K pathway).

Figure 2. Inhibition of HT-1080 cancer cell migration. This 96-well microplate graph illustrates the kinetic measurement of HT-1080 cell migration toward 10% FBS in each well of the Incucyte® Clearview 96-well Plate. Plotted in each well is the cell area on the bottom of the membrane (y-axis) over the course of a 48-hour assay (x-axis). U0126, KU0063794 or Wortmannin were added to 1,000 HT-1080 cells in the upper chamber and incubated at 37°C for approximately 30 minutes prior to exposing the cells to chemoattractant in the lower chamber. The concentration of inhibitors decreases from the top of the plate to the bottom. Positive (with chemoattractant) and negative (without chemoattractant) controls are located in the last row. These data were collected over a 48-hour period at 1-hour intervals.



Cancer Cell Chemotactic Invasion

Directed cell invasion was studied by embedding HT-1080 cells in an extracellular biomatrix, and investigating the ability to specifically inhibit invasion using GM6001. Side-by-side migration and invasion assays were performed (prepared

by embedding 1,000 HT-1080 cells per well in 1 mg/mL Cultrex® Rat Tail Collagen 1) in Incucyte® Clearview Plates (Figure 3) The biomatrix:cell layer was overlaid with three-fold serial dilutions of GM6001, a broad spectrum matrix metalloproteinase (MMP) inhibitor. After compound addition,

10% FBS was added to the reservoir wells and measurements of bottom-side nuclear counts were plotted over 72 hours. Data shows specific GM6001 concentration-dependent inhibition of HT-1080 invasion and no effect on the migratory response of HT-1080 cells toward 10% FBS.

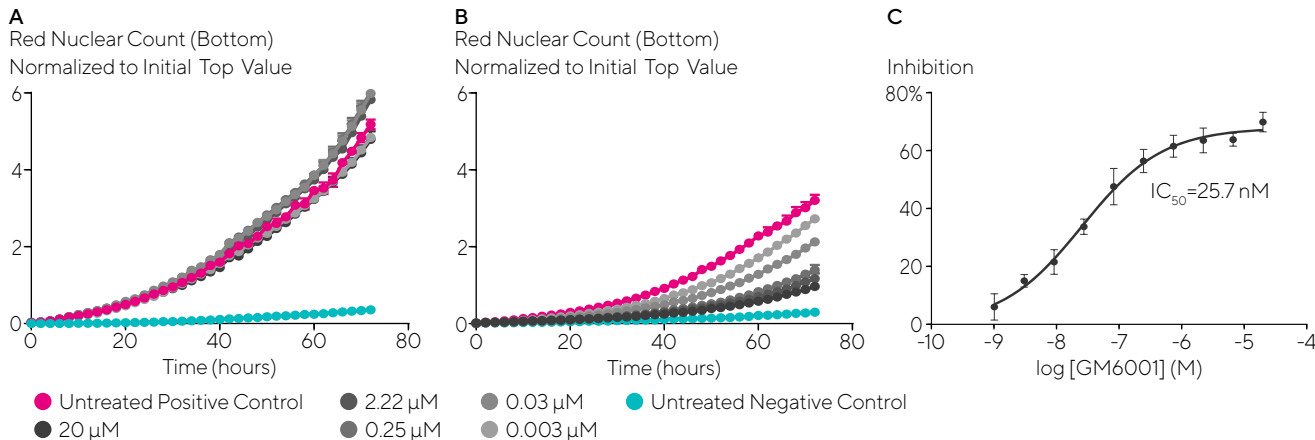


Figure 3. Effect of GM6001 on migration and invasion of HT-1080 cells in a collagen invasion assay. HT-1080 cells were plated at a density of 1,000 cells per well in assay medium (A, migration assay) or embedded in 1 mg/mL neutralized Cultrex® Rat Tail Collagen 1 (B, invasion assay). Serial dilutions of GM6001 were added to the cells in the migration assay or overlaid on the biomatrix:cell layer of the invasion assay at indicated concentrations prior to exposing them to 10% FBS. Analysis of pharmacological response was performed at t=72 hours. Inhibition curve for GM6001 indicating IC_{50} in the invasion assay (C). Data were collected over a 72-hour period at 2-hour intervals. Each data point represents mean \pm SEM, n=4.

Immune Cell Chemotaxis— Non-Adherent Cells

In a model of immune cell chemotaxis, the response of CD3/CD28 activated T cells toward two chemoattractants was investigated: CXCL11 and CXCL12 (aka SDF-1a), ligands for CXCR3 and CXCR4, respectively (Figure 4)². By measuring the loss of cell area on the top of the membrane, we show that activated T cells migrate toward both CXCL11 and CXCL12. Results show the selective CXCR4 antagonist, AMD3100, inhibits chemotaxis toward CXCL12 (IC₅₀ = 279 nM), with no effect on CXCL11-mediated chemotaxis. This experiment was completed on an ICAM-1-coated surface. Interestingly, successful measurements of T cell chemotaxis were also made on fibronectin and Matrigel®/FBS-coated surfaces, while T cells did not migrate on an uncoated surface. This suggests that interactions between integrins and/or receptors on the cell surface and the substrate play a fundamental role in T cell chemotaxis in this assay. This was not the case when tested in a traditional Boyden chamber,

where the surface coating was not required (data not shown).

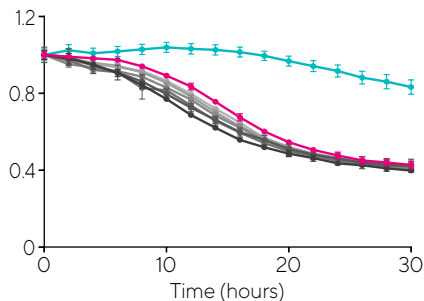
Surface Contact-Mediated Migration

The low pore density of the Clearview Plate membrane ensures that cells must migrate across the biologically relevant surface towards the chemoattractant. Neutrophils seeded on an uncoated Clearview Plate membrane were unable to migrate towards the chemoattractants IL-8 and fMLP; however, those on Matrigel®-coated membranes showed clear chemotactic profiles (data not shown). These data suggest that integrin and/or cell surface receptor interactions with the substrate play a key role in neutrophil chemotaxis in this model. In contrast, no coatings were required for neutrophil migration studies using a 96-well modified Boyden chamber assay (data not shown), suggesting that active migration of neutrophils in a Boyden chamber approach is absent.

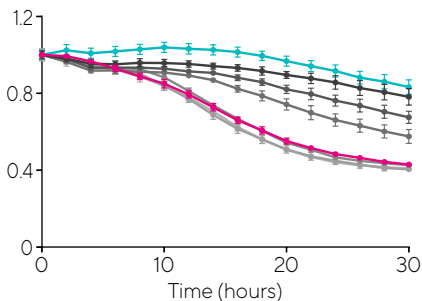
Interestingly, the assay micro-environment is critical in supporting cell motility. Neutrophils suspended

in RPMI supplemented with 0.5% BSA were unable to migrate toward C5a and IL-8 chemoattractant gradients. When media was supplemented with 0.5% HSA, however, neutrophils actively migrated toward both C5a and IL-8 (data not shown). Figure 5 shows that upon visual inspection of the wells, an observed difference in cell morphology of neutrophils isolated in RPMI + 0.5% BSA (rounded phenotype), compared to neutrophils isolated in RPMI + 0.5% HSA (activated phenotype). Furthermore, neutrophils assayed using a modified Boyden-chamber approach responded to both chemoattractants (data not shown), showing no sensitivity to the different albumins present in the assay media. Together, these quantitative and qualitative data suggest that the interaction of cell integrins with the substrate and the overall assay micro-environment are a crucial component in the Incucyte® Chemotaxis Cell Migration Assay (see Chapter 5d - Immune Cell Differentiation, Phagocytosis and Efferocytosis Assays for more details).

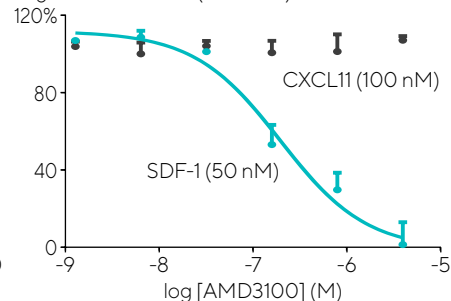
AMD3100 Inhibition of T Cell Chemotaxis
Toward 100 nM CXCL11 Total Phase T Cell
Area $\mu\text{m}^2/\text{well}$ (top count)
Normalized to Initial Value



AMD3100 Inhibition of T Cell Chemotaxis
Toward 50 nM SDF1- α
Area $\mu\text{m}^2/\text{well}$ (top count)
Normalized to Initial Value



Migration Inhibition (30 hours)



● Negative Control ● 6.4 μM ● 160 μM ● 4000 μM
● 1.28 μM ● 32 μM ● 800 μM ● Positive Control

Figure 4. T cell chemotaxis toward CXCL11 and CXCL12 (SDF-1a). T-cells were plated at a density of 5,000 cells per well in the upper chamber of an Clearview 96-well chemotaxis plate coated with ICAM. AMD3100 was added to the cells at indicated concentrations and incubated at room temperature for approximately 1 hour prior to exposing the cells to chemoattractant gradient. CXCL11 or SDF-1a was added to the reservoir plate at 100 nM or 50 nM, respectively, based on EC₅₀ values obtained in agonist curve experiments (data not shown). Analysis of pharmacological response was performed at t=30 hr. Data were collected over a 30-hour period at 2-hour intervals. Each data point represents mean \pm SEM, n=3.

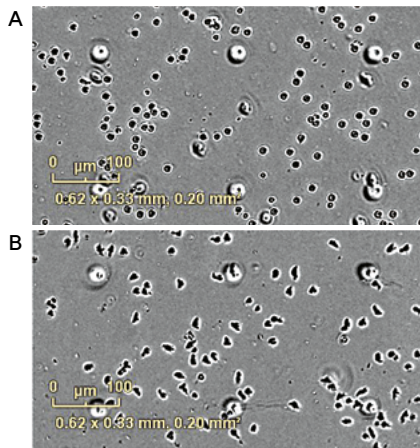


Figure 5. Morphological images. Phase-contrast images of neutrophils isolated in RPMI + 0.5% BSA (A) versus isolation in RPMI + 0.5% HSA (B), seeded on Clearview membranes coated with 50 $\mu\text{g}/\text{mL}$ Matrigel + 10% FBS, showing morphological differences in response to 1 μM C5a ($t=20$ minutes). This difference in phenotype was also observed in neutrophils that were exposed to the chemoattractant IL-8.

Intra- and Inter-Plate Reproducibility Measurements

To assess assay reproducibility and precision of the Incucyte® Chemotaxis Assay, a series of four independent experiments using Jurkat (non-adherent) T cells was performed (Figure 6). Cells were plated at a density of 5,000 cells per well. Two-fold dilutions of CXCL12 were made across columns, and measurements of total phase object area normalized to the initial value were plotted over a 30-hour time course. Highly reproducible well-to-well kinetic measurements, with an average intra-assay CV of 6.3%, were observed. Similar results were obtained when measuring the directed migration of HT-1080 cells toward FBS and neutrophils toward IL-8, C5a and fMLP (data not shown)

Stable Gradient

A long-term, stable gradient is required to support chemotaxis over longer periods of time, and to increase cell participation

rates. In an experiment designed to evaluate the stability of a chemoattractant gradient in the Incucyte® 96-well Clearview Plate and a 96-well modified Boyden-chamber assay, diffusion of a 10,000 kD dextran fluorescently labeled with Alexa Fluor® 594 was monitored over a 72-hour time course in each consumable. As shown in Figure 7, more than 50% of the gradient dissipates in the 96-well traditional Boyden-chamber plate within the first four hours. In contrast, >80% of the gradient remains intact in the Clearview Plate at 72 hours. In a biological test of gradient stability, the HT-1080 cells migrated directionally toward FBS with equal rates in gradients that had been pre-established for 24, 48, and 72 hours, indicating a stable gradient across the membrane (Figure 7). These rates were slightly faster than those for cells migrating toward a gradient that had not been pre-established. This is likely a result of increased cell health when serum-starved cells are plated in established gradients.

Migration (30 hours)

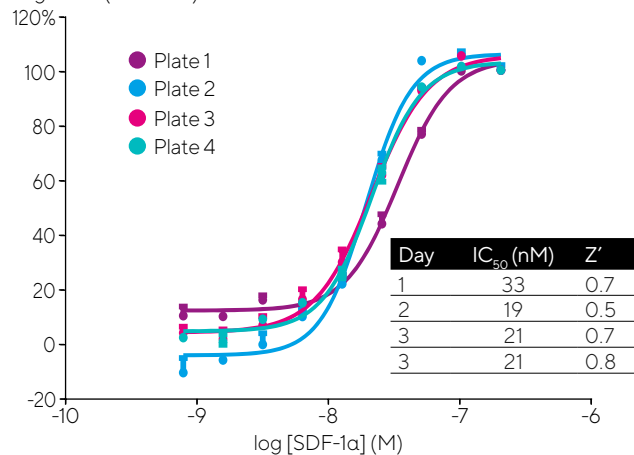
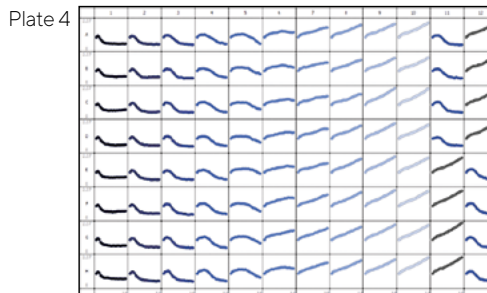
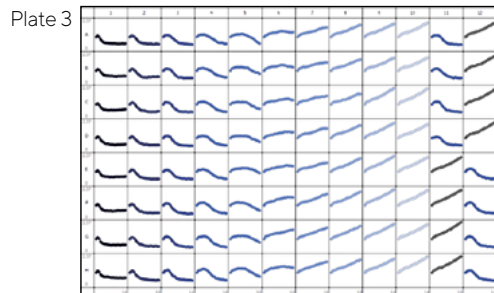


Figure 6. Precision and reproducibility of directed migration of Jurkat T cells toward CXCL12. Jurkat cells were plated at a density of 5,000 cells per well in the upper chamber of the Incucyte® Clearview Plate. Two-fold dilutions of SDF-1α (n=8 per concentration) were added to the reservoir.



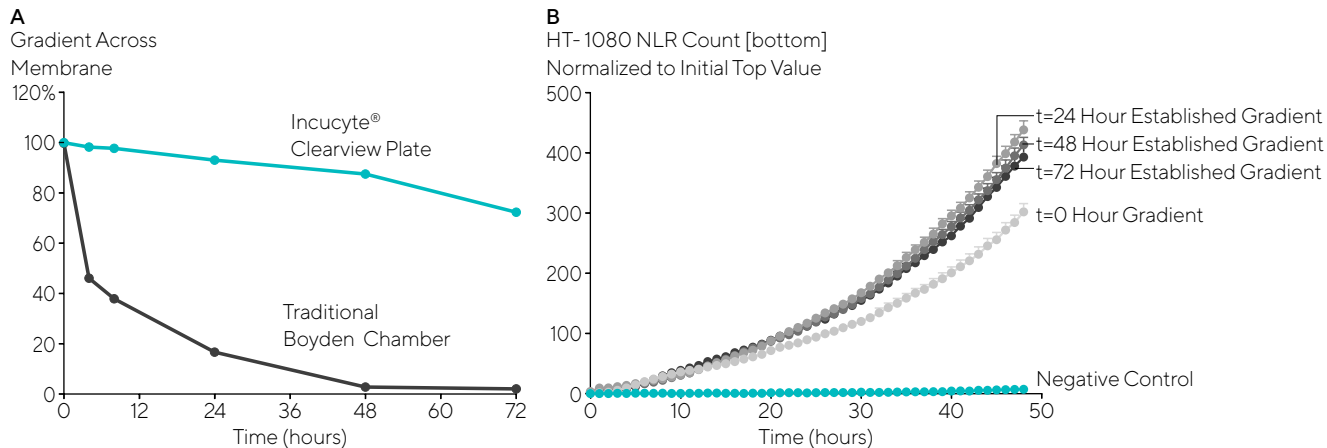


Figure 7. Evaluation of Incucyte® Chemotaxis Assay gradient. (A) 10,000 kDa dextran, labeled with Alexa Fluor® 594, was added to the reservoir plates for the Clearview Plate and 96-well modified Boyden-chamber at a concentration of 10 μ M to establish gradients over 72, 48, 24 and 0 hours. Measurements of diffusion were made by sampling the insert wells on both plates and measuring fluorescent intensity on a microplate reader. Each data point represents mean \pm SEM, N=3. (B). An FBS gradient was established over 72, 48, 24 and t=0 hours in separate wells. Serum starved Nuclight Red HT-1080 cells were added at a density of 500 cells per insert well to the established gradients and FBS-induced chemotactic response was measured. Each data point represents mean \pm SEM, N=3.

Conclusions

The Incucyte® Chemotaxis Assay is a quantitative and reproducible approach for measuring chemotaxis in both adherent and non-adherent cell types. This assay format allows for the kinetic detection of cell migration toward chemotactic gradients on a physiologically relevant substrate, with movies and images that support quantitative measurements and provide associated morphological and phenotypic insights.

Key features demonstrated in the Incucyte® Chemotaxis Assay are:

- Kinetic cell migration is automatically processed on both the top and bottom side of the optically clear membrane, allowing for real-time analysis of chemotactic driven migration of adherent and non-adherent cell types.
- Non-adherent cell migration is precisely quantified in a physiologically relevant environment, while the plate stays stationary, allowing for the evaluation of rare primary hematopoietic cells from the blood.
- Cells are required to migrate across a biologically relevant surface, demonstrating the need for cell-surface interaction, providing an opportunity for evaluation of integrin receptor signaling.
- All data points can be validated by individual images or time-lapse movies to confirm processing metrics, significantly enhancing the confidence in the measured response.

References

1. Taylor, L., Brodermann, M., McCaffary, D., Iqbal, A. J., and Greaves, D. R: **Netrin-1 reduces monocyte and macrophage chemotaxis towards complement component C5a.** *PLOS ONE* (2016) 11(8): e0160685.
2. Kawaguchi A, Orba Y *et al*: **Inhibition of the SDF-1α-CXCR4 axis by the CXCR4 antagonist AMD3100 suppresses the migration of cultured cells from ATL patients and murine lymphoblastoid cells from HTLV-U Tax transgenic mice.** *Blood* 2009, 114: 2961-2968.

Kinetic Transendothelial Migration Assays

Label-Free, Live Cell Imaging Assay to Visualize and Quantify Transendothelial Migration

Introduction

The recruitment of leukocytes to sites of infection and their subsequent migration through the endothelium are critical steps of the immune response. This process of transendothelial migration (TEM) is essential in order for leukocytes to respond to foreign microorganisms, but if uncontrolled, can lead to autoimmune disorders such as inflammatory bowel disease and rheumatoid arthritis. Assays to evaluate the extravasation of leukocytes are also essential for the study of host-defense response and inflammatory disorders.

In this chapter, we will review live-cell transendothelial cell migration assay, which accurately quantifies directional leukocyte migration across an endothelial monolayer in real time. This approach allows for the assay to be completed in a physiologically relevant environment and

automatically analyzes images, alleviating technically challenging and cumbersome quantification steps in traditional approaches.

Incucyte® Transendothelial Migration Assay at a Glance

The Incucyte® Transendothelial Migration Assay is a fully automated solution to quantify directional leukocyte migration across an endothelial monolayer using kinetic, image-based measurements. This label-free assay is suitable for testing multiple cell type pairings, evaluation of immunomodulation with blocking antibodies or inhibitors, along with the associated ability to assess monolayer integrity throughout the assay.

The Transendothelial Migration Assay is conducted in an Incucyte® 96-well Clearview Plate consisting of an optically clear membrane insert and reservoir that

allows for direct visualization of leukocyte migration across an endothelial monolayer. The plate is placed in the Incucyte® Live-Cell Analysis System, a fully automated live-cell analysis system with integrated image analysis tools, thus eliminating laborious endpoint analysis. Kinetic data of the Incucyte® Clearview Plate is supported by images that allow for visualization of endothelial monolayer integrity and leukocyte diapedesis.

Shortcomings of Traditional Assays	Live-Cell Imaging and Analysis Approaches
<ul style="list-style-type: none"> Standard Boyden chamber surfaces are not easily amenable to imaging. 	<ul style="list-style-type: none"> Acquisition of high-definition, phase contrast images enable verification of intact endothelium throughout the experiment.
<ul style="list-style-type: none"> Require use of intrinsically toxic dyes. 	<ul style="list-style-type: none"> Eliminates use of intrinsically toxic dyes.
<ul style="list-style-type: none"> Requires fixing, staining and cell scraping steps. 	<ul style="list-style-type: none"> Fixing, staining and cell scraping steps not required. Quantitate cells on top and bottom of the membrane to confirm movement.

Table 1. Shortcomings of Traditional Assays vs Live-Cell Imaging and Analysis Approaches.

Sample Results

Assessment of Monolayer Integrity and Visualization of TEM

Human umbilical vein endothelial cells (HUVECs) were grown to confluence on top of fibronectin, a physiologically relevant basement membrane. Integrity of the monolayer was evaluated both prior to leukocyte addition, using electrical resistance measurements as well as staining

for E-Selectin, and after leukocyte addition by assessing phase contrast images.

HUVECs were seeded at 6,000 cells per Incucyte® Clearview Insert and allowed to form a monolayer for approximately 24 hrs. Cells were permeabilized and fixed, and VE-cadherin adhesion junctions (green) were visualized from assembled 10x Z-stack confocal images; dashed circles mark membrane pore locations (Figure 1A).

Resistance measurements of HUVEC monolayers cultured on a supporting matrix of fibronectin was measured using a digital multimeter. HUVEC monolayers were grown for 24 hours in EGM-2, then growth medium was removed and 60µL of DPBS-/- was placed into the insert wells and 200 µL into the reservoir wells. The average resistance for inserts containing a monolayer was 31.9±1.7 compared to wells without cells14.9±0.9 (N=9 per condition), indicative of monolayer formation over the insert pores (Figure 1B).

Label-free CD3/CD28 Dynabead activated primary T cells were added to the endothelial monolayer cultured on fibronectin in the presence or absence of migration modulators. Images were acquired every minute (Figure 2) within an Incucyte® Live-Cell Analysis System using a 10x objective. Yellow and orange arrows indicate leukocytes moving between HUVEC cells and eventually down the pores (blue circles) of the Clearview insert.

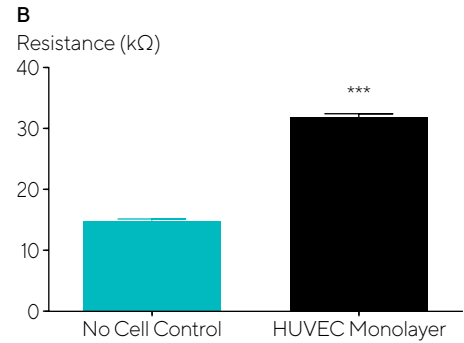
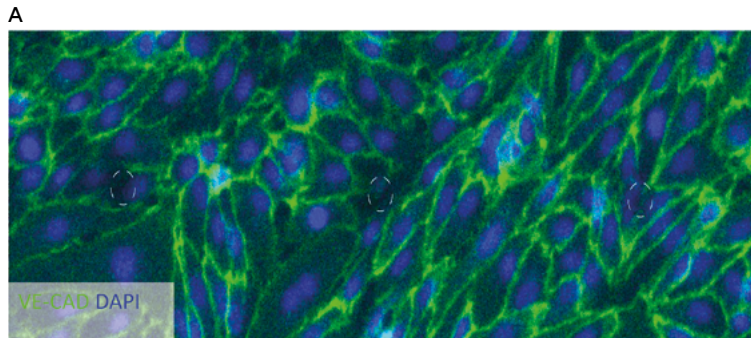


Figure 1. Assessment of monolayer integrity. VE-cadherin adhesion junctions (green) were visualized (A) and monolayer formation confirmed via measurement of resistance across the inserts (B).chemotactic response was measured. Each data point represents mean \pm SEM, N=3.

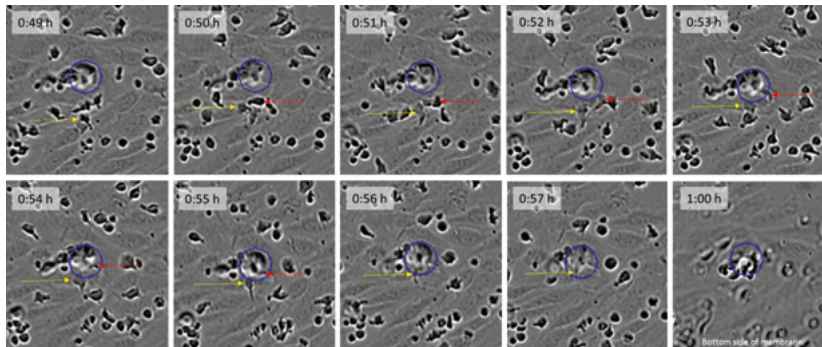


Figure 2. Visualization of leukocyte extravasation.

Real-Time Kinetic Quantitation of Label-Free TEM

CD3/CD28 Dynabead activated primary T-cells were seeded on a HUVEC monolayer cultured on fibronectin in Incucyte® Clearview Plates. Live cell images were captured at regular time intervals, and directed transendothelial migration toward CXCL12 (SDF-1a) was quantified using image analysis algorithms. Significant transendothelial migration, or diapedesis, was observed in response to increasing concentrations of SDF-1a, and could be completely inhibited using high concentrations of AMD3100, a selective inhibitor of CXCR4 and CXCL12 (SDF-1a) mediated chemotaxis.

Whole-well, phase-contrast images represent the top-side of the membrane at t=0 hour time point (Figure 3A). Automated image processing separates T cells (outlined in yellow) from the HUVEC monolayer (Figure 3B). Images are processed as they are acquired, and data can be plotted in real time as a decrease in area on the top side of the membrane for

leukocytes that extravasate the endothelial monolayer and down the pore.

The insert containing T cell:HUVEC monolayer co-cultures was exposed to 3-fold decreasing concentrations of CXCL12 (SDF-1a) (Figure 4A). Images were acquired every 30 minutes and phase analysis was performed. Analysis of pharmacological response was performed at t=6hr; each data point represents mean \pm SEM, N=4 (Figure 4B).

Inhibition of Leukocyte Extravasation

For AMD3100 (CXCR4 receptor antagonist) and BIRT377 (allosteric modulator of LFA- 1) inhibition studies, CD3/CD28 activated T cells were pre-treated for 1 hour at 37°C at indicated inhibitor concentrations, then seeded onto HUVEC monolayers and exposed to 100nM SDF-1a (Figure 5A and C).

Analysis of AMD3100 pharmacological response was performed at t=6 hr. Each data point represents mean \pm SEM, N=4 (Figure 5B). For antibody inhibition,

HUVEC monolayers cultured overnight on fibronectin were \pm pre-treated with neutralizing ICAM-1 for 1 hour at 37°C (Figure 5D). CD3/CD28 Dynabead activated T cells were then plated at a density of 5,000 cells per well on to a HUVEC monolayer then exposed to 100nM SDF-1a (EC80concentration). Images were collected every hour over a 12 hour period and phase analysis performed.

The observed increase in total cell area is due to proliferation of C3/CD28 activated T cells. The inability to fully inhibit TEM via BIRT 377 and neutralizing ICAM-1 is believed to be caused by the centrifugation step, bringing the T cells to the HUVEC monolayer, thus bypassing the cell adhesion step.

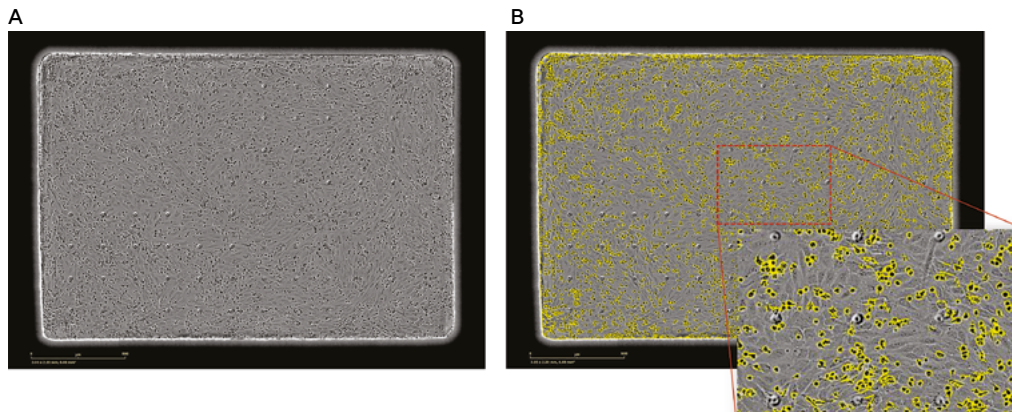


Figure 3. Data quantification and analysis. Whole-well, phase-contrast images represent the top-side of the membrane at t=0 hour time point (A). Automated image processing separates T cells (outlined in yellow) from the HUVEC monolayer (B).

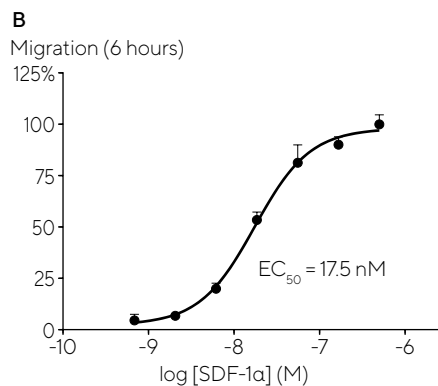
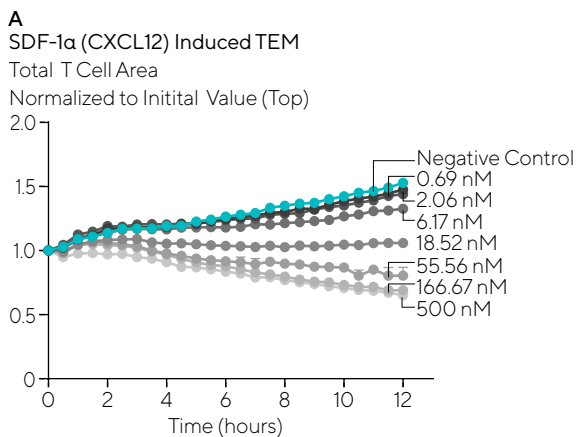
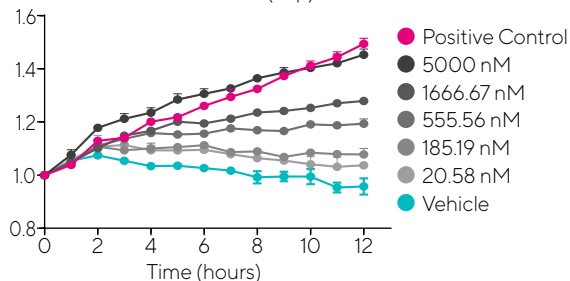


Figure 4. Primary T cells extravasation toward CXCL12. CXCL12 (SDF-1 α) induced TEM (A). Pharmacological response of T cell migration (B).

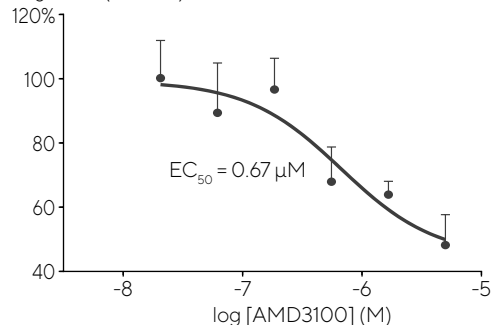
A Inhibition of SDF-1 α Driven T Cell TEM by AMD3100

Total T Cell Area

Normalized to Initial Value (Top)



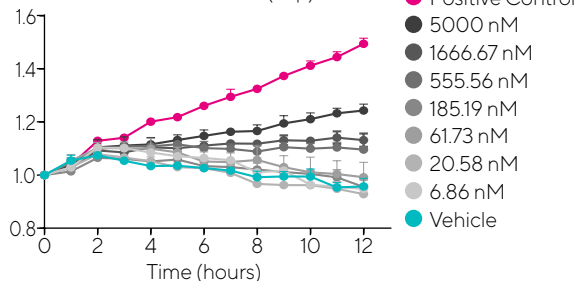
B Migration (6 hours)



C Inhibition of SDF-1 α driven T Cell TEM by BIRT 377

0.8 Total T Cell Area

Normalized to Initial Value (Top)



D Inhibition of SDF-1 α driven T Cell TEM by Neutralizing ICAM-1

0.8 Total T Cell Area

Normalized to Initial Value (Top)

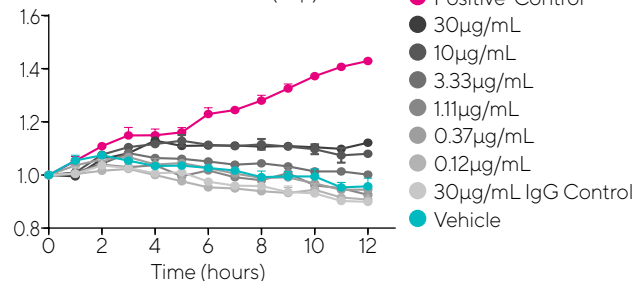


Figure 5. Treatment effects on leukocyte transendothelial migration. Inhibition of CXCL12 (SDF-1 α) driven T cell migration by AMD3100 (A), BIRT 377 (C) and neutralizing ICAM-1. Analysis of AMD3100 pharmacological response (B). Migration across the endothelial layer was at least partially dependent on ICAM-1, as neutralizing ICAM-1 antibodies, and treatments with an allosteric inhibitor of LFA-1, BIRT377, significantly inhibited SDF-1 α mediated diapedesis of T cells.

Conclusions

The Incucyte® Transendothelial Migration Assay can be used for real-time visualization and automated analysis of transendothelial migration in a 96-well format, in real-time.

- Acquisition of high-definition, phase contrast images ensure endothelium integrity throughout the experiment.
- Measurement of leukocyte extravasation is automatically processed without use of intrinsically toxic dyes, fixing, staining and cell scraping steps.
- All data points can be validated by individual images or time-lapse movies to confirm processing metrics, significantly enhancing the confidence in the measured response.

Chapter 7

Kinetic Assays for Quantifying Protein Dynamics

Complementary, Live-Cell Solutions for Studying Protein Dynamics

Proteins—the building blocks of the cell—are required for virtually every biological process, from cell function, to structure and regulation. The study of proteins – how they move, interact and communicate with each other – is thus essential for our understanding of health and disease.

This is particularly true of proteins on the surface of cells involved in cell signaling and ligand binding, which requires the interaction of both extracellular proteins, such as cytokines and hormones, and membrane proteins. Such interactions are often the drivers of disease processes or the basis of drug mechanism of action. Antigen-mediated antibody internalization, for example, plays an important role in several antibody-based therapeutics and in differentiation-induced protein expression changes.

However, despite their importance, our ability to analyze these processes and link

their properties to cell function has been hindered by the methodologies available to study them. Current methodologies for analysis of membrane proteins and their receptor function are limited to single time point analyses, not taking into account the dynamic changes in protein expression due to protein turnover or in response to biochemical cues. While traditional protein assays have provided insights into localization, binding and protein-protein interactions; these single snapshots in time cannot follow the dynamics of proteins in living cells under physiological conditions and therefore are lacking in physiological context.

Incucyte® Live-Cell Analysis System and antibody labeling reagents enable a new assay approach that delivers spatial and temporal information at scale in living cells. The unique antibody reagents can be mixed with any Fc-containing antibody, applied directly to cells and then monitored under physiological conditions for hours or days.

The real-time image acquisition and analysis means it is possible to quantitatively link the dynamics of a target protein with cell morphology, proliferation and function. The protocol is simple despite the richness of data and insight generated, involving a single antibody-labeling step followed by direct addition to cells, thereby removing the need for laborious labeling and blocking procedures and wash steps that can result in unwanted cellular changes and misleading results.

Incucyte® Fabfluor Antibody Labeling Dyes are highly specific and sensitive, amenable to both adherent and non-adherent cell models. The data below exemplifies how the assays can be used to study long-term protein dynamics and their relationship to cell function, morphology, as well as cell-cell interactions.

Live-Cell Imaging and Analysis Approaches to Studying Protein Dynamics

Fluorescently labeled antibodies are widely used as markers for visualizing cell surface protein expression, receptor interactions and antibody internalization. To build on existing methodologies for studying protein expression, a novel strategy was developed based on fluorescently labeled antibody fragments (Fabs) that target the Fc region of any mouse, human or rat antibody. Two types of reagents have been developed, differing in the type of fluorescent molecule conjugated to the Fab and thereby enabling two different applications, antibody internalization and

live-cell immunocytochemistry. These two reagents, when combined with the Incucyte® Live-Cell Analysis System, provide an integrated approach to studying protein dynamics in real-time and under physiological conditions.

How Live-Cell Protein Assays Work

Antibody Internalization Assays

In the antibody internalization assay, a pH-sensitive antibody labeling reagent, Incucyte® Fabfluor-pH Red or Orange Antibody Labeling Dye, allows the specific detection of antibodies as they are internalized into the acidic conditions of endosomes and lysosomes, enabling

real-time, kinetic monitoring over the full time-course of internalization.

Live-Cell Immunocytochemistry

To detect cell surface markers, Incucyte® Fabfluor-488 Antibody Labeling Dye, a Fab conjugated to a continuously fluorescing molecule at physiological pH, is utilized for antibody labeling. Addition of the Incucyte® Fabfluor-antibody complex to living cells enables kinetic detection of cell surface markers, making it possible to track the movement and interaction of cell subsets, reveal the dynamics of their interactions, and link time- and concentration-dependent changes in cell surface protein expression to other morphological and phenotypic parameters.

References

1. Cohen AS, Khalil FK, Welsh EA, Schabath MB, *et al.* **Cell-surface marker discovery for lung cancer.** *Oncotarget* 2017, 8(69): 113373-402.
2. Gundry RL, Boheler KR, Van Eyk JE, and Wollscheid B. **A novel role for proteomics in the discovery of cell-surface markers on stem cells: Scratching the surface.** *Proteomics Clin. Appl* 2008, 2(): 892-903.
3. Macher BA and Yen TY. **Proteins at membrane surfaces – a review of approaches.** *Mol BioSys* 2007, 3(): 705-13.
4. Roesli C, Borgia B, Schliemann C, Gunther M, *et al.* **Comparative analysis of the membrane proteome of closely related metastatic and nonmetastatic tumor cells.** *Cancer Res* 2009, 69(13): 5406-14.
5. Kuhlmann L, Cummins E, Samudio I, and Kislinger T. **Cell-surface proteomics for the identification of novel therapeutic targets in cancer.** *Expert Review of Proteomics* 2018, 15(3): 259-75.
6. Ritchie M, Tchistiakova L, and Scott N. **Implications of receptor-mediated endocytosis and intracellular trafficking dynamics in the development of antibody drug conjugates.** *mAb* 2013, 5(1): 13-21.
7. Beck A, Haeuw JF, Wurch T, Goetsch L, *et al.* **The next generation of antibody-drug conjugates comes of age.** *Discov Med* 2010, 10(53): 329-39.
8. Adams GP and Weiner LM. **Monoclonal antibody therapy of cancer.** *Nat Biotechnol* 2005, 23(9): 1147-57.
9. Liao-Chan S, Daine-Matsuoka B, Heald N, Wong T, *et al.* **Quantitative Assessment of Antibody Internalization with Novel Monoclonal Antibodies against Alexa Fluorophores.** *PLoS ONE* 2015, 10(4): e0124708.
10. Kuo S, Alfano RW, Frankel E and Liu J. **Antibody Internalization after Cell Surface Antigen Binding is Critical for Immunotoxin Development.** *Bioconjugate Chem* 2009, 20(10): 1975-82.

7a

Kinetic Antibody Internalization Assays

Visualization and Quantification of Antibody Internalization, in Real Time

Introduction

The growing focus on antibodies as therapeutics makes it essential to be able to study their dynamics in a realistic cell environment. Antibodies are used both as therapeutic agents that themselves block the activity of certain molecules, or for the targeted delivery of treatments to sites or cells of interest. This includes the delivery of highly toxic drugs to cancer cells via antibody drug conjugates (ADCs), removal or degradation of surface receptors from cancer cells (i.e. EGFR), and antibody immunotherapies used to identify tumor cells for immune cell killing (i.e. ADCC or ADCP).

Each of these therapeutic strategies hold the promise of increased efficacy and reduced side effects, and each requires a series of antibody features, for example, to enable maintenance on the cell surface for identification of tumor cells, or for rapid

internalization when delivering ADCs. To realize their potential, it is important to understand the uptake profile and clearance of antibody candidates, and to be able to measure and optimize functional responses to antibodies for optimal antibody engineering and internalization characteristics. For example, pinocytosis, which is one of the main elimination routes of antibodies, requires antibody optimization for qualitative pharmacokinetic measurements during therapeutic antibody development.

Current methods for measuring antibody internalization have several limitations. These include the requirement to label each antibody, conduct multiple washing steps, and the ability to only do single-time point analysis. This can lead to unnecessary and labor-intensive processes, loss of cells through washing, and missed and incorrect measurements due to limitations of single time-point analysis.

There is an urgent need to have an efficient, affordable method that can be used throughout the entire antibody screening and functional characterization process to fully and rapidly quantify antibody internalization using real time live-cell analysis.

In this chapter, we will illustrate how novel pH-sensitive Fc-targeting antibody labeling reagents allow for real-time rapid, kinetic, high-throughput analysis of antibody internalization in living cells. This is an ideal tool for optimal antibody engineering early in the biologic discovery process.

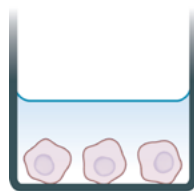
Incucyte® Antibody Internalization Assays at a Glance

The Incucyte® Antibody Internalization Assay uses Incucyte® Fabfluor-pH Red or Orange Antibody Labeling Dye, a novel pH-sensitive Fc-targeting antibody

fragment, isotype-matched to the antibody of interest. The Incucyte® Fabfluor-pH Dye and antibody of interest are mixed in a one-step, no wash, labeling protocol. At pH 7.0, the Fabfluor-Ab complex has little or no fluorescence. When labeled antibodies are added to cells, a fluorogenic signal is seen as the antibody is internalized and processed in acidic (pH 4.5-5.5) lysosomes and endosomes. The full time-course of antibody internalization can then be followed with the Incucyte® Live-Cell Analysis System for real-time analysis of internalization rates. An overview of the workflow is shown in Figure 1.

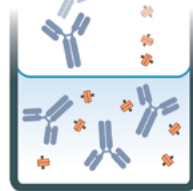
Figure 1. Overview of the Incucyte® Antibody Internalization Assay

1 Seed Cells



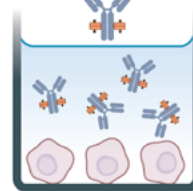
Cell Seeding
Seed cells (50 μ L/well, 5,000-30,000 cells/well), into 96-well plate and leave to adhere (2-24 h, depending on cell type).

2 Label Test Antibody



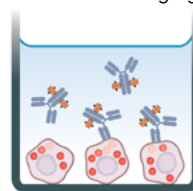
Labeling of Test Antibody with Incucyte® Fabfluor-pH Dye
Mix antibody and Fabfluor Dye at a molar ratio of 1:3 in media, 2x final assay concentration. Incubate for 15 minutes to allow conjugation.

3 Add To Cells



Incucyte® Fabfluor-Labeled Antibody Addition
Add antibody-Fabfluor mix (50 μ L/well) to cell plate.

4 Live-Cell Fluorescent Imaging



Automated Imaging and Quantitative Analysis
Capture images every 15-30 minutes (10x or 20x) in Incucyte® Live-Cell Analysis System for 24-48 hours. Analyze using integrated software.

Shortcomings of Traditional Assays

- Requires **labor-intensive labeling** of each antibody.
- Only provides **single-time point analysis**.
- **Low throughput** due to combination of labeling approach and end-point analysis.

Live-Cell Imaging and Analysis Approaches

- **Rapid, single-step labeling** allows efficient testing of panels of antibodies.
- **Real-time, kinetic measurements** of antibody responses.
- **High-throughput, reproducible antibody screening** validated with individual images.

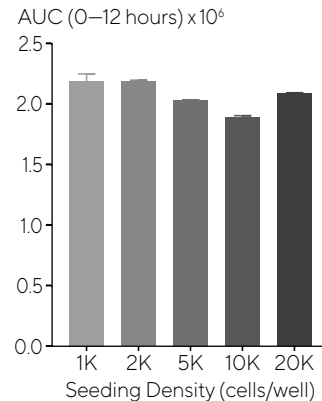
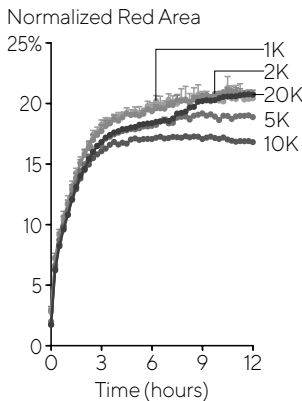
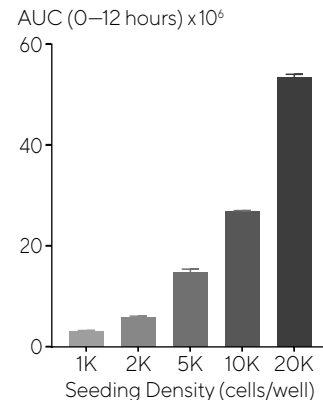
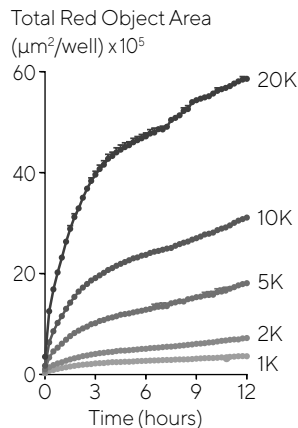
Table 1. Shortcomings of Traditional Assays vs Live-Cell Imaging and Analysis Approaches.

Sample Results

Antibody Internalization With Incucyte® Fabfluor-PH Red Antibody Labeling Dye

Antibody internalization signal increases with cell number, but the Incucyte® Fabfluor-pH Dye can distinguish the true internalization rate signal from that associated with cell proliferation by virtue of collecting both biochemical and morphological data simultaneously. Anti-CD71 internalization (red fluorescence area) was normalized to the total cell area (phase confluence), and the internalization signals over time between different plates were highly similar. This normalization method helps to minimize the impact of variation in cell number between plates and reveals the true internalization rate of your antibody of interest.

Figure 2. Antibody internalization response is cell number dependent. An increasing density of HT-1080 cells were seeded (1-20K/well) and treated with Incucyte® Fabfluor-pH labeled α -CD71 (4 μ g/mL). HD phase contrast and red fluorescence images (10X) were captured every 30 min over 12 h. The time-course of Red Object Area data demonstrates an increasing internalization signal with increasing cell number (A and B). When the Red Object Area is normalized for Phase Area, it is clear the internalization response size is dependent on cell number (C and D). All data shown as a mean of 3 wells \pm SEM, bar graphs shown as area under the curve (AUC) calculated from time-course data.



Specific Detection and Visualization of Internalization

The Incucyte® integrated analysis software robustly detects when an Incucyte® Fabfluor-pH labeled antibody has been internalized. Dual-labeling experiments

were conducted in HT-1080 fibrosarcoma cells using a lysosomal marker (LysoSensor® Green, Thermo Scientific) and an Incucyte® Fabfluor-pH Red-labeled anti-CD71 antibody (Figure 3). After three hours, a strong co-incident signal was

measured: 74% of the red anti-CD71 signal was colocalized with green, confirming that the labeled antibody was internalized in the lysosome.

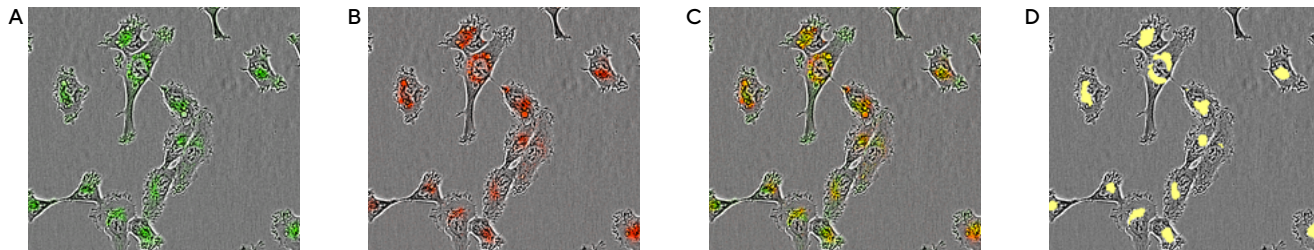
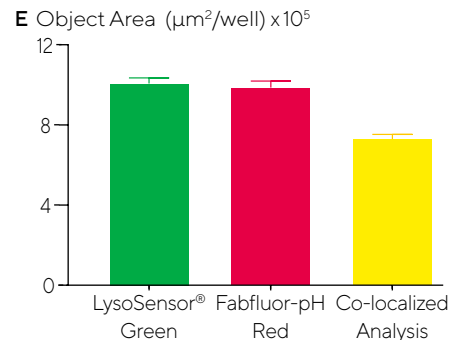


Figure 3. Co-localization of Incucyte® Fabfluor labeled α -CD71 and LysoSensor® Green in HT-1080 cells. Internalization of Incucyte® Fabfluor labeled α -CD71 (4 μ g/mL) was established for 3 h in HT-1080 cells before addition of LysoSensor® Green DND-189 (Thermo, 0.25 μ M). Images show individual LysoSensor® Green and Fabfluor labeled α -CD71 red signal (A and B), co-localization of red and green signals (C), and the co-localized analysis mask shown in yellow (D). (E) Incucyte analysis of the coincidence of the red and green fluorescence confirms co-localization of 74% of the red signal with the green signal. Images captured at 20x magnification, 30 min post LysoSensor® addition, data shown as mean of 4 wells \pm SEM.



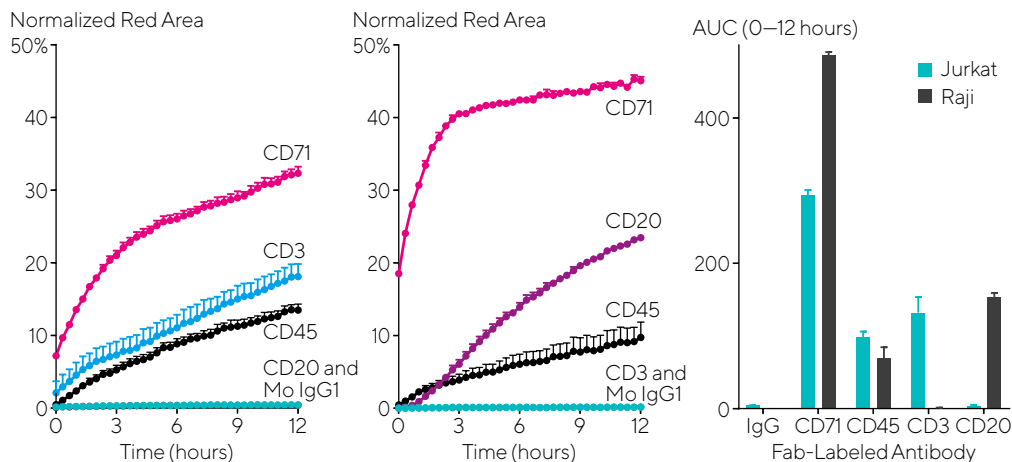
Applicability Across Different Cell Types and Antibodies

To demonstrate the broad application and specificity of the method, internalization was assessed for a range of test antibodies targeted against specific CD markers

expressed in different cell lines (Figure 4). Anti-CD20 was internalized in the B cell line Raji, but not Jurkat, a T cell line. Conversely, anti-CD3 was internalized in Jurkat but not Raji. Antibodies to CD71 and CD45, general lymphocyte markers, were internalized

in both cell types. Importantly, IgG was not internalized in either. These data are in alignment with the known CD surface marker expression of these cell lines, and provide strong confidence in the signal specificity and generic utility of the method.

Figure 4. Internalization of CD surface marker targeted antibodies in lymphocytic cell lines. Jurkat (T cell-like) and Raji (B cell-like) cells (30 K/well) were treated with different Incucyte® Fabfluor labeled antibodies (4 μ g/mL). HD phase contrast and red images were captured every 30 minutes using a 20x objective over 12 hours. Time course data (A and B) and area under the curve (AUC, C) analysis demonstrates the response profile in both cell lines. All data shown as a mean of at least 4 wells \pm SEM, time course data shown as Normalized Red Area.



Quantitative Pharmacological Analysis

Pharmacological, Kinetic Quantification of Antibody Internalization

To illustrate the quantitative nature of the method and suitability for analyzing therapeutic antibodies, we sought to determine EC_{50} values for the internalization of Herceptin (Trastuzumab) and Rituxan (Rituximab), two clinically used monoclonal antibodies. After labeling of each antibody with the Fabfluor-pH Dye, the antibody was serially diluted (1:2) prior to addition to the cells to enable construction of a concentration-response curve. Handling the labeled antibody this way is good practice to eliminate any variation in Fab labeling efficiency which could occur across the concentration range. In BT-474 Her2-positive breast carcinoma cells, clear time and concentration dependent internalization of Herceptin was observed over 48 h. From an area under the time-course (AUC) analysis,

the EC_{50} value for internalization was 323 ng/mL \equiv 2.1 nM, Figure 5). In Raji cells, the EC_{50} value for Rituxan was 426 ng/mL \equiv 2.6 nM, Figure 6). These EC_{50} values are similar to the known KD values for Herceptin and Rituxan for their target receptors (both approximately 5 nM).

Comparison of Multiple Test Antibodies for High-Throughput Screening

The features of the Incucyte® Antibody Internalization Assay are such that it should be facile to parallel label many antibodies and compare their internalization. To validate this, we took 6 different commercially available anti-CD71 antibodies and compared their internalization properties head to head. The antibodies were plated in 96-well plates and labeled in full media with the Incucyte® Fabfluor-pH Dye. Serial dilutions were performed in full media (8 point, 1:2). Labeled IgG and Fabfluor-pH Dye alone were added to control wells. Labeled antibodies were then added to pre-plated HT-1080 cells and monitored for internalization for 12 h.

Of the 6 antibodies, 3 (Ab 1a, Ab2 and Ab 1b) produced large internalization signals and were detected at low concentrations (<0.05 ug ml⁻¹). Reassuringly, Ab 1a and Ab 1b were the same antibody clone from different suppliers, and gave similar internalization responses. Abs 3, 4, and 5 were internalized more weakly and only at higher concentrations (Figure 7). From the control responses, a mean Z' value of 0.82 was determined (2 plates 0.75, 0.87) indicating a microplate assay with high robustness. These data confirm the suitability of the method for comparing the internalization of multiple antibodies at a single target, and illustrate that the internalization profile is a property of the antibody per se. Indeed, the assay precision and work flows are such that 100s of different antibodies could be compared at once and further throughput could be achieved through miniaturization to 384-well format.

Figure 5. Quantitative pharmacological analysis of Incucyte® Fabfluor-pH labeled Herceptin. BT-474 Her2-positive cells were treated with increasing concentrations of Fabfluor-pH labeled Herceptin. The time course graph displays an increase in Normalized Red Area over time with increasing Herceptin concentrations (A). Area under the curve analysis of this response displays a clear concentration dependent response with an EC_{50} of 323 ng/mL (B). All data shown as a mean of 3 wells \pm SEM, time course data shown as Normalized Red Area.

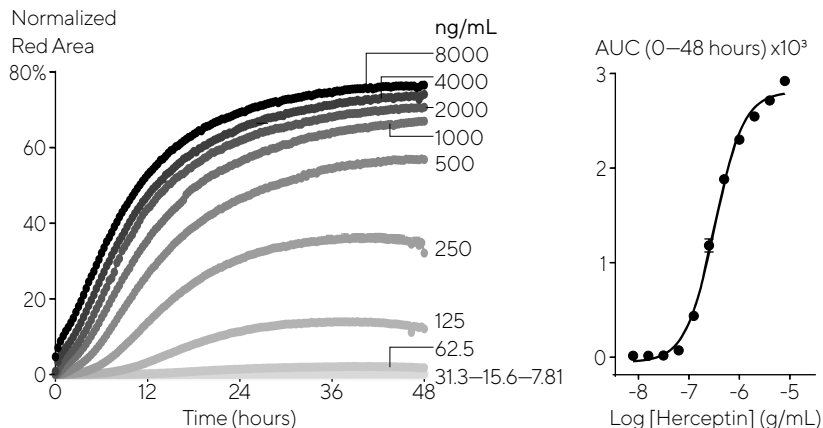
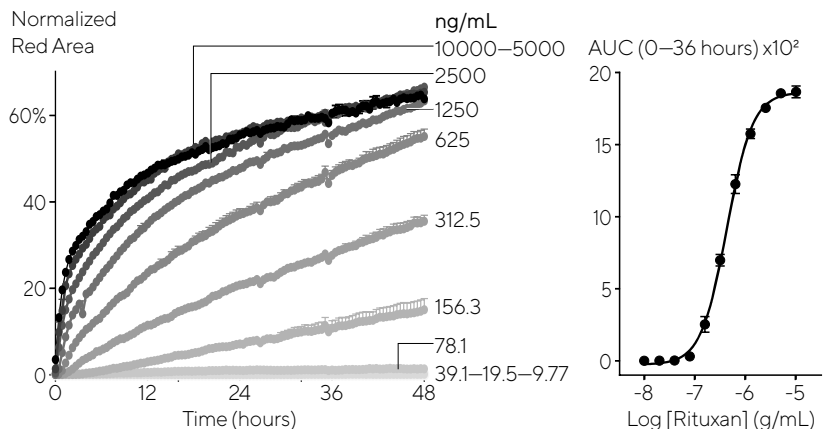
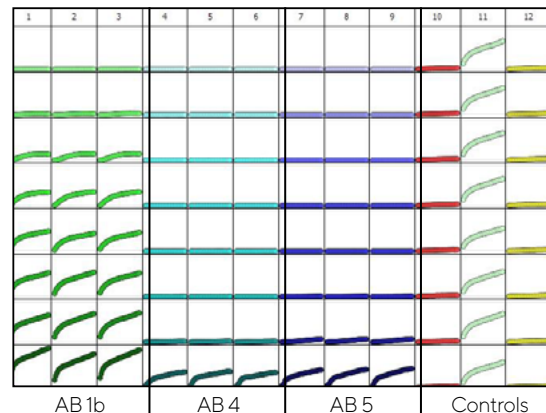
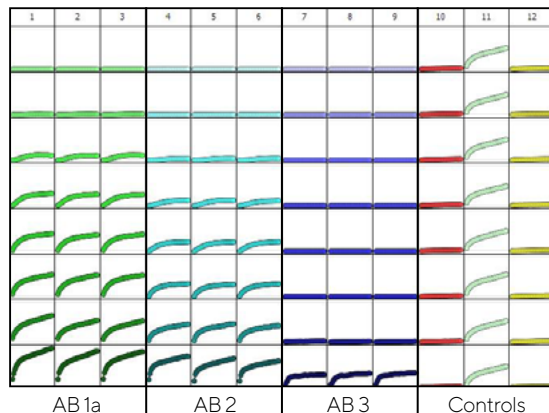


Figure 6. Quantitative pharmacological analysis of Incucyte® Fabfluor-pH labeled Rituxan. Raji cells were treated with increasing concentrations of Fabfluor-pH labeled Rituxan. The time course graph displays an increase in Normalized Red Area over time with increasing Rituxan concentrations (A). Area under the curve analysis of this response displays a clear concentration dependent response with an EC_{50} of 426 ng/mL (B). All data shown as a mean of 3 wells \pm SEM, time course data shown as Normalized Red Area.



A**B**

Red Object Area ($\mu\text{m}^2/\text{well}$) $\times 10^5$, 12 hours

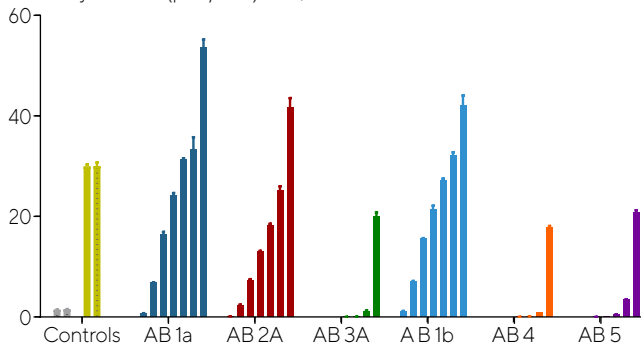


Figure 7. Screening test Abs for internalization. Six different CD71 antibodies including one clone from 2 different suppliers (clone 1a & 1b) were tested head to head in HT-1080 cells. The antibodies were labeled with Incucyte® Fabfluor-pH Dye prior to addition to cells and the internalization signal captured every 30 minutes over 12 hours using a 10x magnification. Incucyte® microplate graphs show clear positive and negative control responses in column 11 and 12 with concentration dependent responses for each antibody across two plates (A). Head to head analysis of antibody data shows a range of responses across these clones (B) control responses at 12 hours display a clear positive response. All data shown as mean of 3 wells \pm SEM, controls shown as mean of 8 wells.

Conclusions

The key features of the approach described in this application note are:

- A single step labeling protocol for easily tagging antibodies of interest with an Fc-targeted Fab coupled pH-sensitive dye (Incucyte® Fabfluor-pH Dye). The labeling method is conducted in full media and is suitable for purified antibodies and antibody supernatants.
- An automated, image-based and real time analysis method (Incucyte® Live-Cell Analysis System) for monitoring internalization in multiple 96-well microplates at once. The format is amenable to both adherent and non-adherent cells.
- An assay system that follows the full time course of the biology and reports internalization with high specificity, sensitivity and morphological information. The use of a pH-sensitive

dye provides for low background signal and obviates the need to separate out fluorescence arising from antibody on the cell surface or in bulk solution.

Taken together, these attributes provide a simple, integrated and quantitative solution for directly studying internalization of antibodies into cells that can easily be scaled to compare many antibodies (10s-100's) in parallel. This method enables antibody internalization measurements to be implemented at earlier stages in the biologics discovery process, and will prove valuable in efficacy, safety and pharmacokinetic optimization of novel therapeutic antibodies. In addition, the method is suited to understanding basic mechanisms of endocytosis, pinocytosis and receptor turnover where antibodies can be employed.

7b

Kinetic Live-Cell Immunocytochemistry Assays

Long-Term Tracking and Quantification of Cell Surface Protein Markers

Introduction

Immunocytochemistry (ICC) is a powerful laboratory technique for visualizing the cellular and subcellular location of proteins using fluorescent-labeled antibodies ('immunofluorescence'). The study of cell protein expression, and the modulation of it, is a crucial method used to understand gene expression, and ultimately the biology of the cell. With cell fixation protocols, labeled antibodies and specialized microscopes, spatial resolution down to the nanometer level can be achieved to evaluate the expression of proteins in the nucleus, specialized organelles and the cell membrane.

Where conventional ICC is less useful, however, is in studying dynamic changes

in protein expression over time and under physiologically relevant conditions. The technique includes a number of lengthy and time-consuming steps – fixing, washes, and staining – which can take anything between six and 24 hours. These procedures can also lead to physical loss of cells, or result in unhealthy cells that are losing their viability because of fixation and are unlikely to give an accurate picture of the biology of interest.

ICC is a widely used technology for studying changes in protein surface molecules – the key communicators that dictate how a cell responds to external stimuli and changes its shape, protein expression and function in response. These cell surface molecules are the targets of many existing and future drugs and being able to monitor their

activity in real-time and in their natural environment is paramount. Consequently, there is a strong unmet need for technical solutions that can allow the tracking of protein distribution and abundance over time in living cells, and link these to cell morphology and function.

In this chapter, we illustrate how kinetic, live-cell analysis of surface protein expression using fluorescently-labeled antibodies opens up new possibilities for connecting long-term dynamic changes in protein abundance and distribution in cells with morphology and function.

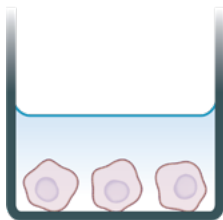
Incucyte® Live-Cell Immunocytochemistry Assay at a Glance

In order to measure the dynamic changes in cell surface protein expression while simultaneously monitoring morphological

changes, Incucyte® Fabfluor-488 Antibody Labeling Dyes are combined with Fc-containing antibodies. These conjugated Fabfluor-Ab complexes are then added directly to live-cells in a single-step mix and read assay. Time-lapse images of cellular fluorescence can then be gathered over hours and days, and automatically

analyzed to provide an index of the levels and pattern of expression over time. An overview of the assay workflow is shown below.ough miniaturization to 384-well format.

1 Seed Cells

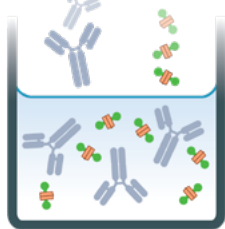


Cell Seeding

Seed cells (50 µl/well, 5-30K/well) into 96-well plate.

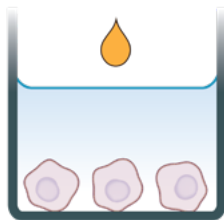
Note: for non-adherent cell types, PLO coat plate prior to cell seeding.

2 Label Test Antibody



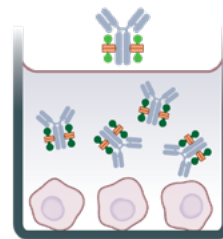
Labeling of Test Antibody with Incucyte® Fabfluor-488 Dye
Mix antibody and Fabfluor-488 Dye at a molar ratio of 1:3 in media, 3x final concentration. Incubate for 15 minutes to allow conjugation.

3 Add Incucyte® Opti-Green



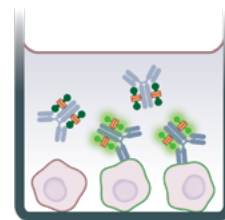
Incucyte® Opti-Green Background Suppressor Addition
Add 50 µl/well, (3x final concentration).

4 Add Labeled AB



Incucyte® Fabfluor-488-labeled Antibody Addition
Add antibody-Fabfluor mix (50 µl/well) to cell plate. Non-adherent cells – spin plate.

5 Live-Cell Fluorescent Imaging



Automated Imaging and Quantitative Analysis
Capture images, (time span and objective depends on assay and cells type, 10x or 20x) in Incucyte® Live-Cell Analysis System.

Figure 1. Overview of Incucyte® Live-Cell Immunocytochemistry Assay workflow.

Key Advantages

- Measure surface protein expression and distribution over time using non-perturbing antibody labeling reagents in physiologically relevant conditions.
- Associate changes in surface protein expression with cell function and morphology to reveal informative, temporal changes in cell behavior.
- Visualize and quantify cell-cell interactions over time in complex co-culture models, revealing insight into the interplay of cells.
- Significantly increase productivity compared to conventional ICC by combining a rapid, single-step labeling protocol with automated acquisition and analysis. (Table 1).

	Incucyte® Live-Cell ICC Approach	Traditional Fix and Stain ICC
Suitable for	▪ Cell surface proteins.	▪ Both intracellular and cell surface proteins.
Optimized for	▪ Protein dynamics and linking changes to function and morphology. Cell identification and cell-cell interactions in motile systems.	▪ In-depth structural/morphological analysis, subcellular distribution, organelles, protein trafficking and redistribution.
Reagents	▪ Primary antibody + Incucyte® Fabfluor-488 + Opti-Green background suppressor.	▪ F-labeled primary or secondary Ab.
Hardware	▪ Incucyte® Live-Cell Analysis System.	▪ Fluorescent microscopes, high-content imagers (Incucyte).
Protocols	▪ Mix and read (one hour prep time).	▪ Fix, wash and stain (6–24 hours?).
Resolution	▪ Cellular, up to 20x magnification.	▪ Subcellular > 100x possible with oil immersion, etc.
Cell Status	▪ Living cells in media/serum.	▪ Dead/dying cells post fixation.
Imaging Paradigm	▪ Repeated imaging over several days, time-lapse movies.	▪ Single time point (“end point”).

Table 1. Comparison of Incucyte® Live-Cell ICC with conventional ‘fix and stain’ ICC.

Sample Results

Quantitative Measurements of Surface Protein Dynamics

Given the current explosion of checkpoint inhibitor cancer therapies, assays that expedite further studies on the regulation of immune-cell signaling pathways in tumors are an area of significant need. The below example illustrates how dynamic changes in cell surface checkpoint proteins can be quantified in living cells in response to an inflammatory stimulus, using Programmed Death Ligand-1 (PD-L1) as an archetype (Figure 2). The Incucyte® Fabfluor-488 Antibody Labeling Dye was conjugated to anti-PD-L1 and applied the mixture to MDA-MB-231 breast cancer cells. Following treatment with IFN- γ , a time- and concentration-dependent increase in PD-L1 labeling was observed over 72 hours. IFN- γ had no effect on the growth rate of MDA-MB-231, indicating that the response was a specific upregulation of PD-L1.

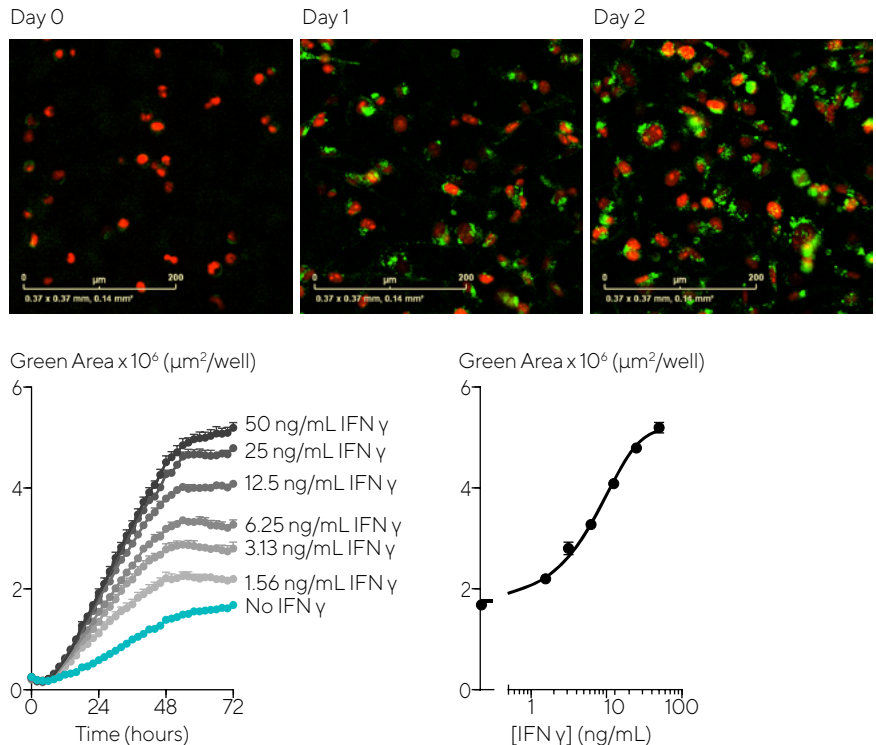


Figure 2. Upregulation of PD-L1 checkpoint protein in tumor cells in response to IFN- γ . Fabfluor-488 Dye was conjugated to anti-PD-L1 Ab (BioLegend) and added to Nuclight Red MDA-MB-231 breast cancer cells in the absence and presence of IFN- γ (+ Incucyte® Opti-Green background suppressor). Quantification of the green fluorescent area shows that IFN- γ induces a time- and concentration-dependent increase in PD-L1 expression, with a mean EC50 value of 9.0 ng/mL. Values are shown as mean \pm SEM, from four wells.

Coupling Protein Dynamics to Morphological Changes

Protein dynamics can also be coupled to morphological changes using Incucyte® Live-Cell Imaging and Analysis. Here, measurements of cell surface markers were linked to morphological changes in human neuroblastoma cells (Figure 3). Here, once treated with a vitamin A derivative to induce differentiation, there was a clear association between the change in neural cell adhesion molecules (NCAMs) observed through live-cell ICC and the increase in neurite length over time.

Coupling Protein Dynamics to Cell Function

Live-cell ICC can also be used to correlate changes in morphology with function. In the below example, the differentiation of human monocytic cells into macrophage-like cells was tracked by Incucyte® Fabfluor-488 labeling of immune cell surface markers (Figure 4). It was found that only phorbol myristate acetate (PMA) produced a marked change in morphology, yielding large, flattened, adherent ‘macrophage-like’ cells. To correlate these observations with function, the ability of differentiated THP-cells to phagocytose Incucyte® pHrodo® labeled apoptotic T cells was measured. Only those cells treated with PMA were phagocytic, illustrating that it is possible to associate protein measurements to the functional properties of cells.

Monitoring Cell-Cell Interactions

Finally, live-cell ICC was used to study the dynamic interactions of immune cells and tumor cells, in a co-culture model system (Figure 5). Close inspection of the Incucyte® time-lapse movies revealed that individual and sometimes multiple immune cells associate with the target cell and remain attached even as the tumor cells move. Using the CD8-labeling antibody it was possible to show that a subset of CD8+ cytotoxic T-lymphocytes specifically engaged with the tumor cells, and even detected a polarity to these cells, where the CD8+ region of the effector cell appeared to contact the target.

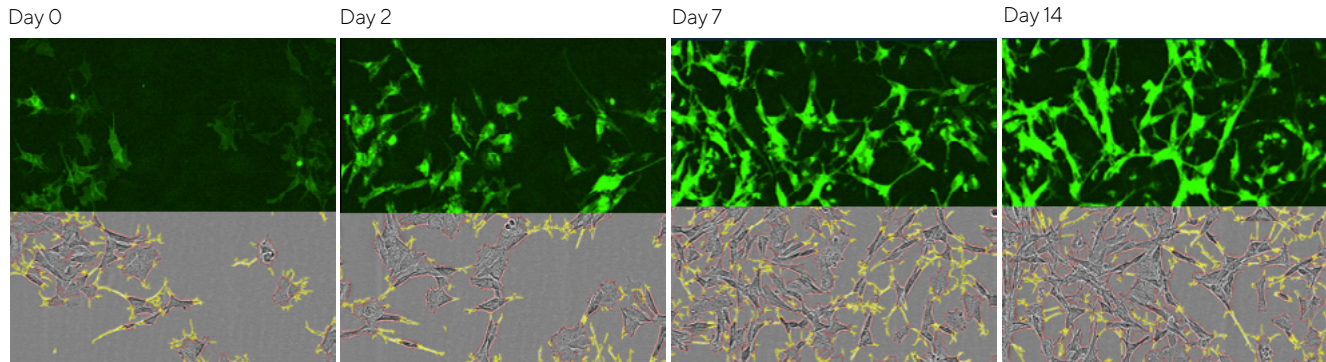
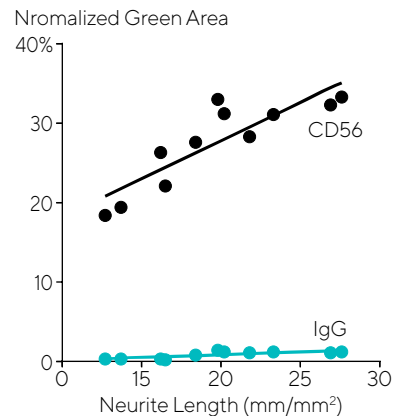
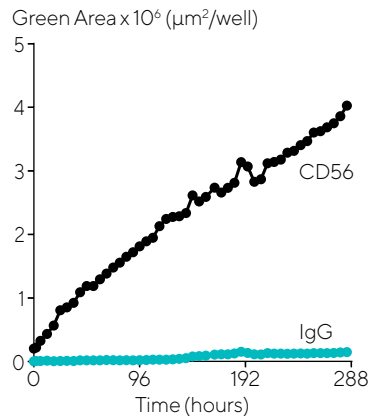


Figure 3. Dynamics of neurite outgrowth and CD56 expression in atRA-differentiated SH-SY-5Y cells. Cells were incubated with FabFluor-488 Dye conjugated anti-CD56 and treated with atRA (50 μ M) at t=0. Blended images show green fluorescence (CD56) and phase morphology. Neurites are masked in yellow (Incucyte[®] Neurotrack Analysis Software Module). The time-course of upregulation of CD56 (mean values \pm SEM, 4 wells) and the relationship between CD56 and neurite outgrowth (normalized to confluence) are shown in panels A and B, respectively. In panel B, each symbol represents data taken at different time-points throughout the experiment. Note the time-dependent increase in Neurite Length and associated CD56 signal (Green Area).



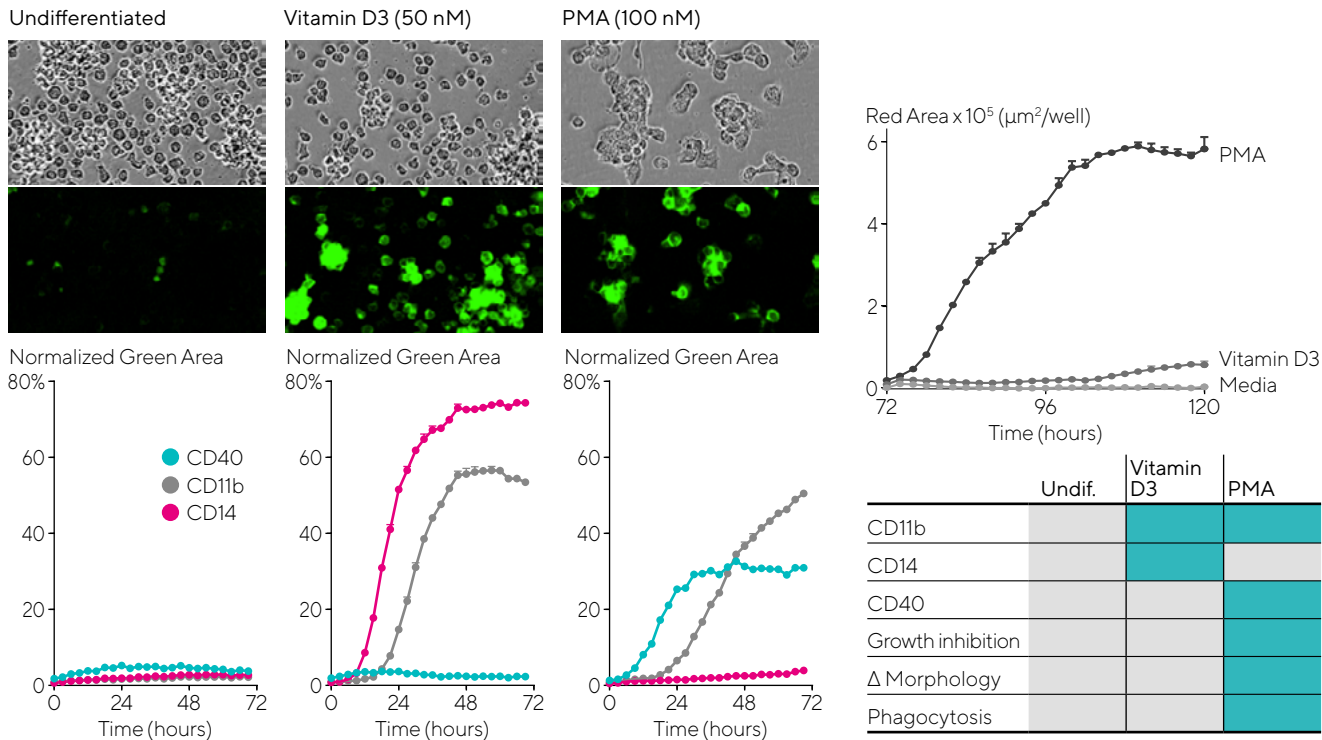
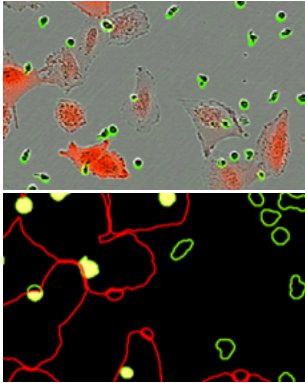
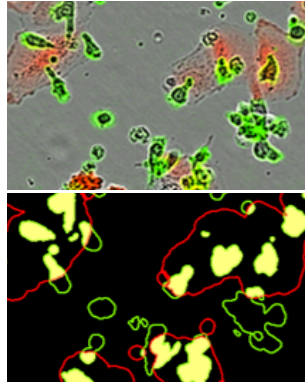


Figure 4. Differentiation of hTHP-1 monocytes: surface marker and functional changes. hTHP-1 cells were exposed to media (undifferentiated), vitamin D3 (50 nM) or PMA (100 nM) in the presence of Incucyte® Fabfluor-488 Dye complexed to CD11b, CD14 or CD40 Abs (+ Incucyte® Opti-Green). Incucyte® images (Top, 20x, every 3h) were analyzed for marker expression (green fluorescent area), normalized for confluency (Center: mean ± SEM, 4 wells). In the lower panel the phagocytic effects were determined by exposing the cells to pHrodo® labeled apoptotic Jurkat cells (1x10⁶ per well) at 72 hours, and measuring red fluorescence. Note the association of the CD40 marker expression with the functional profiles (orange = +ve).

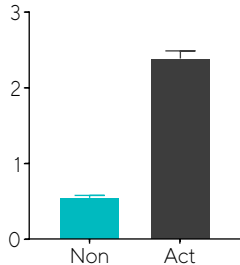
CD45
Non-activated PBMC



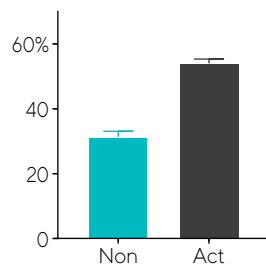
CD45
Activated PBMC



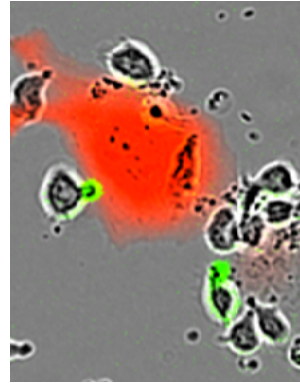
Overlay Area $\times 10^6$ ($\mu\text{m}^2/\text{well}$)



Normalized Overlay Area



CD8



Normalized Overlay Area

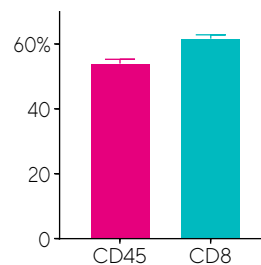


Figure 5: Visualization and quantification of cell-cell interactions. CytoLight Red A549 tumor cells were mixed with either pre-activated (anti-CD3/IL-2) or non-activated PBMC's in the presence of Incucyte® Fabfluor-488- α -CD45 (upper) or CD8 (lower panel). The masked image (center) illustrates the overlay (yellow) of the immune cells (green) and tumor cells (red). The overlay area metric shows the increase in interaction between the two cell types upon activation, either without (upper) or with (middle) normalization to the green area. For CD8, note the clear polarity of the protein signal in the lymphocyte, and formation of the CD8/immune cell 'synapse'.

Conclusions

Incucyte® Live-Cell Immunocytochemistry Assay demonstrates how traditional ICC can be extended from a traditional 'fix and stain' approach to a method that allows for the dynamic monitoring of surface proteins in living cells over several days. Using a simple and robust labeling approach, Incucyte® Fabfluor-488 Antibody Labeling Dyes in conjunction with the Incucyte® Live-Cell Analysis System, enables real-time quantification of dynamic changes in protein abundance and distribution with the ability to associate changes in cell morphology, function as well as study complex cell interactions.

- Live-cell ICC can reveal time- and concentration-dependent changes in cell surface, and can be combined with analyses of other morphological and phenotypic parameters to link surface protein expression changes with cell function over time proteins.

- By labeling different cell surface markers with Incucyte® Fabfluor-488 reagent it becomes possible to track the movement and interaction of subsets of living cells, revealing the dynamics of their interactions.
- Proximity relationships, such as those between the tumor and immune cells presented here, can be observed and quantified at throughput with unprecedented accessibility.
- Incucyte® Fabfluor-488 Antibody Labeling Dye is specific, stable under physiological conditions for long incubations, and allows image analysis without disturbing the biology, health or proliferation of cells.
- The reagent has been used successfully with a range of antibodies in a variety of cells displaying surface proteins –

including immune cells, nerve cells and tumor cells.

- The reagent removes the need for researchers to source antibodies with appropriate fluorescent tags for their molecule of interest.
- The Incucyte® Live-Cell Immunocytochemistry Assay saves time – assay leverages automated acquisition and analysis of data and can be carried out simultaneously in up to six 384-well plates, without laborious fixation and washing protocols.

Chapter 8

Kinetic Assays for Utilizing Complex Models

Live-Cell Microplate Assays for Studying Growth and Health of Three-Dimensional Cultures

It is well established that conventional monolayer cultures of tumor cells grown on plastic do not adequately reflect the *in vivo* situation.^{1,2} Yet, *in vitro* culture models of cancer cells are still an integral component of clinical drug development and for the advancement of our understanding of cancer cell biology. 3D cell culture models, although still relatively new compared to traditional 2D monolayer cultures, are increasingly adopted as advanced tools to accelerate drug discovery efforts.³ This shift is most notable in cancer biology, immuno-oncology and hepatotoxicity, where organoids and 3D microtissues can represent more relevant biological features such as hypoxic regions or tumor-immune cell interactions.^{4,5} There are a multitude of approaches to generating these models and they can generally be described as scaffold-free (media-based) or scaffold-based.

Scaffold-free models are easily achieved

using round-bottom ultra-low attachment (ULA) microplates to promote spheroid self-assembly. These models generally yield a single tumor spheroid per well and exhibit key features of solid tumors; larger spheroids consisting of proliferating, quiescent, and necrotic zones resulting from a radial gradient of nutrients, metabolites and oxygen.

Current scaffold-based models rely primarily on an extracellular matrix (ECM) such as Matrigel® or collagen and attempt to recapitulate both physical and biochemical characteristics of the tumor microenvironment. Generally, these models employ the use of flat bottom plates and result in multiple tumor spheroids per well.

Choosing a model depends on the scientific question or objective at hand. Single spheroid models may be more

representative of large solid tumors and can be made with high reproducibility which is desirable for drug testing. Multi-spheroid models capture the inherent heterogeneity of tumor cells and are considered by many to be more physiologically relevant.

Employing these complex models is challenging due to inherent limitations for studying cell growth, kinetics, and other characteristics in this 3D setting. These include time-consuming, expensive or laborious workflows, labeling requirements that can affect cell biology, and single time-point or indirect read-outs that do not report the full experimental time-course and potentially miss valuable information about size or growth, or shifts in the characteristics of cell populations.

The Incucyte® Live-Cell Analysis System, for both scaffold-free and scaffold-

based 3D spheroid models, avoids such limitations by providing simple, cost-conscious protocols that result in 3D cultures amenable to imaging, employing either label-free techniques or use non-perturbing reagents, and enabling real-time monitoring of morphological and cell health measurements without removing precious samples from the incubator. The approach works both with single spheroids grown in round-bottomed ULA wells in 96- and 384-well formats, and multi-spheroid cultures grown on plates coated with Matrigel® to reproduce the ECM scaffold.

Incucyte® Live-Cell Imaging and Analysis has many advantages over traditional cell analysis methods (summarized in Table 1). In the following chapter, the assays are described in detail, demonstrating their potential as a valuable tool for insightful scientific discovery and drug screening and development.

Table 1. Shortcomings of Traditional Assays vs Live-Cell Imaging and Analysis Approaches.

Shortcomings of Traditional Assays	Live-Cell Imaging and Analysis Approaches
<ul style="list-style-type: none"> ▪ Endpoint collection of data misses important information between imaging intervals that is needed for complete insight into biological processes. 	<ul style="list-style-type: none"> ▪ Continuous long term monitoring captures important kinetic information on cellular processes and morphology, providing for additional mechanistic details.
<ul style="list-style-type: none"> ▪ Repeated removal of cells from incubator for lengthy image acquisition results in loss of control for O₂ and CO₂ and multiple environmental fluctuations. 	<ul style="list-style-type: none"> ▪ Uninterrupted environmental control within incubator, coupled with automated image acquisition (DF Brightfield, HD Phase, and fluorescent) results in a continuous physiologically-relevant environment.
<ul style="list-style-type: none"> ▪ Incorporation of labels that can perturb cells and may confound interpretation. 	<ul style="list-style-type: none"> ▪ Label-free analysis of growth and shrinkage.
<ul style="list-style-type: none"> ▪ Additional time required for development and optimization of image acquisition parameters. 	<ul style="list-style-type: none"> ▪ Non-perturbing, optimized, validated cell health reagents for enhanced physiological relevance.
<ul style="list-style-type: none"> ▪ Complex image processing requires expert operation and training for data generation and analysis. 	<ul style="list-style-type: none"> ▪ Automated acquisition and analysis of high quality, high contrast images, combined with lab-tested protocols, to quickly gather reproducible, quantitative data for pharmacological screening in 96 and 384-well formats.
	<ul style="list-style-type: none"> ▪ Purpose built software tools and guided interface enables non-expert operators to perform image processing and generate publication-ready graphics.

How Live-Cell Spheroid Assays Work

Multi-spheroid Assay

Scaffold-based, multi-spheroid assay allows for the study of cell cultures in a more physiologically relevant, 3D format. This assay permits the tracking and quantification of spheroid formation, cell-cell, and cell-ECM interactions in real time inside a tissue culture incubator. The assay is characteristic of multi-tumor spheroids that form and grow by natural aggregation and is well suited for use with patient specific samples.

Single Spheroid Assay

This assay provides an integrated solution to automatically track and quantify single tumor spheroid formation, growth, and health in real time with minimal environmental disturbance inside a tissue culture incubator, providing

additional physiological insights. This model is designed to model larger solid tumors using tumor cell lines, allowing for the formation of uniform, size-controlled spheroids and the creation of proliferating, quiescent and necrotic cells with exposure to a nutrient gradient. The assay is also designed to closely control and standardize spheroid size across wells and assays for compatibility with drug discovery screening paradigms.

Single Spheroid Invasion Assay

This assay combines an optimized single tumor invasion protocol along with proprietary image and acquisition and analysis, to mimic and quantify metastatic potential over time. The assay builds on the single spheroid assay by embedding spheroids in an extracellular matrix, providing the supportive scaffold for non-adherent growth and invasion from the spheroid body allowing evaluation of metastasis progress in real time.

References

1. Antoni D, Burckel H, Josset E, and Noel G. **Three-dimensional cell culture: a breakthrough in vivo.** *Int J Mol Sci.* Mar 11; 16(3); 5517-27 (2015).
2. Cui X, Hartanto Y, and Zhang H. **Advances in multicellular spheroids formation.** *J R Soc Interface.* Feb; 14(127) (2017).
3. Fang Y and Eglen RM. **Three-Dimensional Cell Cultures in Drug Discovery and Development.** *SLAS Discov.* Jun; 22(5); 456-472 (2017).
4. Costa EC *et al.* **3D tumor spheroids: an overview on the tools and techniques used for their analysis.** *Biotechnol Adv. Dec; 34(8);1427-1441* (2016).
5. Zanon M. *et al.* **3D tumor spheroid models for in vitro therapeutic screening: a systematic approach to enhance the biological relevance of data obtained.** *Sci Rep.* Jan 11;6:19103 (2016).

Incucyte® User Publications

3D Killing Assays

1. Catchpole I, *et al.* **Engineering T-cells for adoptive cell therapy to overcome TGF- β -mediated immunosuppression in the tumour microenvironment.** *Annals of Oncology; 28 (S11)* mdx711.081, 100P (2018).

Invading Cells from 3D Spheroid

2. Fujita, M, Imadome, K, and Imai, T. **Metabolic characterization of invaded cells of the pancreatic cancer cell line, PANC-1.** *Cancer Sci.*, 2017, 108(5); 961-971 (2018).

Tumorsphere Growth Kinetics and Cell Number

3. Cazet AS, *et al.* **Targeting stromal remodeling and cancer stem cell plasticity to overcome chemoresistance in triple negative breast cancer.** Pre-print under review Cold Spring Harbor Laboratory, *bioRxiv* preprint (2018)
URL: <https://www.biorxiv.org/content/10.1101/215954v1>
4. Galbraith MD, *et al.* **CDK8 Kinase Activity Promotes Glycolysis.** *Cell Rep, Cell Rep*, 21(6); 1495-1506, (2018)
5. Cesi G, *et al.* **ROS production induced by BRAF inhibitor treatment rewires metabolic processes affecting cell growth of melanoma cells.** *Cancer, Mol. Cancer* 16(1); 102, 42894 (2018).

Mammosphere Growth

6. Fetting LM *et al.* **Cross talk between progesterone receptors and retinoic acid receptors in regulation of cytokeratin 5-positive breast cancer cells.** *Oncogene*, 36(44);6074-6084 (2018).

Neurosphere Growth Kinetics

7. Griesinger AM *et al.* **Neuro NF- κ B upregulation through epigenetic silencing of LDOC1 drives tumor biology and specific immunophenotype in Group A ependymoma.** *Neuro-Oncology*, Volume 19, Issue 10, 1 October; 1350-1360 (2017).

8a

Kinetic Multi-Spheroid Assays

Integrated Turnkey Solution for Reproducible Analysis of Multi-Spheroid Cultures

Introduction

The use of multi-cell tumor spheroids as a model for oncology research has expanded rapidly in recent years. As 3D spheroid protocols become more accessible to researchers, the experimental models have become more complex with correspondingly greater translational potential.

Multi-spheroid models have a number of advantages over conventional cell culture. In 2D cell culture, tumor cells are grown in monolayers under conditions that are quite different from the physiological conditions of a tumor. They are grown on a rigid, non-biological surfaces, have an abundance of oxygen, and an excess of nutrients produces hyper-nourished cells with unrestricted and non-physiological proliferation characteristics. Using such cells for drug screening introduces

unwanted bias, with a tendency to identify molecules that work only against a uniform population of proliferative cells, and overestimating efficacy.

A more realistic approach involves recreating more physiologic heterogeneity inherent to a 3D tumor structure and providing a microenvironment more closely recapitulating *in vivo* conditions, which includes key interactions between the tumor and the extracellular matrix (ECM).

Scaffold-based 3D spheroid models, in which tumor cell aggregates are grown in ECM scaffolds such as Matrigel®, more closely recapitulate physiological growth conditions of tumors, enabling the study of interactions between tumor cells and the microenvironment. Tumor cells grown in 3D scaffold-based culture can form cell-cell and cell-matrix interactions. The heterogeneous nature of the tumor

microenvironment can also be studied through the use of co-culture models, such as tumor cells with fibroblasts or immune populations.

This chapter illustrates how Incucyte's multi-spheroid assays can provide a rapid method for the pharmacological investigation of potential drug candidates. The approach allows the measurement of real-time viability and toxicity measurements in a meaningful, multicellular *in vitro* model that better reflects the heterogeneous nature of tumors and allows deeper study of their potential physiological interactions with the tumor microenvironment.

Incucyte® Multi-Spheroid Assays at a Glance

The Incucyte® Multi-Spheroid Assays combine the Incucyte® proprietary depth of focus brightfield (DF Brightfield) image acquisition mode with a 3D multi-spheroid model grown on a layer of extracellular matrix in a 96-well format. Multiple protocols have been developed to suit various experimental objectives and cost considerations.

After coating either flat-bottom or round-bottom culture plates¹ with Matrigel®, cells are added to the wells with or without Incucyte® Cell Health Reagents. An optional layer of Matrigel can be added to “sandwich” the cultures and surround them with ECM. The cells are then automatically scanned in the Incucyte® Live-Cell Analysis System every six hours to monitor multi-spheroid formation.

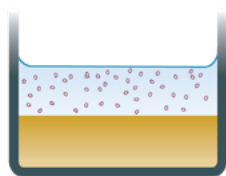
After treatments are added, the spheroid growth and shrinkage assay is initiated and monitored by repeat scanning every six hours in the Incucyte® Live-Cell Analysis System for up to two weeks. Spheroid size is reported based on DF Brightfield image analysis and can be accessed in real time or on demand as needed. The simple protocol is shown below:

1 Coat Plate (Day 0)



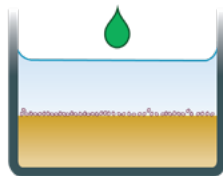
Coat plate (50% Matrigel, 40 μ l/well). Polymerize at 37°C for 30 minutes.

2 Add Cells (Day 0)



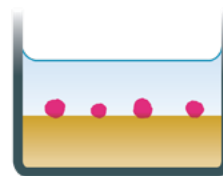
Add cells in media (100 or 150 μ l/well) with or without cell health reagent, respectively.

3 Add Reagent (Day 0, optional)



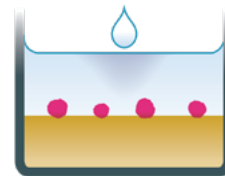
Add cell health reagent (50 μ l/well) at 3x final assay concentration.

4 Monitor Formation (Day 0–3)



Place inside the Incucyte and scan every six hours to monitor multi-spheroid formation.

5 Add Treatments (Day 3)



Add treatments and continue to monitor growth in the Incucyte® Live-Cell Analysis System.

Figure 1. Overview of workflow for generation and analysis of multi-spheroid cultures in an Incucyte® Live-Cell Analysis System.

1. Protocols have been developed using either 96-well flat bottom or round bottom plates to address cost concerns when utilizing Matrigel. Round bottom plate protocols use four times less Matrigel than flat bottom plate protocols.

Key Advantages

- Quantify label-free growth and investigate morphology of multiple spheroids grown on ECM inside a standard tissue culture incubator, ensuring improved physiological relevance.
- Multiplex kinetic viability and toxicity measurements using non-perturbing Incucyte® Cell Health Reagents to investigate drug mechanisms of action.
- Generate reproducible data suitable for pharmacological analysis with lab-tested and cost-conscious protocols, high quality images, and unbiased analysis.
- Rapidly create concentration response curves from thousands of images generated in 96-well plates.

Figure 2. The Incucyte® proprietary image acquisition technique, DF Brightfield for 3D Cultures, generates high contrast, extended depth of focus images when used in conjunction with the Incucyte® Multi-Spheroid Assay. Subsequent segmentation and analysis with Incucyte® image processing algorithms results in reproducible data without operator bias.

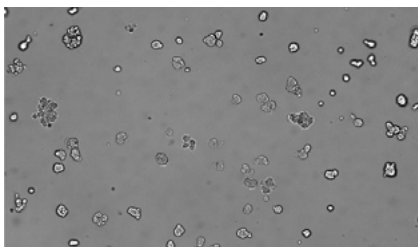
Application of Incucyte® Multi-Spheroid Live-Cell Assays

Combining the Incucyte® DF Brightfield image acquisition with a 3D multi-spheroid cell model on ECM allows for monitoring and quantification of changes over time and under more physiological relevant conditions. As the spheroids remain undisturbed within the incubator while images are taken, it is possible to visualize and quantify spheroid growth, measure cell health, and better understand mechanisms of drug action.

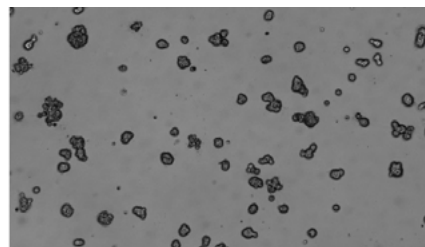
Label-Free Image Acquisition Using Novel DF Brightfield Reveals Morphology and Enables Quantification of Spheroid Growth Over Time

Introduction of a new, enhanced depth of focus brightfield (DF Brightfield) image acquisition enables imaging of multiple tumor spheroids on a layer of extracellular matrix (Figure 2). This enhanced image acquisition results in high contrast brightfield images that can be reliably segmented and analyzed using Incucyte® purpose-built processing algorithms.

Traditional Brightfield



DF Brightfield



The novel DF Brightfield image capture provides high-quality images of multi-spheroids formed from a range of tumor cells (Figure 3). Within just three days, different tumor cell lines begin to show distinctive morphology, demonstrating the physiological relevance of the models.

The Incucyte® Spheroid Analysis Software Module enables label-free, kinetic quantification of growing and shrinking multi-spheroids over time. Figure 4 illustrates the growth curves of three multi-spheroid tumor models over several days and demonstrates the

inhibitory effects of the cytotoxic drug camptothecin (CMP) on their growth trajectories.

Segmented DF Brightfield images compare vehicle and CMP treated conditions at 168 h. Time courses show the individual well total Brightfield Object area (μm^2) (y-axis) over 168 h and illustrate specific cell type-dependent kinetic profile of spheroid growth and shrinkage. Data were collected over 168 hour period at 6 hour intervals. All images captured at 10x magnification. Each data point represents mean \pm SEM, n=6 wells.

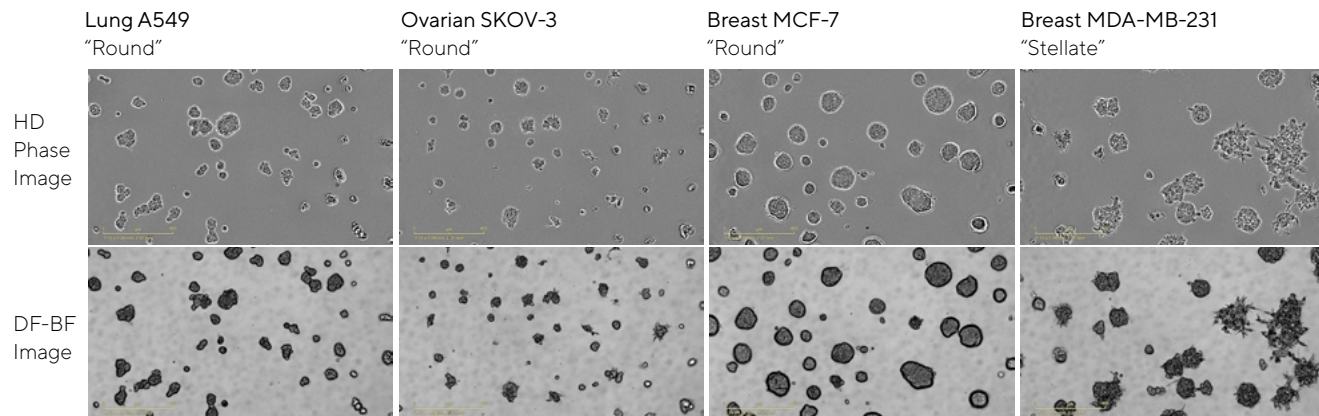


Figure 3. High quality HD Phase and DF Brightfield (DF BF) images of multi-spheroids formed from a range of tumor cell lines (5 d post seeding) on a Matrigel® base. Three day post seeding, A549, SKOV-3 and MCF-7 cells formed round aggregates, while MDA-MB-231 multi-spheroids exhibited stellate branching distinctive of an invasive morphology.

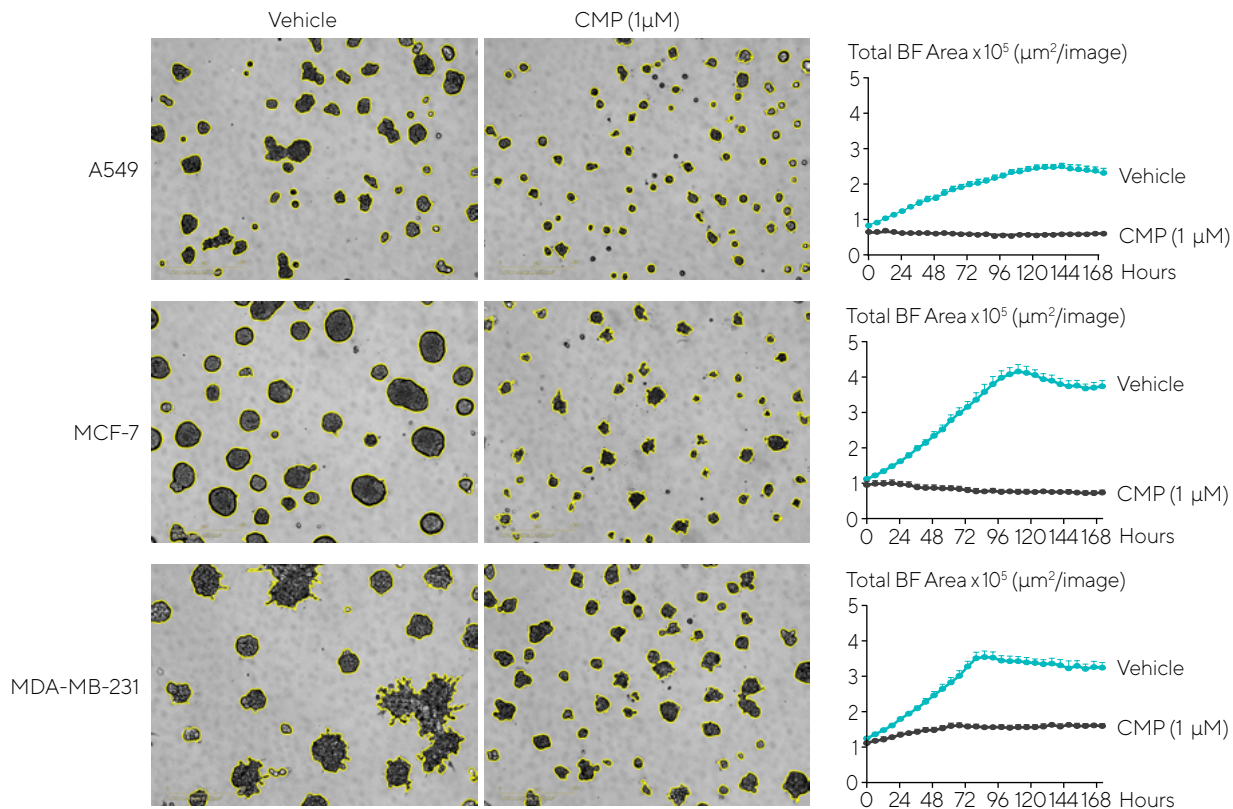


Figure 4. Real-time quantification of the growth of A549, MCF-7 and MDA-MB-231 spheroids. Cells were seeded in flat-bottom 96-well plates (2,000 cells per well) on a bed of Matrigel® and spheroids allowed to form (72 h). Spheroids were treated with either vehicle (0.1% DMSO) or CMP (10 μ M).

Fluorescent Readouts of Stably Expressing Nuclear Restricted Fluorescent Protein Act as a Surrogate for Cell Viability

When a range of antibodies were tested against different cell surface markers in various lymphocyte cell lines (Figure 4) it was found that the internalization patterns

corresponded with the known surface marker expression of these cells. Labeling antibodies with Incucyte® Fabfluor-pH Red Antibody Labeling Dye showed that anti-CD20 was internalized in a B cell line, but not a T cell line, whereas anti-CD3 was internalized in T cells and not B cells. Antibodies to CD71 and CD45, which

are general lymphocyte markers, were internalized in both cell types. Crucially, the non-specific mouse IgG was not internalized in any of the cell lines. These data demonstrate the broad application and specificity across different cell types and molecules.

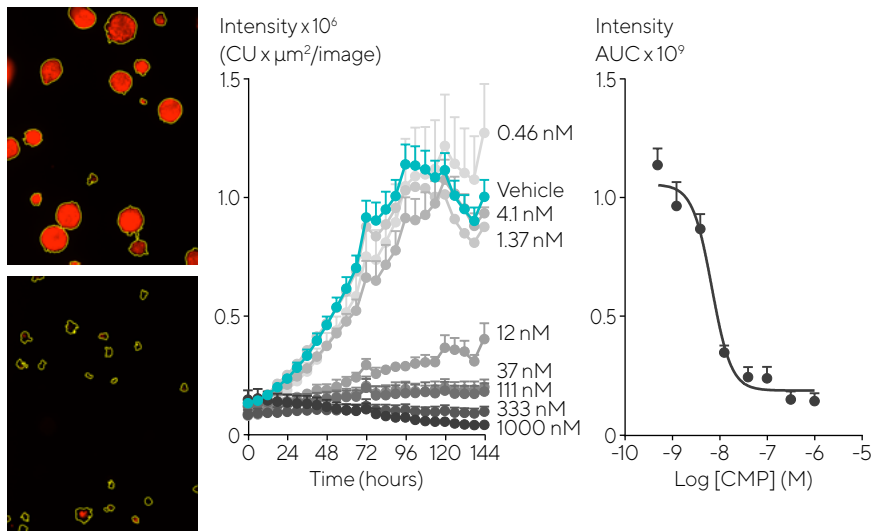
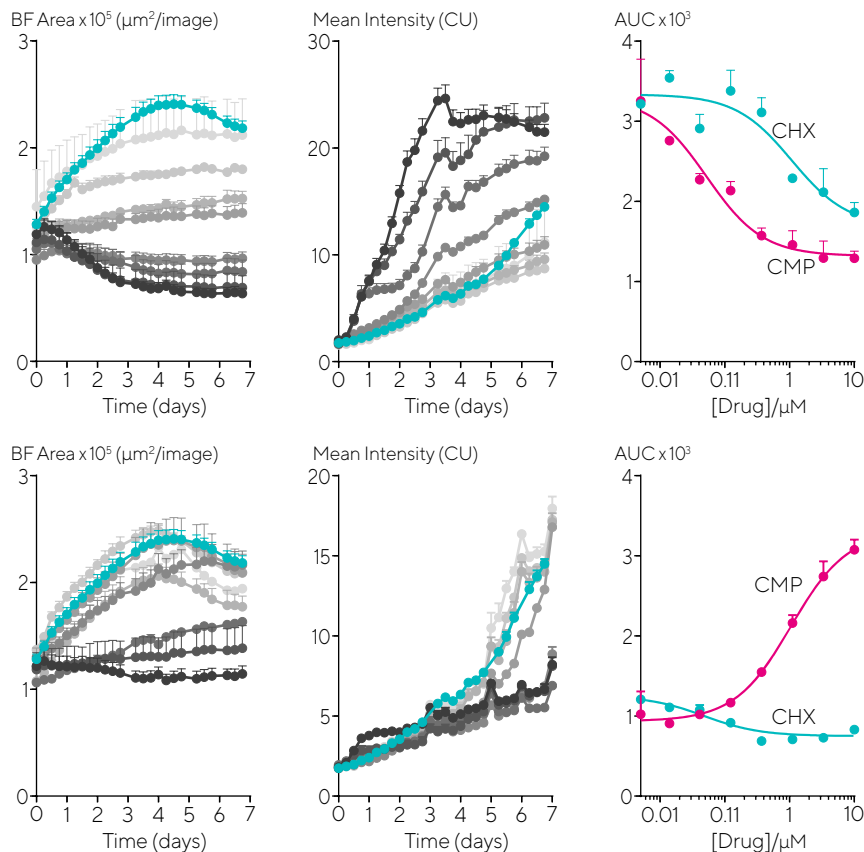


Figure 5. Analysis of spheroids expressing Incucyte® Nuclight Red Lentivirus enables determination of spheroid viability. Representative images taken at 144 h show a strong red fluorescent signal in a vehicle control spheroid, in contrast to a marked loss of red fluorescence in the CMP treated spheroid. The yellow boundary in the images represents the DF Brightfield mask outline. Monitoring the integrated intensity from within the DF Brightfield boundary highlights increasing fluorescence under vehicle control conditions corresponding to the growth of the spheroid. Upon treatment with CMP (0.4 nM - 1 μM), a concentration-dependent reduction in integrated fluorescence is observed, with complete loss of fluorescence at the highest concentration tested after 144 h.

Multiplexed Viability and Toxicity Measurements Enable Investigation of Mechanisms of Action

In addition to screening for cytotoxicity, live-cell multi-spheroid assays can be used in conjunction with Incucyte® Cell Health Reagents to determine the mechanism of action of drugs by combining data on size with levels of cytotoxicity and apoptosis (Figure 6). The power of the assay is illustrated, distinguishing the cytotoxic effects of CMP from that of cycloheximide (CHX). The ability to multiplex reagents with fluorescent-expressing cell lines provides a depth of information on drug mechanism of action under realistic physiological conditions.

Figure 6. Cytotoxic and cytostatic mechanisms of action can be differentiated by measuring spheroid size and apoptosis. A549 cells were plated at a density of 2,000 cells per well and spheroid allowed to form (96 h). Spheroids were treated with increasing concentrations of CMP (top row, 4 nM – 10 μ M) or CHX (bottom row, 4 nM – 10 μ M) in the presence of Incucyte® Annexin V Green Dye (1%). Images were taken every 6 h for 10 d. Time courses show change in size (Brightfield area) or apoptosis (Incucyte® Annexin V Green fluorescence intensity) over time. Concentration response curves show the different profiles of cytotoxic and cytostatic mechanisms.



By enabling long term, continuous live-cell analysis under uninterrupted incubation, the Incucyte® Multi-Spheroid Assay makes it possible to derive meaningful EC_{50} values for drugs by deriving concentration response curves over several days without disturbing cell biology. In Figure 7, this is demonstrated for CMP and CHX, and this approach is used to further validate drug mechanism of action observed through earlier analysis.

Reproducible, Quantitative Data at Throughput Suitable for Pharmacological Testing

A pharmacological study performed in MCF-7 breast cancer cells illustrates the potential of the Incucyte® Multi-Spheroid Assay for drug toxicity testing (Figure 8). The ability to view spheroids in 96-well plates over time provides a rapid method for comparing the potencies and toxicities of different compounds within the same assay.

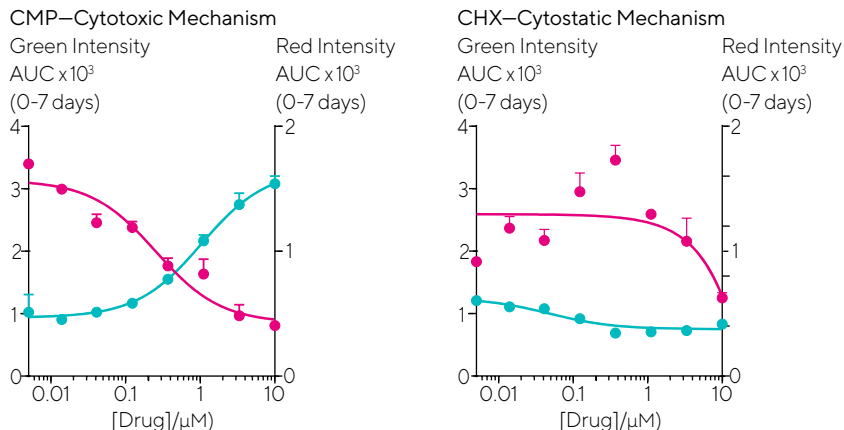


Figure 7. Determination of EC_{50} values of CMP and CHX using the Incucyte® Live-Cell Analysis System to confirm mechanisms of action in response to cytotoxic (CMP) and cytostatic (CHX) drugs. Incucyte® Nuclight Red A549 Cells (2k/well) were seeded in the presence of Incucyte® Annexin V Green Dye (1%, apoptosis marker) and spheroids allowed to form for 3 days. Spheroids were then treated with a concentration range of either CMP, CHX, or vehicle control, and the cells were imaged every 6 hours for 7 days. Both CMP (cytotoxic) and CHX (cytostatic) drugs caused a concentration-dependent inhibition of spheroid growth (total BF time courses, not shown). The CMP EC_{50} , calculated using AUC from 0-7 days after treatment, showed a concentration-dependent loss of viability and increase in apoptosis, while CHX EC_{50} values showed little change in viability and no increase in apoptosis.

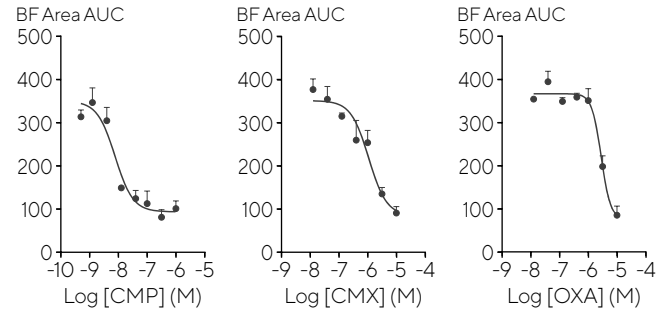
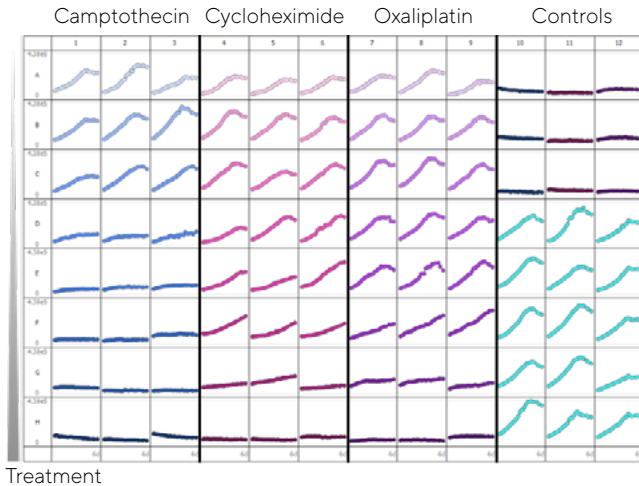


Figure 8. Effect of CMP, cisplatin (CIS) and oxaliplatin (OXA) on growth of MCF-7 cells in a 3D spheroid assay. MCF-7 cells were plated at a density of 1,000 cells per well and spheroids allowed to form (72 hours). Cells were then treated with serial dilutions of compounds and the kinetics of spheroid growth were obtained. Plate view shows the individual well Total Brightfield Area (μm^2) over time. Concentration response curves represent the area under curve of the Total Brightfield Area time course (μm^2) from 0 - 168 h post-treatment. Data were collected over 168 h period at 6 h intervals. Each data point represents mean \pm SEM, n=3 wells.

Conclusions

The use of multi-spheroid assays as model systems for the evaluation of new treatments and study of disease has expanded in recent years. However, despite their ability to measure indicators of cell health, such as cytotoxicity and apoptosis, common assays rely on indirect, end-point measurements that are subject to artefacts and cannot be readily verified by morphological changes. The Incucyte® Multi-Spheroid Assay is a rapid method for the pharmacological investigation of potential drugs in a meaningful multicellular model, which allows researchers to:

- Study spheroid morphology, growth and shrinkage using a label-free, scaffold-based, kinetic 96-well plate assay without removing cultures from the incubator and without need for a predefined endpoint selection.
- Link morphology, growth, and toxicity via direct, kinetic measurements by combining novel DF Brightfield image acquisition and analysis with Incucyte® Cell Health Reagents.
- Investigate mechanisms of action with multiplexed viability and toxicity measurements using non-perturbing reagents and cell lines that stably express fluorescent proteins.
- Produce reproducible well-to-well kinetic data in live spheroid cultures, in response to different compounds and conditions, using lab-tested protocols, high quality images, and unbiased analysis.
- Carry out automated analysis of multiple conditions or variables under more physiologically relevant conditions, minimizing interference with cell biology.

8b

Kinetic Single Spheroid Assays

Reproducible Quantitative Analysis of Single Spheroid Growth and Health Over Time

Introduction

Single spheroids exhibit several physiological traits including relevant morphology, increased cell survival, and a hypoxic core that make them ideally suited to the study of larger solid tumors.

These scaffold-free (media-based) models are easily achieved using round-bottom ultra-low attachment (ULA) microplates to promote spheroid self-assembly. They generally yield a single tumor spheroid per well. By virtue of their size, they exhibit the key features of solid tumors: they are comprised of proliferating and quiescent cells, and contain necrotic zones resulting from a gradient of nutrients, metabolites and oxygen that recapitulates the authentic heterogeneity within a tumor.

Single spheroids formed in ultra-low attachment (ULA) plates also avoid the use of complex and poorly characterized

biomatrices, and are ideal for studies that require high levels of well-to-well consistency.

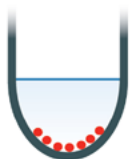
A growing body of evidence suggests that more relevant and translational observations can be made in 3D multi-cell tumor models compared to 2D monolayer models. Most currently available 3D techniques for generating and quantifying spheroids are time consuming, laborious, costly and can lack reproducibility.

In this chapter, we describe the validation and application of miniaturized Incucyte® live-cell single tumor spheroids formed in ULA plates and monitored up to two weeks. These assays are flexible, simple to run, and provide automated and direct measures of tumor size and health in real time.

Incucyte® Single Spheroid Assays at a Glance

Cells of interest are harvested, counted, and plated onto ULA round bottom 96- or 384-well plates and then centrifuged. Spheroid formation is monitored every six hours using DF Brightfield and HD phase contrast image acquisition until they reach the desired size. Test compounds are then added, and the spheroid growth and shrinkage assay is initiated. Automated monitoring continues every six hours for up to two weeks, with tumor spheroid size measurements made available in real time. The simple protocol is shown on the next page.

1 Cell Seeding (Day 0)



Seed cells into 96W or 384W Ultra Low Attachment plate. Centrifuge.

2 Spheroid Formation (Day 0–3)



Place inside the Incucyte® Live-Cell Analysis System and scan every six hours.

3 Add Treatments (Day 3)



Add treatments to plate. Monitor spheroid growth and shrinkage.

Key Advantages

- Quantify growth and investigate morphology of single spheroids grown in ultra-low attachment (ULA) round bottom plates without the need of labels, and leaving cells undisturbed inside a standard tissue culture incubator.
- Investigate mechanisms of action or immune modulation with kinetic viability and toxicity measurements using non-perturbing reagents.
- Lab-tested protocols, high quality images, and unbiased analysis delivers robust data suitable for pharmacological analysis.
- Automated acquisition and analysis tools enable rapid creation of concentration response curves from thousands of images generated from 96- or 384-well plates.

Figure 1. Overview of workflow for generation and analysis of single spheroid cultures in an Incucyte® Live-Cell Analysis System.

Application of Incucyte® Single Spheroid Live-Cell Assays

Incucyte® DF Brightfield Image Acquisition (described in Incucyte® Multi-Spheroid Assays, Figure 2) enables robust measurement of spheroid size, yielding information on spheroid growth rates and morphology without the need for labels. Following treatment with cytotoxic compounds, a strong brightfield signature is obtained which, when combined with fluorescence analysis using Incucyte® Cell Health Reagents, provides insight into the viability of tumor spheroids in response to different treatments.

Label-Free Monitoring of Spheroid Growth and Morphology Over Time

Figure 2 illustrates how the Incucyte® DF

Brightfield analysis can provide kinetic measurements of single spheroid size over time. The size of tumor spheroids was measured using an automated algorithm that masked the largest Brightfield object in the field of view. Changes in the size of spheroids derived from three types of tumor cell were monitored in response to camptothecin, allowing growth response curves to be generated in the absence and presence of the drug.

Reproducible, Quantitative Data to Conduct Pharmacological Analysis

To demonstrate the pharmacological utility of the single spheroid assay, we performed a comparison of three different drugs using 3D

spheroids derived from the SKOV-3 ovarian cancer line (Figure 3). The data shows a concentration-dependent inhibitory growth effect for all compounds, and illustrates how compound potencies can be directly compared within the same assay.

Miniaturizing the 3D spheroid cultures makes it possible to optimize the assay further by testing different seeding densities for multiple cell types in a single experiment. This is demonstrated below using three cell types plated at four different densities (Figure 4). The data demonstrates the cell area dependence with seeding density and differential growth profile across the cell types.

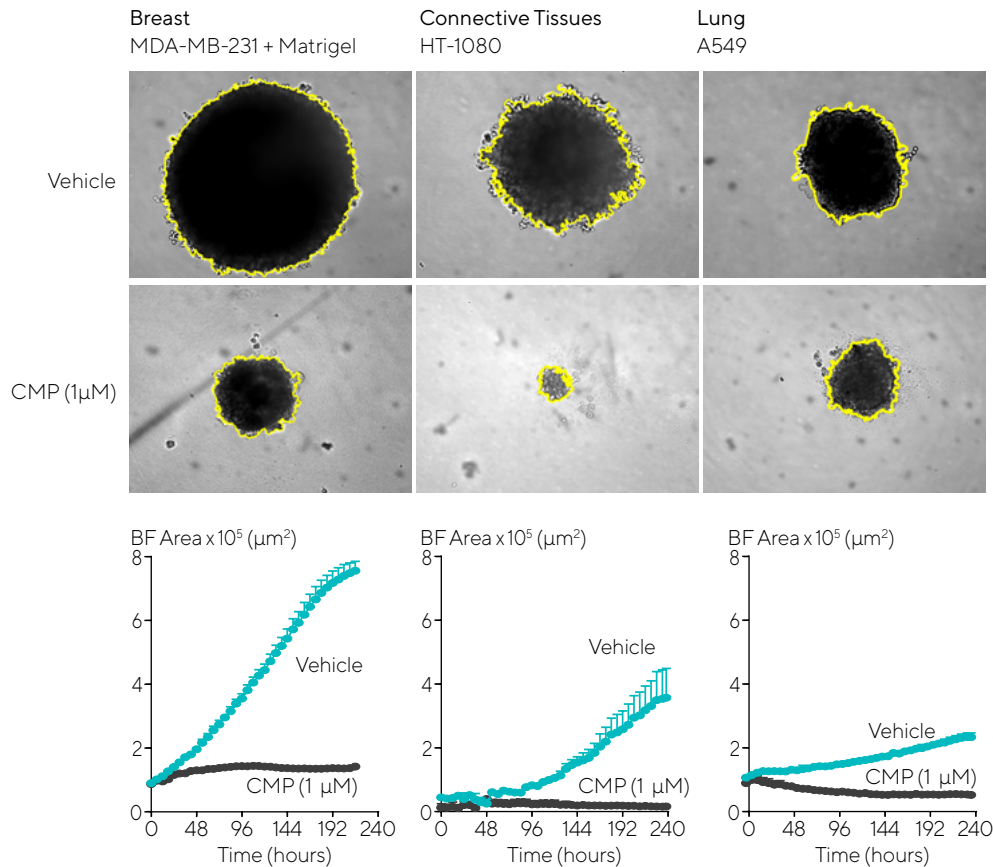


Figure 2. Brightfield analysis enables accurate kinetic quantification of spheroids. The differential pharmacological effect of 1 μ M camptothecin (CMP) on growth of MDA-MB-231, HT-1080 and A549 cells in a 3D spheroid assay. Cells were grown in ULA round-bottom 96-well plates (2,500 cells per well) for 72 h and treatment with \pm 1 μ M CMP followed. Segmented DF Brightfield images compare treated vs. un-treated conditions at 240 hours. Time courses illustrate the specific cell type-dependent kinetic profile of spheroid growth and shrinkage. The graphs display the Largest Brightfield Object Area (μ m²) (y-axis) over the course of a 240-hour assay (x-axis) at 6 hour intervals. All images captured at 10x magnification. Each data point represents mean \pm SEM, n=4.

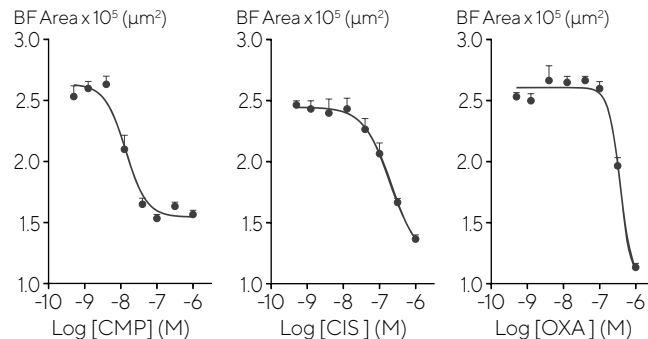
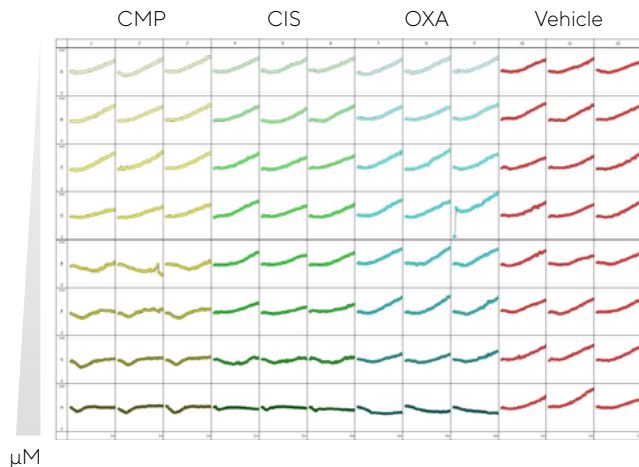


Figure 3. Effect of CMP, cisplatin (CIS) and oxaliplatin (OXA) on growth of SKOV-3 cells in a 3D spheroid assay. SKOV-3 cells were plated at a density of 5,000 cells per well and spheroids were allowed to form (72 h). Cells were then treated with serial compound dilutions and kinetics of spheroid growth and shrinkage were obtained. Plate graph shows the individual well Largest Brightfield Area (μm^2) over time. IC_{50} curves represent the Largest Brightfield area (μm^2) at 204 hour post-treatment. Data were collected over 240 hour period at 6 hour intervals. Each data point represents mean \pm SEM, $n=8$.

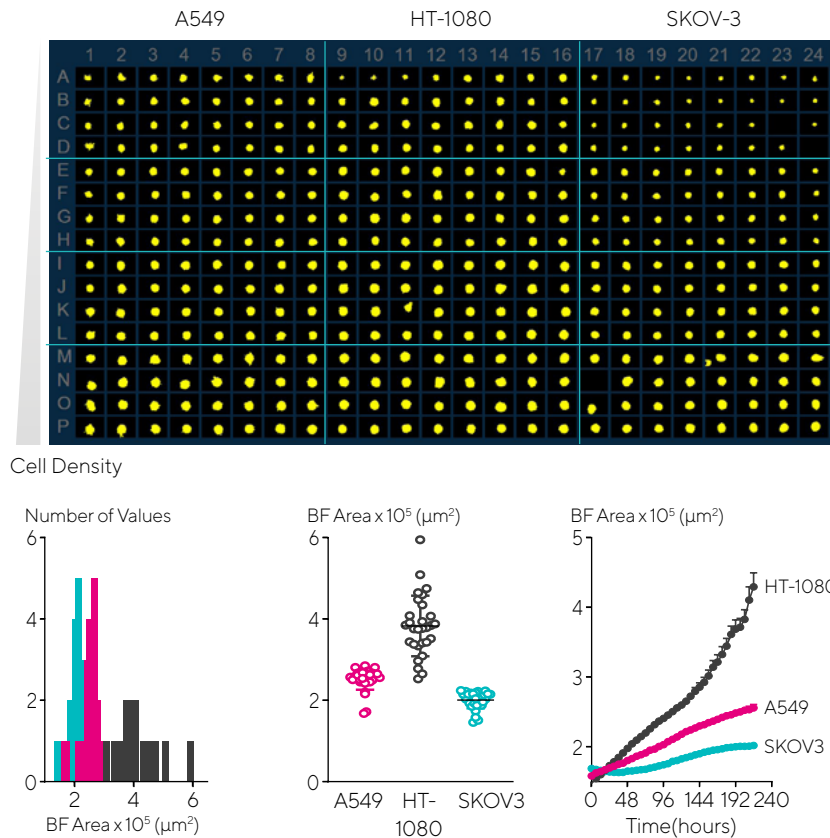


Figure 4. Miniaturizing spheroid growth and shrinkage assay for assay optimization. Comparison of temporal growth profiles of A549, HT-1080 and SKOV-3 cells in a miniaturized 3D spheroid assay. All cells seeded at a density ranging from 310 to 7,500 cells per well plated in a ULA round-bottom 384-well plate. Media was replenished 72 hours post seeding. Microplate overview image shows DF Brightfield segmentation mask at 204 hour post-media replenishment. Histogram compares the distribution frequency of the Brightfield area (μm^2) across all cell types plated at 2,500 cells per well at this time point. Variability plot analysis shows the Largest Brightfield Object Area of individual wells at 204 hours. Time-course plots represent the differential temporal profile of the Largest Brightfield Object Area metric (μm^2) across the cell types. Data were collected over a 204 hour period at 6 hour intervals, all images captured at 10x magnification. Each data point represents mean \pm SEM, n=32.

Viability and Toxicity Measurements Using Non-Perturbing Reagents Enable Investigation of Drug Mechanisms of Action

Masking of the DF Brightfield channel allows measurement of other parameters of interest when non-perturbing reagents

are employed. In Figure 5, the effects of CMP on cell viability were studied by stably expressing a red fluorescent protein (using Incucyte® Nuclight Red Lentivirus) in the spheroids. Applying the 'fluorescence within the Brightfield boundary' feature in

the Incucyte® Spheroid Analysis Software Module negates the need to apply a fluorescence mask, and removes the impact of threshold settings.

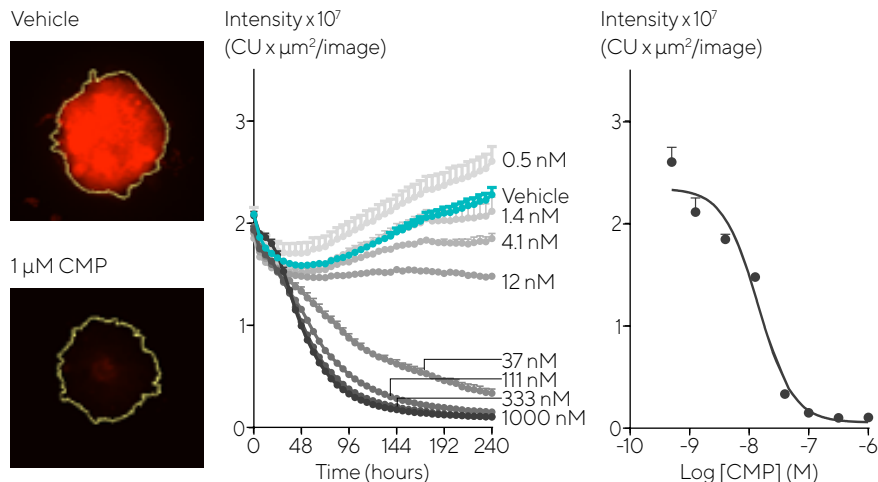


Figure 5. Analysis of spheroids expressing fluorescent proteins enables spheroid viability determination. Representative images taken at 240 hours show a strong red fluorescent signal in a vehicle control spheroid, in contrast to a marked loss in red fluorescence in the CMP-treated spheroid. The yellow boundary in the images represents the Brightfield mask outline. Monitoring the Integrated Fluorescent Intensity from within the Brightfield boundary highlights a gradual increase in fluorescence under vehicle control conditions (red symbols) corresponding to the growth of the spheroid. Upon treatment with CMP, a concentration-dependent reduction in Integrated Fluorescent Intensity is observed, with abolishment of fluorescence with the highest concentration tested after 240 hours.

A similar approach was used with Incucyte® Cell Health Reagents to determine the mechanism of cell death after treatment with CMP (Figure 6). Little or no reduction in spheroid size was observed with the Brightfield images, but fluorescence analysis revealed a concentration-dependent effect with increases in the mean intensity within the

Brightfield boundary, suggesting induction of apoptosis.

Finally, data is presented showing how combining the DF Brightfield and Incucyte® Cell Health Reagents can be used in single spheroids to determine the mechanism of action of compounds (Figure 7). CMP caused a marked increase

in fluorescence intensity, suggesting a cytotoxic mechanism, whereas CHX only caused a notable increase in fluorescence at the highest concentration tested. The clear separation between the size and cytotoxicity readouts supports the known cytostatic mechanism of CHX.

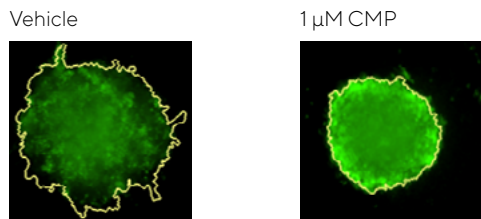


Figure 6. Effect of CMP on A549 cells reported by Incucyte® Annexin V Green Dye in a 3D spheroid assay. A549 cells were seeded at a density of 2,500 cells per well in ULA round bottom plates and spheroids were formed for 96 hours. Spheroids were treated with CMP (0.4 nM - 1 μ M) or vehicle (0.1% DMSO) and apoptosis was reported using Incucyte® Annexin V Green Dye.

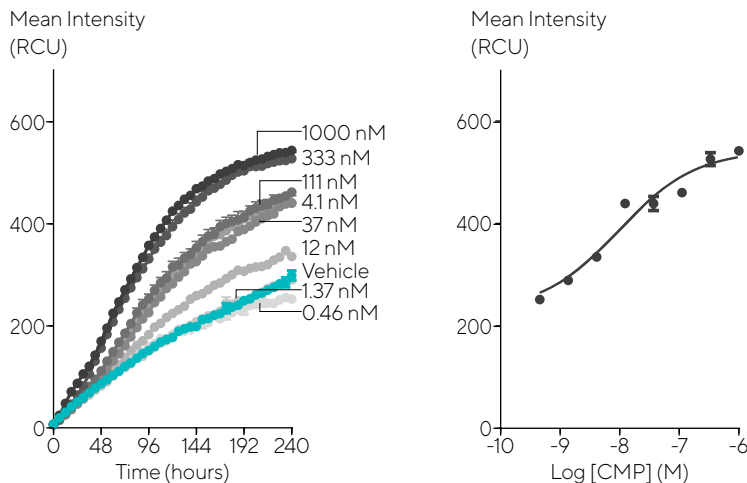
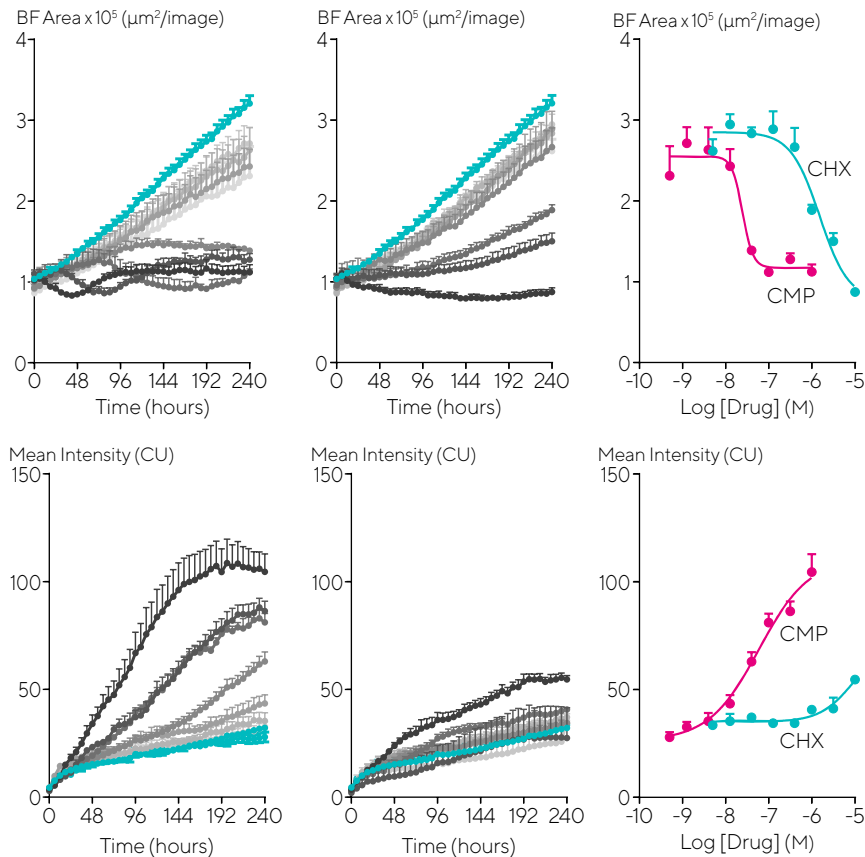


Figure 7. Cytotoxic and cytostatic mechanisms of action can be differentiated by measuring spheroid size and viability. SKOV-3 cells were plated at a density of 2,500 cells per well and spheroid allowed to form (96 hours). Spheroids were treated with increasing concentrations CMP (0.5 nM – 1 μ M, left panels) or CHX (1.4 nM – 10 μ M, middle panels) in the presence of Incucyte® Cytotox Green Dye (25 nM). Images were taken every 6h for 10 days. Time courses show change in Brightfield Area (top row) or Mean Fluorescent Intensity (bottom row) over time. Concentration response curves (right panels) show the different profiles of cytotoxic and cytostatic mechanisms.

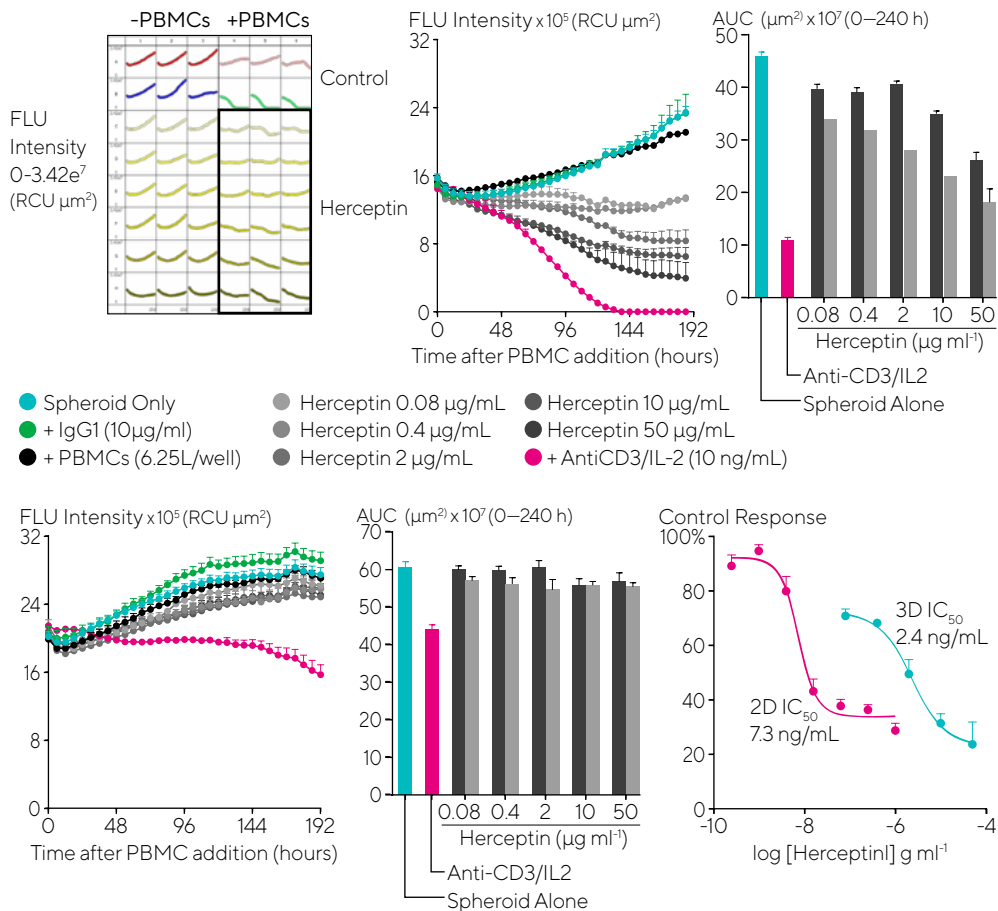




Flexible Assay Format Can Be Adapted for Co-Culture Studies Using Relevant Immune-Oncology Cell Models

In order to further demonstrate the utility of the Incucyte® Single Spheroid Assay as a translational cell-based assay, an immune cell killing model was optimized and employed to assess the efficacy of novel immune modulators. Figure 8 illustrates new insights for greater translational relevance can be gained by utilizing 3D antibody-dependent cell-mediated cytotoxicity (ADCC) spheroid assays, as compared to 2D ADCC assays, for the examination of immune modulators, such as Herceptin. Such models may uncover important information regarding dose response kinetics.

Figure 8. Herceptin-induced ADCC in HER2-positive SKOV-3 cells. HER2-positive SKOV-3 or HER2 negative Nuclight Red A549 spheroids (2.5K/well) were seeded with PBMCs (6.25K/well) and treated with Herceptin (mAb targeting HER2 receptors). Herceptin-induced cytotoxicity was observed and measured in SKOV-3 but not A549 spheroids. A similar assay was conducted in a 2D culture model. SKOV-3 cells (1.6K/well) were seeded overnight prior to the addition of PBMCs (8K/well) and subsequent treatment with Herceptin. SKOV-3 tumor spheroids appear to exhibit ~300-fold lower Herceptin sensitivity in comparison to 2D. Note the apparent 34% inhibition of the 3D spheroid at the lowest test concentration (0.08 $\mu\text{g}/\text{ml}$), suggesting that a biphasic concentration response curve may exist; the outermost cells behave as in the 2D model, whereas the spheroid center has lower sensitivity.



Conclusions

3D micro-tissues and organoids are becoming increasingly popular for their more relevant morphology and cell survival, but current methods for assessing the growth and vitality of these models are limited. Most assays require cell labeling and only provide a single time point readout. By contrast, the Incucyte® Single Spheroid Assay allows:

- Label-free study of spheroid morphology, growth and shrinkage in 96- and 384-well format.
- Generation of kinetic measurements and cell-dependent growth curves for spheroids derived from different types of cells.
- Monitoring of spheroid viability over time and in different treatment conditions using Incucyte® Cell Health Reagents and/or stable expression of fluorescent reporter proteins and the ability to link this to morphological observations.
- Miniaturization of the assay to provide a high-throughput method of producing reproducible, quantitative pharmacological data in physiologically relevant cell models simultaneously for a variety of test compound.
- Flexibility in cell types and co-culture, enabling extension of the assay for study of immune modulators.
- Incucyte® Single Spheroid Assay provides a valuable and timely addition to the toolkit of those working in basic biology, medical research, and pharmacological drug development who seek to better understand cellular responses.

8c

Single Spheroid Invasion Assay

Real Time Quantification of 3D Invasion

Introduction

Cell invasion, a hallmark of malignant cancers, is an essential part of cancer metastasis from the primary site to a secondary location and is responsible for cancer-related deaths^{1,2}.

The ability of tumor cells to form a metastatic tumor involves cellular changes to acquire an invasive phenotype, starting with loss of adhesion and rearrangement of the cytoskeleton to enable movement through the tumor microenvironment, which includes the supportive extracellular matrix (ECM) that must be degraded. In order to accurately study cancer cell metastasis and develop novel cancer therapeutics, accurate models and subsequent analysis must be employed.

Conventional *in vitro* invasion models, such as the filter based transwell invasion assay and scratch wound invasion assays, are widely used to assess tumor cell invasion. However,

these models require the cells to grow on flat surfaces, allowing them to spread in single planes. While cost effective, these models lack the multi-dimensional complex tumor architecture and nutrient gradients found *in vivo*. Moreover, these 2D models typically require manual image acquisition and time consuming analysis in order to track dynamic biological movement.

The Incucyte® Single Spheroid Invasion Assay combines a validated three dimensional (3D) tumor invasion model along with proprietary image acquisition and analysis, to more effectively mimic metastatic phenotype and continuously analyze phenotypic changes over time. The Incucyte® Single Spheroid Invasion Assay provides the supportive scaffold for non-adherent growth of cancer cells in spherical populations, allowing for nutrient gradients to form as they would *in vivo*. Moreover, embedding cancer cells

within ECM may better mimic the physical forces acting on cells during invasion as they breakdown the matrix and invade from the spheroid body. In this chapter, we illustrate how the Incucyte® Single Spheroid Invasion Assay using the Incucyte® Live-Cell Analysis System and purpose build software tools enables straightforward evaluation of invasions and the metastasis progress.

Incucyte® Single Spheroid Invasion Assays at a Glance

To study the invasive potential and capacity of malignant tumor cells, an optimized protocol for the Incucyte® Single Spheroid Invasion Assay is combined with automated imaging and analysis via the Incucyte® Live-Cell Analysis System. To form single spheroids for the evaluation of invasiveness, cells of

interest are harvested and plated into an ultra-low attachment (ULA) round-bottom 96-well plate and centrifuged. Spheroid formation is monitored using Incucyte® Brightfield (BF) and HD phase contrast image acquisition and analyzed using the Incucyte® Spheroid Analysis Software Module to ensure desired spheroid size.

In order to embed the single spheroid to evaluate invasive potential, Matrigel® is added to the formed spheroid and allowed to polymerize prior to the addition of treatments. Continuous automated monitoring of spheroid body and invasive structures are then performed in real time. The simple protocol is shown below:

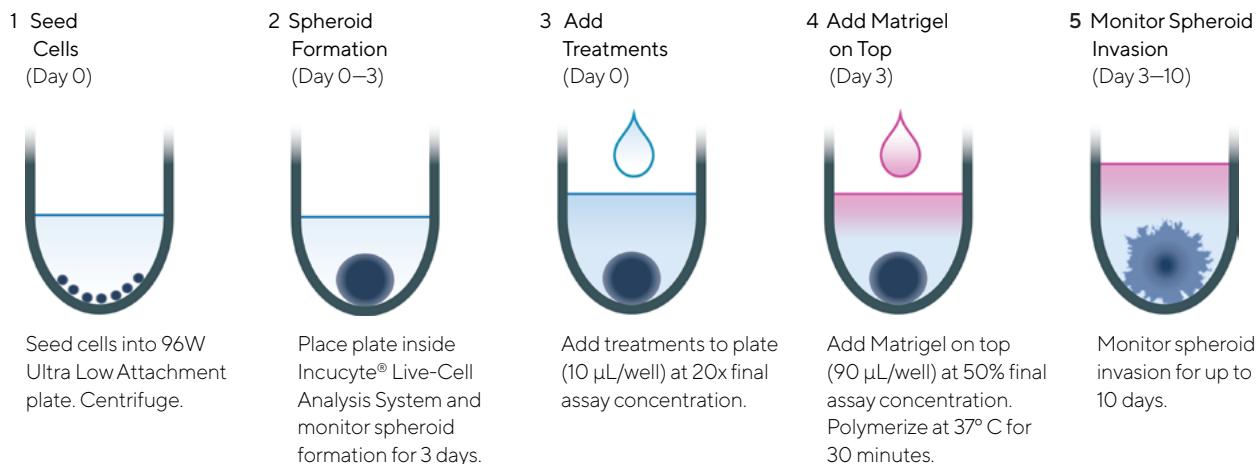


Figure 1. Overview of workflow for generation and analysis of single spheroid invasion in an Incucyte® Live-Cell Analysis System.

Key Advantages

- Quantify label-free invasion and investigate inhibitors of metastasis in a physiologically relevant environment.
- Investigate the metastatic potential of solid tumors in real-time to reveal differences in growth characteristics.
- Lab-tested 96-well protocol to create uniform spheroids suitable for highly reproducible invasion assays with unbiased image analysis.
- Automatically acquire, analyze and graph images from up to six 96-well plates in parallel and get to answers faster.

Sample Results

Quantifying Single Spheroid Invasive Properties Over Time

The Incucyte® Single Spheroid Invasion Assay relies on accurate image segmentation to quantify invasive capabilities of a range of cell types as well as assess cell invasion modulating compounds. Figure 2 illustrates the utility of using Incucyte® Live-Cell Imaging and Analysis for acquisition and analysis for segmentation of invading tumor phenotypes using U87-MG, a human brain glioblastoma cell line. In this experiment, U87-MG spheroids were seeded in a ULA round bottom 96-well plate and allowed to form spheroids for 3 days. Post spheroid formation, Matrigel® was added in the presence and absence of actin

polymerization inhibitor, Cytochalasin D (Cyto D) and depth of focus (DF) Brightfield images were acquired every 6 hours. Incucyte® Spheroid Analysis Software Module was used to quantify changes in spheroid size and invading cell area over time. Figure 2 illustrates the software's ability to accurately segment the whole spheroid area (yellow outline mask) and the invading cell area (blue outline mask), noting extensive invasive phenotype of vehicle treated compared to Cyto D treated spheroids. Kinetic plots highlight the ability to measure differences in invasive phenotype between treated (Cyto D) and untreated (vehicle) spheroids.

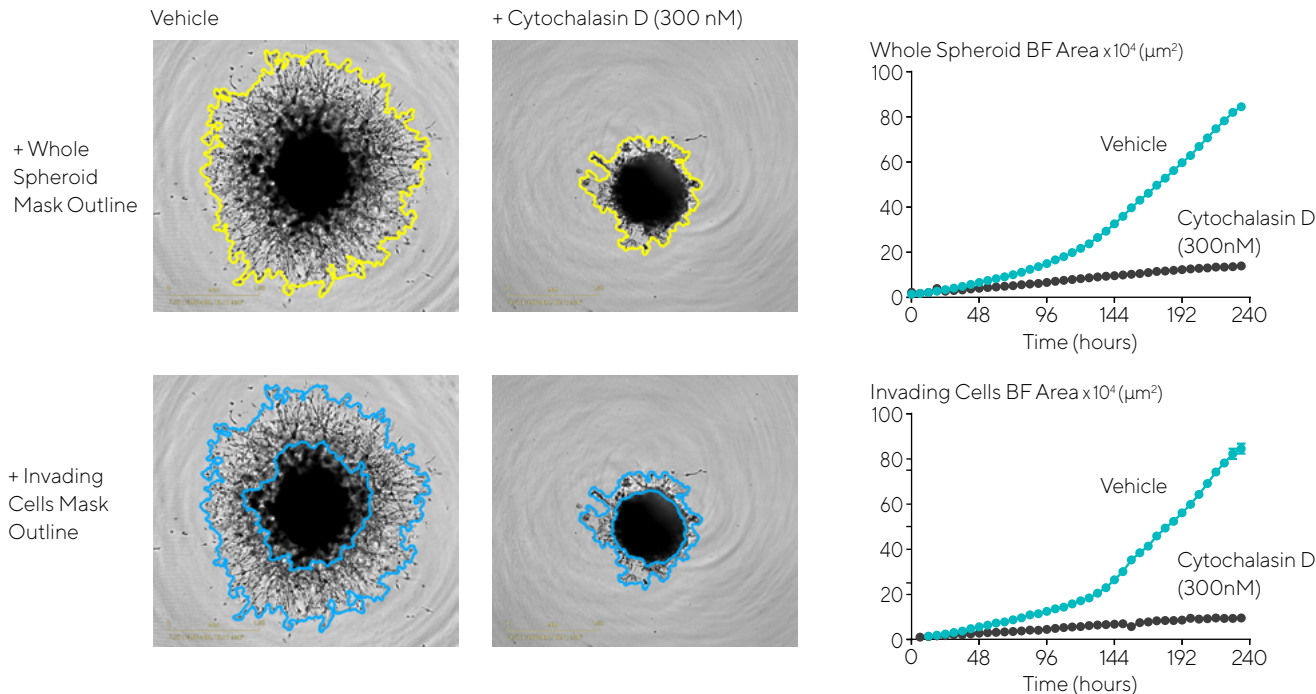


Figure 2. Quantification of single spheroid invasion using Incucyte® real-time analysis. U87-MG cells were seeded in a ULA round bottom 96-well plate (2,500 cells/well) and allowed to form spheroids for 3 days. Spheroids were subsequently treated with vehicle or Cyto D prior to embedding in Matrigel® (4.5 mg/mL). Incucyte® DF Brightfield images (5 days post treatment) show effect of Cyto D on spheroid invasion (whole spheroid; yellow outline mask or invading cells; blue outline mask). Time course plots show the individual well BF area (Whole Spheroid BF or Invading Cell BF Areas, μm^2) over time (hours). Data were collected over a 240 hour period at 6-hour intervals. Each data point represents mean \pm SEM, $n=4$ wells.

Cell Type Specific Spheroid Invasive Potential

To assess the metastatic potential of tumor cells in 3D, comparison of three different tumor cells were assessed. U87-MG (glioblastoma), A172 (glioblastoma) and HT-1080 (fibrosarcoma) spheroids were formed for 72 h in ULA round bottom 96-well plates and subsequently embedded in 4.5 mg/mL of Matrigel®.

Changes in tumor spheroid invasive properties were quantified over 7 days via quantification of invading cell area segmentation of DF Brightfield images shown in blue (Figure 3, images). To account for variation in size following spheroid formation, the whole spheroid area was normalized to spheroid size at $t = 0$ h and automatically plotted over time. U87-MG spheroids exhibited the greatest invasive potential. At 168 hours, whole spheroid area of U87-MG spheroids (ratio: 32) increased to approximately 2x and 4x the size of HT-1080 (ratio: 18) and A172 (ratio: 8) spheroids respectively (Figure 3, whole spheroid area ratio time course). Though different in overall size, A172 and HT-1080 spheroids

showed comparable invasive potential over time (~10 fold at 168 hours) (Figure 3, invading cell area time course).

Data highlights the ability of the Incucyte® Live-Cell Analysis System to accurately identify invading cell area from spheroid body area across a range of cell types, displaying differential spheroid metastatic potential between the cell types. Differences in invasive potential shown across cell types, may suggest distinct mechanisms of cell motility and invasive modalities¹.

Impact of Matrigel® Concentration on Spheroid Invasive Capacity

Metastasis is a multistep process in which ECM and cancer cell cytoskeleton interactions are pivotal in promoting the invasive potential of tumor cells².

To understand the relationship between ECM properties (e.g. rigidity), invasive capacity and invasive phenotype, HT-1080 spheroids were embedded in increasing concentrations of Matrigel® (1.13 – 4.5 mg/mL).

Quantification of DF Brightfield images demonstrated that HT-1080 spheroid invasive capacity is Matrigel® concentration-dependent. (Figure 4A, B). Images also emphasized that Matrigel® concentration effected the density and elongation of spindle-like protrusions (invadopodia) extending from the body of the spheroid, as highlighted at the highest concentration of Matrigel® (4.5 mg/mL) (Figure 4A, zoomed images).

Interestingly, a bell-shaped relationship of ECM concentration on spheroid invasion capacity was revealed in U87-MG and A172 spheroids with the greatest invading cell area attained at 2.25 mg/mL Matrigel® (Figure 4C). While an extension of the concentration range is required to confirm this observation, others have reported that at an optimal matrix concentration, cells at the periphery of the spheroid readily align with matrix fibers and rapidly invade the surrounding ECM, whereas at higher concentrations, cell motility is reduced by the rigidity of the matrix³.

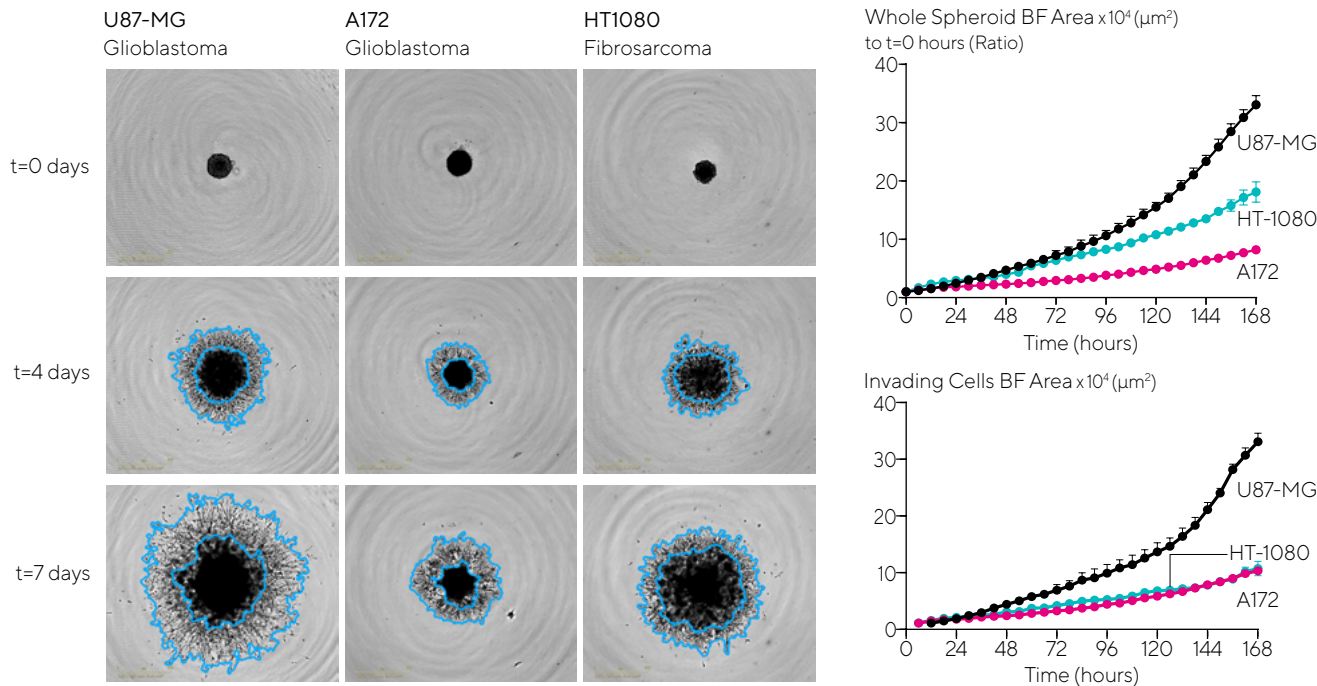


Figure 3. Assess cell type specific invasive capabilities over time. U87-MG, A172 and HT-1080 cells were seeded in ULA round bottom 96-well plates (2,500 cells/well; U87-MG, HT-1080 or 5,000 cells/well; A172) and allowed to form spheroids (3 days) prior to Matrigel® addition (4.5 mg/mL). BF images and time courses of spheroid area (Whole Spheroid BF Area normalized to t = 0h or Invading Cell BF Area) show differences in invasive capacity across cell types. Invading cell area mask outline shown in blue, illustrates the extent of invasive capacity. Data were collected over 168 hours at 6-hour intervals. All images captured at 4x magnification. Each data point represents mean \pm SEM, n=4 wells.

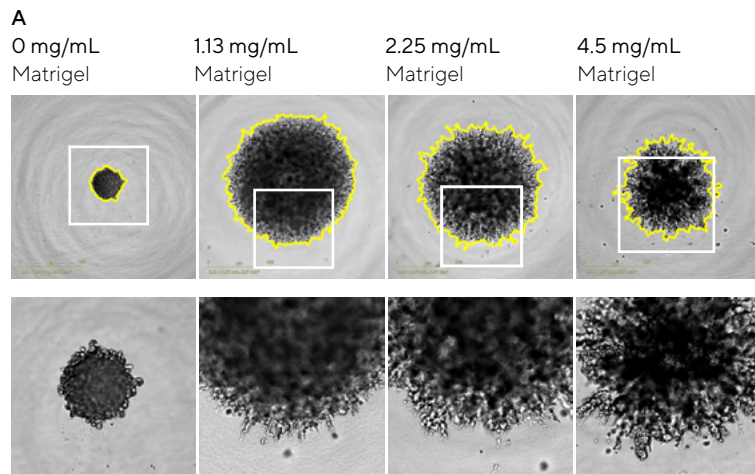
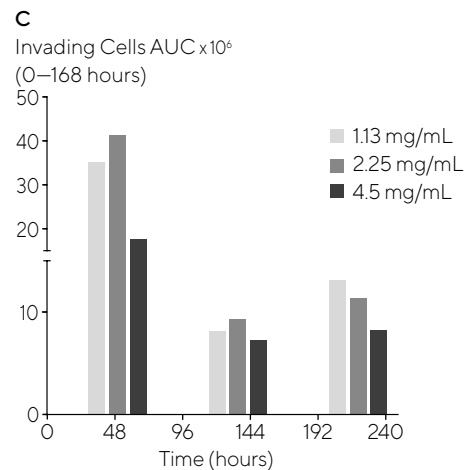
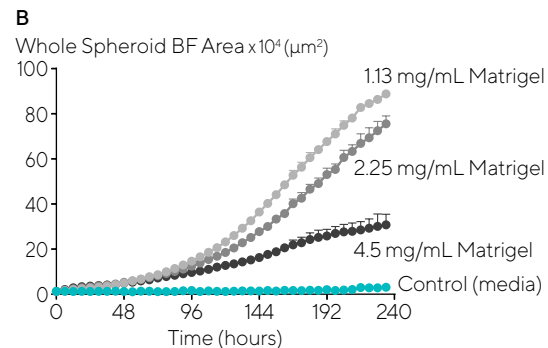


Figure 4. Effects of Matrigel® concentration on spheroid invasion. HT-1080 cells were seeded in a ULA round bottom 96-well plate (2,500 cells/well) and allowed to form spheroids (3 days) prior to Matrigel® addition at varying concentrations (1.13 - 4.5 mg/mL). BF images (7 day) show effects of Matrigel® concentration on spheroid invasive capacity (A, whole spheroid area outline in yellow). Time course shows individual well Whole Spheroid BF Area (μm^2) over time (hours) and dependency on Matrigel® concentration (B). Bar chart represents area under the curve (AUC) analysis of the Invading Cell BF Area time course data (0-7 days, post Matrigel® addition) across multiple cell types (C). Data were collected over 240 hours at 6-hour intervals. All images captured at 4x magnification. Each data point represents mean \pm SEM, n=4 wells.



96-Well 3D Single Spheroid Invasion Assay for Pharmacological Analysis

To exemplify the amenability of Single Spheroid Invasion Assay for testing anti-metastatic compounds, a pharmacological study was performed in U87-MG, A172 and HT-1080 cells. Spheroids (formed over 3 days in ULA round bottom 96-well plates)

were treated with a range of invasion modulating compounds and subsequently embedded in Matrigel® (2.25 mg/mL or 4.5 mg/mL) to initiate invasion.

The Incucyte® real-time, automated Vessel Views and time course Microplate Graphs enabled rapid assessment of

compound effects on spheroid invasion. Cyto D and PP242 caused a concentration dependent inhibition of U87-MG spheroid invasion, while little effect was observed by Blebbistatin (Figure 5).

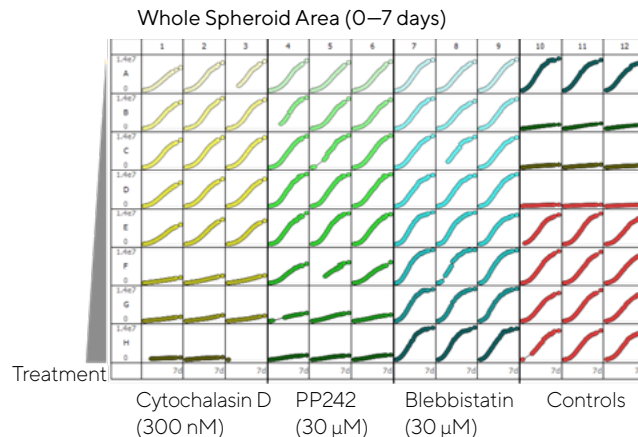
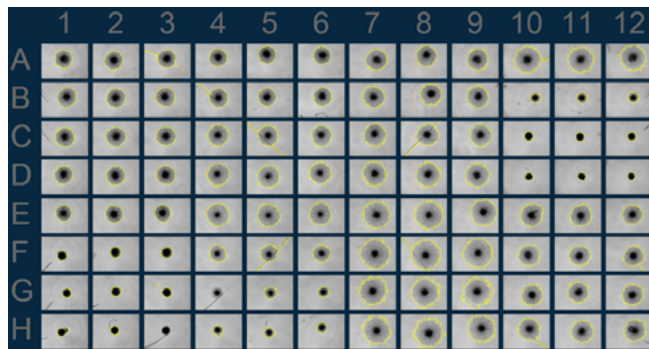


Figure 5. Rapid visualization and assessment of treatment effects using Incucyte® Vessel Views. U87-MG cells were seeded in ULA round bottom 96-well plates (2,500 cells/well) and allowed to form spheroids (3 days). Spheroids were then treated with serial dilutions of anti-metastatic compounds and embedded in Matrigel® (4.5 mg/mL) to induce invasion (up to 10 days). Incucyte® Vessel View and Incucyte® Microplate Graphs show effects of treatments on spheroid invasion (Whole Spheroid BF Area; yellow outline mask) 5 days post treatment.

Elucidating Treatment Effects on Single Spheroid Invasion and Proliferation

The validity of 3D in vitro spheroid invasion models to assess the metastatic effects of treatments relies on their ability to distinguish effects on spheroid invasion and spheroid proliferation and growth. Being able to discriminate between the area covered by cells within the spheroid body from that covered by the invading cell region (invadopodia) is key. Here we illustrate how the Single Spheroid Invasion Assay and associated quantification and analysis approaches is able to address this.

A panel of known anti-metastatic compounds were tested for their effects on U87-MG spheroid invasion. Representative DF Brightfield images revealed a wide range of inhibitory effects on spheroid invasion (Figure 6A). With the exception of Blebbistatin, which appeared pro-invasive, all compounds inhibited spheroid invasion

as reported by a reduction in both whole spheroid and invading cell areas (Figure 6B, teal and grey bars respectively). While comparable attenuation of spheroid size was observed with both Cyto D (90% at 300 nM) and PP242 (80% at 30 μ M), a striking and marked inhibition of the invading cell area (invadopodia) was only evident with Cyto D (Figure 6A, size of blue mask, Figure 6B grey bars).

Normalization of the invading cell area to the whole spheroid area revealed that although similar in overall size 96 hours post treatment, 80% (PP242) and 30% (Cyto D) of the total spheroid size was attributed to the invading cell region (Figure 6C). Performing a simple subtraction of the invading cell area from the whole spheroid area, provides a measure for the size of the spheroid body and hence, a measure for spheroid proliferation in this model of spheroid

invasion. The reduced size of PP242 treated spheroids and the comparable sizes of both Cyto D and vehicle (in the absence of Matrigel®) treated spheroids, further supports the anti-proliferative rather than anti-invasive properties of PP242 (Figure 6D).

To validate this analysis approach, a separate study conducted in the absence of Matrigel® permitted assessment of compound effects on spheroid proliferation alone. After formation, U87-MG spheroids were treated with compounds in the absence of Matrigel®. Effects on spheroid growth and changes in spheroid size (Largest BF Area metric) were quantified using the Incucyte® Live-Cell Analysis System. Figure 6E further supports and shows the inhibitory effects of PP242 (30 μ M), but not Cyto D (300 nM) on spheroid growth.

A

Vehicle (+Matrigel) Cytochalasin D (300nM)

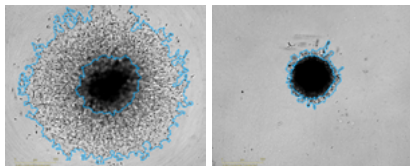
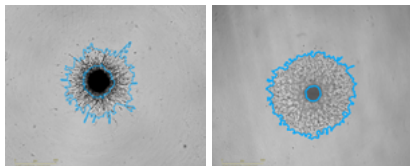
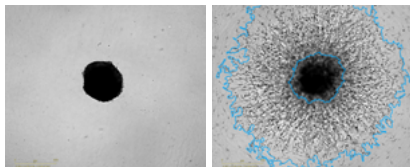
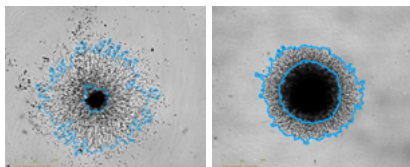
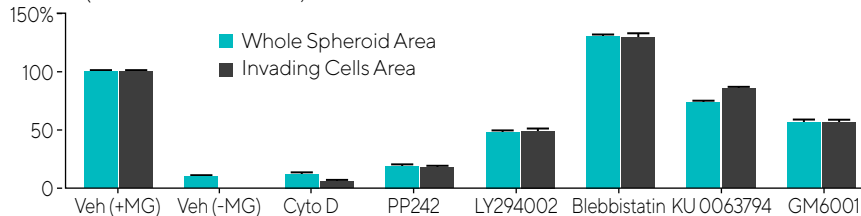
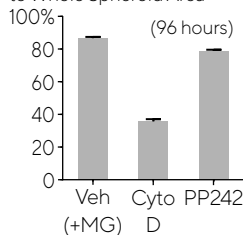
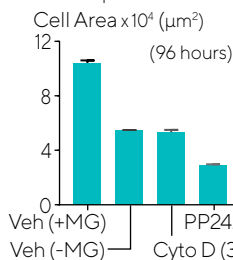
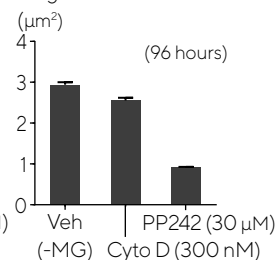
PP242 (30 μ M) LY294002 (30 μ M)Vehicle (-Matrigel) Blebbistatin (30 μ M)KU0063794 (30 μ M) GM6001 (30 μ M)**B** Control (BF Area AUC 0–162 hours)**C** Invading Cell Area Normalized to Whole Spheroid Area**D** Whole Spheroid–Invading**E** Largest BF Area x 10⁴

Figure 6. Effect of cell signaling inhibitors on spheroid invasion. U87-MG cells were seeded in a ULA round bottom 96-well plate (2,500 cells/well) and allowed to form spheroids (3 days) prior to treatment with a range of known inhibitors and embedded in Matrigel® (4.5 mg/mL). Incucyte® Brightfield images (A) (4 days post treatment) show treatment effects on spheroid invasion. Bar chart (B) represents the area under the curve (AUC) analysis of the Whole Spheroid and Invading Cell BF Area (μm^2) time course data (0–162 hours, post treatment). Data normalization (96 hours post treatment) show effect of Cyto D and PP242 on invading cell regions (C). Subtraction of Invading Cell BF Area from Whole Spheroid BF Area (D). In a separate but identical study performed in the absence of Matrigel® shows size (Largest BF Area) of spheroids 96 hours post treatment with Cyto D and PP242 (E). Data were collected over a 162 hour period at 6-hour intervals. Each data point represents mean \pm SEM, $n=3$.

Conclusions

The Incucyte® Single Spheroid Invasion Assay, consisting of optimized protocol and purpose-built software, facilitates the kinetic acquisition and quantification of 3D invasion from single spheroids. This assay mimics *in vivo* tumor cell physiology through the use embedding cancer cells in an extracellular scaffold and analyzing dynamic changes in tumor invasion from the stable environment of the tissue culture incubator. This live-cell technique provides the ability to monitor 3D spheroids long term to better understand processes like metastatic cell invasion and phenotypic responses to therapeutics within the same cell sample.

- A validated protocol to reproducibly embed single spheroids in in an extracellular matrix, allowing cancer cells to mimic the *in vivo* architecture, growing and invading in a three dimensional model.

- Use of purpose built software to automatically acquire images and perform label-free analysis to reveal cell-type specific temporal invasive potential and track Matrigel® concentration-dependent effects on spheroid invasion capacity.
- Verification of all data and time points via inspection of individual images or time-lapse movies to observe changes in cell morphology.
- The utility of our 3D tumor invasion model for real-time compound profiling in a 96-well format to identify and distinguish new or existing compounds effects on tumor invasion.

References

1. Oraiopoulou, *et al.* **Integrating in vitro experiments with in silico approaches for Glioblastoma invasion: the role of cell-to-cell adhesion heterogeneity.** *Nature: Scientific Reports.* 2018. 8: 16200.
2. Goertzen, *et al.* **Three-Dimensional quantification of spheroid degradation-dependent invasion and invadopodia formation.** *Biol Proceed Online.* 2018; 20:20.
3. Ahmadzadeh, *et al.* **Modeling the two-way feedback between contractility and matrix realignment reveals a nonlinear mode of cancer cell invasion.** *PNAS.* 2017; 114 (9) E1617-E1626.

Chapter 9

Kinetic Assays for Studying Neuronal Cell Models

Assays for Studying Neuronal Cell Health, Function and Morphology Long-Term

Effective modeling for neurological disease, injury, and development is critical for identifying novel and effective treatments. However, due to the complexity and plasticity of the nervous system, inaccessibility of human diseased tissue, sensitivity of neurons to perturbation, and lack of translational value of animal models, elucidating the function of the nervous system and identifying novel treatments is challenging. With advances in stem cell technologies, the promise to create differentiated neurons and support cells (e.g. microglia, astrocytes) that accurately represent human phenotypes in order to build translational and patient-specific human models now exists. To fulfill this promise, considerable work is required to optimize the reprogramming and differentiation methods, and to build and validate cellular bioassays that are representative of the native human pathophysiology. To facilitate the evaluation and

characterization of human induced pluripotent stem cells (hiPSCs), many technologies are employed to measure various aspects of cell health, morphology and function, such as immunocytochemistry methods, microelectrode electrophysiology techniques, and flow cytometry. Unfortunately, they are not amenable to monitoring long-term changes (days and weeks) and sample preparation can perturb fragile neuronal cells, thus compromising accurate analysis of dynamic biological changes and responses to treatment. The ability to evaluate long-term changes and characterize complex biological models in a non-invasive manner from a physiologically relevant environment offers considerable advantages in characterizing the function of the nervous system.

The Incucyte® Live-Cell Analysis System addresses the inherent shortcomings of traditional assays through non-invasive,

automated time-lapse imaging and analysis from within a cell incubator. Phase-contrast, brightfield and fluorescence images are acquired under uninterrupted environmental control, and then analyzed and quantified in real time to report changes in morphology, movement, activity and function. Time-lapse videos can be created to verify the experimental outcomes. The critical attributes are:

1. Long-term monitoring of biological events that unfold over days, weeks or even months.
2. Sufficient miniaturization, throughput and ease of use to enable replication, controls and overall experimental productivity.

The attributes of live-cell analysis offer simple and reliable assays which offer new biological insights into basic and advanced neuronal cell models. In the subsequent chapters, the assays are described in

detail, demonstrating their utility for characterizing and validating translational cell models for the discovery of novel neurotherapeutics.

Live-Cell Imaging and Analysis Approaches for Studying Neuronal Cell Dynamics

Building on existing methodologies employed to study cell health, morphology and function, novel strategies were developed in order to quantify long-term changes in neurite dynamics, neuronal activity, as well as readouts for neuroimmune functions, such as phagocytosis and chemotaxis of microglia. Incucyte® Live-Cell Imaging and Analysis consists of instrumentation, software modules, lab-tested protocols and reagents that enable continuous interrogation of sensitive neuronal cell models. In order to accomplish this, instrumentation was designed to quantify cell behavior with uninterrupted incubation provided by a cell culture incubator and a mobile optical train that enables samples to stay stationary and reduce physical disturbance. Purpose-built software analysis modules automatically segment and analyze images to create full

time course plots for each well in 96- and 384-well plates. Finally, combining novel, non-perturbing reagents that deploy longer wavelength fluorophores designed for neuronal-specific measurements along with lab-tested protocols ensures reproducible and unprecedented access to phenotypic information. The flexibility of this instrument, novel reagents, and standardized protocols, combined with higher throughput capabilities and capacity for long-term, unperturbed culture enables this system to overcome many of the challenges associated with traditional endpoint workflows.

How Live-Cell Assays for Neuroscience Work

Incucyte® Neurite Analysis Assays

In the Neurite Analysis Assay, the Incucyte® Neurotrack Analysis Software Module is employed for automated quantification of neurite dynamics using image software analysis. This assay permits the analysis of neurons in monoculture (label-free) or in co-

culture with astrocytes, using a non-perturbing Incucyte® Neurolight Red or Orange Lentivirus for continuous analysis of neurite length and branch points. Furthermore, the neurite analysis assay can be multiplexed with cell health reagents, Incucyte® Annexin V Red, Orange or NIR Dye, to determine the onset of apoptosis in real time.

Kinetic Neuronal Activity Assay

To detect changes in neuronal activity, an end-to-end solution consisting of instrumentation, software and reagent is employed. Addition of a genetically-encoded calcium indicator, Incucyte® Neuroburst Orange Lentivirus, allows for efficient, non-perturbing labeling of living neurons for the long-term detection of neuronal activity via calcium binding. The Incucyte® Neuronal Activity Analysis Software Module captures and analyzes short-term calcium flux kinetics for every active cell within each well to reveal the extent of connections in a network and automatically quantifies longitudinal changes of activity for the characterization of neuronal cell models.

Kinetic Neuroimmune Assays

To quantify neuroimmune function, such as phagocytosis, the Incucyte® pHrodo® Orange or Red Cell Labeling Kit utilizes a pH-sensitive fluorescent probe to quantify cell clearance of diseased or dying cells or neuronal-associated proteins to efficiently study the full time course of phagocytosis in the model of your choice.

To evaluate microglial response, the Incucyte® Chemotaxis Assay enables real-time visualization and quantification of cell migration in response to a chemical stimulus. Using an optically clear membrane, visual assessments of morphology can be linked to real-time measurements to gain deep phenotypic insights.

References

1. Ransohoff RM. **All (animal) models (of neurodegeneration) are wrong. Are they also useful?** *J Exp Med*. 2018, Dec 3;215(12):2955-2958.
2. Zhang X, Hu D, Shang Y, Qi X. **Using induced pluripotent stem cell neuronal models to study neurodegenerative diseases.** *Biochim Biophys Acta Mol Basis Dis*. 2019, Mar 18. pii: S0925-4439(19)30078-X.
3. Zhao X, Bhattacharyya A. **Human Models Are Needed for Studying Human Neurodevelopmental Disorders.** *J Hum Genet*. 2018, Dec 6;103(6):829-857.
4. Li L, Chao J, Shi Y. **Modeling neurological diseases using iPSC-derived neural cells: iPSC modeling of neurological diseases.** *Cell Tissue Res*. 2018, Jan;371(1):143-151.
5. Xiao-hong Xu and Zhong Zhong. **Disease modeling and drug screening for neurological diseases using human induced pluripotent stem cells.** *Acta Pharmacol Sin*. 2013, Jun; 34(6): 755-764.
6. Niu W and Parent JM. **Modeling Genetic Epilepsies In A Dish.** *Dev Dyn*. 2019 Jun 26.
7. Song, J-J et al. **Cografting astrocytes improves cell therapeutic outcomes in Parkinson's disease model.** *Journal of Clinical Investigation*. 2018, 128(1):463-482.
8. Chandrakanthan, V et al. **PGlial cells are functionally impaired in juvenile neuronal ceroid lipofuscinosis and detrimental to neurons.** *Acta Neuropathologica Communications*, 2017, 5:74.
9. Wetzel-Smith, M et al. **PA rare mutation in UNC5C predisposes to late-onset Alzheimer's disease and increases neuronal cell death.** *Nature Medicine*, 2014, 20(12) 1452.
10. Harvey, R. **"Primary Neuronal Cell Culture Tips and Tricks"**, *Biocompare*, posted October 22, 2014, Accessed July 16, 2019. <https://www.biocompare.com/Bench-Tips/168348-Improve-the-Viability-of-Your-Primary-Neuronal-Cell-Culture-with-These-Tips-Tricks/>

9a

Kinetic Neurite Analysis Assays

Quantification and visualization of neurite outgrowth, disruption and cell health

Introduction

Neurite dynamics are central to the study of neuropathological disorders, neuronal injury and regeneration, embryonic development and neuronal differentiation. During these processes, the integrity of neuronal networks is slowly altered, accompanied by changes in neurite outgrowth and disruption that may lead to impaired neuronal connectivity. Characterizing the dynamic changes of neurites *in vitro*, and how they interact with other cells or environmental stimuli, can be invaluable for optimizing *in vitro* models, identifying diseased cells from a heterogeneous population, studying phenotypic effects from genetic manipulation, or performing drug pharmacology studies.

Traditional *in vitro* approaches for analyzing neuronal structures rely on endpoint

assays and imaging techniques that require immunochemical staining. Neuronal cultures are exposed to a treatment condition, fixed and stained at a pre-determined time post-treatment, and then imaged using either high content imaging or traditional fluorescent microscopes. Images are then analyzed to generate measurements of neurite length and branch points. Although this method has been an important tool in neurobiology, the process is labor-intensive, perturbing to fragile neurites, and produces only a single time point of data. In sum, the approach lacks temporal insight and is subject to artifact. Concatenated endpoints may be utilized to address the lack of temporal insight, but require large cell numbers and are subject to further artifacts caused by differences in cell plating or other variable culture conditions.

Continuous real-time imaging and analysis

offers a significant advantage over endpoint assays in that it provides a more physiologically relevant and dynamic approach to visualizing and analyzing neurite outgrowth and disruption. It is achieved using non-destructive, cell-sparing, repeated measurements of the same neuronal networks over extended periods of time (days or weeks), without perturbing cell health or delicate neurite structures. Conducting experiments at these time scales offers a significant advantage when investigating chronic toxicity, as toxic effects develop unpredictably over time.

In this chapter, we will examine kinetic approaches for measuring changes in neurite outgrowth or disruption in both mono- and co-culture cell models. Cultures can be measured and visually validated for days, weeks, or even months, and at microplate throughput, making

these approaches particularly well-suited for the optimization and analysis of neuronal cell models as well as for conducting pharmacological studies and investigations of drug mechanisms of action.

Incucyte® Neurite Analysis Assays at a Glance

In order to measure neurite dynamics, the Incucyte® Live-Cell Analysis System automatically acquires and analyzes images over days or weeks in 96- or 384-well formats. Image acquisition is achieved without the motion of a motorized stage that can be disruptive to sensitive cells; instead, the optical train moves while cells stay stationary. In addition, cells are not subject to loss of environmental control at any point in the experiment. Post-image acquisition, the Incucyte® Neurotrack Analysis Software Module is used to segment neuronal cell bodies and


neurites and quantify biologically relevant processes such as neurite initiation, neurite extension, branching, and loss of neurite length due to retraction. Either label-free or fluorescent methods may be employed depending on the cell culture

model utilized and the scientific question at hand.

For studies of neurite outgrowth and branching in simple mono-culture systems, neurite parameters are derived 'label-free'

Table 1. Shortcomings of Traditional Assays vs Live-Cell Imaging and Analysis Approaches.

Shortcomings of Traditional Assays	Live-Cell Imaging and Analysis Approaches
<ul style="list-style-type: none">▪ Data obtained from a single, pre-defined time point yields minimal dynamic insight.	<ul style="list-style-type: none">▪ Continuous, real-time data can be collected over days, weeks, or months without loss of environmental control or physical movement of cultures.
<ul style="list-style-type: none">▪ Concatenated end-point experiments are subject to cell seeding artifacts and require large cell numbers.	<ul style="list-style-type: none">▪ The same network of cells is repeatedly interrogated over time, yielding maximum information from precious cells.
<ul style="list-style-type: none">▪ Fixation and immunostaining steps are labor-intensive and destroy delicate neurites.	<ul style="list-style-type: none">▪ Neurites are identified without fixation and multiple wash steps. Label-free and non-perturbing fluorescent approaches are available.
<ul style="list-style-type: none">▪ Co-cultures cannot be studied as the entire population is analyzed indiscriminately.	<ul style="list-style-type: none">▪ Purpose built software tools and guided interface enables non-expert operators to perform image processing and generate publication-ready graphics.



using phase-contrast images. Cell bodies are segmented from background based on texture and/or brightness, and neurites (linear features) are segmented based on width and brightness. By normalizing the neurite length to the number of cell bodies, it is possible to directly compare the rates of outgrowth.

When studying neurite retraction, or in cases where co-cultures are required, neuronal fluorescent labeling methods can be employed. In these cases, phase-contrast images alone may not be able to discriminate the neuronal projections from either neurite debris or support cells. In order to identify neuronal processes, neurons are transduced in a single step protocol using the Incucyte® Neurolight Lentivirus Reagent. This

VSV-G pseudotyped lentivirus encodes a non-perturbing fluorescent protein driven off of a synapsin promoter to strengthen neuronal expression and minimize non-neuronal crossover. Phototoxicity associated with repeat exposure to short wavelength lights must also be avoided when analyzing sensitive neuronal models, so longer wavelength fluorophores (e.g. orange, red) are preferred.¹ Once fluorescent images are acquired, Neurotrack algorithms are employed to quantitatively assess neurite morphology and reveal temporal information.

Both label-free and fluorescent Incucyte® Neurite Analysis Assays can be combined with apoptosis measurements to gain further insight into neurotoxic effects. Multiplexing apoptosis measured using

Incucyte® Annexin V NIR Dye and phase contrast neurite measurements enables real-time tracking of neuronal morphology and cell health within the same population of cells in every single well.

Sample Results

Automated Analysis and Visualization in Label-Free Monocultures

The Incucyte® Live-Cell Analysis System takes non-invasive phase-contrast images of neuronal cultures for a complete time course of neurite dynamics (Figure 1, left). Neurotrack Analysis Software produces data on neurite dynamics by analyzing these images. The software analyzes an HD phase image of neurons in two steps:

1. Cell bodies are segmented from background based on texture and/or brightness, and are masked as cell body clusters (Figure 1, upper right). The number of clusters and the total area of clusters are normalized to image area.
2. Linear features are detected based on width and brightness, and are masked as neurites (Figure 1, lower right). The total neurite length and the total number of branch points are normalized to image area. The segmentation mask can be refined and filtered to tailor the mask to the specific cell type. Every time point of the assay generates metrics from the automated software analysis, which quantifies biologically relevant processes such as neurite initiation, neurite extension, branching, and loss of neurite length due to retraction or disintegration. Quantification of cell body cluster count and area provides methods to measure cell body size or proliferation, as well as providing two metrics for normalization.

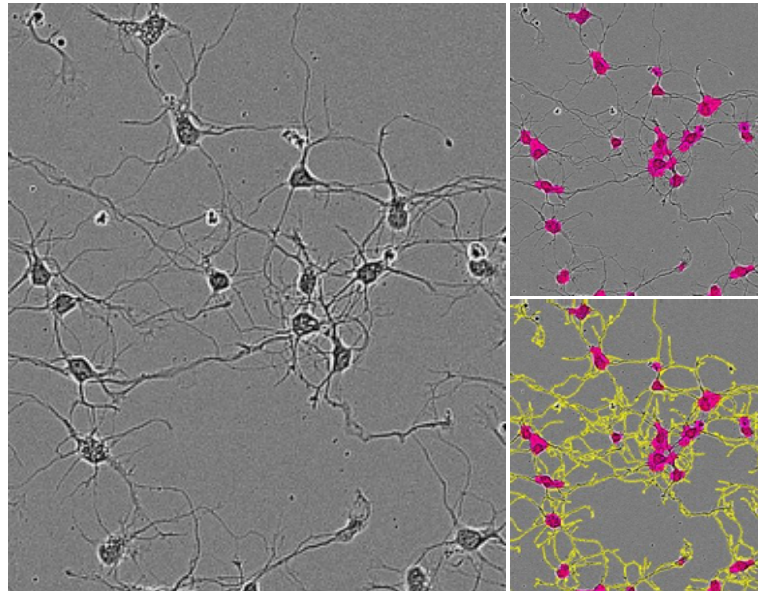


Figure 1. Analysis of rat E18 cortical neurons structures using label-free segmentation masking. Phase image of neurons (top) after 5 days *in vitro* (DIV). Cell body cluster mask applied to image (top right). Neurite mask and cell body cluster mask applied to image (bottom right).

To validate the data generated provided by the Neurotrack Analysis Software, data from a live-cell Incucyte® Neurite Analysis Assay was compared to end-point data derived from fixed cells imaged on a high content screening system (Figure 2). At the three different time points, Neurotrack Analysis Software quantified neurite length in unfixed cells over the course of a 6.5 day assay with a sensitivity statistically identical to the fixing/immunostaining method quantified using a high content screening system.

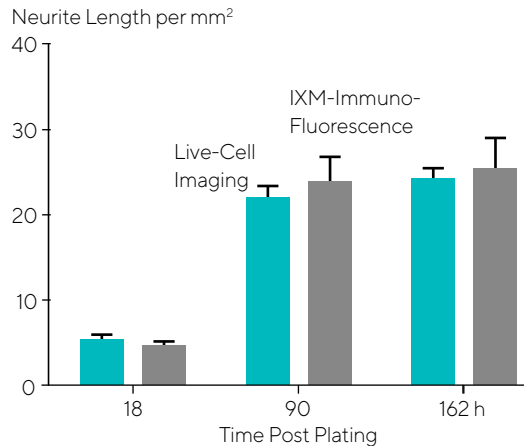


Figure 2: Comparison of automated Incucyte® Neurotrack analysis to traditional fixed-point staining. Three 96- well plates from the same E18 rat cortical prep were seeded at 8,000 cells/well. One plate was imaged in the Incucyte® Live-Cell Analysis System at each of three different time points post-plating (18, 90, and 162 hours). These images were quantified with Incucyte® Neurotrack Analysis Software to measure Neurite Length/mm². Immediately after imaging in an Incucyte® Live-Cell Analysis System, plates were removed from the incubator, fixed, and immunostained for β -tubulin to mark the neurite structures. Cells were then imaged in an Image Xpress Micro high-content screening system and MetaXpress software was used to quantify neurite length/mm². The two data sets are statically indistinguishable at each time point. Error bars represent standard deviation, n=6.

Real-Time Quantification of Neurite Outgrowth in Co-Culture Models

To identify and measure neuronal processes in co-cultures containing neurons and astrocytes, incorporation of a neuronal-specific fluorescent label is required. Figure 3 shows primary rat cortical neurons labeled with Incucyte® Neurolight Orange Lentivirus in co-culture with rat primary astrocytes to

measure changes in neurite length over time. Rat cortical neurons were seeded in a 96-well poly-D-lysine coated microtiter plate and allowed to adhere for 4 hours in an incubator. Neurons were then infected with Incucyte® Neurolight Orange, exposing the cells to lentivirus (MOI 1) for 16-24 h. After the incubation period, the lentivirus was removed and media replaced followed by addition of

astrocytes. The microtiter plate was placed in an Incucyte® Live-Cell Analysis System, where phase and fluorescent images (4 images per well, 20x) were captured every 6 hours for the entire assay duration and automatic analysis of fluorescent images was performed to identify both cell body clusters and neurite length.

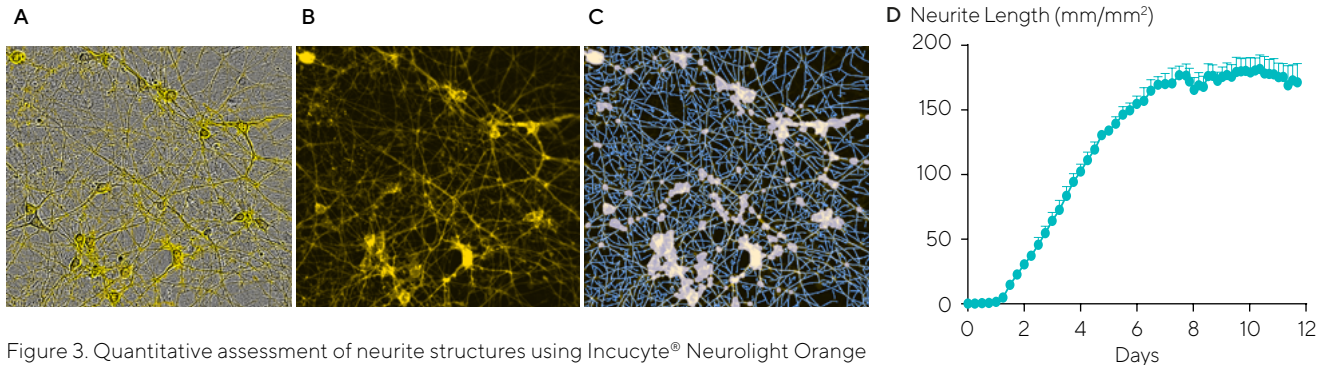


Figure 3. Quantitative assessment of neurite structures using Incucyte® Neurolight Orange Lentivirus in co-culture with astrocytes. (A) Merged HD phase and fluorescent image of rat cortical neurons in co-culture with rat astrocytes at 7 days post-infection. (B) Fluorescent only image is analyzed via automated image processing to identify (C) both cell body and neurite masks and (D) to quantify neurite length over 12 days.

Real-Time Quantification of Neurite Retraction in Co-Culture Models

To illustrate the use of neurite analysis in a model of neurodegenerative disease and neurotoxicity, rat cortical neurons expressing Incucyte® Neurolight Orange were co-cultured with rat astrocytes and exposed to glutamate. Figure 4 illustrates the use of the Incucyte® Live-Cell Analysis System and Neurotrack Analysis Software to analyze phenotypic retraction of neurites, providing quantitative pharmacology. As shown in Figure 4A, the addition of glutamate to co-cultures of primary neurons and astrocytes at day 9 produced a concentration- and time-dependent decrease in neurite length. Measurements of neurite length at 286 hours after plating were fitted with a Hill equation, yielding a 29 μM IC_{50} for glutamate-induced decreases in neurite length with a 73% decline at maximal glutamate concentrations (Figure 4B). To investigate a potential mechanism mediating this toxicity, the neuron-astrocyte co-cultures were exposed on day 9 to MK-801, a specific NMDA receptor antagonist, 10 minutes prior to addition of a maximally effective glutamate concentration (250 μM). MK-801 afforded full protection from the effects of glutamate on neurite length (Figure 4C) with an IC_{50} value of 0.44 nM at 298 hours (Figure 4D), suggesting that the effects of glutamate on neurite length are mediated, at least in part, by NMDA receptors.

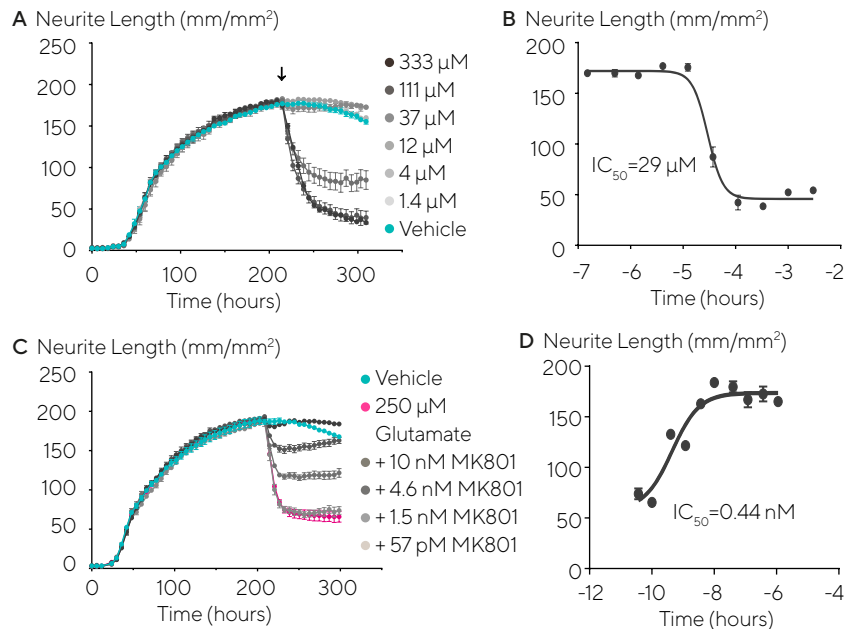


Figure 4. Glutamate-induced retraction of neurite projections. Time-course of effects of glutamate addition at day 9 (arrow) on neurite length is shown in A (mean + SEM, n=4). (B) Concentration-response analysis for data in A (mean + SEM, n=4) taken at 286 hour time-point. (C) Addition of increasing concentrations of MK-801 10 minutes prior to addition of 250 μM glutamate (arrow) protects neurites from glutamate toxicity (mean + SEM, n=4). (D) Concentration-response data for MK-801 effects measured at 298 hours (mean + SEM, n=4).

Live-Cell Analysis Utility for Characterization and Development of iPSC-Derived Neuronal Models

Neurite analysis can also be used to characterize and optimize basic culture conditions when plating and maintaining iPSC. An example of this is shown in Figure 5 where the culture of iCell® Neurons (Cellular Dynamics International) were tested in three

common culture substrates (PDL, PLO, PEI) w/w/o secondary laminin or Matrigel coating. iCell Neurons were seeded at 50,000 cells/well on PDL, PLO or PEI +/-Matrigel or +/-laminin, and images were captured at 10X magnification. Different morphologies were observed between the coatings, with dramatic cell clustering and radial neurite cabling demonstrated with PDL and PLO,

while the morphology of the monolayer on PEI plates were more homogenous and representative of classical neurite outgrowth. Secondary coating with either laminin or Matrigel produced a neuronal monolayer with more pronounced neurite outgrowth, and laminin was chosen for further experimentation.

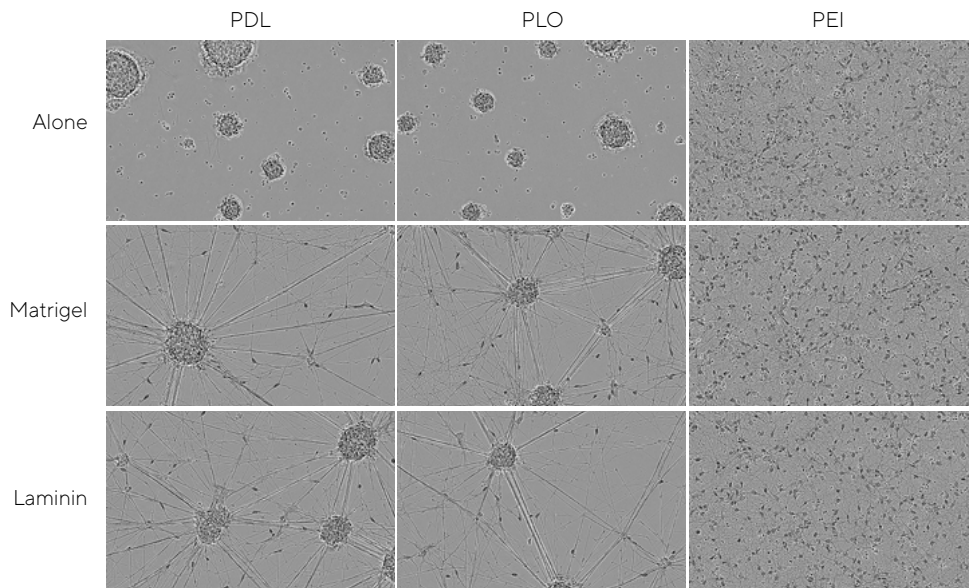
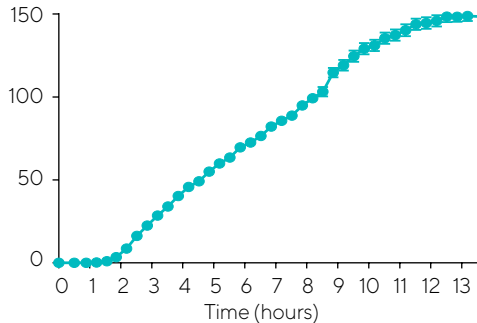


Figure 5. Determination of optimal adherence and morphology of iCell Neuron monocultures seeded on PEI + laminin. iCell Neurons were seeded at 50,000 cells/well on PDL, PLO or PEI +/-Matrigel or +/- laminin. Cells plated on PDL or PLO formed large neurospheres by DIV14 in the presence or absence of additional laminin or Matrigel coating. Cells plated on PEI +/- laminin or Matrigel displayed a more homogenous monolayer. All images captured at 10x magnification.

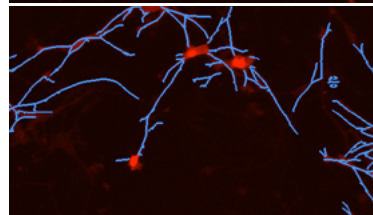
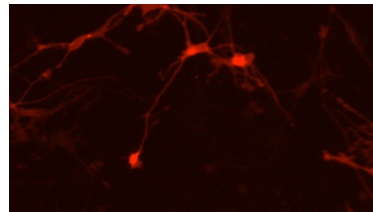
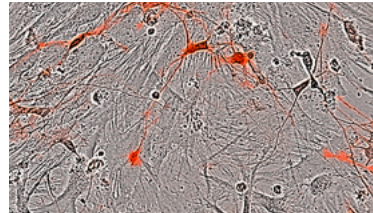
Once culture conditions were optimized for iCell Neurons in monoculture on PEI + laminin, they were subsequently tested to evaluate if the conditions translated to iCell Neurons plated in co-culture with primary rat astrocytes. iCell Neurons and primary rat astrocytes were seeded at 10,000 and 15,000 cell/well respectively. The iCell Neurons were then infected with Incucyte® Neurolight Red Lentivirus, images captured at 20X magnification, and neurite length was assessed with fluorescent Neurotrack Analysis Software Module (Figure 6), which demonstrated robust neurite outgrowth. Although iCell Neurons in co-culture with astrocytes did not display a dramatic difference in morphology or neurite length with other coating conditions (data not shown), we recommend seeding on PEI + laminin to maintain consistency with monoculture experiments.

PEI + Laminin Mean Neurite Length

Neurite Length Red (mm/mm²)



PEI/laminin
DIV 6



PEI/laminin
DIV 14

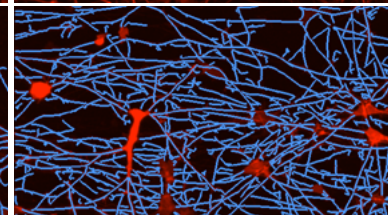
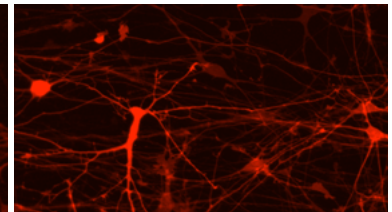
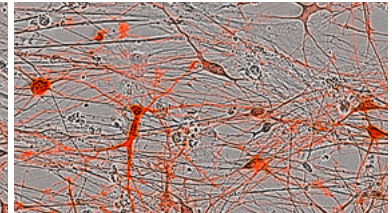
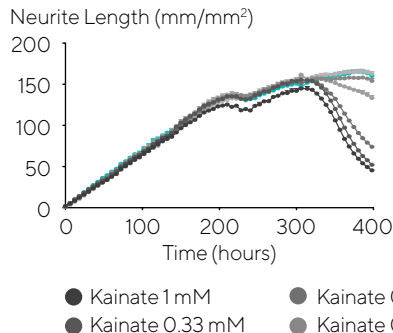


Figure 6. PEI + laminin coating enables robust neurite outgrowth in iCell Neuron co-culture with primary rat astrocytes. Cell culture plates were coated with PEI + laminin. All images captured at 20X magnification. Each data point represents mean \pm SEM, n=4.

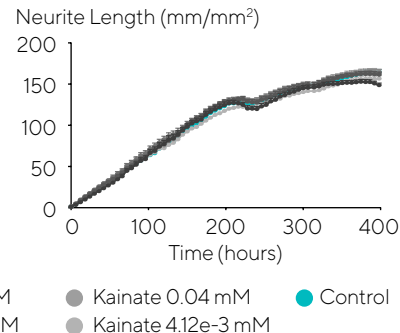
Multiplexed, Kinetic Measurements of Neurite Dynamics and Cell Health

The flexibility of the Incucyte® Live-Cell Analysis System, integrated software, and associated non-perturbing reagents enables users to multiplex kinetic measurements of neurite length and branch points with cell health readouts in one assay platform, which spares precious sample, augments standardization, and enhances throughput for both mono-culture and co-culture workflows. Figure 7 shows the use of fluorescent (co-culture) Neurotrack Analysis Software multiplexed with Incucyte® Annexin V NIR Dye to quantitatively characterize potential long term neurotoxic effects of glutamate and kainate in hiPSC-derived neurons (iGluta Neuron). Addition of both glutamate and kainate at DIV14 produced a concentration- and time-dependent decrease in neurite length with concomitant increase in cell death in iGluta Neurons in co-culture with primary rat astrocytes. To investigate a potential mechanism mediating this toxicity, AMPA receptor and NMDA receptor antagonists (NBQX and MK801, respectively) were added at DIV14 along with glutamate or kainate. NBQX and MK801 reduced the neurotoxic effects of both glutamate and kainate, suggesting that these effects are, at least in part, glutamate receptor-mediated.

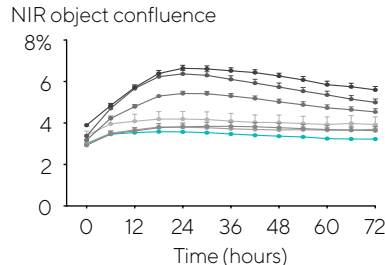
Neurite Length—Fluorescent Neurotrack



Addition of NBQX and MK801



Cell Viability—Incucyte® Annexin V NIR



Addition of NBQX and MK801

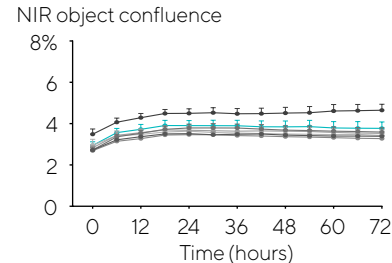


Figure 7. Kainate exposure concentration- and time-dependently decreases neurite length and increases cell death in iGluta Neuron co-culture. Time course of the effects of kainate addition at day 14 (arrow) on neurite length (top panels) and cell viability (bottom panels). Kainate causes a concentration-dependent decrease in neurite length with concomitant decrease in cell viability (increased Incucyte® Annexin V NIR fluorescence). Addition of NBQX (20 μ M) and MK801 (10 μ M) protects iGluta Neurons from kainate toxicity. Each data point represents mean \pm SEM, n=6.

Conclusions

Incucyte® Neurite Analysis Assays enable long-term examination of neurite dynamics in primary, immortalized and iPSC-derived neuronal models. These assays are ideal for both optimizing *in vitro* models and performing drug pharmacology studies. By acquiring images in a physiologically relevant environment, and using robust, integrated software analysis, neurite analysis can be extended from a traditional 'fix-and-stain' approach, to kinetic, non-invasive evaluation of mono- or co-culture models to detect pharmacological and genetic manipulations that alter neurite formation, elongation, and disruption. This approach also allows users to optimize the culture conditions and maintenance of iPSC-derived neuronal models as well as providing a method to analyze cell health by deploying longer wavelength, non-perturbing fluorophores. Incucyte® Live-Cell Imaging and Analysis for real-time, long-term quantitative analysis of neuronal morphology and cell health fills a critical need in the study of human neurophysiological disorders and iPSC-derived neurons.

- The assay is flexible and can be utilized to study neurite outgrowth or retraction in a wide range of cell types, from large immortalized cell lines to primary neurons and iPSCs, in mono- or co-culture.
- Sensitive, kinetic measurements of neurite length, branch points, and cell body clusters capture a complete description of a highly dynamic process that cannot be provided by single time point data alone. Arbitrarily defined endpoints are not required.
- Assays are conducted in an optimal environment so that neurite dynamics can be studied over extended time periods (days or weeks), ideal for studying effects that may not present until later points in time. Cells do not experience loss of environmental control or physical movement as data is collected.
- All data and time points can be verified by inspecting individual images and/or time-lapse movies. Observation of cell morphology provides additional validation and insight into the biological effect of treatment groups.
- Assays are either label-free or employ non-perturbing Incucyte® reagents that can be multiplexed (e.g. to readout neurite length and cell death). Cell sparing, lab-tested protocols are provided to minimize troubleshooting.
- Images are automatically acquired and analyzed in 96- or 384-well format using an intuitive user interface. This allows for rapid assay optimization.
- Low well-to-well variability and minimal user effort make the assay amenable to medium throughput screening.
- The combination of long-term image-based analysis and microplate throughput in a physiologically relevant environment enables efficient optimization of culture conditions and maintenance of iPSC-derived neuronal models.

References

1. Laissue P, *et al.* 2017. **Assessing phototoxicity in live fluorescence imaging.** *Nature Methods*; 14: 657–661.

Incucyte® User Publications

1. Bressan RB, *et al.* **Efficient CRISPR/Cas9-assisted gene targeting enables rapid and precise genetic manipulation of mammalian neural stem cells.** *Development*, 2017, Feb 15; 144(4):635–648.
2. Cavaliere F, *et al.* **In vitro α -synuclein neurotoxicity and spreading among neurons and astrocytes using Lewy body extracts from Parkinson disease brains.** *Neurobiol Dis.*, 2017, Jul; 103:101–112.
3. Hong W, *et al.* **Diffusible, highly bioactive oligomers represent a critical minority of soluble A β in Alzheimer's disease brain.** *Acta Neuropathol.*, 2018, Jul; 136(1):19–40.
4. Jin, M, *et al.* **An in vitro paradigm to assess potential anti-A β antibodies for Alzheimer's disease.** *Nat Commun.* 2018, Jul 11; 9(1):2676.
5. Kobayashi W, *et al.* **Culture systems of dissociated mouse and human pluripotent stem cell-derived retinal ganglion cells purified by two-step immunopanning.** *Invest Ophthalmol Vis Sci.* 2018 Feb 1;59(2):776–787.
6. Li S, *et al.* **Decoding the synaptic dysfunction of bioactive human AD brain soluble A β to inspire novel therapeutic avenues for Alzheimer's disease.** *Acta Neuropathol Commun.* 2018 Nov 8;6(1):121.
7. Muñoz SS, *et al.* **The serine protease HtrA1 contributes to the formation of an extracellular 25-kDa apolipoprotein E fragment that stimulates neuritogenesis.** *J Biol Chem.*, 2018, Mar 16; 293(11):4071–4084.
8. Robinson M, Douglas S, and Michelle Willerth S. **Mechanically stable fibrin scaffolds promote viability and induce neurite outgrowth in neural aggregates derived from human induced pluripotent stem cells.** *Sci Rep.*, 2017, Jul 24; 7(1):6250.
9. Vadodaria KC, *et al.* **Altered serotonergic circuitry in SSRI-resistant major depressive disorder patient-derived neurons.** *Mol Psychiatry.* 2019 Jun;24(6):808–818.

Kinetic Neuronal Activity Assays

Long-Term Quantification of Synaptic Activity and Network Connectivity

Introduction

The most fundamental function of the nervous system is the transmission and integration of information via electrical and chemical signals that pass from axon termini to receiving dendrites of neighboring neurons. In order to coordinate complex processes, this primary function of integration and propagation of cellular signals must be achieved. Activity measurements are therefore critical for characterizing the generation and maturation of neuronal networks to gain functional insights into relevant neuronal models and disease states. Model systems gaining the most traction in the field of neuroscience are human induced pluripotent stem cell (hiPSC)-derived neurons, which offer the opportunity to study basic neuronal development as well as representative disease conditions as they differentiate, mature and become

functionally active. However, current technologies have limited ability to generate the information needed to develop these models and determine when they become functionally active.

Traditionally, neuronal activity measurements are made using sophisticated microelectrode electrophysiology techniques or microscopic analysis of calcium oscillations. Electrophysiology techniques, such as patch clamp measurements and multi-electrode arrays (MEA), may provide exquisite resolution of electrical changes, however these measurements are often derived at a single point in time without confirmation of cell morphology. Furthermore, MEA methods require neuronal cultures to be grown at high densities which sacrifices representation of *in vivo* conditions. Analysis of calcium oscillations offers the opportunity to

analyze morphological changes associated with neuronal activity, however also fail to capture long-term changes of neuronal activity and cannot detect the formation of a mature, connected neuronal network.

Live-cell analysis alleviates many of these challenges by allowing for chronic evaluation (over days, weeks, or months) of neuronal activity and connectivity from thousands of cells per well, via non-destructive, repeated imaging of the same sample in a physiologically relevant environment. In this chapter, we illustrate how the Neuronal Activity Assay using the Incucyte® Live-Cell Analysis System in conjunction with fit-for-purpose software tools and a non-perturbing reagent enables kinetic quantification of activity and connectivity at a microplate scale.

Kinetic Neuronal Activity Assays at a Glance

To evaluate long-term neuronal activity measurements, Incucyte® Live-Cell Imaging and Analysis employs an end-to-end solution consisting of instrumentation, software, and reagent utilized in a physiologically relevant environment. The Incucyte® Neuroburst Orange Lentivirus is a genetically encoded calcium indicator that can be expressed in a variety of neuronal cell types, including iPSC-derived models, to gain insight into the dynamic changes in activity via measurements of calcium oscillations. In order to acquire these neuronal activity changes, the reagent encodes a fluorescent protein that is excited at a higher wavelength to avoid phototoxic damage to the sensitive neurons that are being analyzed. The Incucyte® Live-Cell Analysis System and

Incucyte® Neuronal Activity Analysis Software Module captures these short-term calcium oscillations via high speed movie acquisition (3 fps for 30-180s) in every well of a 96-well microtiter plate. Acquired fluorescent Incucyte® movies are then analyzed to quantify the orange fluorescent signal to derive the active neuronal count and connectivity over the course of the experiment, enabling continuous characterization of developing networks as they become functional and mature. This approach provides researchers the opportunity to continuously analyze the same population of cells long-term, from days to weeks to months, in order to gain insight into how and when neurons become active and how their activity changes over time.

Shortcomings of Traditional Assays	Live-Cell Imaging and Analysis Approaches
<ul style="list-style-type: none"> ▪ Data obtained from at a single point in time yields minimal insight as neuronal networks develop and mature. 	<ul style="list-style-type: none"> ▪ Long-term, kinetic evaluation shows longitudinal changes in network activity to determine when neurons become active and how their activity changes over time.
<ul style="list-style-type: none"> ▪ Measurement of activity from a limited number of cells or by using concatenated single time point data causes high variability in assay results. 	<ul style="list-style-type: none"> ▪ Burst rate of thousands of cells in every well of a 96-well plate is measured with high accuracy via continuous interrogation in the same population of cells over days, weeks, or month.
<ul style="list-style-type: none"> ▪ Lack of environmental control and physical movement of plate during analysis disturbs sensitive neuronal structures and the biology of interest. 	<ul style="list-style-type: none"> ▪ Uninterrupted environmental control provided by a tissue culture incubator, coupled with a non-perturbing reagent and automated image acquisition without physical movement of sample, protects sensitive neuronal structures and maintains integrity of data.
<ul style="list-style-type: none"> ▪ Poor/no visualization of cell morphology and limited spatial resolution does not allow for evaluation of cell health or neuronal network formation. 	<ul style="list-style-type: none"> ▪ Qualitatively monitor cell morphology using HD phase image and quantify functional connectivity of entire network of active objects in each well of a 96-well plate.
<ul style="list-style-type: none"> ▪ Complex instrumentation and image processing requires expert operation and training for data generation and analysis. 	<ul style="list-style-type: none"> ▪ Purpose built software tools and guided interface enables scientific discovery for even first time users.

Sample Results

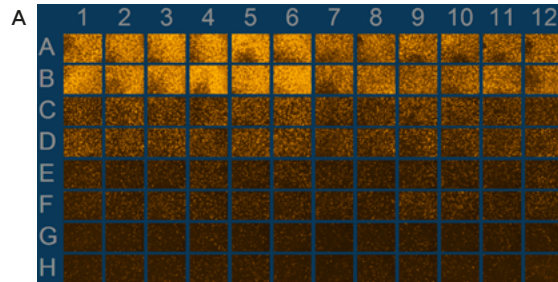
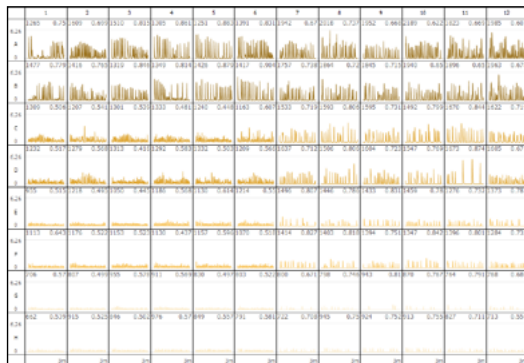
Monitoring Neuronal Activity via Detection of Calcium Oscillations
Incucyte® Neuroburst Orange Lentivirus is a neuronal specific, live-cell genetically-encoded calcium indicator (GECI) that, when used along with Incucyte® Live-Cell Analysis System and Incucyte® Neuronal Activity Analysis Software Module, enables automated quantification of transient calcium oscillations of thousands of functional neurons within a culture over long periods of time. Optimizing cell seeding densities for use with the Incucyte® Neuroburst Orange Lentivirus for monitoring neuronal activity is illustrated on the next page (Figure 1) using a primary model for neuronal activity; co-culture of primary rat neurons (E18) and primary rat astrocytes. In this experiment, E18 rat cortical neurons were plated at decreasing cell densities (5-40K/well) in co-culture with a fixed number of rat astrocytes (15K per well). As visualized in Figure 1A, fluorescence intensity within the range image strongly

Table 1. Shortcomings of Traditional Assays vs Live-Cell Imaging and Analysis Approaches.

correlates with cell density, with the highest amount of activity observed at 40K neurons/well. The range image also provides the researcher with a qualitative assessment of morphology, toxicity, and transduction efficiency. Summary traces of neuronal activity provide a quantitative assessment of activity within each well, and density of neurons tested was optimal for visualization of neuronal activity within each scan (Figure 1B) and detection of active objects over the full 12-day time course (Figure 1C).

B Summary Trace Activity at Day 12

Neurons
per well



C Number of Active Objects Over 12 Days

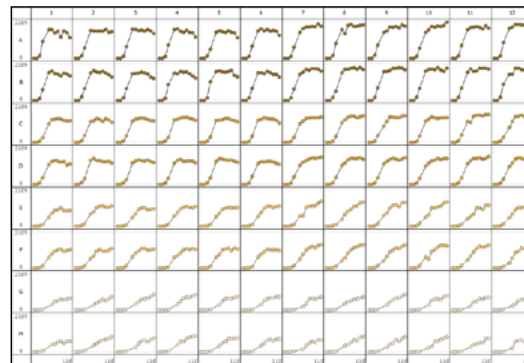


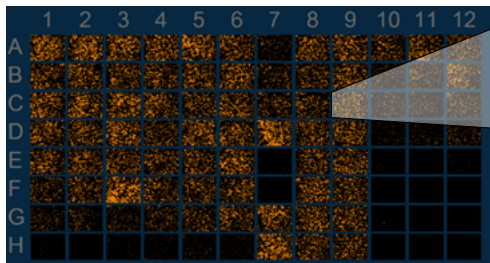
Figure 1. Optimizing cell seeding densities for use with Incucyte® Neuroburst Orange Lentivirus for monitoring neuronal activity. Primary rat cortical neurons were seeded at 40K (rows A and B), 20K (rows C and D), 10K (rows E and F), and 5K (rows G and H) cells/well. All densities of neurons were plated in a co-culture with primary rat astrocytes seeded at 15K cells/well and transduced with the Neuroburst Orange Lentivirus. (A) 96-well Vessel View of the range image over the course of the scan provides a snapshot of active wells at each time point. (B) Summary traces of fluorescence intensity across all active objects for the 96-well plate at day 12 provide an overview of activity and display metrics of bursting intensity, active object number and mean correlation. (C) 96-well throughput with high kinetic reproducibility over 12 days in culture.

The Incucyte® Live-Cell Analysis System automatically captures and analyzes short-term, calcium flux kinetics for every active cell within each well of a 96-well plate using Incucyte® Stare Mode movie acquisition. Each scan consists of a 30-180 second movie, captured at a rate of three frames per second, then distilled into a single range image to allow for simple

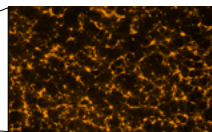
viewing and image processing. This image represents the range of intensities that are detected from each cell within the culture over the specified scan time. Using this image, automated image segmentation tools are used to identify active objects (cells) within each well. Based on the changing fluorescent intensity of each individual cell, intensity traces are

displayed for every active cell in the culture. Scanning is typically completed once every 24 hrs. Once these data are collected, several automated metrics are calculated for each well and at each scan time, allowing for simple visualization of changing metrics over the full time-course of the experiment (Figure 2).

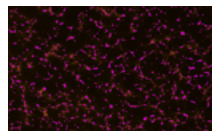
A Vessel View



B Active Object Mask



Fluorescent range image



Active object mask

C Summary Trace – Mean Intensity Over 3 Minutes

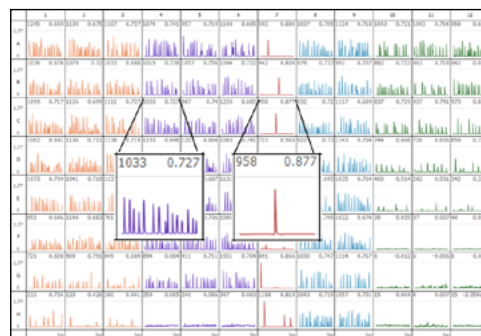


Figure 2. Identification and masking of active neurons using integrated Incucyte® Neuronal Activity Analysis Software Module. Incucyte® rCortical Neurons seeded at 15,000 cells/well in a co-culture model with Incucyte® rAstrocytes were subsequently infected with the Incucyte® Neuroburst Orange Lentivirus. Vessel View (A) displays a summary of active objects (range image) in each well of a 96-well plate acquired during movie acquisition on day 8, revealing differences in activity across the microplate. Identification of each active object via masking (shown in purple) of the range image (B) is performed using the integrated Incucyte® Neuronal Activity Analysis Software Module. 96-well Summary Traces for movies acquired at a given time-point (C) provide a full 96-well view of burst intensity, active object count (left inset value) and mean correlation (right inset value).

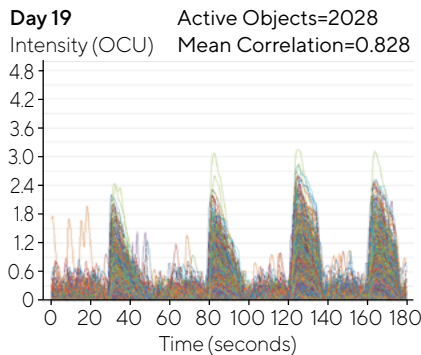
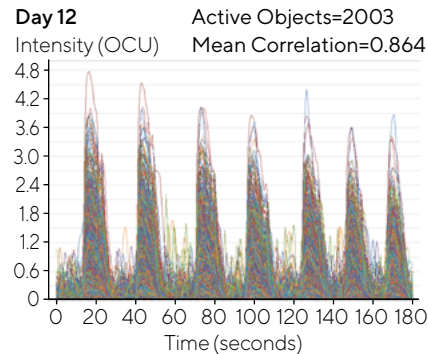
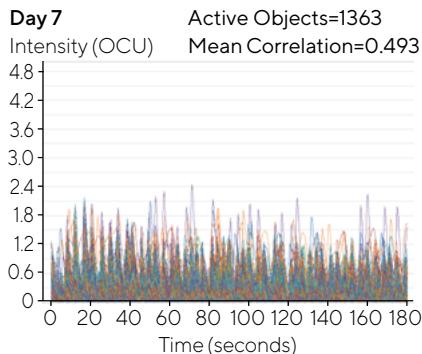
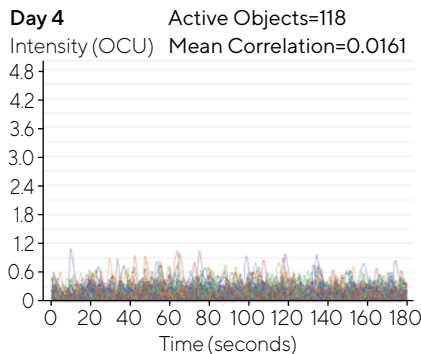
Characterizing Changes in Neuronal Activity Through Chronic Analysis

A key value of live-cell analysis is the ability to quantify longitudinal changes in activity for the characterization of neuronal cell models in physiologically relevant conditions. In Figure 3, iPSC-derived iCell® GlutaNeurons in co-culture with rat astrocytes co-were transduced with Incucyte® Neuroburst Orange Lentivirus. After 24 hours, the lentivirus reagent was removed and live-cell analysis of calcium oscillations were captured every 24 hours for 20 days. Automated image processing identifies thousands of active neurons—many more than MEA—in each well of a 9 mean burst rate and mean correlation of the samples being analyzed. Importantly, this analysis of the same population of cells is repeated over many days and weeks to build understanding of the development of the network and any long-term plastic changes.

Kinetic Profiles of Different iPSC-Derived Neurons

Four different types of iPSC-derived neurons were evaluated over 30–50 days in culture to profile their functional activity. These included iCell GlutaNeurons (Figure 4A), iCell GABANeurons (Figure 4B), iCell DopaNeurons (Figure 4C) co-cultured with primary rat astrocytes, as well as CNS.4U neurons (Figure 4D). iCell GlutaNeurons, described as human glutamatergic-enriched cortical neurons derived from iPSCs, displayed a rapid induction of calcium burst activity in >1500 cells that became highly correlated within 10 days of co-culture. iCell GABANeurons, characterized as a culture of >95% pure population of GABAergic (inhibitory) neurons, also displayed a rapid increase in the number of cells with calcium burst activity within the first week of co-culture. However, iCell GABANeurons did not display significant correlation at any time-point tested, in line with their inhibitory

phenotype. A closer examination of cellular activity at day 14, displayed as object traces over the full 3 min scan (Figure 4A and 4B), supports the observation of a significant number of active cells in both the iCell Gluta- and GABANeurons; the former displaying higher calcium burst intensity and synchronicity when compared to the latter. Interestingly, the kinetics of iCell DopaNeuron activity was strikingly similar to iCell GlutaNeurons, illustrating a very rapid induction of highly active, highly correlated networks within the first 10 days of culture. Ncardia's CNS.4U cells represent an *in vitro* co-culture model of hiPSC-derived neurons and astrocytes. These cells showed significant activity from nearly 1200 cells within the first week of culture and an increase in correlated activity (network connectivity) at approximately day 34 in culture, reaching a correlation of 0.7 at day 45 when the experiment was terminated.



Kinetic Quantification

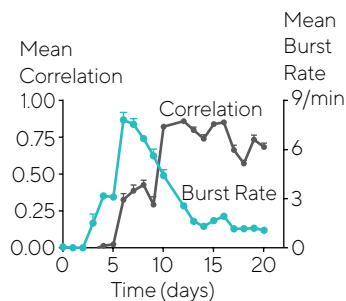


Figure 3. Long-term characterization of changes in spontaneous neuronal activity in iCell GlutaNeurons. iCell GlutaNeurons (Cellular Dynamics International) were seeded at 30K cells/well with a co-culture of rat astrocytes (15K cells/well) on PEI/laminin coated 96-well culture plates. Neurons were transduced with Incucyte® Neuroburst Orange Lentivirus at DIV 2, and spontaneous neuronal activity was analyzed over a period of 20 days. Active object traces provide detailed insight into the dynamic changes in neuronal activity and connectivity for every acquired movie and are qualitatively confirmed with movie viewing tools. Kinetic quantification of longitudinal, dynamic changes in neuronal activity of mean burst rate and mean correlation over time shows that during neuronal network maturation, an increase in burst rate occurs, peaking at day 5. Time course data also shows an increase in neuronal synaptic connections, as noted in an increase in correlation.

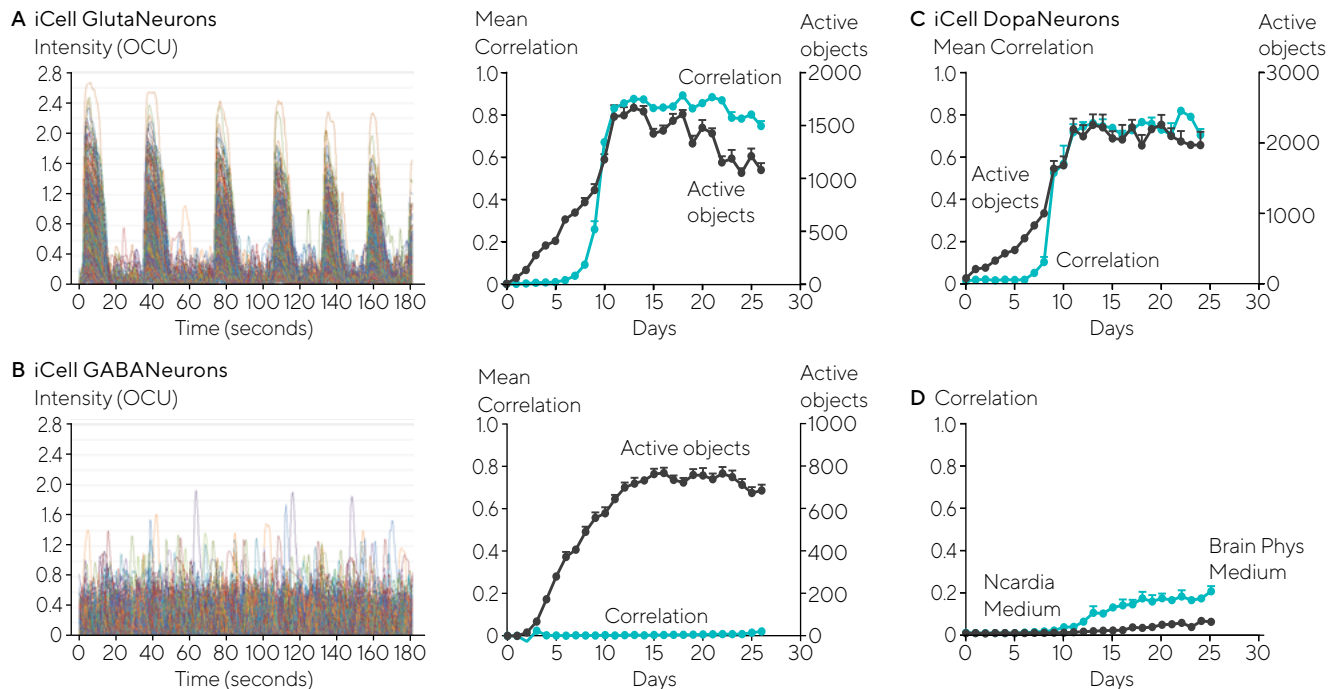


Figure 4. Comparison of differences in functional activity in iPSC-derived neurons. iCell GlutaNeurons, iCell GABANeurons, iCell DopaNeurons (Cellular Dynamics International) and CNS.4U neurons (Ncardia) were all seeded at 20K cells/well. iCell GlutaNeurons, iCell GABANeurons and iCell DopaNeurons were also plated with a co-culture of rat astrocytes seeded at 15K cells/well. Neurons were infected with Neuroburst Orange Lentivirus, and active object number and mean correlation were quantified for up to 45 days. Example calcium oscillation traces and kinetic graphs of activity metrics over time for iCell GlutaNeurons (A) and iCell GABANeurons (B). Mean correlation and active object number were quantified for iCell DopaNeurons (25 days) (C) and CNS.4U neurons (45 days) (D). Data points represent Mean \pm SEM.

Measuring Impact of Culture Conditions on Neuronal Activity in iPSC-Derived Neurons

To evaluate the impact of cell culture conditions on neuronal function, complete BrainPhys® Neuronal Medium, a serum-free, neurophysiological basal medium specifically developed for improved neuronal function, was evaluated to test whether the media could affect the function of iPSC-derived neurons, Peri.4Ucells, iPSC-derived peripheral neurons (Ncardia). Neurons were cultured in either BrainPhys medium or the media provided by the manufacturer (Neuro.4U; Figure 5). Qualitative inspection of cell morphology did not reveal obvious differences in cell health or neuronal network structure. Quantitative measurements of neuronal function indicate that both media types support neuronal activity with noticeably increased activity observed within the first three days of culture. However, the number of active objects observed in

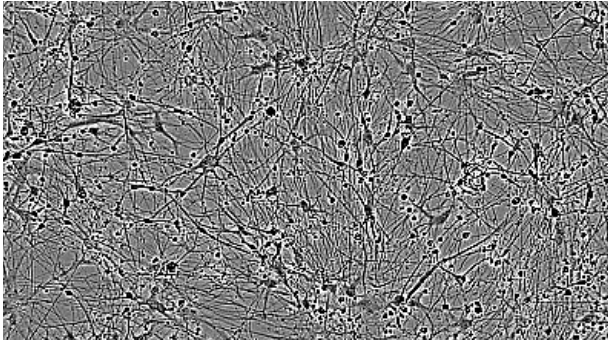
the Ncardia medium were higher than in complete BrainPhys medium. Interestingly, although the synchronicity of cells in both culture conditions remained low for the extent of the 25 day experiment, higher synchronicity was observed in co-cultures grown in BrainPhys medium compared to Ncardia medium. Although changes in environmental conditions (media and supplements) did not appear to affect qualitative observations of neuronal morphology and network complexity, these data illustrate that there were significant alterations in neuronal function and connectivity.

Measurements of Neuronal Structure Versus Function to Investigate Neurotoxic Effects

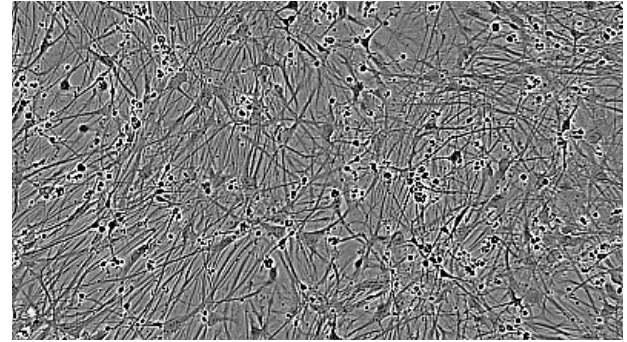
Additional insights can be obtained when measurements of neuronal structure and function are combined. Figure 6 shows how this was applied to study the potential neurotoxic effects of paclitaxel (Taxol®), which can sometimes be associated with

neuropathic effects such as numbness and loss of sensory function. To study potential neurotoxic effects, primary rat cortical neurons were first co-cultured with primary rat astrocytes for 11 days, allowing the cultures to mature and stabilize. Baseline measurements of activity and morphology were made each day using Incucyte® Neuroburst Orange and Incucyte® Neurolight Orange respectively (Figure 6). At day 11, cultures were treated with a range of concentrations of Taxol. Activity and morphology were monitored for a further 11 days in culture. Figure 6 illustrates that by day 21, at sub-nanomolar (<10⁻⁹ M) concentrations of Taxol only small changes in neurite length were observed, while a reduction in neuronal activity occurred (Figure 6C). Individual well traces indicated both concentration- and time- dependent responses of neuronal activity following Taxol treatment as shown in Figure 6D.

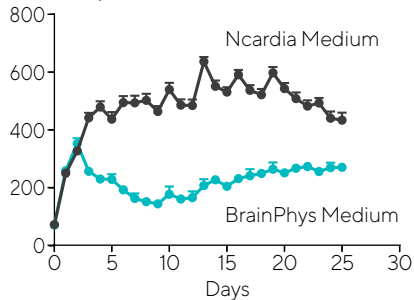
A Ncardia Medium



B BrainPhys Medium



C Active Objects



D Correlation

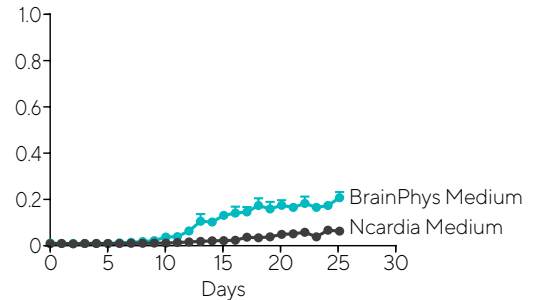


Figure 5. Impact of culture conditions on neuronal activity in iPSC-derived Peri/4U cells. Peri.4U neurons were seeded at 25K cells/wells with a co-culture of primary rat astrocytes seeded at 15K cells/well on 96-well culture plates. Neurons were infected with Neuroburst Orange Lentivirus at day 2. Cells were then cultured in Complete BrainPhys Medium or Neuro.4U Medium. Morphology of the neurons was not affected by media differences (A and B). Active object number (C) and mean correlation (D) were plotted over 25 days in culture. Data points represent Mean \pm SEM.

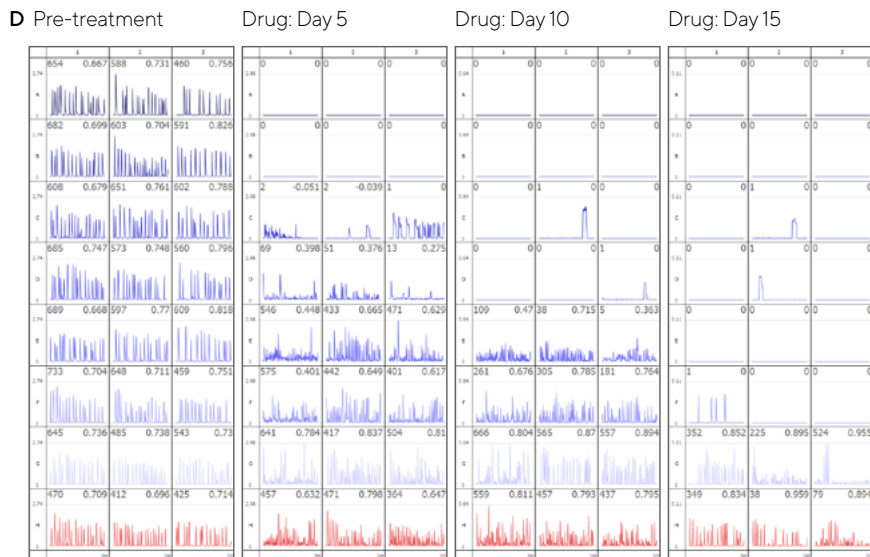
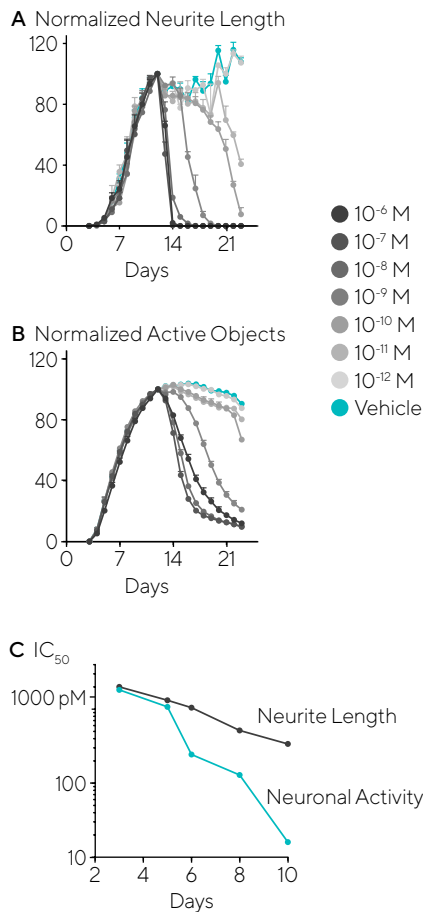


Figure 6. Taxol-induced changes in neurite length and neuronal activity in primary rat neurons. Rat cortical neurons seeded at 30K cells/well were co-cultured with rat astrocytes seeded at 15K cells/well and transduced with Neuroburst Orange or NeuroLight Orange at day 3 in culture. Live-cell analysis measurements were made each day using the Incucyte® Live-Cell Analysis System. After 11 days, neural networks had fully formed and stabilized. Taxol or vehicle control was then added and cultures were monitored for an additional 11 days. Time-courses of neurite development (A) and neuronal activity (B) prior to, and after the addition of, control or increasing concentrations of Taxol are shown. Potency (IC_{50} values) plotted against time post-treatment for neuronal activity (grey) and neurite length (orange) (C). Data is expressed as % neurite length or active object count, normalized to the pre-treatment value. Data points represent Mean \pm SEM. Neuronal activity summary traces at pre-treatment and at 5, 10 and 15 days post-treatment display decreased activity levels over the course of the experiment (D).

Conclusions

The Incucyte® Neuronal Activity Assay, consisting of instrumentation, software, and reagent, provides access to complex, neuronal activity and connectivity measurements as neurons and their networks mature and become functionally active through chronic evaluation of the same population of cells. This assay achieves long-term evaluation in a variety of neuronal cell models, such as primary cells and hiPSC-derived neurons, to evaluate when they become active and how this activity changes overtime without removing cells from the physiologically-relevant environment of a tissue culture incubator. Overall, live-cell analysis provides a valuable compliment to established techniques such as electrophysiology, for building and validating translational cell models for the discovery of novel neurotherapeutics.

- A non-invasive imaged-based approach allows quantitative monitoring of neuronal activity as neurons mature and networks develop; the need to select an arbitrary point in time to perform a single measurement is alleviated.

- Use of a genetically encoded calcium sensor (Incucyte® Neuroburst Orange Lentivirus) is non-perturbing and can be used with a variety of neuronal cell types (such as primary neurons and iPSC-derived models) to analyze short-term calcium flux kinetics.
- Acquisition of longer wavelength fluorophores (excitation > 500 nm) allows for chronic analysis of the same population of cells over weeks to months to detect functional changes and reveal differences among various iPSC-derived neuronal models or to measure impact of culture conditions on neuronal activity.
- Capture of spontaneous calcium oscillations from thousands of neurons allows for highly reproducible kinetic profiling to determine both activity and connectivity using Incucyte® Neuronal Activity Analysis Software Module.
- Additional insights can be obtained when measurements of neuronal structure and function are combined. As an example

of utility when investigating potential neurotoxic effects, concentration response curves of paclitaxel were generated in an established co-culture of primary rat cortical neurons and astrocytes, revealing a substantial reduction in neuronal activity with only small changes in neurite length after 10 days of treatment.

Kinetic Neuroimmune Assays

Real-Time Quantification of Chemotaxis and Phagocytosis to Evaluate Neuroimmune Function

Introduction

Several neurological disorders have been linked with the dysfunction of the immune system, including multiple sclerosis, Alzheimer's disease and brain cancers. Being the primary innate immune cells of the brain, microglia, play a role in both the etiology of such disease progression as well as in healthy brain development and maintenance. In their role as resident brain macrophages, microglia are responsible for immunosurveillance and neuroprotection, regulating brain development primarily through phagocytosis and the release of various immune proteins. However, with age, microglia become increasingly dysfunctional and lose their neuroprotective properties. Thus, studying the role of these innate immune cells is crucial in understanding the inflammatory response under both normal and degenerative conditions of the brain.

To evaluate microglia behavior and their impact on the regulation of functional neurons, detailed *in vitro* methodology is required. In particular, the cell models used, such as microglia cell lines, stem cell-derived microglia cultures and primary dissociated cell cultures, as well as their culture conditions is of pivotal importance to characterize the underlining functions of microglia. Assays designed to evaluate these models typically focus on the morphology of activated cells, their migratory response, and the ability to phagocytize diseased or dying cells as well as pathogens, employing technologies such as flow cytometry and Boyden chamber assays. However, the techniques used to study microglia behavior is typically endpoint, are performed in environments that are not representative of physiological conditions, include cumbersome assay preparation steps and do not offer insight into morphological changes associated with microglial activation.

Live-cell imaging and analysis addresses these inherent drawbacks via non-invasive, repeated monitoring of the same population of cells within a standard cell culture incubator. The includes incorporation of reagents and consumables that allow for real-time, quantification and visualization of microglial behavior, alleviating technically challenging preparation and quantification steps associated with traditional techniques. In this chapter, we will examine kinetic approaches that can shed new light on the function of microglia in order to characterize microglial response to neurodegeneration therapeutic interventions.

Incucyte® Neuroimmune Assays at a Glance

In order to measure microglia function over time, various quantitative and qualitative assays are employed. Incucyte® HD phase imaging allows for visual observation of activation-associated morphology changes, giving detailed insight into cellular changes associated with neurodegenerative diseases.

Incucyte® Chemotaxis Assays are fully automated solutions to quantify directional migration in response to a stimulus. Utilizing a proprietary migration microplate, the Incucyte® Clearview 96-Well Plate, label-free analysis and precise quantification of the chemotactic response is generated throughout the experiment. In addition, visual assessment of morphological changes associated with stimuli response as the membrane of the plate is optically clear (see Chapter 6c - Kinetic Chemotaxis Assays for more details).

Incucyte® Phagocytosis Assays enable real-time, automated analysis of both phagocytosis and efferocytosis within your

cell culture incubator. Using non-perturbing, pH sensitive fluorescent probes, visualization and quantification of phagocytosis can be achieved in real-time over the entire assay time course.

Shortcomings of Traditional Assays	Live-Cell Imaging and Analysis Approaches
<ul style="list-style-type: none">▪ Requires fixation and immunostaining steps.	<ul style="list-style-type: none">▪ Real-time, label-free measurement of chemotaxis migration without fixing, staining or cell scraping steps.
<ul style="list-style-type: none">▪ Measurements at user-defined time points.	<ul style="list-style-type: none">▪ Real-time automated analysis in 96- or 384-well formats.
<ul style="list-style-type: none">▪ Inability to visualize, confirm morphological changes.	<ul style="list-style-type: none">▪ Direct visualization of morphological changes associated with biological response.
<ul style="list-style-type: none">▪ Requirement for large number of cells for single-point measurements.	<ul style="list-style-type: none">▪ Analyze sensitive and rare cells with a cell sparing, highly reproducible 96- or 384-well assays.

Table 1. Shortcomings of Traditional Assays vs Live-Cell Imaging and Analysis Approaches.

Sample Results

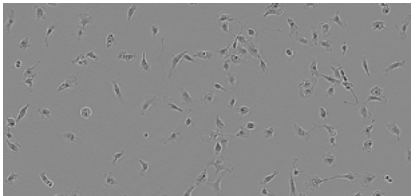
Differential Morphology of Microglia

Finding the optimal *in vitro* model for studying microglia in the pathogenesis of neurodegenerative disorders can be difficult. Current options for studying

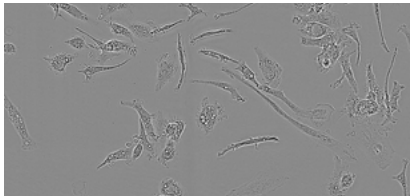
microglia, include immortalized cell lines, primary cell lines and human induced pluripotent stem cell (hiPSC)-derived microglia. In order to evaluate morphological characteristics of each of these models, we imaged rat primary microglia, two different sources of hiPSC-derived microglia, and three immortalized

microglia cell lines. Dramatic differential morphology was observed depending on species and source (Figure 1). Evaluation of imaged-based changes in morphology gives insight into *in vitro* culture conditions, cell activation status and reprogramming events for the development of therapeutic targets for neurodegenerative disorders.

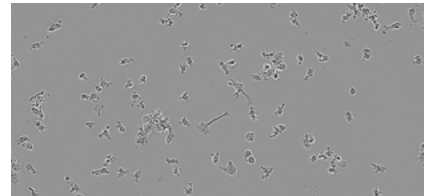
Rat Primary Microglia



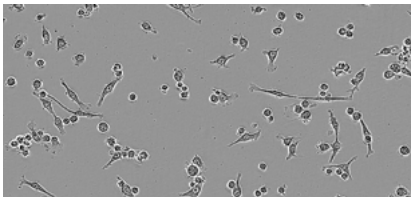
Axol iPSC-Derived Microglia



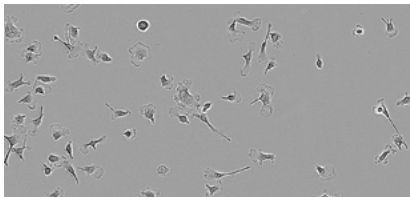
CDI iPSC-Derived Microglia



BV-2



C8-B4



HMC3

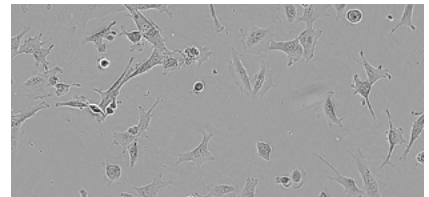


Figure 1. Visualization of morphological differences in microglia. Representative images from: rat primary microglia (Brain Bits – top left), iPSC-derived microglia (Axol BioSciences – top middle), iPSC-derived microglia (Cellular Dynamics International – top right), immortalized murine microglia cell lines BV-2 (bottom left) and C8-B4 (bottom middle), and HMC3 human immortalized microglia (bottom right).

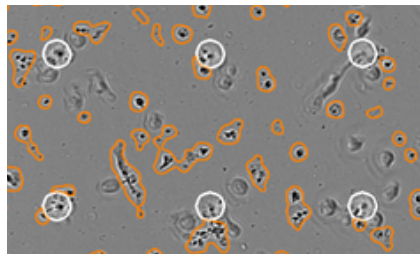
Automated Quantification of Microglia Migrations

In addition to providing insight into the morphology of microglia, the Incucyte® Live-Cell Analysis System can also be utilized to quantify migratory capability of these cells via Incucyte® Chemotaxis Assays. Microglia are the resident immune cells of the brain, responding to extracellular signals and migrating towards

the site of infection or neuronal damage. In a model of microglia migration response, iPSC-derived microglia (CDI) were seeded in an Incucyte® Clearview 96-well Plate and exposed to C5a, a protein fragment involved in cell recruitment and activation of phagocytosis. After cell addition on the top membrane of the Incucyte® Clearview 96-well Plate, three-fold dilutions of C5a were added to reservoir wells. Cells then

migrated to the bottom of the membrane toward C5a. Label-free measurements of bottom-side confluence were analyzed in real time using the Incucyte® Chemotaxis Analysis Software Module. Data shows concentration-dependent chemotactic migration of iPSC-derived microglia towards C5a over a period of 24 hours (Figure 2).

Rat Primary Microglia



Axol iPSC-Derived Microglia

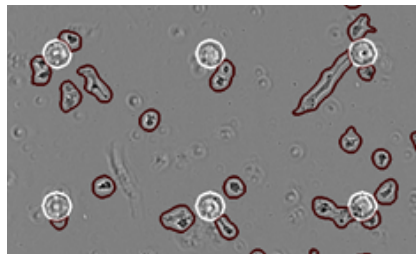
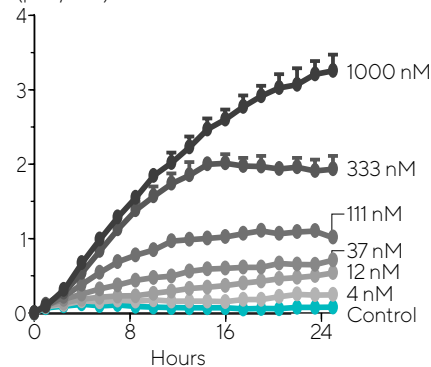


Figure 2. Concentration-dependent migration of iPSC-derived microglia (CDI) toward C5a. iPSC-derived microglia (CDI) were plated in the top chamber of the Incucyte® Clearview 96-Well Plate at a density of 4,000 cells/well. Serial dilutions of C5a, starting at 1 nM, were added to the bottom reservoir wells and automated imaging and analysis was performed (data collected at 1-hour intervals). Images represent the top and bottom side of the membrane at the 30-hour time point. Automated image processing separates cells located on the top (outlined in yellow) and the bottom (outlined in black) surface of the membrane. Pores are outlined in white. Images are processed as they are acquired, and data can be plotted in real time.

Concentration-Dependent Movement Towards C5a

Phase Area Bottom x 10⁵
(μm²/well)



Specific Detection and Visualization of Cell Engulfment by Microglia

Another important function of microglia cells is the phagocytosis of cellular debris and dead neurons. To visualize and quantify the phagocytic potential of microglia, the non-perturbing pH sensitive Incucyte® pHrodo® Orange Cell Labeling Dye was used. Neuro-2a (N2A) target cells were treated with staurosporine to induce apoptosis and subsequently labelled with the Incucyte® pHrodo® Orange Cell Labeling Kit. The target cells were added to wells containing iPSC-derived microglia and imaged in real time real time to visualize and quantify the engulfment of the labeled apoptotic N2A cells (Figure 3). As the engulfed cell enters the acidic phagosome of the microglia, the change in pH results in an orange fluorescent signal which is automatically segmented

and quantified by integrated Incucyte® software. To verify sensitivity of the assay, increasing densities of pHrodo labelled apoptotic N2A cells were added to pre-plated rat primary microglia. Data reveals a N2A density-dependent response of orange intensity due to phagocytosis by microglia, and no fluorescent signal in wells containing only apoptotic N2A cells. (Figure 4).

Differential Effects of Inhibitors on Efferocytosis and Phagocytosis

The Incucyte® Phagocytosis Assays can also be used to evaluate pharmacological effects on microglial engulfment of dead or dying cells as well as bacterial particles. By looking at different types of target material, we can understand how treatments impact different phagocytic processes, as the receptors that mediate

efferocytosis (uptake of dying/dead cells) are different from those that mediate phagocytosis of bacteria and other cellular debris. The BV-2 microglia cell line was used to evaluate the effect of cytochalasin D and cilengitide on both the efferocytosis of apoptotic N2A cells and the phagocytosis of pHrodo® labeled E. coli Bioparticles. Cytochalasin D is an inhibitor of actin polymerization and elicited a concentration-dependent inhibition of both efferocytosis and phagocytosis. Cilengitide is an inhibitor of $\alpha V\beta 3$ and $\alpha V\beta 5$ integrins, and it selectively attenuated the efferocytosis of N2A cells with minimal effect on the phagocytosis of bioparticles. These data support the role of $\alpha V\beta 3$ and $\alpha V\beta 5$ integrins in the cell interactions required for efferocytosis, but not in the phagocytosis of bacteria-based bioparticles.

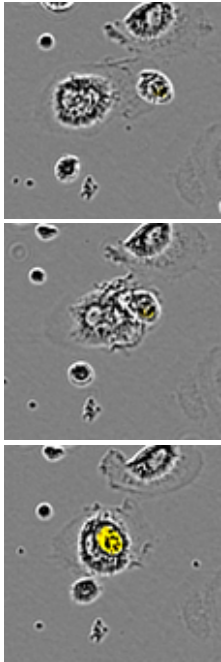
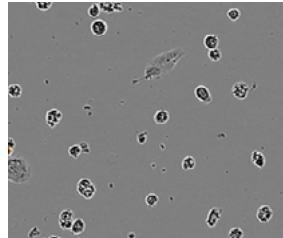
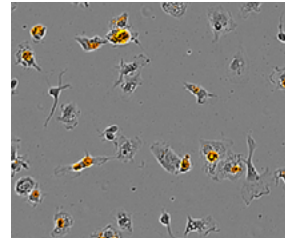


Figure 3. HD phase and fluorescent visualization of N2A engulfment by microglia. Time-lapse visualization of iPSC-derived microglia (Axol BioSciences) engulfing Incucyte® pHrodo® Orange-labeled apoptotic N2A cells. Images verify the entry of apoptotic target cells into the phagosome of microglia.

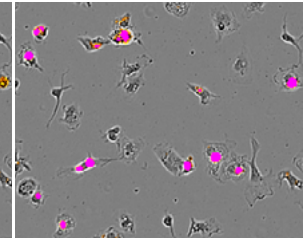
Apoptotic N2A Alone



Microglia with N2A



Fluorescent image



Fluorescent image with mask

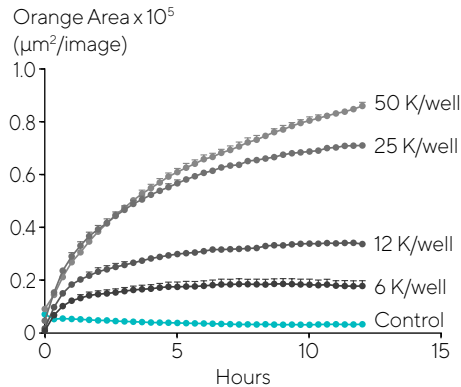
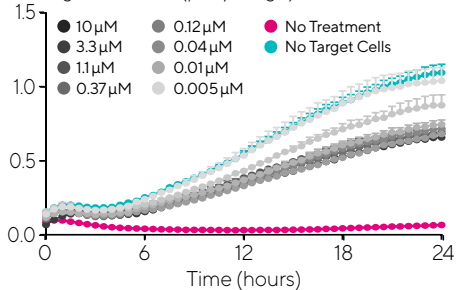


Figure 4. Visualization and quantification of apoptotic N2A engulfment by microglia. N2A cells were pre-treated with staurosporine (24 hrs), labeled with the Incucyte® pHrodo® Orange Cell Labeling Kit, and added to pre-plated primary rat microglia (Brain Bits, 20,000 cells/well). N2A cells alone have minimal fluorescence (left image). Engulfment of labeled apoptotic N2A cells by microglia causes an increase in orange fluorescence (fluorescent image) that is automatically segmented to quantify N2A density-dependent efferocytosis over time (right).

Cytochalasin D

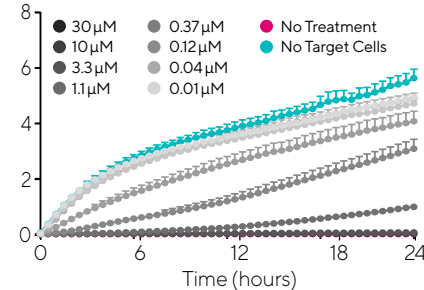
Efferocytosis

Orange Area $\times 10^5$ ($\mu\text{m}^2/\text{image}$)



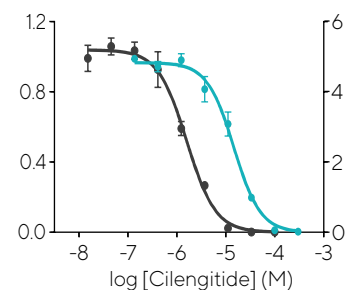
Phagocytosis

Orange Area $\times 10^5$ ($\mu\text{m}^2/\text{image}$)



Efferocytosis

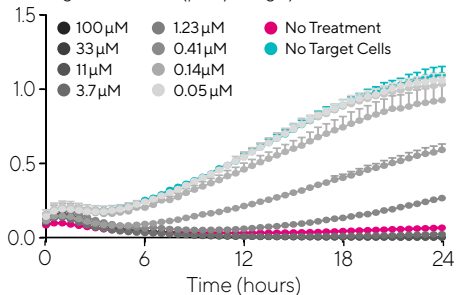
Phagocytosis



Cilengitide

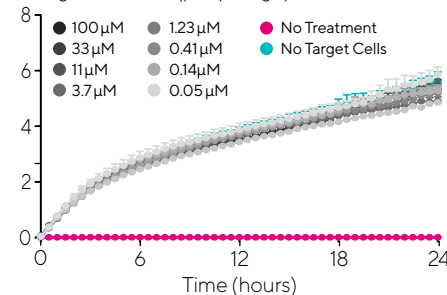
Efferocytosis

Orange Area $\times 10^5$ ($\mu\text{m}^2/\text{image}$)



Phagocytosis

Orange Area $\times 10^5$ ($\mu\text{m}^2/\text{image}$)



Efferocytosis

Phagocytosis

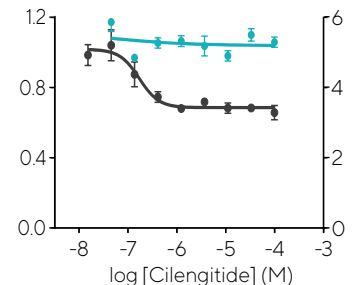


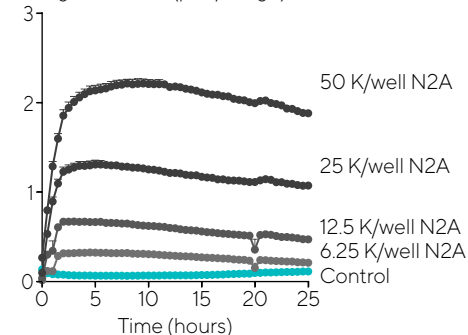
Figure 5. Quantitative pharmacological analysis of relevant target material. BV-2 effector cells (20,000 cells/well) efferocytose apoptotic N2A cells (left column) or E. coli Bioparticles (middle column). Cytochalasin D (top row) elicits a concentration-dependent inhibition of both efferocytosis and phagocytosis, yielding IC_{50} values of 0.16 μM and 1.5 μM , respectively. Cilengitide, and inhibitor of $\alpha\text{V}\beta 3$ and $\alpha\text{V}\beta 5$ integrins, selectively attenuates efferocytosis (IC_{50} value of 0.16 μM), with minimal effect on phagocytosis at the highest concentration tested (100 μM).

Microglial Phagocytosis of Disease-Related Peptides

Microglia are also responsible for the clearance of other cellular debris and peptides associated with neurological disorders. In order to evaluate the engulfment of relevant disease-associated peptides, the Incucyte® pHrodo Orange Cell Labeling Kit was used to label apoptotic N2A cells, beta-amyloid, alpha-synuclein and myelin basic protein. Using iPSC-derived microglia, we observed a concentration-dependent phagocytic clearance of physiologically relevant material (Figure 6). These data support the use of pHrodo-labeled material to study microglia function in maintaining brain homeostasis to clear potential toxic factors.

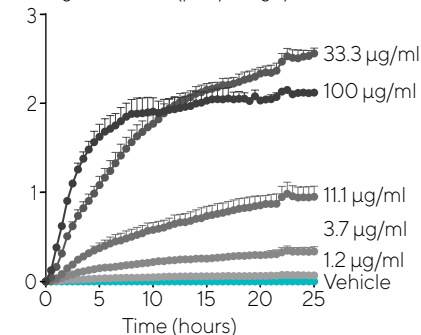
Apoptotic N2A

Orange Area $\times 10^5$ ($\mu\text{m}^2/\text{image}$)



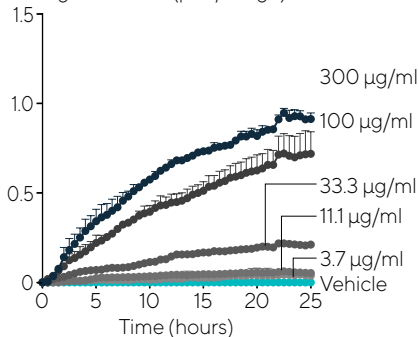
Beta-Amyloid (1-42)

Orange Area $\times 10^5$ ($\mu\text{m}^2/\text{image}$)



Alpha-Synuclein

Orange Area $\times 10^5$ ($\mu\text{m}^2/\text{image}$)



Myelin basic protein

Orange Area $\times 10^5$ ($\mu\text{m}^2/\text{image}$)

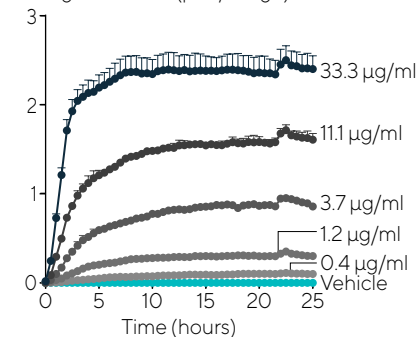


Figure 6. Comparison of phagocytic clearance of neuro-associated peptides in an iPSC-derived microglial cell model. iPSC-derived microglia (Axol BioSciences) seeded at 30,000 cells/well phagocytose physiologically relevant target material. Kinetic graphs display concentration-dependent response to pHrodo labeled apoptotic Neuro-2A, beta-amyloid, alpha-synuclein and myelin basic protein.

Conclusions

These results exemplify the Incucyte® Live-Cell Analysis System's capability for analysis of neuroimmune function in live-cell models. Using non-perturbing reagents, a proprietary microplate, and purpose-built software analysis, microglia can be kinetically evaluated to monitor cell morphology, movement and function in a single, flexible platform. Specifically, this system allows for image-based evaluation of changes in microglia morphology during cell activation and reprogramming events as well as the kinetic quantification of microglia chemotaxis and phagocytosis in response to physiologically relevant material. The Incucyte® approach for real-time, long-term quantitative analysis of neuroimmune

modulation is suited for development and characterization of therapeutic approaches for neurodegenerative disorders.

- System allows for users to optimize culture conditions and maintenance of different *in vitro* models by providing automated analysis of cell morphology, movement and function.
- Image-based acquisition enables qualitative assessment of morphological changes in different microglia *in vitro* models.
- Kinetic measurements of microglia chemotaxis and phagocytosis capture

a complete account of dynamic cell function and movement.

- All data and time points can be verified by inspecting individual images and/or time-lapse movies.
- Low well-to-well variability and minimal user effort make the assay amenable to medium throughput screening in a 96- or 384-well format.
- This approach also provides a sensitive method to detect experimental manipulations that alter neuroimmune function to study microglia function in maintaining brain homeostasis.

Incucyte® User Publications

1. Balaban S, *et al.* Adipocyte lipolysis links obesity to breast cancer growth: adipocyte-derived fatty acids drive breast cancer cell proliferation and migration. *Cancer Metab*, 2017, Jan 5:1.
2. Bohlen C. J. *et al.* 2017 Diverse requirements for microglial survival, specification, and function revealed by defined-medium cultures. *Neuron*, 94 (4): 759-773.e8.
3. Brosius Lutz A. *et al.* 2017 Schwann cells use TAM receptor-mediated phagocytosis in addition to autophagy to clear myelin in a mouse model of nerve injury. *Proc. Natl. Acad. Sci. USA*; 114 (38): E8072-E8080.
4. Sellgren C. M. *et al.* Increased microglial synapse elimination in patient-specific models of schizophrenia. <https://www.biorxiv.org/content/10.1101/231290v1> Preprint bioRxiv, 231290.
5. Zorina Y. *et al.* Human IgM antibody rHlgM22 promotes phagocytic clearance of myelin debris by microglia. *Sci. Rep.*; 8: 9392.



Appendix: Live-Cell Assay Protocols and Product Guides

A. Cell Culture Quality Control

D. Cell Migration and Invasion

B. Cell Health & Proliferation

E. Protein Dynamics

F. Complex Cell Models

C. Immune Cell Models

G. Neuronal Cell Models

Sales and Service Contacts

North America

Essen BioScience Inc.
300 West Morgan Road
Ann Arbor, Michigan, 48108
USA
Telephone +1 734 769 1600

E-Mail:
orders.US07@sartorius.com

Europe

Essen BioScience Ltd.
Units 2 & 3 The Quadrant
Newark Close
Royston Hertfordshire
SG8 5HL
United Kingdom
Telephone +44 1763 227400

E-Mail:
euorders.UK03@sartorius.com

APAC

Sartorius Japan K.K.
4th Floor Daiwa Shinagawa North
Bldg.
1-8-11 Kita-Shinagawa
Shinagawa-ku, Tokyo
140-0001
Japan
Telephone: +81 3 6478 5202

E-Mail:
orders.US07@sartorius.com



Find more information at
www.sartorius.com/incucyte

E-mail: AskAScientist@sartorius.com

Specifications subject to change without notice.

© 2020, Essen BioScience, Inc., part of the Sartorius Group. All Rights Reserved. Incucyte and all names of Incucyte products are registered trademarks and the property of Essen BioScience unless otherwise specified. Incucyte is a Sartorius brand.

Version 4 / 2020 / 09

www.sartorius.com/incucyte